Quantum Science and Technology

Quantum Science and Technology

Aims and Scope

The book series Quantum Science and Technology is dedicated to one of today's most active and rapidly expanding fields of research and development. In particular, the series will be a showcase for the growing number of experimental implementations and practical applications of quantum systems. These will include, but are not restricted to: quantum information processing, quantum computing, and quantum simulation; quantum communication and quantum cryptography; entanglement and other quantum resources; quantum interfaces and hybrid quantum systems; quantum memories and quantum repeaters; measurement-based quantum control and quantum feedback; quantum nanomechanics, quantum optomechanics and quantum transducers; quantum sensing and quantum metrology; as well as quantum effects in biology. Last but not least, the series will include books on the theoretical and mathematical questions relevant to designing and understanding these systems and devices, as well as foundational issues concerning the quantum phenomena themselves. Written and edited by leading experts, the treatments will be designed for graduate students and other researchers already working in, or intending to enter the field of quantum science and technology.

Renato Portugal

Quantum Walks and Search Algorithms

Springer

Renato Portugal
Department of Computer Science
National Laboratory of Scientific
Computing (LNCC)
Petrópolis, RJ, Brazil

ISBN 978-1-4614-6335-1 ISBN 978-1-4614-6336-8 (eBook)
DOI 10.1007/978-1-4614-6336-8
Springer New York Heidelberg Dordrecht London

Library of Congress Control Number: 2013930230

Printed on acid-free paper

Springer is part of Springer Science+Business Media (www.springer.com)

Preface

This is a textbook about *quantum walks* and *quantum search algorithms*. The reader will take advantage of the pedagogical aspects of this book and learn the topics faster and make less effort than reading the original research papers, often written in jargon. The exercises and references allow the readers to deepen their knowledge on specific issues. Guidelines to use or to develop computer programs for simulating the evolution of quantum walks are also available.

There is a gentle introduction to quantum walks in Chap. 2, which analyzes both the discrete- and continuous-time models on a discrete line state space. Chapter 4 is devoted to Grover's algorithm, describing its geometrical interpretation, often presented in textbooks. It describes the evolution by means of the *spectral decomposition* of the evolution operator. The technique called *amplitude amplification* is also presented. Chapters 5 and 6 deal with analytical solutions of quantum walks on important graphs: line, cycles, two-dimensional lattices, and hypercubes using the Fourier transform. Chapter 7 presents an introduction of quantum walks on generic graphs and describes methods to calculate the limiting distribution and the mixing time. Chapter 8 describes spatial search algorithms, in special a technique called *abstract search algorithm*. The two-dimensional lattice is used as example. This chapter also shows how Grover's algorithm can be described using a quantum walk on the complete graph. Chapter 9 introduces Szegedy's quantum-walk model and the definition of the quantum hitting time. The complete graph is used as example. An introduction to quantum mechanics in Chap. 2 and an appendix on linear algebra are efforts to make the book self-contained.

Almost nothing can be extracted from this book if the reader does not have a full understanding of the postulates of quantum mechanics, described in Chap. 2, and the material on linear algebra described in the appendix. Some extra bases are required: It is desirable that the reader has (1) notions of quantum computing, including the circuit model, references are provided at the end of Chap. 2, and (2) notions of classical algorithms and computational complexity. Any undergraduate or graduate student with this background can read this book. The first five chapters are more amenable to reading than the remaining chapters and provide a good basis for the area of quantum walks and Grover's algorithm. For those who have strict interest

in the area of quantum walks, Chap. 4 can be skipped and the focus should be on Chaps. 2, 5–7. Grover's algorithm plays an essential role in Chaps. 8 and 9. Chapter 6 is very technical and repetitive. In a first reading, it is possible to skip the analysis of quantum walks on finite lattices and hypercubes in Chap. 6 and in the subsequent chapters. In many passages, the reader must go slow, perform the calculations and fill out the details before proceeding. Some of those topics are currently active research areas with strong impact on the development of new quantum algorithms.

Corrections, suggestions, and comments are welcome, which can be sent through webpage (qubit.lncc.br) or directly to the author by email (portugal@lncc.br).

Petrópolis, RJ, Brazil Renato Portugal

Acknowledgments

I am grateful to SBMAC, the Brazilian Society of Computational and Applied Mathematics, which publishes a very nice periodical of booklets, called Notes of Applied Mathematics. A first version of this book was published in this collection with the name *Quantum Search Algorithms*. I thank SBC, the Brazilian Computer Society, which developed a report called Research Challenges for Computer Science in Brazil that calls attention to the importance of fundamental research on new technologies that can be an alternative to silicon-based computers. I thank the Computer Science Committee of CNPq for its continual support during the last years, providing essential means for the development of this book. I acknowledge the importance of CAPES, which has an active section for evaluating and assessing research projects and graduate programs and has been continually supporting science of high quality, giving an important chance for cross-disciplinary studies, including quantum computation.

I learned a lot of science from my teachers, and I keep learning with my students. I thank them all for their encouragement and patience. There are many more people I need to thank including colleagues of LNCC and the group of quantum computing, friends and collaborators in research projects and conference organization. Many of them helped by reviewing, giving essential suggestions and spending time on this project, and they include: Peter Antonelli, Stefan Boettcher, Demerson N. Gonçalves, Pedro Carlos S. Lara, Carlile Lavor, Franklin L. Marquezino, Nolmar Melo, Raqueline A. M. Santos, and Angie Vasconcellos.

This book would not have started without an inner motivation, on which my family has a strong influence. I thank Cristina, João Vitor, and Pedro Vinicius. They have a special place in my heart.

Contents

Chapter 1
Introduction

Quantum mechanics has changed the way we understand the physical world and has introduced new ideas that are difficult to accept, not because they are complex, but because they are different from what we are used to in our everyday lives. Those new ideas can be collected in four postulates or laws. It is hard to believe that Nature works according to those laws, and the difficulty starts with the notion of the superposition of contradictory possibilities. Do you accept the idea that a billiard ball could rotate around its axis in both directions at the same time?

Quantum computation was born from this kind of idea. We know that digital classical computers work with zeroes and ones and that the value of the bit cannot be zero and one at the same time. The classical algorithms must obey Boolean logic. So, if the coexistence of bit-0 and bit-1 is possible, which logic should the algorithms obey?

Quantum computation was born from a paradigm change. Information storage, processing and transmission obeying quantum mechanical laws allowed the development of new algorithms, faster than the classical analogues, which can be implemented in physics laboratories. Nowadays, quantum computation is a well-established area with important theoretical results within the context of the theory of computing, as well as in terms of physics, and has raised huge engineering challenges to the construction of the quantum hardware.

The majority of people, who are not familiar with the area and talk about quantum computers, expect that the hardware development would obey the famous Moore's law, valid for classical computer development for fifty years. Many of those people are disappointed to learn about the enormous theoretical and technological difficulties to be overcome to harness and control memory size of a few atoms, where quantum laws hold in their fullness. The construction of the quantum computer requires a technology beyond the semiclassical barrier, which guides the construction of semiconductors used in classical computers, and something equivalent, completely quantum, should be developed to implement elementary logical operations in some sub-nano scale.

R. Portugal, *Quantum Walks and Search Algorithms*, Quantum Science and Technology, DOI 10.1007/978-1-4614-6336-8_1,

The processing of classical computers is very stable. Depending on the calculation, an inversion of a single bit could invalidate the entire process. But we know that long computations, which require inversion of billions of bits, are performed without problems. Classical computers are error prone because its basic components are stable. Consider, for example, a mechanical computer. It would be very unusual for a mechanical device to change its position, especially if we put a spring to keep it stable in the desired position. The same is true for electronic devices, which remain in their states until an electrical pulse of sufficient power changes this. Electronic devices are built to operate at a power level well above the noise and this noise is kept low by dissipating heat into the environment.

The laws of quantum mechanics require that the physical device must be isolated from the environment, otherwise the superposition vanishes, at least partially. It is a very difficult task to isolate physical systems from their environment. Ultra-relativistic particles and gravitational waves pass through any blockade, penetrate into the most guarded places, obtain information, and convey it out of the system. This process is equivalent to a measurement of a quantum observable, which often collapses the superposition and slows down the quantum computer, making it almost, or entirely, equivalent to the classical one. Techniques for signal amplification and noise dissipation cannot be applied to quantum devices in the same way they are used in conventional devices. This fact raises questions about the feasibility of quantum computers. On the other hand, theoretical results show that there are no fundamental issues against the possibility of building quantum hardware. Researchers say that it is only a matter of technological difficulty.

There is no point in building quantum computers if we are going to use them in the same way we use classical computers. Algorithms must be rewritten and new techniques for simulating physical systems must be developed. The task is more difficult than for classical computer. So far, we do not have a quantum programming language. Also, quantum algorithms must be developed using concepts of linear algebra. Quantum computers with a large enough number of qubits are not available, as yet, to be used in simulations. This is slowing down the development in the area.

The concept of quantum walks provides a powerful technique for building quantum algorithms. This area was developed in the beginning as the quantum version of the concept of classical random walk, which requires the tossing of a coin to determine the direction of the next step. The laws of quantum mechanics state that the evolution of an isolated quantum system is deterministic. Randomness shows up only when the system is measured and classical information is obtained. This explains why the name "quantum random walks" is seldom used. The coin is introduced in quantum walks by enlarging the space of the physical system. Time proceeds in discrete units. There are at least two such models. They are called *discrete-time quantum walks*. Surprisingly, there is another model that does not require an extra space dimension, in addition to where the walker moves, and time is continuous. This model is called *continuous-time quantum walk*. Those models cannot be obtained one from the other, via time limit or discretization and they have some fundamental differences.

Chapter 2
The Postulates of Quantum Mechanics

It is impossible to present quantum mechanics in a few pages. Since the goal of this book is to describe quantum algorithms, we limit ourselves to the *principles* of quantum mechanics and describe them as "game rules." Suppose you have played checkers for many years and know several strategies, but you really do not know chess. Suppose now that someone describes the chess rules. Soon you will be playing a new game. Certainly, you will not master many chess strategies, but you will be able to play. This chapter has a similar goal. The postulates of a theory are its game rules. If you break the rules, you will be out of the game.

At best, we can focus on four postulates. The first describes the arena where the game goes on. The second describes the dynamics of the process. The third describes how we adjoin various systems. The fourth describes the process of physical measurement. All these postulates are described in terms of linear algebra. It is essential to have a solid understanding of the basic results in this area. Moreover, the postulate of composite systems uses the concept of tensor product, which is a method of combining two vector spaces to build a larger vector space. It is also important to be familiar with this concept.

2.1 State Space

The *state* of a physical system describes its physical characteristics at a given time. Usually we describe some of the possible features that the system can have, because otherwise, the physical problems would be too complex. For example, the spin state of a billiard ball can be characterized by a vector in $\mathbb{R}^3$. In this example, we disregard the linear velocity of the billiard ball, its color or any other characteristics that are not directly related to its rotation. The spin state is completely characterized by the axis direction, the rotation direction and rotation intensity. The spin state can be described by three real numbers that are the components of a vector, whose direction characterizes the rotation axis, whose sign describes to which side of the billiard

R. Portugal, *Quantum Walks and Search Algorithms*, Quantum Science and Technology, DOI 10.1007/978-1-4614-6336-8_2,

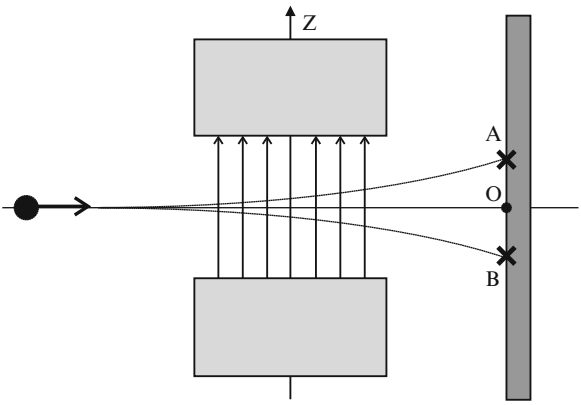

Fig. 2.1 Scheme of an experimental device to measure the spin state of an electron. The electron passes through a magnetic field having vertical direction. It hits A or B depending on the rotation direction. The distance of the points A and B from point O depends on the rotation speed. The results of this experiment are quite different from what we expect classically

ball is spinning and whose length characterizes the speed of rotation. In classical physics, the direction of the rotation axis can vary continuously, as well as the rotation intensity.

Does an *electron*, which is considered an elementary particle, *i.e.* not composed of other smaller particles, rotates like a billiard ball? The best way to answer this is by experimenting in real settings to check whether the electron in fact rotates and whether it obeys the laws of classical physics. Since the electron has charge, its rotation would produce magnetic fields that could be measured. Experiments of this kind were performed at the beginning of quantum mechanics, with beams of silver atoms, later on with beams of hydrogen atoms, and today they are performed with individual particles (instead of beams), such as electrons or photons. The results are different from what is expected by the laws of the classical physics.

We can send the electron through a magnetic field in the vertical direction (direction z), according to the scheme of Fig. 2.1. The possible results are shown. Either the electron hits the screen at the point A or point B. One never finds the electron at point O, which means no rotation. This experiment shows that the *spin* of the electron only admits two values: *spin up* and *spin down* both with the same intensity of "rotation." This result is quite different from classical, since the direction of the rotation axis is quantized, admitting only two values. The rotation intensity is also quantized.

Quantum mechanics describes the electron spin as a unit vector in the Hilbert space $\mathbb{C}^2$. The *spin up* is described by the vector

$$|0\rangle = \begin{bmatrix} 1 \\ 0 \end{bmatrix}$$

and *spin down* by the vector

$$|1\rangle = \begin{bmatrix} 0 \\ 1 \end{bmatrix}.$$

This seems a paradox, because vectors $|0\rangle$ and $|1\rangle$ are orthogonal. Why use orthogonal vectors to describe *spin up* and *spin down*? In $\mathbb{R}^3$, if we add *spin up* and *spin down*, we obtain a rotationless particle, because the sum of two opposite vectors of equal length gives the zero vector, which describes the absence of rotation. In the classical world, you cannot rotate a billiard ball to both sides at the same time. We have two mutually excluded situations. It is the *law of excluded middle*. The notions of *spin up* and *spin down* refer to $\mathbb{R}^3$, whereas quantum mechanics describes the behavior of the electron before the observation, that is, before entering the magnetic field, which aims to determine its state of rotation.

If the electron has not entered the magnetic field and if it is somehow isolated from the macroscopic environment, its spin state is described by a linear combination of vectors $|0\rangle$ and $|1\rangle$

$$|\psi\rangle = a_0|0\rangle + a_1|1\rangle, \tag{2.1}$$

where the coefficients a_0 and a_1 are complex numbers that satisfy the constraint

$$|a_0|^2 + |a_1|^2 = 1. \tag{2.2}$$

Since vectors $|0\rangle$ and $|1\rangle$ are orthogonal, the sum does not result in the zero vector. Excluded situations in classical physics can coexist in quantum mechanics. This coexistence is destroyed when we try to observe it using the device shown in Fig. 2.1. In the classical case, the spin state of an object is independent of the choice of the measuring apparatus and, in principle, has not changed after the measurement. In the quantum case, the spin state of the particle is a mathematical idealization which depends on the choice of the measuring apparatus to have a physical interpretation and, in principle, suffers irreversible changes after the measurement. The quantities $|a_0|^2$ and $|a_1|^2$ are interpreted as the probability of detection of spin up or down, respectively.

2.1.1 State–Space Postulate

An *isolated physical system* has an associated Hilbert space, called the *state space*. The state of the system is fully described by a unit vector, called the *state vector* in that Hilbert space.

Notes

1. The postulate does not tell us the Hilbert space we should use for a given physical system. In general, it is not easy to determine the dimension of the Hilbert space of the system. In the case of electron spin, we use the Hilbert space of dimension 2, because there are only two possible results when we perform an experiment to determine the vertical electron spin. More complex physical systems admit more possibilities, which can be an infinite number.

2. A system is isolated or *closed* if it does not influence and is not influenced by the outside. In principle, the system need not be small, but it is easier to isolate small systems with few atoms. In practice, we can only deal with approximate isolated systems, so the state–space postulate is an idealization.

The state–space postulate is impressive, on the one hand, but deceiving, on the other hand. The postulate admits that classically incompatible states coexist in superposition, such as rotating to both sides simultaneously, but this occurs only in isolated systems, *i.e.* we cannot see this phenomenon, as we are on the outside of the insulation (let us assume that we are not *Schrödinger's cat*). A second restriction demanded by the postulate is that quantum states must have unit norm. The postulate constraints show that the quantum superposition is not absolute, *i.e.* is not the way we understand the classical superposition. If quantum systems admit a kind of superposition that could be followed classically, the quantum computer would have available an exponential amount of parallel processors with enough computing power to solve the problems in *class NP-complete*.[1] It is believed that the quantum computer is exponentially faster than the classical computer only in a restricted class of problems.

2.2 Unitary Evolution

The goal of physics is not simply to describe the state of a physical system at a given time, rather the main objective is to determine the state of this system in future. A theory makes predictions that can be verified or falsified by physical experiments. This is equivalent to determining the dynamical laws the system obeys. Usually, these laws are described by differential equations, which govern the time evolution of the system.

2.2.1 Evolution Postulate

The *time evolution* of an isolated quantum system is described by a *unitary transformation*. If the state of the quantum system at time t_1 is described by vector $|\psi_1\rangle$, the system state $|\psi_2\rangle$ at time t_2 is obtained from $|\psi_1\rangle$ by a unitary transformation U, which depends only on t_1 and t_2, as follows:

$$|\psi_2\rangle = U|\psi_1\rangle. \tag{2.3}$$

[1] The class NP-complete consists of the most difficult problems in the class NP (*Non-deterministic Polynomial*). The class NP is defined as the class of computational problems that have solutions whose correctness can be "quickly" verified.

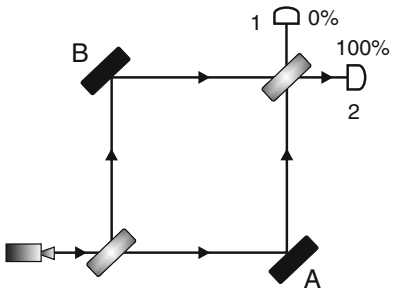

Fig. 2.2 Schematic drawing of an experimental device, which consists of a light source, two half-silvered mirrors A and B, fully reflective mirrors, detectors 1 and 2. The interference produced by the last half-silvered mirror makes all light to go to the detector 2

Notes

1. The action of a unitary operator on a vector preserves its norm. Thus, if $|\psi\rangle$ is a unit vector, $U|\psi\rangle$ is also a unit vector.
2. A *quantum algorithm* is a prescription of a sequence of unitary operators applied to an initial state takes the form

$$|\psi_n\rangle = U_n \cdots U_1 |\psi_1\rangle.$$

   The qubits in state $|\psi_n\rangle$ are measured, returning the result of the algorithm. Before measurement, we can obtain the initial state from the final state because unitary operators are invertible.
3. The evolution postulate is to be written in the form of a differential equation, called *Schrödinger equation*. This equation provides a method to obtain operator U once given the physical context. Since the goal of physics is to describe the dynamics of physical systems, the Schrödinger equation plays a fundamental role. The goal of computer science is to analyze and implement algorithms, so the computer scientist wants to know if it is possible to implement some form of a unitary operator previously chosen. Equation (2.3) is useful for the area of quantum algorithms.

Let us analyze a second experimental device. It will help to clarify the role of unitary operators in quantum systems. This device uses *half-silvered mirrors* with 45° incident light, which transmit 50% of incident light and reflect 50%. If a single photon hits the mirror at 45°, with probability 1/2, it keeps the direction unchanged and with probability 1/2, it is reflected. These half-silvered mirrors have a layer of glass that can change the phase of the wave by 1/2 wavelength. The complete device consists of a source that can emit one photon at a time, two half-silvered mirrors, two fully reflective mirrors and two photon detectors, as shown in Fig. 2.2. By tuning the device, the result of the experiment shows that 100% of the light reaches detector 2.

There is no problem explaining the result using the interference of electromagnetic waves in the context of the *classical physics*, because there is a phase change in the light beam that goes through one of the paths producing a destructive

interference with the beam going to the detector 1 and constructive interference with the beam going to the detector 2. However, if the light intensity emitted by the source is decreased such that one photon is emitted at a time, this explanation fails. If we insist on using classical physics in this situation, we predict that 50% of the photons would be detected by detector 1 and 50% by detector 2, because the photon either goes through the mirror A or goes through B, and it is not possible to interfere since it is a single photon.

In *quantum mechanics*, if the set of mirrors is isolated from the environment, the two possible paths are represented by two orthonormal vectors $|0\rangle$ and $|1\rangle$, which generate the state space that describes the possible paths to reach the photon detector. Therefore, a photon can be in superposition of "*path A*," described by $|0\rangle$, together with "*path B*," described by $|1\rangle$. This is the application of the first postulate. The next step is to describe the dynamics of the process. How is this done and what are the unitary operators in the process? In this experiment, the dynamics is produced by the half-silvered mirrors, since they generate the paths. The action of the half-silvered mirrors on the photon must be described by a unitary operator U. This operator must be chosen so that the two possible paths are created in a balanced way, *i.e.*

$$U|0\rangle = \frac{|0\rangle + \mathrm{e}^{\mathrm{i}\phi}|1\rangle}{\sqrt{2}}. \tag{2.4}$$

This is the most general case where paths A and B have the same probability to be followed, because the coefficients have the same modulus. To complete the definition of operator U, we need to know its action on state $|1\rangle$. There are many possibilities, but the most natural choice that reflects the experimental device is $\phi = \pi/2$ and

$$U = \frac{1}{\sqrt{2}}\begin{bmatrix} 1 & i \\ i & 1 \end{bmatrix}. \tag{2.5}$$

The state of the photon after passing through the second half-silvered mirror is

$$\begin{aligned} U(U|0\rangle) &= \frac{(|0\rangle + i|1\rangle) + i(i|0\rangle + |1\rangle)}{2} \\ &= i|1\rangle. \end{aligned} \tag{2.6}$$

The intermediate step of the calculation was displayed on purpose. We can see that the paths described by $|0\rangle$ algebraically cancel, which can be interpreted as a destructive interference, while the $|1\rangle$-paths interfere constructively. The final result shows that the photon that took path B remains, going directly to the detector 2. Therefore, quantum mechanics predicts that 100% of the photons will be detected by detector 2.

2.3 Composite Systems

The *postulate of composite systems* states that the state space of a *composite system* is the *tensor product* of the state space of the components. If $|\psi_1\rangle, \ldots, |\psi_n\rangle$ describe the states of n isolated quantum systems, the state of the composite system is $|\psi_1\rangle \otimes \cdots \otimes |\psi_n\rangle$.

An example of a composite system is the memory of a *n-qubit* quantum computer. Usually, the memory is divided into sets of qubits, called *registers*. The state space of the computer memory is the tensor product of the state space of the registers, which is obtained by repeated tensor product of the Hilbert space $\mathbb{C}^2$ of each *qubit*.

The state space of the memory of a 2-qubit quantum computer is $\mathbb{C}^4 = \mathbb{C}^2 \otimes \mathbb{C}^2$. Therefore, any unit vector in $\mathbb{C}^4$ represents the quantum state of two qubits. For example, the vector

$$|0,0\rangle = \begin{bmatrix} 1 \\ 0 \\ 0 \\ 0 \end{bmatrix}, \tag{2.7}$$

which can be written as $|0\rangle \otimes |0\rangle$, represents the state of two electrons both with spin up. Analogous interpretation applies to $|0,1\rangle$, $|1,0\rangle$, and $|1,1\rangle$. Consider now the unit vector in $\mathbb{C}^4$ given by

$$|\psi\rangle = \frac{|0,0\rangle + |1,1\rangle}{\sqrt{2}}. \tag{2.8}$$

What is the spin state of each electron in this case? To answer this question, we have to factor $|\psi\rangle$ as follows:

$$\frac{|0,0\rangle + |1,1\rangle}{\sqrt{2}} = \big(a|0\rangle + b|1\rangle\big) \otimes \big(c|0\rangle + d|1\rangle\big). \tag{2.9}$$

We can expand the right-hand side and match the coefficients setting up a system of equations to find a, b, c, and d. The state of the first qubit will be $a|0\rangle + b|1\rangle$ and second will be $c|0\rangle + d|1\rangle$. But there is a big problem: the system of equations has no solution, *i.e.* there are no coefficients a, b, c, and d satisfying (2.9). Every state of a composite system that cannot be factored is called *entangled*. The quantum state is well defined when we look at the composite system as a whole, but we cannot attribute the states to the parts.

A single qubit can be in a superposed state, but it cannot be entangled, because its state is not composed of subsystems. The qubit should not be taken as a synonym of a particle, because it is confusing. The state of a single particle can be entangled when we are analyzing more than a physical quantity related to it. For example, we may describe both the position and the rotation state. The position state may be entangled with the rotation state.

Exercise 2.1. Consider the states

$$|\psi_1\rangle = \frac{1}{2}\big(|0,0\rangle - |0,1\rangle + |1,0\rangle - |1,1\rangle\big),$$

$$|\psi_2\rangle = \frac{1}{2}\big(|0,0\rangle + |0,1\rangle + |1,0\rangle - |1,1\rangle\big).$$

Show that $|\psi_1\rangle$ is not entangled and $|\psi_2\rangle$ is entangled.

Exercise 2.2. Show that if $|\psi\rangle$ is an entangled state of two qubits, then the application of a unitary operator of the form $U_1 \otimes U_2$ necessarily generates an entangled state.

2.4 Measurement Process

In general, measuring a quantum system that is in the state $|\psi\rangle$ seeks to obtain classical information about this state. In practice, measurements are performed in laboratories using devices such as lasers, magnets, scales, and chronometers. In theory, we describe the process mathematically in a way that is consistent with what occurs in practice. Measuring a physical system that is in an unknown state, in general, disturbs this state irreversibly. In those cases, there is no way to know or recover the state before the measurement. If the state was not disturbed, no new information about it is obtained. Mathematically, the disturbance is described by a *orthogonal projector*. If the projector is over an one-dimensional space, it is said that the quantum state *collapsed* and is now described by the unit vector belonging to the one-dimensional space. In the general case, the projection is over a vector space of dimension greater than 1, and it is said that the collapse is partial or, in extreme cases, there is no change at all in the quantum state of the system.

The measurement requires the interaction between the quantum system with a macroscopic device, which violates the *state–space postulate*, because the quantum system is not isolated at this moment. We do not expect the evolution of the quantum state during the measurement process to be described by a unitary operator.

2.4.1 Measurement Postulate

A *projective measurement* is described by a Hermitian operator O, called *observable* in the state space of the system being measured. The observable O has a *diagonal representation*

$$O = \sum_{\lambda} \lambda P_{\lambda}, \tag{2.10}$$

where P_λ is the projector on the eigenspace of O associated with the eigenvalue λ. The possible results of measurement of the observable O are the eigenvalues λ.

If the system state at the time of measurement is $|\psi\rangle$, the probability of obtaining the result λ will be $\|P_\lambda|\psi\rangle\|^2$ or, equivalently,

$$p_\lambda = \langle\psi|P_\lambda|\psi\rangle. \tag{2.11}$$

If the result of the measurement is λ, the state of the quantum system immediately after the measurement will be

$$\frac{1}{\sqrt{p_\lambda}} P_\lambda|\psi\rangle. \tag{2.12}$$

Notes

1. There is a correspondence between the physical layout of the devices in a physics lab and the observable O. When an experimental physicist measures a quantum system, she or he gets real numbers as result. Those numbers correspond to the eigenvalues λ of the Hermitean operator O.
2. The states $|\psi\rangle$ and $e^{i\phi}|\psi\rangle$ have the same *probability distribution* p_λ when one measures the same observable O. The states after measurement differ by the same factor $e^{i\phi}$. The term $e^{i\phi}$ multiplying a quantum state is called *global phase factor* whereas a term $e^{i\phi}$ multiplying a vector of a sum of vectors, such as $|0\rangle + e^{i\phi}|1\rangle$, is called *relative phase factor*. The real number ϕ is called *phase*.

Since the possible outcomes of a measurement of observable O obey a probability distribution, we can define the *expected value* of a measurement as

$$\langle O\rangle = \sum_\lambda p_\lambda \lambda, \tag{2.13}$$

and the *standard deviation* as

$$\Delta O = \sqrt{\langle O^2\rangle - \langle O\rangle^2}. \tag{2.14}$$

It is important to remember that the mean and standard deviation of an observable depends on the state that the physical system was in just before the measurement.

Exercise 2.3. Show that $\langle O\rangle = \langle\psi|O|\psi\rangle$.

Exercise 2.4. Show that if the physical system is in a state $|\psi\rangle$ that is an eigenvector of O, then $\Delta O = 0$, that is, there is no uncertainty about the result of the measurement of the observable O. What is the result of the measurement?

Exercise 2.5. Show that $\sum_\lambda p_\lambda = 1$ for any observable O and any state $|\psi\rangle$.

Exercise 2.6. Suppose that the physical system is in generic state $|\psi\rangle$. Show that $\sum_\lambda p_\lambda^2 = 1$ to an observable O, if and only if $\Delta O = 0$.

2.4.2 Measurement in Computational Basis

The *computational basis* of space $\mathbb{C}^2$ is the set $\{|0\rangle, |1\rangle\}$. For one qubit, the observable of the *measurement in the computational basis* is Pauli matrix Z, whose spectral decomposition is

$$Z = (+1)P_{+1} + (-1)P_{-1}, \tag{2.15}$$

where $P_{+1} = |0\rangle\langle 0|$ and $P_{-1} = |1\rangle\langle 1|$. The possible results of the measurement are ± 1. If the state of the qubit is given by (2.1), the probabilities associated with possible outcomes are

$$p_{+1} = |a_0|^2, \tag{2.16}$$

$$p_{-1} = |a_1|^2, \tag{2.17}$$

whereas the states immediately after the measurement are $|0\rangle$ and $|1\rangle$, respectively. In fact, each of these states has a global phase that can be discarded. Note that

$$p_{+1} + p_{-1} = 1,$$

because state $|\psi\rangle$ have unit norm.

Before generalizing to n qubits, it is interesting to reexamine the process of measurement of a qubit with another observable given by

$$O = \sum_{k=0}^{1} k|k\rangle\langle k|. \tag{2.18}$$

Since the eigenvalues of O are 0 and 1, the above analysis holds if we replace $+1$ by 0 and -1 by 1. With this new observable, there is a one-to-one correspondence in the nomenclature of the measurement result and the final state. If the result is 0, the state after the measurement is $|0\rangle$. If the result is 1, the state after the measurement is $|1\rangle$.

The *computational basis* of the Hilbert space of n qubits in decimal notation is the set $\{|0\rangle, \ldots, |2^n - 1\rangle\}$. The *measurement in the computational basis* is associated with observable

$$O = \sum_{k=0}^{2^n-1} k\, P_k, \tag{2.19}$$

where $P_k = |k\rangle\langle k|$. A generic state of n qubits is given by

$$|\psi\rangle = \sum_{k=0}^{2^n-1} a_k|k\rangle, \tag{2.20}$$

where amplitudes a_k satisfying the constraint

$$\sum_k |a_k|^2 = 1. \tag{2.21}$$

The measurement result is an integer value k in the range $0 \leq k \leq 2^n - 1$ with a probability distribution given by

$$\begin{aligned} p_k &= \langle \psi | P_k | \psi \rangle \\ &= | \langle k | \psi \rangle |^2 \\ &= |a_k|^2. \end{aligned} \tag{2.22}$$

Equation (2.21) ensures that the sum of the probabilities is 1. The n-qubit state immediately after the measurement is

$$\frac{P_k|\psi\rangle}{\sqrt{p_k}} \simeq |k\rangle. \tag{2.23}$$

For example, suppose that the state of two qubits is given by

$$|\psi\rangle = \frac{1}{\sqrt{3}} \left(|0,0\rangle - i|0,1\rangle + |1,1\rangle \right). \tag{2.24}$$

The probability that the result is 00, 01 or 11 in binary notation is $1/3$. Result 10 is never obtained, because the associated probability is 0. If the measurement result is 00, the system state immediately after will be $|0,0\rangle$. Similarly for 01 and 11. For the measurement in the computational basis, it makes sense that the result is *state* $|0,0\rangle$, because there is a correspondence between eigenvalue 00 and state $|0,0\rangle$.

The result of the measurement specifies to which vector of the computational basis state $|\psi\rangle$ is projected. The result does not provide the value of coefficient a_k, that is, none of the 2^n amplitudes a_k describing state $|\psi\rangle$ are revealed. Suppose we want to find number k as a result of an algorithm. This result should be encoded as one of the vectors of the computational basis, which spans the vector space to which state $|\psi\rangle$ belongs. It is undesirable, in principle, that the result itself is associated with one of the amplitudes. If the desired result is a non-integer real number, then the k most significant digits should be coded as a vector of the computational basis. After a measurement, we have a chance to get closer to k. A technique used in quantum algorithms is to amplify the value of a_k making it as close to 1 as possible. A measurement at this point will return the value k with high probability. Therefore, the number that specifies a *ket*, for example number k of $|k\rangle$ is a possible outcome of the algorithm, while the amplitudes of the quantum state are associated with the probability of obtaining a result.

The description of the measurement process of observable (2.19) is equivalent to simultaneous measurements or in a cascade of observables Z, *i.e.* one observable Z for each qubit. The possible results of measuring Z are ± 1. Simultaneous measurements, or in a cascade of n qubits, result in a sequence of values ± 1. The relationship between a result of this kind and the one described before is obtained by replacing $+1$ by 0 and -1 by 1. We will have a binary number that can be converted into a decimal number which is one of the values k of (2.19).

For example, for 3 qubits the result may be $(-1, +1, +1)$, which is equivalent to $(1, 0, 0)$. Converting to base ten, we get number 4. The state after the measurement will be obtained using the projector

$$\begin{aligned} P_{-1,+1,+1} &= |1\rangle\langle 1| \otimes |0\rangle\langle 0| \otimes |0\rangle\langle 0| \\ &= |1,0,0\rangle\langle 1,0,0| \end{aligned} \tag{2.25}$$

over the state system of the three qubits followed by *renormalization*. The renormalization in this case replaces the coefficient by 1. The state after measurement will be $|1,0,0\rangle$. So far using the computational basis, for both observables (2.19) and Z's, we can simply say that the result is $|1,0,0\rangle$, because we automatically know that the eigenvalues of Z in question are $(-1,+1,+1)$ and the number k is 4.

A simultaneous measurement of n observables Z is not equivalent to measure observable $Z \otimes \cdots \otimes Z$. The latter observable returns a single value, which can be $+1$ or -1, whereas with n observables Z, simultaneously or not, we obtain n values ± 1. Measurements on a cascade are performed with observable $Z \otimes I \otimes \cdots \otimes I$, $I \otimes Z \otimes \cdots \otimes I$, and so on. They can also be performed simultaneously. Usually, we use a more compact notation, Z_1, Z_2, successively, where Z_1 means that observable Z was used for the first qubit and the identity operator for the remaining qubits. Since these observables commute, the order is irrelevant and the limits imposed by the *uncertainty principle* do not apply. Measurement of observables of this kind is called *partial measurement* in the computational basis.

Exercise 2.7. Suppose that the state of a qubit is $|1\rangle$.

1. What is the mean value and standard deviation of the measurement of observable X?
2. What is the mean value and standard deviation of the measurement of observable Z? Compare with Exercise 2.4.

2.4.3 Partial Measurement in Computational Basis

The term *measurement in the computational basis* of n qubits implies a measurement of all n qubits. However, it is possible to perform a *partial measurement*, *i.e.* to measure some qubits. The result in this case is not necessarily a state of the computational basis. For example, we can measure the first qubit of system described by the state $|\psi\rangle$ of (2.24). It is convenient to rewrite that state as follows:

$$|\psi\rangle = \sqrt{\frac{2}{3}}|0\rangle \otimes \frac{|0\rangle - i|1\rangle}{\sqrt{2}} + \frac{1}{\sqrt{3}}|1\rangle \otimes |1\rangle. \tag{2.26}$$

We can see that the measurement result is either 0 or 1. The probability of obtaining 1 is $1/3$, because the only way to get 1 for a measurement of the first qubit is to obtain 1 as well, for the second qubit. Therefore, the probability of obtaining 0 is $2/3$, and the state immediately after the measurement in this case is

$$|0\rangle \otimes \frac{|0\rangle - i|1\rangle}{\sqrt{2}}.$$

Only the qubits involved in the measurement are projected on the computational basis. The states that have 0 in the first qubit survive and the final state must be renormalized. The remaining qubits may be in superposition. In this example, when the result is 0, the state of the second qubit is a superposition, when the result is 1, the state of the second qubit is $|1\rangle$.

If we have a system composed of subsystems A and B, a partial measurement is a measurement of an observable of the type $O_A \otimes I_B$, where O_A is an observable of system A and I_B is the identity operator of system B. Physically, this means that the measuring apparatus interacted only with the subsystem A. Equivalently, a partial measurement interacting only with subsystem B is a measurement of an observable of the type $I_A \otimes O_B$.

If we have a register of m qubits together with a register of n qubits, we can represent the computational basis in a compact form $\left\{|i, j\rangle : 0 \leq i \leq 2^m - 1, 0 \leq j \leq 2^n - 1\right\}$, where i and j are both represented in base ten. A generic state will be represented by

$$|\psi\rangle = \sum_{i=0}^{2^m-1} \sum_{j=0}^{2^n-1} a_{ij} |i, j\rangle. \tag{2.27}$$

Suppose we measure all qubits of the first register in the computational basis, *i.e.* we measure observable $O_A \otimes I_B$, where

$$O_A = \sum_{k=0}^{2^m-1} k P_k. \tag{2.28}$$

The probability of obtaining value $0 \leq k \leq 2^m - 1$ is

$$\begin{aligned} p_k &= \langle\psi| \left(P_k \otimes I\right) |\psi\rangle \\ &= \sum_{j=0}^{2^n-1} \left|a_{kj}\right|^2. \end{aligned} \tag{2.29}$$

The set $\{p_0, \ldots, p_{2^m-1}\}$ is a probability distribution and therefore satisfies

$$\sum_{k=0}^{2^m-1} p_k = 1. \tag{2.30}$$

If the measurement result is k, the state immediately after the measurement will be

$$\frac{1}{\sqrt{p_k}} (P_k \otimes I) |\psi\rangle = \frac{1}{\sqrt{p_k}} |k\rangle \left(\sum_{j=0}^{2^n-1} a_{kj} |j\rangle \right). \tag{2.31}$$

Note that the state after the measurement is a superposition of the second register. A measurement of observable (2.28) is equivalent to measure observables $Z_1, \ldots, Z_m$.

Exercise 2.8. Suppose that the state of two qubits is given by

$$|\psi\rangle = \frac{3}{5\sqrt{2}}|0,0\rangle - \frac{3\,i}{5\sqrt{2}}|0,1\rangle + \frac{2\sqrt{2}}{5}|1,0\rangle - \frac{2\sqrt{2}\,i}{5}|1,1\rangle. \tag{2.32}$$

1. Describe completely the measurement process of observable Z_1, that is, obtain the probability of each outcome and the corresponding states after the measurement. Suppose that, after measuring Z_1, we measure Z_2. Describe all resulting cases.
2. Now invert the order of the observable and describe the whole process.
3. If the intermediate quantum states are disregarded, is there a difference when we invert the order of the observable? Note that the measurement of Z_1 and Z_2 may be performed simultaneously. One can move the qubits without changing the quantum state, which may be entangled or not, and put each of them into a measuring device, both adjusted to measure observable Z, as in Fig. 2.1.
4. For two qubits, the state after the measurement of the first qubit in the computational basis can be either $|0\rangle|\alpha\rangle$ or $|1\rangle|\beta\rangle$, where $|\alpha\rangle$ and $|\beta\rangle$ are states of the second qubit. In general, we have $|\alpha\rangle \neq |\beta\rangle$. Why is this not the case in previous items?

Further Reading

The amount of good books about quantum mechanics is very large. For the first contact, we suggest [31, 66, 69]. For a more complete approach, we suggest [23]. For a more conceptual approach, we suggest [25, 65]. For those who are only interested in the application of quantum mechanics to quantum computing, we suggest [41, 57, 64, 67, 68].

Chapter 3
Introduction to Quantum Walks

Quantum walks play an important role in the development of quantum algorithms. Algorithms based on quantum walks generally use a technique called *amplitude amplification*, which was introduced in Grover's algorithm. This technique differs from the ones used in algebraic algorithms, in which the Fourier transform plays the main role. However, it is possible to go beyond Grover's algorithm in terms of efficiency. The best algorithm to solve the *element distinctness problem* is based on quantum walks. This problem consists in determining whether there are repeated elements in a set of elements. When Grover's algorithm is used, the solution is less efficient.

Before describing the area of quantum walks, we will briefly review the area of *classical random walks* with a focus on the *expected distance* from the origin induced by the *probability distribution*. We will compare the results to the *quantum expected distance*. We will see that the probability of finding the walker away from the origin is greater in the quantum case. This fact is the main reason why algorithms based on quantum walks can be faster than those based on classical random walks.

3.1 Classical Random Walks

3.1.1 Random Walk on the Line

The simplest example of random walk is the classical motion of a particle on a line, the direction of which is determined by a non-biased coin. Toss the coin, if it is tails, the particle will jump one unit rightward, if it is heads, the particle will jump one unit leftward. This process is repeated every time unit. Because this process is probabilistic, we cannot know for sure where the particle will be at a later time, but we can calculate the probability p of it being at a given point n at time t. Suppose the particle is at the origin at time $t = 0$. Then $p(t = 0, n = 0) = 1$, as shown in the table in Fig. 3.1. For $t = 1$, the particle can be either in the position $n = -1$

R. Portugal, *Quantum Walks and Search Algorithms*, Quantum Science and Technology, DOI 10.1007/978-1-4614-6336-8_3,

t \ n	-5	-4	-3	-2	-1	0	1	2	3	4	5
0						1					
1					$\frac{1}{2}$		$\frac{1}{2}$				
2				$\frac{1}{4}$		$\frac{1}{2}$		$\frac{1}{4}$			
3			$\frac{1}{8}$		$\frac{3}{8}$		$\frac{3}{8}$		$\frac{1}{8}$		
4		$\frac{1}{16}$		$\frac{1}{4}$		$\frac{3}{8}$		$\frac{1}{4}$		$\frac{1}{16}$	
5	$\frac{1}{32}$		$\frac{5}{32}$		$\frac{5}{16}$		$\frac{5}{16}$		$\frac{5}{32}$		$\frac{1}{32}$

Fig. 3.1 Probability of the particle being in the position n at time t, assuming it starts the random walk at the origin. The probability is zero in empty cells

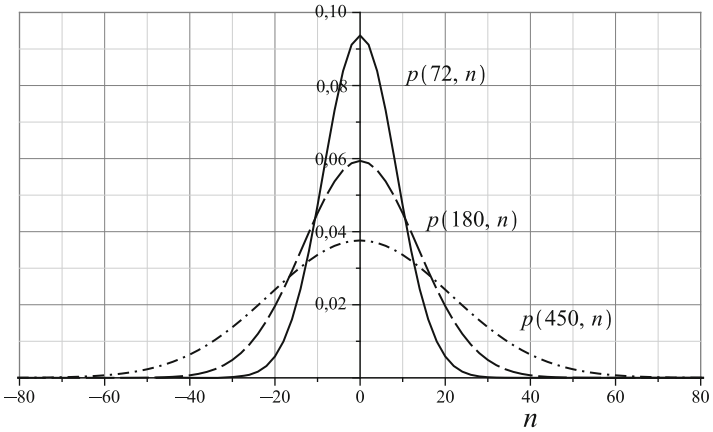

Fig. 3.2 Probability distribution of the random walk in a classical one-dimensional lattice for $t = 72$, $t = 180$ and $t = 450$

with probability $1/2$ or in $n = 1$ with probability $1/2$. The probability of it being in the position $n = 0$ becomes zero. Following this reasoning, we can confirm all probabilities described in the table in Fig. 3.1.

A generic term in this table is given by

$$p(t,n) = \frac{1}{2^t}\binom{t}{\frac{t+n}{2}}, \tag{3.1}$$

where $\binom{a}{b} = \frac{a!}{(a-b)!b!}$. This equation is valid only if it $t + n$ is even and $n \leq t$. If $t + n$ is odd or $n > t$, the probability will be zero. For a fixed value of t, $p(t,n)$ is a *binomial distribution*. For relatively large values of fixed t, the probability as a function of n has a characteristic curve. In Fig. 3.2, three of these curves are shown for $t = 72$, $t = 180$, and $t = 450$. Strictly, the curves are envelopes of the

distribution of points, because the probability is zero for odd values of n when t is even. Another way to interpret the curves of the figure is as the sum $p(t,n) + p(t+1,n)$, *i.e.* we have two overlapping distributions.

We can see in Fig. 3.2 that the height of the midpoint of the curve decreases as a function of time, whereas the width increases. It is natural to ask what the *expected distance* from the origin induced by the probability distribution is. It is important to determine how far away from the origin we can find the particle as time goes on. The expected distance is a statistical quantity that captures this idea and is equal to the *position standard deviation* when the probability distribution is symmetrical. The *average position* (or *expected position*) is

$$\begin{aligned} \langle n \rangle &= \sum_{n=-\infty}^{\infty} n\, p(t,n) \\ &= 0, \end{aligned} \tag{3.2}$$

it follows that the standard deviation of the probability distribution is

$$\begin{aligned} \sqrt{\langle n^2 \rangle - \langle n \rangle^2} &= \sqrt{\sum_{n=-\infty}^{\infty} n^2\, p(t,n)} \\ &= \sqrt{t}\,. \end{aligned} \tag{3.3}$$

Another way to calculate the standard deviation is by converting the binomial distribution into an expression that is easier to handle analytically. By expanding the binomial factor of (3.1) in terms of factorials, and using Stirling's approximation for large values of t, the probability distribution of the random walk can be approximated by the expression

$$p\,(t,n) \simeq \frac{2}{\sqrt{2\pi\, t}}\, \mathrm{e}^{-\frac{n^2}{2t}}. \tag{3.4}$$

For a fixed value of t and without the factor 2 in the numerator, this function is called *Gaussian* or *normal distribution*. The width of the normal distribution is defined as half the distance between the inflection points. By equating the second derivative $\partial^2 p/\partial n^2$ to zero, we eventually obtain the width $\sqrt{t}$. The standard deviation is the width of the normal distribution.

Exercise 3.1. The goal of this exercise is to help to obtain (3.1). First show that at time t, the total number of possible paths of the particle is 2^t. At time t, the particle is in position n. Suppose that the particle has moved a steps rightward and b steps leftward. Find a and b as functions of t and n. Now focus on the steps rightward. In how many ways can the particle move a steps rightward in t units of time? Or, equivalently, we have t objects, in how many ways can we select a objects? Show that the probability of the particle being in the position n is given by (3.1).

Exercise 3.2. The goal of this exercise is to help the calculation of the sum in (3.3). Change the dummy index to obtain a finite sum starting at $n = 0$ and running over even values of n when t is even and running over odd values of n when t is odd. After that you can use (3.1). Rename the dummy index in order to use the identities

$$\sum_{n=0}^{t} \binom{2t}{n} = 2^{2t-1} + \frac{1}{2}\binom{2t}{t}, \quad \sum_{n=0}^{t} n \binom{2t}{n} = t\,2^{2t-1},$$
$$\sum_{n=0}^{t} n^2 \binom{2t}{n} = t^2 2^{2t-1} + t\,2^{2t-2} - \frac{t^2}{2}\binom{2t}{t}$$

and simplify the result to show that

$$\sum_{n=-\infty}^{\infty} n^2\, p(t,n) = t.$$

Exercise 3.3. Show that (3.4) can be obtained from (3.1) through *Stirling's approximation*, which is given by

$$t! \approx \sqrt{2\pi t}\; t^t\, \mathrm{e}^{-t},$$

when $t \gg 1$. [Hint: Use Stirling's approximation and simplify the result trying to factor out the fraction n/t. Take the *natural logarithm* of the expression, expand the logarithm, and use the asymptotic expansion of the logarithm. Note that terms of the type n^2/t^2 are much smaller than n^2/t. At the end, take the exponential of the result.]

3.1.2 Classical Discrete Markov Chains

A *classical Markov chain* is a stochastic process that assumes values in a discrete set and obeys the following property: the next state of the chain only depends on the current state, *i.e.* it is not influenced by the past states. The Markov chain can be viewed as a directed graph where the states are represented by vertices and directed edges indicate what the possible next states are. The next state is randomly determined. Note that the set of states is discrete, whereas the evolution can be discrete or continuous. Therefore, the term discrete or continuous in this area only refers to time.

Let us start by describing the *classical discrete Markov chains*, *i.e.* chains with discrete time variable. At each step, the Markov chain has an associated probability distribution, which is the set of probabilities of the walker being in the states or vertices. We can describe the probability distribution with a vector, after choosing an order for the states. Let $\Gamma(X, E)$ be a graph with set of vertices $X = \{x_1, \ldots, x_n\}$

($|X| = n$) and set of edges E. The probability distribution is described by a vector of the form

$$\begin{bmatrix} p_1(t) \\ \vdots \\ p_n(t) \end{bmatrix},$$

where $p_1(t)$ is the probability of the walker being at vertex x_1 at time t. Similarly for the other entries. If the process begins with the walker in the first vertex, we have $p_1(0) = 1$ and $p_i(0) = 0$ for $i = 2, \ldots, n$. In a Markov chain, we cannot precisely tell where the walker will be in the future. However, we can determine the probability distribution, if we know the *transition matrix* M, also called *probability matrix* or *stochastic matrix*.

If the probability distribution is known at the time t, we obtain the distribution at time $t + 1$ by employing the formula

$$p_i(t + 1) = \sum_{j=1}^{n} M_{i\,j}\; p_j(t). \tag{3.5}$$

To ensure that $p_i(t + 1)$ is a probability distribution, *i.e.* $p_i \geq 0, \forall i$ and $\sum_i p_i = 1$, matrix M must satisfy the following properties: the entries must be nonnegative real numbers and the sum of the entries of any column must be equal to 1. In vector form, we have

$$\vec{p}(t + 1) = M\; p(t). \tag{3.6}$$

Because the matrix is in the left position, this version is called *left stochastic matrix*. There is a corresponding description that uses a transposed vector of probabilities (row vector) and the matrix is on the right position. In this case, the sum of the entries of each line of M should result in one.

The entry M_{ij} of the stochastic matrix is the probability of the walker, who is in vertex x_j, to go to vertex x_i. The simplest case is when the graph is undirected and

$$M_{ij} = \frac{1}{d_j},$$

where d_j is the *degree* or *valence* of vertex x_j. If there is no edge from x_j to x_i, then $M_{ij} = 0$. In this case, the walker goes to one of the adjacent vertices and transition probability is the same for all of them. The stochastic matrix is related to the *adjacency matrix* (A) of the graph by formula $M_{ij} = A_{ij}/d_j$. The adjacency matrix of an undirected graph is a symmetric Boolean matrix specifying whether two vertices x_i and x_j are connected (entry A_{ij} is 1) or not (entry A_{ij} is 0).

Let us take the *complete graph* with n vertices as an example. All vertices are connected by undirected edges. Therefore, the degree of each vertex is $n - 1$.

The vertices do not have *loops*, so $M_{i\,i} = 0, \forall i$. The stochastic matrix is

$$M = \frac{1}{n-1}\begin{bmatrix} 0 & 1 & 1 & \cdots & 1 \\ 1 & 0 & 1 & \cdots & 1 \\ 1 & 1 & 0 & \cdots & 1 \\ \vdots & \vdots & \vdots & \ddots & \vdots \\ 1 & 1 & 1 & \cdots & 0 \end{bmatrix}. \tag{3.7}$$

If the initial condition is a walker located on the first vertex, the probability distributions in the first steps will be

$$\vec{p}(0) = \begin{bmatrix} 1 \\ 0 \\ \vdots \\ 0 \end{bmatrix}, \quad \vec{p}(1) = \frac{1}{n-1}\begin{bmatrix} 0 \\ 1 \\ \vdots \\ 1 \end{bmatrix}, \quad \vec{p}(2) = \frac{1}{(n-1)^2}\begin{bmatrix} n-1 \\ n-2 \\ \vdots \\ n-2 \end{bmatrix}.$$

The probability distribution at a generic step t is

$$\vec{p}(t) = \begin{bmatrix} f_n(t-1) \\ f_n(t) \\ \vdots \\ f_n(t) \end{bmatrix}, \tag{3.8}$$

where function $f_n(t)$ is

$$f_n(t) = \frac{1}{n}\left(1 - \frac{1}{(1-n)^t}\right). \tag{3.9}$$

Note that when $t \to \infty$, the probability distribution goes to the uniform distribution, which is the *limiting distribution* of this graph.

As motivation for the next section, we make some observations about the dynamical structure of discrete Markov chains. Equation (3.6) is a *recursive equation* that can be solved and written as

$$\vec{p}(t) = M^t\, \vec{p}(0), \tag{3.10}$$

where $\vec{p}(0)$ is the initial condition. Matrix M can be used one step at a time. The successive applications generate the probability distribution at any time. This description is more general than the deterministic description. In a deterministic process, only one possibility evolves over time. Therefore, we do not have a position vector or an *evolution matrix*. The position is a scalar, the dynamics of which is described by a function of time. In the stochastic case, we must consider all possible

evolutions and describe them in a matrix structure, despite the fact that we know only one possibility actually occurs in a specific situation. The matrix structure of the stochastic evolution will be used in the next section to describe the quantum evolution. However, the physical interpretation of what happens at the physical level is clearly different from the actual stochastic process, since in the quantum case it is not correct to say that only one of the possibilities occurs. From the mathematical point of view, there is a radical change, because the evolution matrix is not applied directly to the probability distribution and the matrix entries need not be positive real numbers. In the quantum case, the matrix entries can be negative or complex numbers and the evolution matrix is applied to the vector of *probability amplitudes*.

Exercise 3.4. The purpose of this exercise is to obtain the expression (3.8). By inspecting the stochastic matrix of the complete graph, show that $p_2(t) = p_3(t) = \cdots = p_n(t)$ and $p_1(t+1) = p_2(t)$. Considering that the sum of entries of the vector of probabilities is 1, show that $p_2(t)$ satisfies the following recursive equation:

$$p_2(t) = \frac{1 - p_2(t-1)}{n-1}.$$

Using that $p_2(0) = 0$, solve the recursive equation and show that $p_2(t)$ is given by $f_n(t)$, as in (3.9).

Exercise 3.5. Obtain an expression for M^t in terms of function $f_n(t)$, where M is the stochastic matrix of the complete graph. From the M^t expression, show that $\vec{p}(t)$ obeys (3.8).

Exercise 3.6. Consider a cycle with n vertices and take as initial condition a walker located in one of the vertices. Obtain the stochastic matrix of this graph. Describe the probability distribution for the first steps and compare to the values in Fig. 3.1. Obtain the distribution at a generic time and find the limiting distribution for the odd cycle. [Hint: To find the distribution for the cycle, use the probability distribution of the line.]

Exercise 3.7. Let M be a generic stochastic matrix. Show that M^t is a stochastic matrix for any positive integer t.

3.2 Discrete-Time Quantum Walks

The construction of quantum models and their equations is usually performed by a process called *quantization*. Momentum and energy are replaced by operators acting on a Hilbert space, whose size depends on the physical system freedom degrees. The state of the quantum system is described by a vector in the Hilbert space and the evolution of the system is governed by a unitary operation, if the system is totally isolated from interactions with the macroscopic world around. If the system has more than one component, the Hilbert space is the tensor product of the Hilbert

spaces of the components. As the evolution of isolated quantum systems is unitary, there is no room for *randomness*. Therefore, in principle, the name *quantum random walk* is contradictory. In literature, the term *quantum walk* has been used instead, but quantum systems that are not totally isolated from the environment may have randomness. In addition, at some point we measure the quantum system to obtain information about it. This process generates a probability distribution.

The first model of quantization of classical random walks that we will discuss is the *discrete-time model* or simply *discrete model*. In the quantum case, the walker's position n should be a vector in a Hilbert space $\mathcal{H}_P$ of infinite dimension, the computational basis of which is $\{|n\rangle : n \in \mathbb{Z}\}$. The evolution of the walk should depend on a quantum "coin." If one obtains "heads" after tossing the "coin" and the walker is described by vector $|n\rangle$, then in the next step it will be described by $|n+1\rangle$. If it is "tails," it will be described by $|n-1\rangle$. How do we include the "coin" in this scheme? We can think in physical terms. Suppose an electron is the "random" walker on a one-dimensional lattice. The state of the electron is described not only by its position in the lattice but also by the value of its spin, which may be spin up or spin down. Thus, the spin value can determine the direction of motion. If the electron is in position $|n\rangle$ and its spin is up, it should go to $|n+1\rangle$ keeping the same spin value. Similarly, when its spin is down, it should go $|n-1\rangle$. The Hilbert space of the system should be $\mathcal{H} = \mathcal{H}_C \otimes \mathcal{H}_P$, where $\mathcal{H}_C$ is the two-dimensional Hilbert space associated with the "coin," the computational basis of which is $\{|0\rangle, |1\rangle\}$. We can now define the "coin" as any unitary matrix C with dimension 2, which acts on vectors in Hilbert space $\mathcal{H}_C$. It is called *coin operator*.

The shift from $|n\rangle$ to $|n+1\rangle$ or $|n-1\rangle$ must be described by a unitary operator, called the *shift operator* S. It should operate as follows:

$$S|0\rangle|n\rangle = |0\rangle|n+1\rangle, \tag{3.11}$$

$$S|1\rangle|n\rangle = |1\rangle|n-1\rangle. \tag{3.12}$$

If we know the action of S on the computational basis of $\mathcal{H}$, we have a complete description of this linear operator. Therefore, we can deduce that

$$S = |0\rangle\langle 0| \otimes \sum_{n=-\infty}^{\infty} |n+1\rangle\langle n| + |1\rangle\langle 1| \otimes \sum_{n=-\infty}^{\infty} |n-1\rangle\langle n|. \tag{3.13}$$

We can re-obtain (3.11) and (3.12) by applying S to the computational basis.

At the beginning of the quantum walk, we must apply the coin operator C to the initial state. This is analogous to tossing a coin in the classical case. C produces a rotation of the coin state. If the coin is initially described by one of the states of the computational basis, the result may be a superposition of states. Each term in this superposition will generate a shift in one direction. We would like to choose a fair coin in order to generate a symmetrical walk around the origin. Let us take the initial state with the particle located at the origin $|n=0\rangle$ and the coin state with spin up $|0\rangle$. So

$$|\psi(0)\rangle = |0\rangle|n = 0\rangle, \tag{3.14}$$

where $|\psi(0)\rangle$ denotes the state at the initial time and $|\psi(t)\rangle$ denotes the state of the quantum walk at time t.

The coin used for most one-dimensional quantum walks is the Hadamard operator

$$H = \frac{1}{\sqrt{2}}\begin{bmatrix} 1 & 1 \\ 1 & -1 \end{bmatrix}. \tag{3.15}$$

One step consists of applying H in the state of the coin, *i.e.* applying $H \otimes I$, where I is the identity operator of the Hilbert space $\mathcal{H}_P$, followed by the application of the shift operator S:

$$\begin{aligned} |0\rangle \otimes |0\rangle &\xrightarrow{H\otimes I} \frac{|0\rangle + |1\rangle}{\sqrt{2}} \otimes |0\rangle \\ &\xrightarrow{S} \frac{1}{\sqrt{2}}\big(|0\rangle \otimes |1\rangle + |1\rangle \otimes |-1\rangle\big). \end{aligned} \tag{3.16}$$

The result is a superposition of the particle both in position $n = 1$ and in position $n = -1$. The superposition of positions is a result of the superposition generated by the coin operator. We can see that the coin H is non-biased when applied to $|0\rangle$, since the amplitude of the right part is equal to the amplitude of the left part. If we apply H to $|1\rangle$, there is a sign difference between the amplitudes of the right and left parts. When we calculate the probability of finding the particle at position n, the sign plays no role. So we can call H a non-biased coin.

What is the next step? In the quantum case, we need to measure the quantum system in the state (3.16) to know what the position of the particle is. If we measure it using the computational basis of $\mathcal{H}_P$, we will have a 50% chance of finding the particle at position $n = 1$ and a 50% chance of finding it at the position $n = -1$. This result is the same, compared to the first step of the classical random walk. If we repeat the same procedure successively, *i.e.* (1) we apply the coin operator, (2) we apply the shift operator, and (3) we measure using the computational basis, we will re-obtain the classical random walk. Our goal is to use quantum features to obtain new results, which cannot be obtained in the classical context. When we measure the particle position after the first step, we destroy the correlations between different positions, which are typical of quantum systems. If we do not measure and apply the coin operator followed by the shift operator successively, the quantum correlations between different positions can have constructive or destructive interference, effectively generating a behavior different from the classical context, which is a characteristic of quantum walks. We will see that the probability distribution does not go to the normal distribution and the standard deviation is not $\sqrt{t}$.

The quantum walk consists in applying the unitary operator

$$U = S\,(H \otimes I), \tag{3.17}$$

t \ n	-5	-4	-3	-2	-1	0	1	2	3	4	5
0						1					
1					$\frac{1}{2}$		$\frac{1}{2}$				
2				$\frac{1}{4}$		$\frac{1}{2}$		$\frac{1}{4}$			
3			$\frac{1}{8}$		$\frac{1}{8}$		$\frac{5}{8}$		$\frac{1}{8}$		
4		$\frac{1}{16}$		$\frac{1}{8}$		$\frac{1}{8}$		$\frac{5}{8}$		$\frac{1}{16}$	
5	$\frac{1}{32}$		$\frac{5}{32}$		$\frac{1}{8}$		$\frac{1}{8}$		$\frac{17}{32}$		$\frac{1}{32}$

Fig. 3.3 Probability of finding the quantum particle in position n at time t, assuming that the walk starts at the origin with the quantum coin in "heads" state

a number of times without intermediate measurements. One step consists in applying U one time, which is equivalent to applying the coin operator followed by the shift operator. In the next step, we apply U again without intermediate measurements. A time t, the state of the quantum walk is given by

$$|\psi(t)\rangle = U^t|\psi(0)\rangle. \tag{3.18}$$

Let us calculate the initial steps explicitly to compare with the classical random walk. We will take (3.14) as initial condition. The first step will be equal to (3.16). The second step can be calculated using the formula $|\psi(2)\rangle = U|\psi(1)\rangle$ and so on.

$$\begin{aligned}
|\psi(1)\rangle &= \frac{1}{\sqrt{2}}\big(|1\rangle|-1\rangle + |0\rangle|1\rangle\big)\\
|\psi(2)\rangle &= \frac{1}{2}\Big(-|1\rangle|-2\rangle + (|0\rangle + |1\rangle)|0\rangle + |0\rangle|2\rangle\Big)\\
|\psi(3)\rangle &= \frac{1}{2\sqrt{2}}\Big(|1\rangle|-3\rangle - |0\rangle|-1\rangle + (2|0\rangle + |1\rangle)|1\rangle + |0\rangle|3\rangle\Big)
\end{aligned} \tag{3.19}$$

These few initial steps have already revealed that the quantum walk differs from the classical random walk in several aspects. We use a non-biased coin, but the state $|\psi(3)\rangle$ is not symmetric with respect to the origin. The table in Fig. 3.3 shows the probability distribution up to the fifth step, without intermediate measurements. Besides being asymmetric, the probability distribution is not concentrated in the central points. A comparison with the table in Fig. 3.1 clearly illustrates this fact.

We would like to find the probability distribution for a number of steps much larger than 5. However, the calculation method we are using is not suitable to be manually done. Suppose our goal is to calculate $p(100, n)$, *i.e.* the probability distribution of the hundredth step. Firstly, we have to calculate $|\psi(100)\rangle$. There are at least three methods to perform a computational implementation.

The first method uses a recursive formula obtained as follows: the generic state of the quantum walk can be written as a linear combination of the computational basis as

$$|\psi(t)\rangle = \sum_{n=-\infty}^{\infty} \big(A_n(t)|0\rangle + B_n(t)|1\rangle\big)|n\rangle, \tag{3.20}$$

where the coefficients satisfy the constraint

$$\sum_{n=-\infty}^{\infty} |A_n(t)|^2 + |B_n(t)|^2 = 1, \tag{3.21}$$

ensuring that $|\psi(t)\rangle$ has norm equal to 1 in all steps. When applying $H \otimes I$ followed by the shift operator in expression (3.20), we can obtain recursive formulas involving the coefficients A and B, which are given by

$$A_n(t+1) = \frac{A_{n-1}(t) + B_{n-1}(t)}{\sqrt{2}},$$
$$B_n(t+1) = \frac{A_{n+1}(t) - B_{n+1}(t)}{\sqrt{2}}.$$

Using the initial condition

$$A_n(0) = \begin{cases} 1, \text{ if } n = 0; \\ 0, \text{ otherwise,} \end{cases}$$

and $B_n(0) = 0$, we can calculate the probability distribution using the formula

$$p(t,n) = |A_n(t)|^2 + |B_n(t)|^2. \tag{3.22}$$

This approach is suitable to be implemented in the mainstream programming languages, such as `C`, `Fortran`, `Java`, or `Python`.

The second method is to calculate matrix U explicitly. We have to calculate the tensor product $H \otimes I$ according to the formula described in Appendix A. The tensor product is also required to obtain a matrix representation of the shift operator as defined in (3.13). These operators act on vectors in an infinite vector space. However, the number of nonzero entries is finite. Therefore, these arrays must have dimensions slightly larger than 200×200. After calculating U, we calculate U^{100}, and the product of U^{100} with the initial condition $|\psi(0)\rangle$, written as a column vector with a compatible number of entries. The result is $|\psi(100)\rangle$. Finally, we can calculate the probability distribution. This method is suitable to be implemented in computer algebra systems, such as `Mathematica`, `Maple`, or `Sage`, and is inefficient in general.

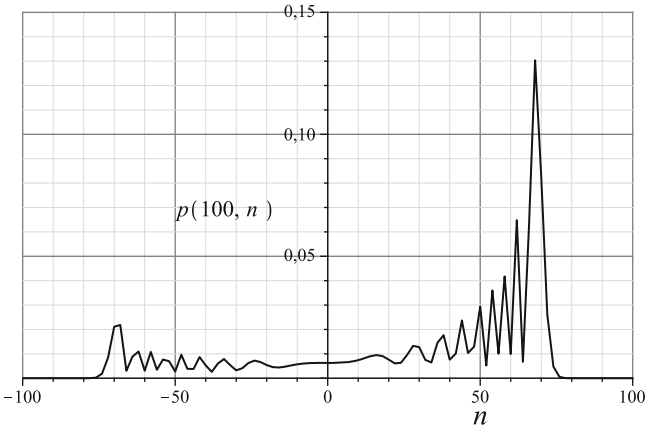

Fig. 3.4 Probability distribution after 100 steps of a quantum walk with the Hadamard coin starting from the initial condition $|\psi(0)\rangle = |0\rangle|n = 0\rangle$. The points where the probability is zero were excluded (n odd)

The third method is to *download* program *QWalk*[1] and follow the instructions on how to choose the initial condition and the coin operator. A short description of this program can be found in Sect. 5.2.5. This is the simplest method by far.

By employing any of the aforementioned methods the graph in Fig. 3.4 for the probability distribution after 100 steps will be obtained. Analogous to the classical random walk, we will ignore the null values of the probability. At $t = 100$, the probability is zero for all odd values of n. The asymmetry of the probability distribution is evident. The probability of finding the particle on the right side of the origin is larger than on the left. In particular, for n around $100/\sqrt{2}$, the probability is much higher than at the origin. This fact is not exclusive to the value $t = 100$. It is valid for any value of t. This suggests a *ballistic* behavior of the quantum walk. The particle can be found away from the origin as if it were in a uniform motion rightward. It is natural to ask whether this pattern would be held if the distribution were symmetric around the origin.

In order to obtain a symmetrical distribution, one must understand why the previous example has a tendency to go rightward. The Hadamard coin introduces a negative sign when applied to state $|1\rangle$. This means there are more cancelations of terms with coin state equals $|1\rangle$ than of terms with coin state equals $|0\rangle$. Since the coin state $|0\rangle$ induces movement rightward and $|1\rangle$ leftward, the final effect is the asymmetry with large probabilities on the right. We can confirm this analysis by calculating the resulting probability distribution when the initial condition is

$$|\psi(0)\rangle = -|1\rangle|n = 0\rangle.$$

[1] http://qubit.lncc.br/qwalk

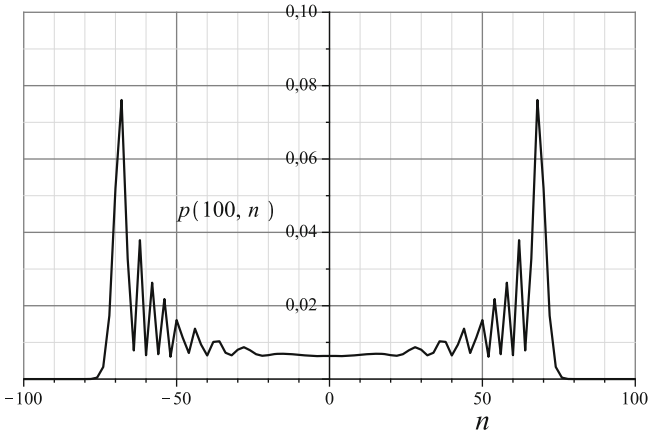

Fig. 3.5 Probability distribution after 100 steps of a quantum walk with the Hadamard coin starting from the initial condition (3.23)

In this case, the number of negative terms will be greater than positive terms and there will be more cancelations of terms with the coin state in $|0\rangle$. The final result will be the mirror distribution in Fig. 3.4 around the vertical axis. To obtain a symmetrical distribution, one must superpose the quantum walks resulting from these two initial conditions. This superposition should not cancel terms before the calculation of the probability distribution. The trick is to multiply the imaginary complex number i to the second initial condition and add to the first initial condition, as follows:

$$|\psi(0)\rangle = \frac{|0\rangle - i\,|1\rangle}{\sqrt{2}}|n = 0\rangle. \tag{3.23}$$

The entries of the Hadamard coin are real numbers. When we apply the evolution operator, terms with the imaginary unit are not converted into terms without the imaginary unit and vice versa. There will be no cancelations of terms of the walk that goes rightward with the terms of the walk that goes leftward. At the end, the probability distributions are added. In fact, the result is the graph in Fig. 3.5.

If the probability distribution of the quantum walk is symmetric, the expected value of the position will be zero, *i.e.* $\langle n\rangle = 0$. The question now is how the standard deviation $\sigma(t)$ behaves as a function of time. The formula for the standard deviation of the probability distribution is

$$\sigma(t) = \sqrt{\sum_{n=-\infty}^{\infty} n^2\, p(t,n)}, \tag{3.24}$$

where $p(t,n)$ is the probability distribution of the quantum walk with initial condition given by (3.23). The analytical calculation is quite elaborate and will be

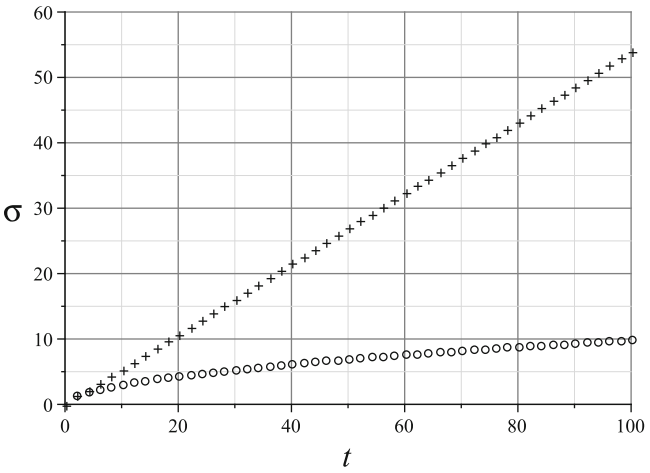

Fig. 3.6 Standard deviation of the quantum walk (*crosses*) and the classical random walk (*circles*) against the number of steps

performed in another chapter. For now, we will numerically calculate the sum of (3.24) by employing some computational implementation. The graphs in Fig. 3.6 show the standard deviation as a function of time for both the quantum walk (cross-shaped points) and classical random walk (circle-shaped points). In the classical case, we have $\sigma(t) = \sqrt{t}$. In the quantum case, we obtain a line, the slope being around 0.54, *i.e.* $\sigma(t) = 0.54\,t$

The linear dependence of the position standard deviation against time is an impressive result. Consider the following extreme situation: Suppose the particle has a probability of exactly one to go rightward. After t steps, it will certainly be found in the position $n = t$. This movement is called *ballistic*. It is the motion of a free particle with unit velocity. The standard deviation in this case is obtained by replacing $p(t,n)$ by $\delta_{t\,n}$ in (3.24). The result is $\sigma(t) = t$. The quantum walk is ballistic, but the scape velocity is almost half of the free particle velocity. However, the quantum particle can be randomly found on the right or on the left side of the origin after measurement, which is a characteristic of random walks. The quantum probability distribution is spread in the interval $\left[-t/\sqrt{2}, t/\sqrt{2}\right]$, while the classical distribution is a Gaussian centered at the origin.

Exercise 3.8. Obtain states $|\psi(4)\rangle$ and $|\psi(5)\rangle$ by continuing the sequence of the states of (3.19) and check that the probability distribution coincides with the one described in the table in Fig. 3.3.

3.3 Classical Markov Chains

The discrete-time quantum walk model is not the only way to *quantize* classical random walks. We will describe a new quantum walk model that does not use a coin to determine the direction to move. The *continuous-time Markov chains* served as the inspiration for the quantization that generated this new model.

When time is a continuous variable, the walker can go from vertex x_j to an adjacent vertex x_i at any time. One way to visualize the problem is to think of probability as if it were a liquid seeping from x_j to x_i. In the beginning, the walker is likely to be found in x_j. As time goes by, the probability of being found in one of the neighboring vertices increases and the probability of staying in x_j decreases. We have a transition rate which we denote by γ, assumably constant for all vertices (homogeneity and isotropy) and for all times. Therefore, the transition between neighboring vertices occurs with a probability γ per unit time. To address problems with continuous variables, we generally use an *infinitesimal* time interval, set up the differential equation of the problem, and solve the equation. If we take an infinitesimal time interval ϵ, the probability of the walker going from vertex x_j to x_i will be $\gamma\epsilon$. Let d_j be the degree of the vertex x_j. Vertex x_j has d_j neighboring vertices. It follows that the probability of the walker being in one of the neighboring vertices after time ϵ is $d_j\gamma\epsilon$. Therefore, the probability of staying in x_j is $1-d_j\gamma\epsilon$. In the continuous case, the entry $M_{ij}(t)$ of the transition matrix at time t is defined as the probability of the particle, which is in vertex x_j, going to the vertex x_i in the time interval t. So

$$M_{ij}(\epsilon) = \begin{cases} 1 - d_j\gamma\epsilon + O(\epsilon^2), & \text{if } i = j; \\ \gamma\epsilon + O(\epsilon^2), & \text{if } i \neq j. \end{cases} \tag{3.25}$$

Let us define an auxiliary matrix, called *generating matrix* given by

$$H_{ij} = \begin{cases} d_j\gamma, \text{ if } i = j; \\ -\gamma, \text{ if } i \neq j \text{ and adjacent;} \\ 0, \text{ if } i \neq j \text{ and non-adjacent.} \end{cases} \tag{3.26}$$

If we play a dice twice, the probability of getting six both times is the product of the probability of each move, as the moves are independent events. The same occurs in a Markov chain, because the next state of a Markov chain only depends on the current configuration of the chain. We can multiply the transition matrix at different times, so

$$M_{ij}(t+\epsilon) = \sum_k M_{ik}(t) M_{kj}(\epsilon). \tag{3.27}$$

The index k runs over all vertices; however, this is equivalent to running only over the vertices adjacent to x_j. In fact, if the particle is at vertex x_j, the probability of it going to x_k in the time interval ϵ is $M_{kj}(\epsilon)$ whatever the value of k is. If there is no edge joining x_j and x_k for a specific k, $M_{kj}(\epsilon) = 0$.

By isolating the term $k = j$ and using the (3.25) and (3.26), we obtain

$$\begin{aligned} M_{ij}(t+\epsilon) &= M_{ij}(t)M_{jj}(\epsilon) + \sum_{k\neq j} M_{ik}(t)M_{kj}(\epsilon) \\ &= M_{ij}(t)(1-\epsilon H_{jj}) - \epsilon \sum_{k\neq j} M_{ik}(t)H_{kj}. \end{aligned}$$

By moving the first term on the right-hand side to the left-hand side and dividing it by ϵ, we obtain

$$\frac{\mathrm{d}M_{ij}(t)}{\mathrm{d}t} = -\sum_k H_{kj}M_{ik}(t). \tag{3.28}$$

The solution of this differential equation with initial condition $M_{ij}(0) = \delta_{ij}$ is

$$M(t) = \mathrm{e}^{-Ht}. \tag{3.29}$$

The verification is simple, if we expand the exponential function in *Taylor series*. With the transition matrix in hand, we can obtain the probability distribution at time t. If the initial distribution is $\vec{p}(0)$, we have

$$\vec{p}(t) = M(t)\,\vec{p}(0). \tag{3.30}$$

It is interesting to compare this form of evolution of the continuous-time Markov chain with discrete-time chain, given by (3.10).

Exercise 3.9. Show that the uniform vector is an eigenvector of H with eigenvalue 0. Use this fact to show that the uniform vector is the eigenvector of $M(t)$ with eigenvalue 1. Show that $M(t)$ is a stochastic matrix for all $t \in \mathbb{R}$.

Exercise 3.10. What is the relationship between H and the Laplacian matrix of the graph?

Exercise 3.11. Show that the probability distribution satisfies the following differential equation:

$$\frac{\mathrm{d}p_i(t)}{\mathrm{d}t} = -\sum_k H_{ki}\,p_k(t).$$

3.4 Continuous-Time Quantum Walks

In the passage from the *classical random walk* model to the *quantum walk* model, we used the standard process of quantization which consists in replacing the vector of probabilies to a state vector or vector of probability amplitudes and the transition matrix by a unitary matrix. It was also necessary to join the Hilbert space associated

with the coin and the Hilbert space associated with the shift operator, which was accomplished with the tensor product, according to the postulates of Quantum Mechanics.

In the passage from the *continuous-time Markov chains* model to the *continuous-time quantum walk* model, again we use a quantization process in this new context. Note that the continuous-time Markov chain has no coin associated. Therefore, we simply convert the vector that describes the probability distribution to a state vector and the transition matrix to an equivalent unitary operator. We must pay attention to the following detail: matrix H, given by (3.26) is Hermitian, so matrix M given by (3.29) is not unitary. There is a very simple way to make M unitary within the context of Hilbert spaces, which is to replace H by $\mathrm{i}H$, *i.e.* to multiply H by the *imaginary unit*. Let us define the evolution operator of the continuous-time quantum walk as

$$U(t) = \mathrm{e}^{-\mathrm{i}Ht}. \tag{3.31}$$

If the initial condition is $|\psi(0)\rangle$, the quantum state at time t is

$$|\psi(t)\rangle = U(t)|\psi(0)\rangle \tag{3.32}$$

and the probability distribution is

$$p_k = \left|\langle k|\psi(t)\rangle\right|^2, \tag{3.33}$$

where k runs over all vertices of the graph or states of the Markov chain and $|k\rangle$ is the state of the computational basis corresponding to the vertex x_k.

As a first application, let us consider the continuous-time quantum walk on the line. The vertices are integer points (discrete space). Equation (3.26) is reduced to

$$H_{ij} = \begin{cases} 2\gamma, & \text{if } i = j; \\ -\gamma, & \text{if } i \neq j \text{ and adjacent;} \\ 0, & \text{if } i \neq j \text{ and non-adjacent.} \end{cases} \tag{3.34}$$

So

$$H|n\rangle = -\gamma\,|n-1\rangle + 2\gamma\,|n\rangle - \gamma\,|n+1\rangle. \tag{3.35}$$

The analytical calculation of operator $U(t)$ will be guided in Exercise 3.12. The numerical calculation of this operator is relatively simple. Figure 3.7 shows the probability distribution of the continuous-time quantum walk at $t = 100$ for $\gamma = \left(2\sqrt{2}\right)^{-1}$ with the initial condition $|\psi(0)\rangle = |0\rangle$. This graph can be generated by the program in Fig. 3.8 or 3.9.

The comparison of the graph in Fig. 3.7 with the graph in Fig. 3.5 is revealing. There are many common points in the overall comparison between the evolution of discrete-time and continuous-time quantum walks; however, they differ in several details. From the global point of view, the probability distribution of the continuous-time walk has two major external peaks and low probability near the origin.

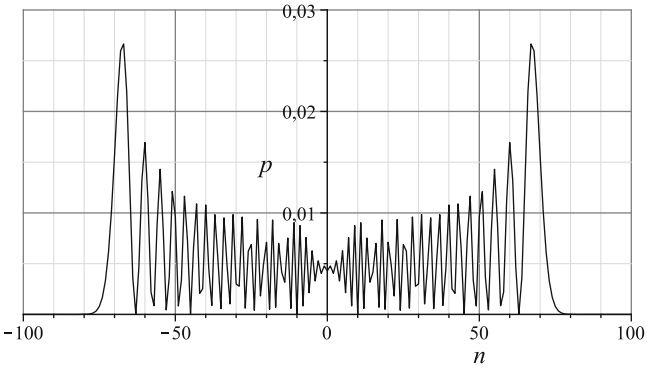

Fig. 3.7 Probability distribution at $t = 100$ for $\gamma = \left(2\sqrt{2}\right)^{-1}$ of a continuous-time quantum walk with initial condition $|\psi(0)\rangle = |0\rangle$

```
t = 100;
n = 100;
gamma = 1./(2.*Sqrt[2.]);
H = Table[If[i == j, 2.*gamma,
     If[i == j+1 || i == j-1, -gamma, 0]],
          {i, 2*n+1}, {j, 2*n+1}];
expH = MatrixExp[-I*t*H];
Psi = expH.Table[If[i == n+1, 1, 0], {i, 2*n+1}];
ListLinePlot[Table[{i-1-n, Abs[Psi[[i]]]^2}, {i,2*n+1}]]
```

Fig. 3.8 Script in *Mathematica* that generates the graph of the probability distribution of the continuous-time quantum walk of Fig. 3.7

Fig. 3.9 Script in *Maple* that generates the graph of the probability distribution of the continuous-time quantum walk of Fig. 3.7

```
with(LinearAlgebra):
t := 100:
n := 100:
gamma0:= 1/(2.*sqrt(2.)):
H := Matrix(2*n+1, 2*n+1,
     (i,j) -> `if`(i=j, 2*gamma0,`if`(i=j+1 or
                    i=j-1, -gamma0, 0.))):
expH := MatrixExponential(-I*H*t):
Psi_t := expH . Vector([0$n, 1., 0$n]):
plot([seq([i-n, abs(Psi_t[i+1])^2], i=0..2*n)]);
```

The same with the discrete-time walk. In the discrete-time walk, these features can be amplified or reduced by choosing an appropriate coin or, equivalently, changing the walker's initial condition. In the continuous-time walk, the dispersion is controlled by the constant γ. If one decreases γ, the distribution shrinks around the origin, maintaining the same pattern.

The most relevant comparison in this context refers to the standard deviation. How does the standard deviation of the continuous-time walk compare to discrete-time walk? The probability distribution of the continuous-time walk is symmetric

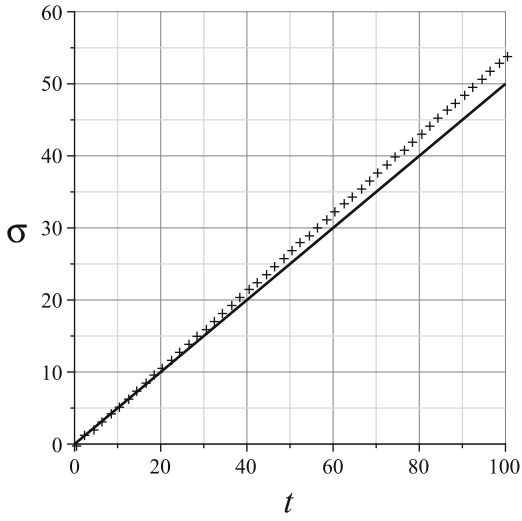

Fig. 3.10 Standard deviation against time for the continuous-time quantum walk with $\gamma = \left(2\sqrt{2}\right)^{-1}$ (*solid line*) and the discrete-time quantum walk analyzed in Sect. 3.2 (*cross-shaped points*)

in relation to the origin in this case. Then, the expected position is zero, *i.e.* $\langle n \rangle = 0$. The standard deviation $\sigma(t)$ is given by (3.24), as in the discrete-time case. The probability distribution is $p(t, n)$

$$p(t, n) = \left| \langle n | U(t) | \psi(0) \rangle \right|^2. \tag{3.36}$$

As before, we can numerically calculate the sum of (3.24). The graphs in Fig. 3.10 show the standard deviation as a function of time for both the continuous-time quantum walk (solid line) and the discrete-time quantum walk (cross-shaped points). In the continuous-time case, we obtain a line, the slope being about 0.5, or $\sigma(t) = 0.5\,t$. In the discrete-time case, we had already obtained a line, with the slope of approximately 0.54. Again, these values are not critical, since in the continuous-time case, this value depends on the choice of γ, while in the discrete-time case, it depends on the coin. What really matters is that the standard deviation is linear, *i.e.* $\sigma(t)$ is proportional to t, contrasting with the classical case where $\sigma(t)$ is proportional to $\sqrt{t}$.

After analyzing two quantization models of classical random walks, the following question naturally arises: are discrete and continuous-time models equivalent? In several applications, these models have very similar behaviors. Both have quantum characteristics that are distinctly different from classical characteristics. In particular, both models have a standard deviation that depend linearly on the time and, with respect to algorithmic applications, they improve the time complexity for many problems when compared to classical algorithms. Nevertheless, when the smallest details are analyzed, it is possible to prove that these models are not equivalent. The optimal algorithms for *spatial search* problems in lattices have different time complexities for each model. Considering these models are

not equivalent in terms of solving specific problems, another question naturally arises: which one is better or more efficient to solve computational problems? This question is still subject to current research. It seems that the discrete-time model is winning the race, since it has approximately a quadratic speedup when searching for a marked vertex in a two-dimensional lattice with periodic boundary conditions compared to the equivalent classical algorithm. The continuous-time model has no gain in this context.

Exercise 3.12. Show that for any time t, matrix H of the continuous-time quantum walk on the line obeys

$$H^t|0\rangle = \gamma^t \sum_{n=-t}^{t} (-1)^n \binom{2t}{t-n} |n\rangle.$$

From this expression, compute $U(t)|0\rangle$ in terms of two nested sums. Invert the sums, use the identity

$$\mathrm{e}^{-2\,\mathrm{i}\,\gamma\,t} J_{|n|}(2\,\gamma\,t) = \mathrm{e}^{\frac{\pi \mathrm{i}}{2}|n|} \sum_{k=|n|}^{\infty} \frac{(-\mathrm{i}\gamma t)^k}{k!} \binom{2\,k}{k-n},$$

where J is the Bessel function of first kind with integer n, to show that the wave function of the continuous-time walk on the line at time t is

$$|\psi(t)\rangle = \sum_{n=-\infty}^{\infty} \mathrm{e}^{\frac{\pi \mathrm{i}}{2}|n| - 2\,\mathrm{i}\,\gamma\,t} J_{|n|}(2\,\gamma\,t)\,|n\rangle.$$

Show that the probability distribution is

$$p(t,n) = \left| J_{|n|}(2\,\gamma\,t) \right|^2.$$

Use this result to depict the graphs of the probability distributions with the same parameters in Fig. 3.7, both for continuous and discrete values of n.

Further Reading

Classical random walks are addressed in many books. Extensive materials can be found in [27, 38, 39]. Identities with binomial expressions used in Exercise 3.2 can be found in [29] and on *Henry Gould*'s webpages,[2] or be deduced from the methods presented in [30]. *Stirling's approximation* can be found in [27]. The main results about classical discrete Markov chains can be found in [24]. Reference [60] is very useful in this context.

[2] http://www.math.wvu.edu/~gould

The quantum algorithm for the *element distinctness problem*, mentioned in the beginning of this chapter, was proposed in [9] by *Andris Ambainis*. A good reference for an initial contact with the area of quantum walks is the review article of *Julia Kempe* [42], which has been highly influential. Reference [5] was the first one to introduce the quantum walk notion in detail with the aim at presenting new quantum phenomena strikingly different from the classical ones. A detailed analysis of quantum walks on the line is presented in [7, 63]. Reference [3] is a key paper addressing quantum walks on generic graphs. *Program QWalk* is described in [56] and is available in the *Computer Physics Communications* library.[3] Further information at http://qubit.lncc.br/qwalk.

Reference [26] introduced the concept of *continuous-time quantum walk*. The application of quantum walks to develop quantum algorithms was strongly influenced by this reference. The continuous-time quantum walk on the line was studied in [22]. Attempts to connect discrete and continuous-time are described in [20, 73]. The link between *universal quantum computation* and quantum walks is addressed in [21] (continuous-time) and in [48] (discrete-time).

[3] http://cpc.cs.qub.ac.uk/summaries/AEAX_v1_0.html

Chapter 4
Grover's Algorithm and Its Generalization

Grover's algorithm is a *search algorithm* originally designed to look for an element in an unsorted database with no repeated elements. If the database elements are stored in a random order, the only available method to find a specific element is an exhaustive search. Usually, this is not the best way to use databases, especially if it is queried several times. It is better to sort the elements, which is an expensive task, but performed only once. In the context of quantum computing, storing data in superposition or in an entangled state for a long period of time is not an easy task. Because of that, Grover's algorithm is introduced following an alternative route, which shows its wide applicability.

Grover's algorithm can be straightforwardly generalized to search databases with repeated elements, if we know beforehand the number of repetitions. The details of this generalization are worked out in this chapter, because it is important in the context of quantum search algorithms. The *counting problem* and searching without knowing the number of repetitions are not addressed here.

In this chapter, we show that Grover's algorithm is *optimal* up to a multiplicative constant, that is, it is not possible to improve its *computational complexity*. If N is the number of database entries, it takes $O(\sqrt{N})$ steps to find the marked element with high probability using $O(\log N)$ storage space.

At the heart of Grover's algorithm lies a method called *amplitude amplification*, which can be used in many quantum algorithms once its structure is extracted. The details of this method are presented at the end of this chapter.

4.1 Grover's Algorithm

Suppose that f is a function with domain $\{0, \ldots, N-1\}$, where $N = 2^n$ and n is some positive integer, and image

$$f(x) = \begin{cases} 1, & \text{if } x = x_0; \\ 0, & \text{otherwise.} \end{cases} \tag{4.1}$$

R. Portugal, *Quantum Walks and Search Algorithms*, Quantum Science and Technology, DOI 10.1007/978-1-4614-6336-8_4,

Algorithm 4.1: Classical search algorithm

Input: N and f as described in Eq (4.1).
Output: x_0.

```
for x = 0 to N − 1 do
    if f(x) = 1 then
        print x
        stop
```

The function image is 1 only for a single point x_0 and 0 for all other points. Suppose we have function f at our disposal, that is, we can evaluate f for any point in the domain; however, we do not know point x_0. The problem is to find which point in the domain has image 1, *i.e.* to find x_0. This is a search problem whose relation to database searching is clear.

What is the *computational complexity* of the best classical algorithm that solves this problem? In this particular problem, the metric employed to measure the complexity is the number of times function f was used. We know no equation for function f and no details of its implementation. It leaves us with the only option: To perform an exhaustive search for point x_0 by *querying* function f. Consequently, the time complexity of the classical algorithm is $\Omega(N)$. Function f is called an *oracle* or *black box*. To evaluate the function at a point is also referred to as *querying* the oracle. Point x_0 is also called a *marked element*.

A concrete way to describe this problem is to ask a programmer to randomly select point x_0 and implement function f using a programming language in a classical computer with a single processor. The programmer must compile the program to hide the value of x_0—it is not allowed to read the code. The function domain is known by us and there is the following *promise*: only one image point is 1, all other image points are 0. A program that solves this problem is described in Algorithm 4.1.

What is the computational complexity of the best *quantum* algorithm that solves the same problem? Grover's algorithm finds x_0 by querying function f $\left\lfloor \frac{\pi}{4}\sqrt{N} \right\rfloor$ times. This is the optimal algorithm. There is a quadratic gain in computational complexity in the transition from the quantum to the classical context. How can we put this problem in a concrete way in the quantum context? Can we write a quantum program equivalent to Algorithm 4.1?

In the quantum context, we must use a unitary operator that plays the role of function f. There is a standard method to construct a unitary operator that implements a generic function. The quantum computer must have two *registers*. The first register stores the domain points and the second stores the image points of function f. A complete description of this operator, which we will call $\mathcal{R}_f$, in the computational basis is

$$\mathcal{R}_f|x\rangle|i\rangle = |x\rangle|i \oplus f(x)\rangle, \tag{4.2}$$

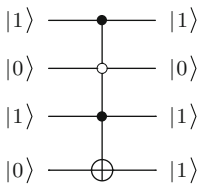

Fig. 4.1 Circuit of operator $\mathcal{R}_f$ when $x_0 = 5$. The value of x_0 determines which control bits should be *white* and which should be *black*. Only the programmer knows which quantum controls are black and white

where operation $\oplus$ is the *binary sum* or *bitwise xor*. The standard method is: repeat the value of x to guarantee *reversibility*, and perform the binary sum of the image of x with the value of the second register. For any function f, the resulting operator will be unitary. For the function of (4.1), the first register must have n qubits and second must have one qubit. If the state of the second register is $|0\rangle$, we can see that the action of $\mathcal{R}_f$ is similar to evaluating function f:

$$\mathcal{R}_f|x\rangle|0\rangle = \begin{cases} |x_0\rangle|1\rangle, & \text{if } x = x_0; \\ |x\rangle|0\rangle, & \text{otherwise.} \end{cases} \tag{4.3}$$

Now we ask a quantum programmer to implement $\mathcal{R}_f$. He uses a *generalized Toffoli gate*. For example, if $x_0 = 5$, the circuit of Fig. 4.1 implements $\mathcal{R}_f$ for $n = 3$. Note that the state of the second register will change from $|0\rangle$ to $|1\rangle$ only if the entry of the first register is 5, otherwise it remains in state $|0\rangle$.

We cannot learn any implementation details about $\mathcal{R}_f$, but we can employ this operator as many times as we wish. What is the algorithm that determines x_0 using $\mathcal{R}_f$ the least number of times?

Grover's algorithm uses a second unitary operator defined by

$$\mathcal{R}_{\mathrm{D}} = \left(2\,|\mathrm{D}\rangle\langle\mathrm{D}| - I_N\right) \otimes I_2, \tag{4.4}$$

where $|\mathrm{D}\rangle$ is the *diagonal state* of the first register (see Appendix). The *evolution operator* that performs one step of the algorithm is

$$U = \mathcal{R}_{\mathrm{D}}\,\mathcal{R}_f. \tag{4.5}$$

The initial condition is

$$|\psi_0\rangle = |\mathrm{D}\rangle|-\rangle. \tag{4.6}$$

The algorithm tells us to apply U recursively $\left\lfloor \frac{\pi}{4}\sqrt{N} \right\rfloor$ times. We measure the first register in the computational basis and the result is x_0 with probability greater than or equal to $1 - \frac{1}{N}$.

Algorithm 4.2: Grover's algorithm

Input: N and f as described in Eq (4.1).
Output: x_0 with probability greater than or equal to $1 - \frac{1}{N}$.

1. Use a 2-register quantum computer with $n + 1$ qubits;
2. Prepare the initial state $|\mathrm{D}\rangle|-\rangle$;
3. Apply U^t, where $t = \left\lfloor \frac{\pi}{4}\sqrt{N} \right\rfloor$ and U is given by (4.5);
4. Measure the first register in the computational basis.

Exercise 4.1. After discarding the second register of $\mathcal{R}_\mathrm{D}$, show that

$$\mathcal{R}_\mathrm{D} = H^{\otimes n}\left(2\,|0\rangle\langle 0| - I\right) H^{\otimes n}.$$

Sketch a circuit that implements $\mathcal{R}_\mathrm{D}$ using Hadamard gates and a generalized Toffoli gate.

4.1.1 Analysis of the Algorithm Using Reflection Operators

The evolution operator and the initial condition of Grover's algorithm have real entries. This means that the entire evolution takes place in a real vector subspace of the Hilbert space $\mathcal{H}^{2N}$. We can give a geometric interpretation to the algorithm and, in fact, visualize the evolution. The key to understanding the operations of the algorithm is to note that operator U is the product of two *reflection operators*. First we check that $\mathcal{R}_f$ is a reflection around the vector space orthogonal to the vector space spanned by $|x_0\rangle|-\rangle$. Vector $|x_0\rangle$ is in the computational basis of $\mathcal{H}^{2N}$ and the orthogonal space is spanned by the other elements in the computational basis. Consider the action of $\mathcal{R}_f$ on vector $|x_0\rangle|-\rangle$. Using (4.3), we obtain

$$\begin{aligned}\mathcal{R}_f\,|x_0\rangle|-\rangle &= \frac{\mathcal{R}_f|x_0\rangle|0\rangle - \mathcal{R}_f|x_0\rangle|1\rangle}{\sqrt{2}} \\ &= \frac{|x_0\rangle|1\rangle - |x_0\rangle|0\rangle}{\sqrt{2}} \\ &= -|x_0\rangle|-\rangle. \end{aligned} \tag{4.7}$$

Then, $\mathcal{R}_f$ reflects $|x_0\rangle|-\rangle$ around the vector space orthogonal to $|x_0\rangle|-\rangle$. Now, consider the action of $\mathcal{R}_f$ on a vector orthogonal to $|x_0\rangle|-\rangle$. Take $|x\rangle|-\rangle$, where $x \neq x_0$. Performing a calculation similar to (4.7), we conclude that

$$\mathcal{R}_f\,|x\rangle|-\rangle = |x\rangle|-\rangle, \quad x \neq x_0. \tag{4.8}$$

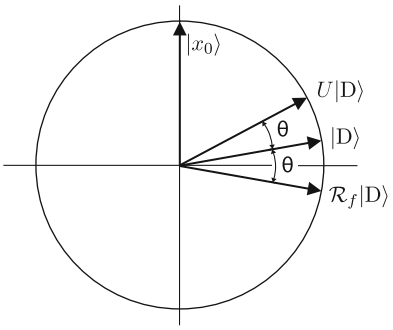

Fig. 4.2 The initial condition of Grover's algorithm is state $|\mathrm{D}\rangle$. After applying operator $\mathcal{R}_f$, state $|\mathrm{D}\rangle$ is reflected around the plane orthogonal to vector $|x_0\rangle$. After applying operator $\mathcal{R}_\mathrm{D}$, vector $\mathcal{R}_f|\mathrm{D}\rangle$ is reflected around $|\mathrm{D}\rangle$. That is, one application of U rotates the initial vector by θ degrees toward vector $|x_0\rangle$

Consider a linear combination with real coefficients of $|x_0\rangle|-\rangle$ with a vector orthogonal to $|x_0\rangle|-\rangle$. The application of $\mathcal{R}_f$ on this linear combination inverts the sign of component $|x_0\rangle|-\rangle$ and preserves the sign of the component orthogonal to $|x_0\rangle|-\rangle$. The geometric interpretation is a reflection.

$\mathcal{R}_\mathrm{D}$ is also a reflection, but around the vector space spanned by $|\mathrm{D}\rangle$. Using (4.4), we conclude that

$$\mathcal{R}_\mathrm{D}\,|\mathrm{D}\rangle|-\rangle = |\mathrm{D}\rangle|-\rangle. \tag{4.9}$$

Take a vector orthogonal to $|\mathrm{D}\rangle|-\rangle$. Using again (4.4), we conclude that the result of applying $\mathcal{R}_\mathrm{D}$ inverts the sign of this vector. Consider a linear combination with real coefficients of $|\mathrm{D}\rangle|-\rangle$ with a vector orthogonal to $|\mathrm{D}\rangle|-\rangle$. After the action of $\mathcal{R}_\mathrm{D}$, the component orthogonal to $|\mathrm{D}\rangle|-\rangle$ inverts the sign while the other remains unchanged. The geometric interpretation is a reflection around $|\mathrm{D}\rangle|-\rangle$.

It is possible to simplify the analysis of Grover's algorithm as follows: Discard the second register, because its state remains unchanged throughout the algorithm. From Fig. 4.2, we can see that the action of U on the initial state returns a vector that is in the vector space spanned by $|x_0\rangle$ and $|\mathrm{D}\rangle$. The same argument holds for future applications of U. Therefore, the entire evolution takes place in a real (two-dimensional) plane. In this case, R_f can be interpreted as a reflection on the vector space spanned by the vector orthogonal to $|x_0\rangle$, which is in the plane of the algorithm. Let us call $\left|x_0^\perp\right\rangle$ the unit vector orthogonal to $|x_0\rangle$, which is in the plane spanned by $|x_0\rangle$ and $|\mathrm{D}\rangle$ and has the smallest angle with $|\mathrm{D}\rangle$. The expression for $\left|x_0^\perp\right\rangle$ in the computational basis is

$$\left|x_0^\perp\right\rangle = \frac{1}{\sqrt{N-1}} \sum_{x \neq x_0} |x\rangle. \tag{4.10}$$

When we analyze the evolution of the algorithm in the plane spanned by vectors $|x_0\rangle$ and $|\mathrm{D}\rangle$, operator $\mathcal{R}_f$ can be replaced by

$$\mathcal{R}_{x_0^\perp} = 2\left|x_0^\perp\right\rangle\left\langle x_0^\perp\right| - I_N, \tag{4.11}$$

which keeps $\left|x_0^{\perp}\right\rangle$ unchanged and inverts the sign of a vector orthogonal to $\left|x_0^{\perp}\right\rangle$. Since we have discarded the second register, we redefine operator $\mathcal{R}_{\mathrm{D}}$ by

$$\mathcal{R}_{\mathrm{D}} = 2\,|\mathrm{D}\rangle\langle\mathrm{D}| - I_N. \tag{4.12}$$

In summary, $\mathcal{R}_{x_0^{\perp}}$ is a reflection around the vector space spanned by $\left|x_0^{\perp}\right\rangle$ and $\mathcal{R}_{\mathrm{D}}$ is a reflection around the vector space spanned by $|\mathrm{D}\rangle$. One step in the evolution is given by operator

$$U = \mathcal{R}_{\mathrm{D}}\mathcal{R}_{x_0^{\perp}}, \tag{4.13}$$

replacing the operator defined by (4.5). The initial condition is $|\mathrm{D}\rangle$.

In real vector spaces, the action of two successive reflections on a real vector $|\psi\rangle$ rotates $|\psi\rangle$ by an angle that is twice the angle between the invariant spaces. The direction of rotation depends on the application order of the reflections. In the case of $\mathcal{R}_{x_0^{\perp}}$ and $\mathcal{R}_{\mathrm{D}}$, the action of U rotates $|\psi\rangle$ by an angle that is twice the angle between $\left|x_0^{\perp}\right\rangle$ and $|\mathrm{D}\rangle$. Because $\mathcal{R}_{x_0^{\perp}}$ is applied first, the rotation angle is positive when coming from $\left|x_0^{\perp}\right\rangle$ to $|\mathrm{D}\rangle$, that is, counterclockwise.

Let $\theta/2$ be the angle between vectors $\left|x_0^{\perp}\right\rangle$ and $|\mathrm{D}\rangle$, which is the complement of the angle between $|x_0\rangle$ and $|\mathrm{D}\rangle$. So,

$$\begin{aligned}\sin\frac{\theta}{2} &= \cos\left(\frac{\pi}{2} - \frac{\theta}{2}\right)\\ &= \langle x_0|\mathrm{D}\rangle\\ &= \frac{1}{\sqrt{N}}.\end{aligned} \tag{4.14}$$

Angle θ is very small when $N \gg 1$, that is, when function f has a large domain. Solving (4.14) for θ and taking the asymptotic expansion, we obtain

$$\theta = \frac{2}{\sqrt{N}} + \frac{1}{3\,N\sqrt{N}} + O\left(\frac{1}{N^2}\right). \tag{4.15}$$

Starting from initial condition $|\mathrm{D}\rangle$, one application of U rotates $|\mathrm{D}\rangle$ approximately by $\frac{2}{\sqrt{N}}$ degrees toward $|x_0\rangle$. This is small progress, but definitely a good one, mainly because it can be repeated. In the time instant

$$t_f = \left\lfloor \frac{\pi}{4}\sqrt{N} \right\rfloor, \tag{4.16}$$

$|\mathrm{D}\rangle$ will have rotated approximately by $\frac{\pi}{2}$ radians. In fact, it will have rotated a little less, because the next term in the expansion (4.15) is positive. The angle between the final state and $|x_0\rangle$ is about $\frac{2}{\sqrt{N}}$ and is at most $\frac{\theta}{2}$. The probability of finding value x_0 when we measure the first register is

$$\begin{aligned} p_{x_0} &= \left|\langle x_0|U^{t_f}|\mathrm{D}\rangle\right|^2 \\ &\geq \cos^2\frac{\theta}{2} \\ &= 1-\frac{1}{N}. \end{aligned} \tag{4.17}$$

The lower bound for the success probability shows that Grover's algorithm has a very high success probability when N is large.

Exercise 4.2. Show algebraically that the product of reflections $\mathcal{R}_{\mathrm{D}}\mathcal{R}_{x_0^\perp}$ rotates a generic vector in the real plane spanned by $|x_0\rangle$ and $\left|x_0^\perp\right\rangle$ by angle $\theta = 2\arccos\left\langle \mathrm{D}\middle|x_0^\perp\right\rangle$.

Exercise 4.3. Using basis $\left\{|x_0\rangle, \left|x_0^\perp\right\rangle\right\}$, show that U is the rotation matrix

$$U = \begin{bmatrix} \cos\theta & \sin\theta \\ -\sin\theta & \cos\theta \end{bmatrix}.$$

What are the expressions of $\cos\theta$ and $\sin\theta$ as functions of N?

Exercise 4.4. Show that

$$U^t|\mathrm{D}\rangle = \sin\left(t\,\theta+\frac{\theta}{2}\right)|x_0\rangle + \cos\left(t\,\theta+\frac{\theta}{2}\right)\left|x_0^\perp\right\rangle.$$

Exercise 4.5. Show that the success probability in Grover's algorithm is exactly 121/128 when $N = 8$.

Exercise 4.6. Calculate the probability of Grover's algorithm returning a value x, obeying $x \neq x_0$, when $N \gg 1$. Check out that the sum of the probabilities, when we consider all cases $x \neq x_0$ and $x = x_0$, is asymptotically equal to 1.

Exercise 4.7. After discarding the second register, show that operator $\mathcal{R}_f$ given by (4.2) can be written as

$$\mathcal{R}_f = I - 2\,|x_0\rangle\langle x_0|, \tag{4.18}$$

or equivalently as

$$\mathcal{R}_f = 2\sum_{x\neq x_0}|x\rangle\langle x| - I. \tag{4.19}$$

What is the spectral decomposition of R_f?

Exercise 4.8. Show that $\mathcal{R}_f$ and $\mathcal{R}_{\mathrm{D}}$ are Hermitian and unitary operators. Can we conclude that the product $\mathcal{R}_{\mathrm{D}}\mathcal{R}_f$ is Hermitian? Show that if U is a non-Hermitian real unitary operator, then it has at least two non-real eigenvalues. If U has only two non-real eigenvalues, what is the relationship between them?

4.1.2 Analysis Using the Spectral Decomposition

Another way to analyze the evolution of Grover's algorithm is through the *spectral decomposition* of U. The characteristic polynomial of U is

$$|\lambda I - U| = (\lambda + 1)^{N-2}\left(\lambda^2 - \frac{2(N-2)}{N}\lambda + 1\right), \tag{4.20}$$

Therefore, the eigenvalues are -1 and $\mathrm{e}^{\pm \mathrm{i}\omega}$, where

$$\cos\omega = 1 - \frac{2}{N}. \tag{4.21}$$

The eigenvalue -1 has multiplicity $N-2$ and a non-orthogonal set of eigenvectors is

$$\left|\alpha_j\right\rangle = \frac{|1\rangle - |j-1\rangle}{\sqrt{2}}, \quad 3 \le j \le N, \tag{4.22}$$

assuming that the marked element is $x_0 = 0$. The remaining two eigenvectors associated with eigenvalues $\mathrm{e}^{\mathrm{i}\omega}$ and $\mathrm{e}^{-\mathrm{i}\omega}$ are, respectively,

$$|\alpha_1\rangle = \frac{1}{\sqrt{2}}\left(\left|x_0^{\perp}\right\rangle - \mathrm{i}\,|x_0\rangle\right), \tag{4.23}$$

$$|\alpha_2\rangle = \frac{1}{\sqrt{2}}\left(\left|x_0^{\perp}\right\rangle + \mathrm{i}\,|x_0\rangle\right), \tag{4.24}$$

where $\left|x_0^{\perp}\right\rangle$ is given by (4.10). The calculation of these eigenvectors is oriented in the exercises.

Eigenvectors of unitary operators associated with distinct eigenvalues are orthogonal to each other. Therefore, $|\alpha_1\rangle$ and $|\alpha_2\rangle$ are orthogonal to each other and are orthogonal to $\left|\alpha_j\right\rangle$, $3 \le j \le N$. To analyze the evolution of Grover's algorithm, we must find the expression of the initial condition $|\mathrm{D}\rangle$ in the eigenbasis of U. Using (4.22), we check that $|\mathrm{D}\rangle$ is orthogonal to $\left|\alpha_j\right\rangle$, for $3 \le j \le N$. Therefore, the initial condition is in the vector space spanned by $|\alpha_1\rangle$ and $|\alpha_2\rangle$. So

$$|\mathrm{D}\rangle = a\,|\alpha_1\rangle + a^*\,|\alpha_2\rangle, \tag{4.25}$$

where

$$\begin{aligned} a &= \langle\alpha_1|\mathrm{D}\rangle \\ &= \frac{\sqrt{N-1}+\mathrm{i}}{\sqrt{2N}}. \end{aligned} \tag{4.26}$$

The entire evolution of the algorithm takes place in the vector space spanned by $|\alpha_1\rangle$ and $|\alpha_2\rangle$. The application of U^t on state $|\mathrm{D}\rangle$ given by (4.25) can be calculated explicitly, because $|\alpha_1\rangle$ and $|\alpha_2\rangle$ are eigenvectors of U with eigenvalues $\mathrm{e}^{\pm \mathrm{i}\omega}$. Therefore, at time t, the state of the quantum computer is

$$U^t|\mathrm{D}\rangle = a\,\mathrm{e}^{\mathrm{i}\omega t}\,|\alpha_1\rangle + a^*\mathrm{e}^{-\mathrm{i}\omega t}\,|\alpha_2\rangle. \tag{4.27}$$

By design, the iterative applications of operator U rotate the state of the quantum computer toward state $|x_0\rangle$, which is almost orthogonal to the initial state $|\mathrm{D}\rangle$ when N is large. For $t_f = \pi/2\omega$, we have $\mathrm{e}^{\mathrm{i}\omega t_t} = \mathrm{i}$ and $\mathrm{e}^{-\mathrm{i}\omega t_f} = -\mathrm{i}$, that is,

$$U^{t_f}|\mathrm{D}\rangle = \mathrm{i}\left(a\,|\alpha_1\rangle - a^*\,|\alpha_2\rangle\right) \tag{4.28}$$

which is orthogonal to $|\mathrm{D}\rangle$. This is the first value of t such that $U^t|\mathrm{D}\rangle$ is orthogonal to $|\mathrm{D}\rangle$.

Using the above equation for $U^{t_f}|\mathrm{D}\rangle$, and (4.23), (4.24), and (4.26), the measurement of the first register in the computational basis returns x_0 with probability

$$\begin{aligned} p_{x_0}(t_f) &= \left|\langle x_0|U^{t_f}|\mathrm{D}\rangle\right|^2 \\ &= 1 - \frac{1}{N}. \end{aligned} \tag{4.29}$$

Because the number of applications of U must be an integer, we must take $\lfloor \pi/2\omega \rfloor$ as the stopping time. Using (4.21) and taking the *asymptotic expansion* in N, we obtain

$$\begin{aligned} \lfloor t_f \rfloor &= \left\lfloor \frac{\pi}{2\arccos\left(1-\frac{2}{N}\right)} \right\rfloor \\ &= \left\lfloor \frac{\pi}{4}\sqrt{N} \right\rfloor + O\left(\frac{1}{\sqrt{N}}\right). \end{aligned} \tag{4.30}$$

Expression (4.29) is a lower bound for $p_{x_0}(\lfloor t_f \rfloor)$.

Exercise 4.9. Show that the entries of matrix $\mathcal{R}_f$ given in (4.18) are $(\mathcal{R}_f)_{ij} = (-1)^{\delta_{ix_0}}\delta_{ij}$ and for matrix $\mathcal{R}_\mathrm{D}$ given by (4.12) are $(\mathcal{R}_\mathrm{D})_{ij} = \frac{2}{N} - \delta_{ij}$. Show that the entries of U are

$$U_{ij} = (-1)^{\delta_{jx_0}}\left(\frac{2}{N} - \delta_{ij}\right).$$

Exercise 4.10. Using Exercise 4.9, show that the characteristic polynomial of U is given by (4.20). Show that the eigenvalues are -1 and $\mathrm{e}^{\pm \mathrm{i}\omega}$, where $\omega = \arccos\left(1 - \frac{2}{N}\right)$.

Exercise 4.11. Use matrix U given in Exercise 4.9 to show that if the marked element is $x_0 = 0$, then matrix $U + I$ is given by

$$U + I = \begin{bmatrix} \frac{2(N-1)}{N} & \frac{2}{N} & \cdots & \frac{2}{N} \\ -\frac{2}{N} & \frac{2}{N} & \cdots & \frac{2}{N} \\ \vdots & \vdots & \ddots & \vdots \\ -\frac{2}{N} & \frac{2}{N} & \cdots & \frac{2}{N} \end{bmatrix}.$$

By inspecting the entries of $U + I$, obtain a basis for the eigenspace associated with eigenvalue -1. Show that vectors $|\alpha_j\rangle$ described in (4.22) is a basis for this eigenspace. Generalize this description to a generic marked element x_0, and show that the subspace spanned by these vectors does not play any role in the dynamics of the algorithm.

Exercise 4.12. The complex eigenvectors of U can be obtained by noting that the x_0-th column of U has a role different from the other columns, which follow the systematic pattern of Grover's operator $\mathcal{R}_{\mathrm{D}}$. An *Ansatz* to find these eigenvectors is a vector that has the same entries, except at position x_0, that is, to take $|\alpha\rangle$ such that $\langle j|\alpha\rangle = b$, for $j \neq x_0$ and $\langle x_0|\alpha\rangle = a$. Find a and b such that $(U - \mathrm{e}^{\pm \mathrm{i}\omega} I)|\alpha\rangle = 0$ and each $|\alpha\rangle$ is a unit vector.

Exercise 4.13. Find an expression for $p_{x_0}(t)$ for a generic (non-integer) t and show that the first maximum point is

$$t_{\max} = \frac{\arctan \sqrt{N-1}}{\omega}.$$

Verify that the stopping time with the best chance of success is the integer closest to $t_{\max}$. Taking the asymptotic expansion in N, show that a lower bound for this probability is $1 - \frac{1}{N}$. Show that the state of the quantum computer is $|x_0\rangle$ at time $t_{\max}$.

4.1.3 Comparison Analysis

We have described two ways to analyze the evolution of Grover's algorithm. In first one, we use the fact that U is a real operator and the product of two reflections. U can be seen as a rotation matrix in a two-dimensional vector space, the rotation angle of which is twice the angle between the vectors that are invariant under the action of the reflection operators. The marked state $|x_0\rangle$ and initial condition $|\mathrm{D}\rangle$ are almost orthogonal when N is large. The strategy of the algorithm is to rotate

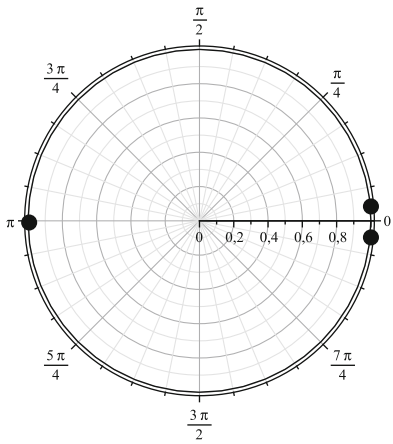

Fig. 4.3 Eigenvalues of the evolution operator of Grover's algorithm for $n = 9$

the initial condition by $\pi/2$ radians and to measure in the computational basis at this point. Since the angle between the final state and the marked state is small, the probability of obtaining x_0 as a result of the measurement is close to 1. The analysis of the algorithm evolution employs a real subspace of the Hilbert space. This analysis is quite attractive for its simplicity but does not have the same degree of generality as the second analysis.

In the second analysis, we use the spectral decomposition of U. The entire evolution is happening in eigenspace spanned by two eigenvectors, which are the only non-real eigenvectors. By definition, the eigenvectors do not rotate under the action of U. However, the initial condition is a linear combination of the two eigenvectors and the coefficients change under the action of U. The strategy is equal to the first case, that is, rotating the initial condition by $\pi/2$ radians. While the first case has an appealing geometric interpretation, the second case allows one to extend the idea behind Grover's algorithm to other search algorithms, in particular, to the *abstract search algorithm*, which aims to find a specially marked vertex in a graph.

To help understand the *abstract search algorithm*, which will be addressed in Chap. 8, let us look at some details of the spectral decomposition of U used in Grover's algorithm. Figure 4.3 shows the geometric configuration of the eigenvalues of U for $N = 512$. The non-real eigenvalues are in symmetrical locations and approach to 1 when N increases. Although they are close, the associated eigenvectors are orthogonal. Note that U does not have eigenvalue 1. If the initial state would have had a large overlap with eigenspace associated with eigenvalue 1, the algorithm would not have worked as desired, because we would not have rotated the initial state by $\pi/2$ radians. Therefore, it is necessary that the initial state has no overlap with eigenspace associated with an eigenvalue 1 of U. In Grover's algorithm, this is true, let us say, by default. This does not happen necessarily in abstract search algorithms. An important detail is that the initial state $|\mathrm{D}\rangle$ is an eigenvector with eigenvalue 1 of operator $\mathcal{R}_{\mathrm{D}}$. This fact plays a key role in the characterization of an abstract search algorithm.

4.2 Optimality of Grover's Algorithm

Grover's algorithm finds the marked element by querying the oracle $O\left(\sqrt{N}\right)$ times. Is it possible to develop an algorithm faster than Grover's algorithm? In this section, we show that Grover's algorithm is *optimal*, that is, no quantum algorithm can find the marked element with less than $\Omega\left(\sqrt{N}\right)$ queries of f using space $O(n)$ and with success probability greater than or equal to $1/2$.

This type of proof should be as generic as possible. We use the standard quantum computing model in which a generic algorithm is a sequence of unitary operators acting iteratively, starting with some initial condition, followed by a measurement at the end. We want to show that: if the oracle is queried less than $\Omega\left(\sqrt{N}\right)$ times, the marked element is not found. Let us assume that the oracle form is $\mathcal{R}_f = I - 2|x_0\rangle\langle x_0|$ as given in (4.18), where x_0 is the marked element. This is not a restriction, because the oracle must somehow distinguish the marked element, and in order to allow other forms of oracles, let us allow the use of any unitary operators U_a and U_b that transform $\mathcal{R}_f$ to $U_a\mathcal{R}_f U_b$ during the execution of the algorithm. More than that, U_a and U_b may change at each step.

Let $|\psi_0\rangle$ be the initial state. The state of the quantum computer after t steps is given by

$$|\psi_t\rangle = U_t\mathcal{R}_f \cdots U_1\mathcal{R}_f U_0|\psi_0\rangle, \tag{4.31}$$

where $U_1, \ldots, U_t$ are generic unitary operators, which are applied to each step after the oracle. There is no restriction on the efficiency of these operators.

The strategy of the proof is to compare state $|\psi_t\rangle$ with state

$$|\phi_t\rangle = U_t \cdots U_0|\psi_0\rangle, \tag{4.32}$$

that is, the equivalent state without the application of the oracles. To make this comparison, we define the quantity

$$D_t = \frac{1}{N}\sum_{x_0=0}^{N-1} \big\||\psi_t\rangle - |\phi_t\rangle\big\|^2, \tag{4.33}$$

which measures the deviation between $|\psi_t\rangle$ and $|\phi_t\rangle$ after t steps. The sum in x_0 is to average over all possible values of x_0 in order to avoid favoring any particular value. Note that $|\psi_t\rangle$ depends on x_0 and, in principle, $|\phi_t\rangle$ does not so depend. If D_t is too small after t steps, we cannot distinguish the marked element.

We will show that the following inequalities are valid:

$$c \leq D_t \leq \frac{4t^2}{N}, \tag{4.34}$$

where c is a strictly positive constant. From this result we can conclude that if we take the number of steps t with a functional dependence in N smaller than $\Omega\left(\sqrt{N}\right)$, for example, $N^{\frac{1}{4}}$, the first inequality is violated. This means that D_t is not big

enough to allow us to distinguish the marked element. In the asymptotic limit, the violation of this inequality is more dramatic showing that, for this number of steps, a sequence of operators that distinguishes the marked element is equivalent to a sequence that does not so distinguish.

Let us start with inequality $D_t \leq 4t^2/N$. This inequality is valid for $t = 0$. Using the method of proof by induction, we assume that the inequality is valid for t and show that it will be valid for $t + 1$. Note that

$$\begin{aligned} D_{t+1} &= \frac{1}{N}\sum_{x_0=0}^{N-1} \left\| U_{t+1}\mathcal{R}_f|\psi_t\rangle - U_{t+1}|\phi_t\rangle \right\|^2 \\ &= \frac{1}{N}\sum_{x_0=0}^{N-1} \left\| \mathcal{R}_f|\psi_t\rangle - |\phi_t\rangle \right\|^2 \\ &= \frac{1}{N}\sum_{x_0=0}^{N-1} \left\| \mathcal{R}_f(|\psi_t\rangle - |\phi_t\rangle) + (R_f - I)|\phi_t\rangle \right\|^2. \end{aligned} \tag{4.35}$$

Using the square of the *triangle inequality*

$$\left\| |\alpha\rangle + |\beta\rangle \right\|^2 \leq \left\| |\alpha\rangle \right\|^2 + 2\,\||\alpha\rangle\|\,\||\beta\rangle\| + \left\| |\beta\rangle \right\|^2, \tag{4.36}$$

where

$$|\alpha\rangle = \mathcal{R}_f(|\psi_t\rangle - |\phi_t\rangle)$$

and

$$\begin{aligned} |\beta\rangle &= (R_f - I)|\phi_t\rangle \\ &= -2\,\langle x_0|\phi_t\rangle\,|x_0\rangle, \end{aligned}$$

we obtain

$$\begin{aligned} D_{t+1} \leq \frac{1}{N}\sum_{x_0=0}^{N-1} \Big(&\left\| |\psi_t\rangle - |\phi_t\rangle \right\|^2 + 4\left\| |\psi_t\rangle - |\phi_t\rangle \right\| \,|\langle x_0|\phi_t\rangle| \\ &+ 4\,|\langle x_0|\phi_t\rangle|^2 \Big). \end{aligned} \tag{4.37}$$

Using the *Cauchy–Schwarz inequality*

$$|\langle\alpha|\beta\rangle| \leq \||\alpha\rangle\|\,\||\beta\rangle\| \tag{4.38}$$

in the second term of inequality (4.37), where

$$|\alpha\rangle = \sum_{x_0=0}^{N-1} \left\| |\psi_t\rangle - |\phi_t\rangle \right\| |x_0\rangle$$

and

$$|\beta\rangle = \sum_{x_0=0}^{N-1} \left|\langle x_0|\phi_t\rangle\right| \, |x_0\rangle$$

and also using the fact that

$$\sum_{x_0=0}^{N-1} \left|\langle x_0|\phi_t\rangle\right|^2 = \langle \phi_t|\phi_t\rangle = 1,$$

we obtain

$$\begin{aligned} D_{t+1} &\leq D_t + \frac{4}{N}\left(\sum_{x_0=0}^{N-1} \big\||\psi_t\rangle - |\phi_t\rangle\big\|^2\right)^{\frac{1}{2}} \left(\sum_{x_0'=0}^{N-1} \left|\langle x_0'|\phi_t\rangle\right|^2\right)^{\frac{1}{2}} + \frac{4}{N} \\ &\leq D_t + 4\sqrt{\frac{D_t}{N}} + \frac{4}{N}. \end{aligned} \tag{4.39}$$

Since we are assuming that $D_t \leq 4\,t^2/N$ from the inductive hypothesis, we obtain $D_{t+1} \leq 4\,(t+1)^2/N$.

We will now show the harder inequality $c \leq D_t$. Let us define two new quantities given by

$$E_t = \frac{1}{N}\sum_{x_0=0}^{N-1} \big\||\psi_t\rangle - |x_0\rangle\big\|^2, \tag{4.40}$$

$$F_t = \frac{1}{N}\sum_{x_0=0}^{N-1} \big\||\phi_t\rangle - |x_0\rangle\big\|^2. \tag{4.41}$$

We obtain an inequality involving D_t, E_t, and F_t as follows:

$$\begin{aligned} D_t &= \frac{1}{N}\sum_{x_0=0}^{N-1} \Big\| \left(|\psi_t\rangle - |x_0\rangle\right) + \left(|x_0\rangle - |\phi_t\rangle\right) \Big\|^2 \\ &\geq E_t + F_t - \frac{2}{N}\sum_{x_0=0}^{N-1} \big\||\psi_t\rangle - |x_0\rangle\big\| \, \big\||\phi_t\rangle - |x_0\rangle\big\| \\ &\geq E_t + F_t - 2\sqrt{E_t\,F_t} \\ &= \left(\sqrt{F_t} - \sqrt{E_t}\right)^2, \end{aligned} \tag{4.42}$$

where, in the first inequality, we use the square of the *reverse triangle inequality*

$$\big\||\alpha\rangle + |\beta\rangle\big\|^2 \geq \big\||\alpha\rangle\big\|^2 - 2\,\||\alpha\rangle\|\,\||\beta\rangle\| + \big\||\beta\rangle\big\|^2 \tag{4.43}$$

and, in the second inequality, we use the Cauchy–Schwarz inequality with vectors

$$|\alpha\rangle = \sum_{x_0=0}^{N-1} \big\||\psi_t\rangle - |x_0\rangle\big\|\ |x_0\rangle,$$

$$|\beta\rangle = \sum_{x_0=0}^{N-1} \big\||\phi_t\rangle - |x_0\rangle\big\|\ |x_0\rangle.$$

We now show that

$$F_t \geq 2 - 2\frac{1}{\sqrt{N}}.$$

Define θ_{x_0} as the phase of $\langle x_0|\phi_t\rangle$, that is,

$$\langle x_0|\phi_t\rangle = \mathrm{e}^{\mathrm{i}\theta_{x_0}}\,\big|\langle x_0|\phi_t\rangle\big|\,.$$

Define the state

$$|\theta\rangle = \frac{1}{\sqrt{N}} \sum_{x_0=0}^{N-1} \mathrm{e}^{\mathrm{i}\theta_{x_0}} |x_0\rangle. \tag{4.44}$$

So,

$$\begin{aligned}\langle\theta|\phi_t\rangle &= \frac{1}{\sqrt{N}} \sum_{x_0=0}^{N-1} \mathrm{e}^{-\mathrm{i}\theta_{x_0}}\,\langle x_0|\phi_t\rangle \\ &= \frac{1}{\sqrt{N}} \sum_{x_0=0}^{N-1} \big|\langle x_0|\phi_t\rangle\big|\,. \end{aligned} \tag{4.45}$$

Using the Cauchy–Schwarz inequality, we obtain $\big|\langle\theta|\phi_t\rangle\big| \leq 1$, and

$$\sum_{x_0=0}^{N-1} \big|\langle x_0|\phi_t\rangle\big| \leq \sqrt{N}. \tag{4.46}$$

To reach the desired result, we use the above inequality and the fact that the real part of $\langle x_0|\phi_t\rangle$ is smaller than or equal to $\big|\langle x_0|\phi_t\rangle\big|$:

$$
\begin{aligned}
F_t &= \frac{1}{N}\sum_{x_0=0}^{N-1} \big\| |\phi_t\rangle - |x_0\rangle \big\|^2 \\
&= 2 - \frac{2}{N}\sum_{x_0=0}^{N-1} \mathrm{Re}\left\{\langle x_0|\phi_t\rangle\right\} \\
&\geq 2 - \frac{2}{N}\sum_{x_0=0}^{N-1} \left|\langle x_0|\phi_t\rangle\right| \\
&\geq 2 - \frac{2}{\sqrt{N}}.
\end{aligned} \tag{4.47}
$$

Now we show that $E_t \leq (2-\sqrt{2})$. After t steps, the state of the quantum computer after the application of the oracles is $|\psi_t\rangle$. Similar to the calculation used for F_t, we have

$$
\begin{aligned}
E_t &= \frac{1}{N}\sum_{x_0=0}^{N-1} \big\| |\psi_t\rangle - |x_0\rangle \big\|^2 \\
&= 2 - \frac{2}{N}\sum_{x_0=0}^{N-1} \mathrm{Re}\left\{\langle x_0|\psi_t\rangle\right\}.
\end{aligned}
$$

Let us assume that the probability of a measurement to return value x_0 is greater than or equal to $1/2$, that is, $\left|\langle x_0|\psi_t\rangle\right|^2 \geq 1/2$ for all x_0. Value $1/2$ is arbitrary. In fact, we can choose any fixed value between 0 and 1, see Exercise 4.14. Instead of using the computational basis, we use basis $\{e^{i\alpha_0}|0\rangle, \ldots, e^{i\alpha_{N-1}}|N-1\rangle\}$, where α_{x_0} for $0 \leq x_0 < N$ is defined as the phase of $\langle x_0|\psi_t\rangle$. This basis transformation does not change the inequalities that we have obtained so far and it does not change measurement results either. In this new basis (tilde basis), $\langle \tilde{x}_0|\psi_t\rangle$ is a real number, that is, $\mathrm{Re}\left\{\langle \tilde{x}_0|\psi_t\rangle\right\} = |\langle \tilde{x}_0|\psi_t\rangle|$. Therefore,

$$
\begin{aligned}
E_t &= 2 - \frac{2}{N}\sum_{x_0=0}^{N-1} \left|\langle \tilde{x}_0|\psi_t\rangle\right| \\
&\leq 2 - \frac{2}{N}\sum_{x_0=0}^{N-1} \frac{1}{\sqrt{2}} \\
&= 2 - \sqrt{2}.
\end{aligned} \tag{4.48}
$$

Using inequalities $E_t \leq (2-\sqrt{2})$ and $F_t \geq 2 - 2/\sqrt{N}$, we obtain

$$
\begin{aligned}
D_t &\geq \left(\sqrt{F_t} - \sqrt{E_t}\right)^2 \\
&\geq \left(\sqrt{2 - \frac{2}{\sqrt{N}}} - \sqrt{2 - \sqrt{2}}\right)^2 \\
&= \left(\sqrt{2} - \sqrt{2 - \sqrt{2}}\right)^2 + O\left(\frac{1}{\sqrt{N}}\right). \qquad (4.49)
\end{aligned}
$$

This completes the proof of inequality $c \leq D_t$ for N large enough. Constant c must obey

$$0 < c < \left(\sqrt{2} - \sqrt{2 - \sqrt{2}}\right)^2.$$

We conclude that an algorithm that is able to find the marked element must obey the inequalities (4.34). Therefore, $cN \leq 4t^2$ or equivalently $t = \Omega\left(\sqrt{N}\right)$. This result implies that the computational complexity of Grover's algorithm is $\Theta\left(\sqrt{N}\right)$ in terms of the number of queries.

Exercise 4.14. Show that if the probability of measurement to return value x_0 is greater than or equal to p, then the value of constant c must obey

$$0 < c < \left(\sqrt{2} - \sqrt{2 - 2\sqrt{p}}\right)^2.$$

To achieve a success probability close to 1, the algorithm must be run $1/p$ times. Since p is constant, this does not change the total cost of $\Omega\left(\sqrt{N}\right)$.

Exercise 4.15. Instead of assuming that $\left|\langle x_0 | \psi_t \rangle\right|^2 \geq \frac{1}{2}$ for all x_0, suppose that the uniform average probability is greater than or equal to $1/2$. Show that one still needs to query the oracle $\Omega\left(\sqrt{N}\right)$ times.

Exercise 4.16. In (4.31) and (4.32), unitary operators $U_0, \ldots, U_t$ can also distinguish the marked element. Is the proof valid if $U_i = U_i' \mathcal{R}_f$ for all i?

Exercise 4.17. What is the value of $\left\| |\alpha\rangle - |\beta\rangle \right\|^2$ for orthogonal states $|\alpha\rangle$ and $|\beta\rangle$? Can you give an interpretation for F_t and explain why it is so close to 2? Is it important that E_t be smaller than 2?

4.3 Search with Repeated Elements

In Sect. 4.1, we have described Grover's algorithm which solves the following problem: Given a Boolean function f, the domain of which is $\{0, \ldots, N-1\}$, where $N = 2^n$ for some positive integer n, find the element x_0 such that $f(x_0) = 1$

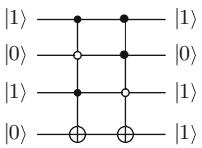

Fig. 4.4 Circuit that implements the case $f(5) = 1$ and $f(6) = 1$. Only the quantum programmer knows where the *black* and *white* controls are. However, we know how many Toffoli gates were used: it is m

assuming that x_0 is the only domain point with image equal to 1. In this section, we address a more general problem. Suppose that function f is a Boolean function as before, but m domain points have image equal to 1. The case $m = 1$ is equal to the previous case. Suppose M is the set of points whose images are equal to 1. The problem is to find an element in M with the least number of queries to function f. If we compare this problem with database searching, we have a database with repeated elements. We can put this problem into a concrete form, as we did in the beginning of Sect. 4.1. We ask a quantum programmer to choose m points in the domain of f without telling us which are the points. We know m, but we do not know the points. For example, if he chooses points 5 and 6, he will use two *generalized Toffoli gates*, as shown in the circuit of Fig. 4.4. Note that the state of the second register will change from $|0\rangle$ to $|1\rangle$ only if the input of the first register is 5 or 6, otherwise the state remains unchanged.

The optimal quantum algorithm that solves this problem is a straightforward extension of Grover's algorithm. As before, we use two registers with $n + 1$ qubits together. The form of operator $\mathcal{R}_f$ is equal to the one described in (4.2), but it returns m values equal to 1 in the second register, while the previous operator returned a single value. Operator $\mathcal{R}_{\mathrm{D}}$ is exactly the same as in (4.4). Each step is driven by $U = \mathcal{R}_{\mathrm{D}}\mathcal{R}_f$ and the initial condition is given by (4.6), as in Grover's algorithm. The number of times operator U is applied changes to $\left\lfloor \frac{\pi}{4}\sqrt{\frac{N}{m}} \right\rfloor$. The algorithm finishes when we measure the first register in the computational basis and the result is an element in M with probability greater than or equal to $1 - \frac{m}{N}$.

4.3.1 Analysis Using Reflection Operators

The analysis of the algorithm can be performed as follows: Consider a subspace of dimension m spanned by vectors $|x\rangle$, $x \in M$. State

$$|M\rangle = \frac{1}{\sqrt{m}} \sum_{x \in M} |x\rangle \tag{4.50}$$

is in this space. It replaces vector $|x_0\rangle$ when the number of marked elements is greater than 1. Define vector $\left|M^{\perp}\right\rangle$ orthogonal to $|M\rangle$ as

$$\left|M^{\perp}\right\rangle = \frac{1}{\sqrt{n-m}} \sum_{x \notin M} |x\rangle. \tag{4.51}$$

The entire algorithm takes place in the two-dimensional vector space spanned by $|M\rangle$ and $\left|M^{\perp}\right\rangle$. In the first-register Hilbert space $\mathcal{H}^N$, operator $\mathcal{R}_f$ has an expression similar to the expression given in (4.11), that is,

$$\mathcal{R}_{M^{\perp}} = 2\left|M^{\perp}\right\rangle\left\langle M^{\perp}\right| - I_N. \tag{4.52}$$

The same geometric interpretation used in Grover's algorithm applies here, but the angle between $\left|M^{\perp}\right\rangle$ and $|\mathrm{D}\rangle$ is

$$\begin{aligned} \frac{\theta}{2} &= \arcsin\left(\left\langle M\middle|\mathrm{D}\right\rangle\right) \\ &= \sqrt{\frac{m}{N}} + O\left(\frac{1}{N}\right), \end{aligned} \tag{4.53}$$

when $N \gg m$. This result explains why the number of steps of the algorithm is $t_f = \left\lfloor \frac{\pi}{4}\sqrt{\frac{N}{m}} \right\rfloor$. The success probability can be calculated in the same way as before

$$\begin{aligned} p_M &\geq \cos^2\left(\frac{\theta}{2}\right) \\ &= 1 - \frac{m}{N}. \end{aligned} \tag{4.54}$$

Exercise 4.18. Show that the generalization of Exercise 4.4 when f has M marked elements is

$$U^t|\mathrm{D}\rangle = \sin\left(t\,\theta + \frac{\theta}{2}\right)|M\rangle + \cos\left(t\,\theta + \frac{\theta}{2}\right)\left|M^{\perp}\right\rangle,$$

where θ is given by (4.53). From this expression, find the best stopping point t_f for the algorithm and show that the success probability p_M obeys (4.54).

Exercise 4.19. What is the computational complexity in terms of the number of queries of function f of the best *classical algorithm* that finds an element in set M with probability $p \geq \frac{1}{2}$.

Exercise 4.20. Show that if $m = \frac{N}{2}$, a marked element is found with probability 1 in a single iteration. Find the best value of the success probability when $m = \frac{N}{4}$.

Exercise 4.21. Suppose that someone measures the first register after r steps. Show that the probability of finding a marked element is

$$\sin^2\left((2r+1)\arcsin\sqrt{\frac{m}{N}}\right).$$

4.3.2 Analysis Using the Spectral Decomposition

The spectral decomposition of U when there is more than one marked element is a straightforward generalization. The characteristic polynomial becomes

$$|\lambda I - U| = (\lambda+1)^{N-m-1}(\lambda-1)^{m-1}\left(\lambda^2 - 2\left(1-\frac{2m}{N}\right)\lambda + 1\right), \tag{4.55}$$

Therefore, the eigenvalues are ± 1 and $\mathrm{e}^{\pm \mathrm{i}\omega}$, where

$$\cos\omega = 1 - \frac{2m}{N}. \tag{4.56}$$

The general structure of the analysis is the same when m is greater than 1. The initial condition is in the vector space spanned by eigenvectors associated with eigenvalues $\mathrm{e}^{\pm \mathrm{i}\omega}$. The number of iterations of the algorithm is $\lfloor \pi/2\omega \rfloor$. Since the expression of ω is now given by (4.56), the number of iterations becomes

$$\begin{aligned} t_f &= \left\lfloor \frac{\pi}{2\arccos\left(1-\frac{2m}{N}\right)} \right\rfloor \\ &= \left\lfloor \frac{\pi}{4}\sqrt{\frac{N}{m}} \right\rfloor + O\left(\frac{1}{\sqrt{N}}\right) \end{aligned} \tag{4.57}$$

when $N \gg m$.

The details of the analysis and the calculation of a lower bound for the success probability are oriented in the following exercises.

Exercise 4.22. Obtain (4.55).

Exercise 4.23. Show that the eigenvectors of U associated with the eigenvalues $\mathrm{e}^{\pm \mathrm{i}\omega}$ are

$$\frac{|M^\perp\rangle \mp \mathrm{i}|M\rangle}{\sqrt{2}},$$

where $|M\rangle$ and $|M^\perp\rangle$ are defined in (4.50) and (4.51), respectively. Show that the initial condition $|\mathrm{D}\rangle$ is in the space spanned by these eigenvectors.

Exercise 4.24. Show that $U^t|\mathrm{D}\rangle$ is orthogonal to $|\mathrm{D}\rangle$ for $t = \frac{\pi}{2\omega}$.

Exercise 4.25. Show that

$$p_M(t) = \left(\sqrt{\frac{M}{N}}\cos(\omega t) + \sqrt{1-\frac{M}{N}}\sin(\omega t)\right)^2$$

for a generic (non-integer) t and show that the first maximum point is given by

$$t_{\max} = \frac{\arctan\sqrt{\frac{N}{M}-1}}{\omega}.$$

Show that in the time instant $t_{\max}$ the state of the quantum computer is in the subspace spanned by the marked elements. Show that this state is $|M\rangle = \frac{1}{\sqrt{m}}\sum_{x\in M}|x\rangle$. Considering the integer nearest to the maximum point as the stopping time, show that the probability of finding a marked element is bounded below by $1-\frac{m}{N}$, asymptotically.

Exercise 4.26. Analyze the algorithm when $m \geq \frac{N}{2}$. What happens to the number of steps and the success probability? Can we efficiently solve this problem with a classical algorithm?

4.4 Amplitude Amplification

The technique called *amplitude amplification* used in quantum algorithms is contrasted with the technique called *probability amplification* used in classical randomized algorithms. An algorithm is said to be randomized if, during its execution, it chooses a path randomly, usually employing a *random number generator*. The algorithm can output different values in two separate rounds, using the same input on each round. For example, a randomized algorithm that outputs a factor of number N may return 3 when $N = 15$ and, in a second round with the same input, may return 5. This never happens in a deterministic algorithm. One of the reasons we need randomized algorithms is that in some problems in which we are faced with several options, it is best to take a random decision instead of spending time analyzing what is the best option.

The two most common classes of randomized algorithms are *Monte Carlo* and *Las Vegas algorithms*. A brief description of these classes is as follows: Monte Carlo algorithms always return an output in a finite pre-determined time, but it may be wrong. The probability of correct response may be small. Las Vegas algorithms return a correct output or an error message, but the running time may be long or infinite. It is usually required that the expected running time is finite. Monte Carlo

algorithms can be converted into Las Vegas algorithms, if a procedure is known that checks whether outputs are correct. Las Vegas algorithms can be converted into Monte Carlo algorithms using the *Markov inequality*.[1]

We will deal with the class of Monte Carlo algorithms. Let p be the probability of returning the correct value. If a procedure that checks the correctness of the output is known, then we can amplify the success probability by running the algorithm many times with the same input each time. We have a collection of outputs and we want to be sure that the correct result is in there. If the algorithm runs n times, the probability of returning a wrong result every time is $(1-p)^n$. Therefore, the probability of returning at least one correct result is $1-(1-p)^n$. This probability is approximately np, if $p \ll 1$. In order to achieve a success probability close to 1, we must take $n = 1/p$ as a first approximation. To analyze the complexity of a Monte Carlo algorithm that returns the correct output with probability p, we must multiply the runtime by a factor $1/p$. If p does not depend on the parameters that measure the input size, then the factor $1/p$ does not change the time complexity. Otherwise, this factor must be considered.

In the quantum case, we amplify amplitudes and consequently the number of rounds is $1/\sqrt{p}$, that is, quadratically smaller compared with the method of probability amplification. In general terms, the method of amplitude amplification can be described as follows: Suppose we have a function $f : \{0,1\}^n \to \{0,1\}$ and know a unitary operator A such that, if we measure the qubits in the computational basis when they are in state $A|\psi_{\text{in}}\rangle$, we obtain a marked element with probability p, where $|\psi_{\text{in}}\rangle$ is the initial state of algorithm A. A marked element x is a point in the domain of f such that $f(x) = 1$. Using f, we can build operator U_f possibly using some extra register, the action of which is

$$U_f|x\rangle = (-1)^{f(x)}|x\rangle. \tag{4.58}$$

There is a quantum procedure that allows us to find a marked element using $O(1/\sqrt{p})$ applications of U_f, with probability approaching 1 when $n \to \infty$. The *amplitude–amplification algorithm* is: Apply U^{t_f} to state $|\psi\rangle$ and measure in the computational basis, where $t_f = \lfloor \pi/4\sqrt{p} \rfloor$, $|\psi\rangle = A|\psi_{\text{in}}\rangle$, and

$$U = (2\,|\psi\rangle\langle\psi| - I)\,U_f.$$

Grover's algorithm and its generalization are the simplest examples that employ the method of amplitude amplification. In this case, operator A is $H^{\otimes n}$, $|\psi_{\text{in}}\rangle$ is $|0\rangle^{\otimes n}$, and $A|0\rangle^{\otimes n}$ is $|\mathrm{D}\rangle$. If we measure the qubits in state $|\mathrm{D}\rangle$ in the computational basis, we obtain a marked element with probability m/N. Therefore, the number of applications of U_f to find a marked element is $O(\sqrt{m/N})$.

[1] Markov's inequality provides an upper bound for the probability that a nonnegative function of a random variable is greater than or equal to some positive constant.

We can provide other examples and at the same time deepen our understanding about the choice $A = H^{\otimes n}$ in Grover's algorithm. Note that

$$\mathcal{R}_{\mathrm{D}} = H^{\otimes n} R_0 H^{\otimes n}, \tag{4.59}$$

where $R_0 = 2|0\rangle\langle 0| - I$, see Exercise 4.1. Can we generalize Grover's algorithm by using a generic operator A in place of $H^{\otimes n}$? The answer is positive if the new version of Grover's algorithm has an evolution operator that is the product of two reflection operators. Operator $\mathcal{R}_{\mathrm{D}}$ is a reflection around vector $|\mathrm{D}\rangle$, which is obtained by applying $H^{\otimes n}$ to $|0\rangle$. If we replace $H^{\otimes n}$ by A, the new operator, which we will call $\mathcal{R}_\psi$, is defined as

$$\mathcal{R}_\psi = A R_0 A^\dagger \tag{4.60}$$

and state $|\psi\rangle$ is defined as

$$|\psi\rangle = A|0\rangle. \tag{4.61}$$

$\mathcal{R}_\psi$ is a reflection operator around vector $|\psi\rangle$. The proof is left as Exercise 4.27. Note that operator A need not be real, as we have been considering so far. The analysis of the algorithm by means of reflections around a real plane is preserved. The choice $A = H^{\otimes n}$ is the simplest one and means that all solutions will be equally considered, that is, with the same real amplitude. This choice is not the most general one, and in any case, it is a straightforward application of the method of amplitude amplification.

The analysis of the *amplitude–amplification algorithm* is very similar to the analysis of the generalized version of Grover's algorithm. Let us disregard the extra register, which is necessary to implement operator U_f, but plays a minor role in the analysis of the algorithm. Suppose that

$$|\psi\rangle = \sum_{x\in\{0,1\}^n} \alpha_x |x\rangle \tag{4.62}$$

and define

$$p_0 = \sum_{f(x)=0} |\alpha_x|^2, \tag{4.63}$$

$$p_1 = \sum_{f(x)=1} |\alpha_x|^2. \tag{4.64}$$

We have $p_0 + p_1 = 1$. If $p_1 = 0$, the method of amplitude amplification does not work because there is no marked element. If $p_1 = 1$, we do not need to amplify the amplitude of the marked elements. So let us assume that $0 < p_1 < 1$. Define states

$$|\psi_0\rangle = \frac{1}{\sqrt{p_0}} \sum_{f(x)=0} \alpha_x |x\rangle, \tag{4.65}$$

$$|\psi_1\rangle = \frac{1}{\sqrt{p_1}} \sum_{f(x)=1} \alpha_x |x\rangle. \tag{4.66}$$

We have

$$|\psi\rangle = \sin\left(\frac{\theta}{2}\right)|\psi_1\rangle + \cos\left(\frac{\theta}{2}\right)|\psi_0\rangle, \tag{4.67}$$

where

$$\sin\left(\frac{\theta}{2}\right) = \sqrt{p_1} \tag{4.68}$$

and $\theta \in (0, \pi)$.

One evolution step is obtained by applying operator

$$U = \mathcal{R}_\psi U_f, \tag{4.69}$$

where $\mathcal{R}_\psi = 2|\psi\rangle\langle\psi| - I$. The initial condition is $|\psi\rangle = A|\psi_{\text{in}}\rangle$, where $|\psi_{\text{in}}\rangle$ is the initial state of the original algorithm. For now, what matters is how many times we have to apply U_f to find a marked element with certainty when $n \to \infty$. The overall efficiency of the amplitude–amplification algorithm depends on operator A and must be eventually considered.

The evolution of the amplitude–amplification algorithm takes place in the real plane spanned by vectors $|\psi_0\rangle$ and $|\psi_1\rangle$, which plays a role similar to vectors $|M\rangle$ and $|M^\perp\rangle$ of Sect. 4.3.1. As in Exercise 4.18 on Page 57, the state of the quantum computer after t steps is given by

$$U^t|\psi\rangle = \sin\left(t\,\theta + \frac{\theta}{2}\right)|\psi_1\rangle + \cos\left(t\,\theta + \frac{\theta}{2}\right)|\psi_0\rangle, \tag{4.70}$$

where θ is given by (4.68). As before, we choose t such that

$$t\,\theta + \frac{\theta}{2} \approx \frac{\pi}{2},$$

which results in $t \approx \pi/2\theta$, if $\theta \ll 1$. Therefore,

$$t = O\left(\frac{1}{\sqrt{p_1}}\right).$$

The number of applications of U_f is asymptotically the square root of the number of times it would take on a classical algorithm.

The stopping time of the amplitude–amplification algorithm depends on θ or, equivalently, p_1. If $A = H^{\otimes n}$, the value of θ is obtained from the number of marked elements. In the general case, this information depends on the modulus of amplitudes α_x of the marked elements.

Exercise 4.27. Show that operator $\mathcal{R}_\psi$ given by (4.60) is a reflection around vector $|\psi\rangle$ given by (4.61), that is, show that $\mathcal{R}_\psi|\psi\rangle = |\psi\rangle$ and $\mathcal{R}_\psi|\psi\rangle^\perp = -|\psi\rangle^\perp$.

Further Reading

The original version of Grover's algorithm is described in [33]. References [32, 34] are also influential. The generalization of the algorithm for searching databases with repeated elements and a first version of the *counting algorithm* are described in [17]. The version of the counting algorithm using *phase estimation* is described in [61]. The geometric interpretation of Grover's algorithm is described in [4]. The analysis using spectral decomposition is discussed in [61] and its connection with the *abstract search algorithm* is briefly described in [10]. The proof of *optimality* of Grover's algorithm is in [16]. A more readable version is in [17] and we have closely followed the proof presented in [64]. Reference [83] presents a more detailed proof. References [18, 41] describe the method of *amplitude amplification* in detail. Reference [41] describes Markov's inequality.

Chapter 5
Quantum Walks on Infinite Graphs

Quantum walks on the line were introduced in Sect. 3.2 in order to highlight some features, which are strikingly different from the *classical random walks*. In this Chapter, we present in detail the analytical calculation of the state of quantum walks on the line. This calculation is a model for the study of quantum walks on many types of graphs. The *Fourier transform* is the key to the success of this calculation.

We also analyze quantum walks on the *two-dimensional infinite lattice*. Since the evolution equations are very complex in this case, the analysis is performed numerically. Among new features that show up in the two-dimensional case, we highlight the fact that there are non-equivalent coins, which generate a wide class of probability distributions.

On infinite graphs, the quantum walk spreads indefinitely. One of the most interesting physical properties is the *expected distance* from the origin, which is measured by the *standard deviation* of the probability distribution. Both the line and the two-dimensional lattice have a standard deviation that is directly proportional to the evolution time in contrast to the standard deviation of the classical random walk, which is proportional to the square root of the evolution time.

Quantum walks can also be defined in higher dimensions, such as, the *three-dimensional infinite lattice*. The results regarding the dependence of the standard deviation against time are similar, the quadratic speedup over the behavior of classical random walk is maintained.

5.1 Line

Suppose that the spatial part for the movement of the quantum walk consists of the integer points in a line. The spatial part has an associated Hilbert space $\mathcal{H}_P$ of infinite dimension, the computational basis of which is $\{|n\rangle : n \in \mathbb{Z}\}$. The coin space $\mathcal{H}_M$ has dimension 2 and its computational basis is $\{|0\rangle, |1\rangle\}$ corresponding to two possible directions of movement, rightward or leftward. Thus, the Hilbert

R. Portugal, *Quantum Walks and Search Algorithms*, Quantum Science and Technology, DOI 10.1007/978-1-4614-6336-8_5,

space associated with the quantum walk is $\mathcal{H}_M \otimes \mathcal{H}_P$, the computational basis of which is $\{|s,n\rangle, s \in \{0,1\}, -\infty \leq n \leq \infty\}$, where we set $s = 0$ as being rightward and $s = 1$ as being leftward. Using these conventions, the *shift operator* is

$$S = \sum_{s=0}^{1} \sum_{n=-\infty}^{\infty} |s, n + (-1)^s\rangle\langle s, n|. \tag{5.1}$$

If $s = 0$, the value of n will be incremented by one unit after one application of S, whereas if $s = 1$, n is decremented by one unit. This expression for S is equal to the expression of (3.13) of Sect. 3.2. To verify this fact one has to expand the sum over index s.

The generic state of the walker at time t is described by

$$|\Psi(t)\rangle = \sum_{s=0}^{1} \sum_{n=-\infty}^{\infty} \psi_{s,n}(t)|s, n\rangle, \tag{5.2}$$

where the coefficients $\psi_{s,n}(t)$ are complex functions, called *probability amplitudes*, which obey the *normalization condition*

$$\sum_{n=-\infty}^{\infty} |\psi_{0,n}(t)|^2 + |\psi_{1,n}(t)|^2 = 1, \tag{5.3}$$

for all time *t*. The probability distribution is given by

$$p_n(t) = |\psi_{0,n}(t)|^2 + |\psi_{1,n}(t)|^2. \tag{5.4}$$

5.1.1 Hadamard Coin

Let us use the *Hadamard operator*

$$H = \frac{1}{\sqrt{2}} \begin{bmatrix} 1 & 1 \\ 1 & -1 \end{bmatrix} \tag{5.5}$$

as coin. Applying the *standard evolution operator*

$$U = S\,(H \otimes I) \tag{5.6}$$

to the generic state, we obtain

$$|\Psi(t+1)\rangle = \sum_{n=-\infty}^{\infty} S\,(\psi_{0,n}(t)H|0\rangle|n\rangle + \psi_{1,n}(t)H|1\rangle|n\rangle)$$

$$= \sum_{n=-\infty}^{\infty} \frac{\psi_{0,n}(t) + \psi_{1,n}(t)}{\sqrt{2}} S|0\rangle|n\rangle + \frac{\psi_{0,n}(t) - \psi_{1,n}(t)}{\sqrt{2}} S|1\rangle|n\rangle$$

$$= \sum_{n=-\infty}^{\infty} \frac{\psi_{0,n}(t) + \psi_{1,n}(t)}{\sqrt{2}} |0\rangle|n+1\rangle + \frac{\psi_{0,n}(t) - \psi_{1,n}(t)}{\sqrt{2}} |1\rangle|n-1\rangle.$$

Using (5.2) on the left side of the above equation, *i.e.* expanding the left hand side in the computational basis, and matching to the corresponding coefficients on the right hand side, we obtain the walker's *evolution equations*

$$\psi_{0,n}(t+1) = \frac{\psi_{0,n-1}(t) + \psi_{1,n-1}(t)}{\sqrt{2}}, \tag{5.7}$$

$$\psi_{1,n}(t+1) = \frac{\psi_{0,n+1}(t) - \psi_{1,n+1}(t)}{\sqrt{2}}. \tag{5.8}$$

These equations were used in Sect. 3.2 to generate the graphs of probability distributions through numerical simulation.

Our goal is to calculate the probability distribution analytically. However, (5.7) and (5.8) cannot be solved easily at least in the way they are presently described. Fortunately, in this case, there is an alternative way to address the problem. There is a special basis called *Fourier basis* that diagonalizes the shift operator. This will help in the diagonalization of the evolution operator.

Exercise 5.1. Instead of using operator H as coin, take the Pauli matrix X. Obtain the evolution equations of the walker on the line and solve analytically taking as initial condition a walker at the origin with an arbitrary state for the coin state. Calculate the standard deviation.

5.1.2 Fourier Transform

The *Fourier transform* of a discrete function $f : \mathbb{Z} \to \mathbb{C}$ is a continuous function $\tilde{f} : [-\pi, \pi] \to \mathbb{C}$ defined by

$$\tilde{f}(k) = \sum_{n=-\infty}^{\infty} \mathrm{e}^{-\mathrm{i}kn} f(n), \tag{5.9}$$

where $\mathrm{i} = \sqrt{-1}$. The inverse transform is given by

$$f(n) = \int_{-\pi}^{\pi} \frac{\mathrm{d}k}{2\pi}\, \mathrm{e}^{\mathrm{i}kn}\, \tilde{f}(k). \tag{5.10}$$

This is a special case of a more general class of Fourier transforms, which is useful in our context. Note that if n had units (*e.g.* meters), k should have the inverse unit (1/meters), since the product kn is the argument of the exponential function and therefore must be *dimensionless*. The physical interpretation of the variable k is the *wave number*.

In (5.2), the coefficients $\psi_{s,n}(t)$ are discrete functions in variable n. We can calculate the Fourier transform of $\psi_{s,n}(t)$ with respect to the index n as follows:

$$\tilde{\psi}_s(k,t) = \sum_{n=-\infty}^{\infty} \mathrm{e}^{-\mathrm{i}kn}\, \psi_{s,n}(t), \tag{5.11}$$

where k is a continuous variable defined in the interval $[-\pi, \pi]$. The goal now is to obtain the evolution equations for $\tilde{\psi}_s(k,t)$. If we solve these new equations, we will obtain $\psi_{s,n}(t)$ through the inverse transform.

There is another way to use the Fourier transform. Instead of transforming function $f : \mathbb{Z} \to \mathbb{C}$, we transform the computational basis of $\mathcal{H}_P$. We use the formula

$$|\kappa_k\rangle = \sum_{n=-\infty}^{\infty} \mathrm{e}^{\mathrm{i}kn} |n\rangle \tag{5.12}$$

to define vectors $|\kappa_k\rangle$, where k is a continuous variable defined in the interval $[-\pi, \pi]$, as before. Note that we are using the positive sign in the exponential. The problem with this method is that $|\kappa_k\rangle$ has infinity norm. This can be solved by redefining $|\kappa_k\rangle$ as follows

$$|\kappa_k\rangle = \lim_{L\to\infty} \frac{1}{\sqrt{2L+1}} \sum_{n=-L}^{L} \mathrm{e}^{\mathrm{i}kn} |n\rangle. \tag{5.13}$$

The same change should be applied to (5.11) for the sake of consistency. Since the *normalization constant* is not relevant, we will continue to use (5.12) as the definition of $|\kappa_k\rangle$ and (5.11) as the definition of $\tilde{\psi}_s(k,t)$ to simplify the calculation. This transform defines a new orthonormal basis $\{|\kappa_k\rangle : -\pi \le k \le \pi\}$ called *Fourier basis*. In this basis, we can express the state of the quantum walk as

$$|\Psi(t)\rangle = \int_{-\pi}^{\pi} \frac{\mathrm{d}k}{2\pi} \sum_{s=0}^{1} \tilde{\psi}_s(k,t)\, |s\rangle |\kappa_k\rangle. \tag{5.14}$$

Note that the above equation decomposes $|\psi(t)\rangle$ in the Fourier basis, the coefficients of which are $\tilde{\psi}_s(k,t)$. Equation (5.2) decomposes $|\psi(t)\rangle$ in the computational basis, the coefficients of which are $\psi_{s,n}(t)$.

Exercise 5.2. Show that (5.2) and (5.14) are equivalent, if the Fourier basis is defined by formula (5.12).

Let us calculate the action of the shift operator on the new basis, *i.e.* its action on $|s\rangle|\kappa_k\rangle$. Using (5.12) and the definition of S, we have

$$\begin{aligned} S|s\rangle|\kappa_k\rangle &= \sum_{n=-\infty}^{\infty} \mathrm{e}^{\mathrm{i}kn} S|s,n\rangle \\ &= \sum_{n=-\infty}^{\infty} \mathrm{e}^{\mathrm{i}kn}|s\rangle|n+(-1)^s\rangle. \end{aligned}$$

Renaming index n in such way that $n' = n + (-1)^s$, we obtain

$$\begin{aligned} S|s\rangle|\kappa_k\rangle &= \sum_{n'=-\infty}^{\infty} \mathrm{e}^{\mathrm{i}\,(n'-(-1)^s)\,k}|s\rangle\big|n'\big\rangle \\ &= \mathrm{e}^{-(-1)^s\,\mathrm{i}\,k}|s\rangle|\kappa_k\rangle. \end{aligned} \tag{5.15}$$

The result shows that the action of the shift operator S over a state of the Fourier basis only changes its phase, *i.e.* $|s\rangle|\kappa_k\rangle$ is an eigenvector associated with the eigenvalue $\mathrm{e}^{-(-1)^s\,\mathrm{i}\,k}$. The next task is to find the eigenvectors of the evolution operator U. If we diagonalize U, we will be able to find an analytical expression for the state of the quantum walk as a function of time.

Applying U to vector $|s'\rangle|\kappa_k\rangle$ and using (5.15), we obtain

$$\begin{aligned} U\big|s'\big\rangle|\kappa_k\rangle &= S\left(\sum_{s=0}^{1} H_{s,s'}|s\rangle|\kappa_k\rangle\right) \\ &= \sum_{s=0}^{1} \mathrm{e}^{-(-1)^s\,\mathrm{i}\,k} H_{s,s'}|s\rangle|\kappa_k\rangle. \end{aligned} \tag{5.16}$$

The components of U in the Fourier basis are

$$\langle s,\kappa_k|U\big|s',\kappa_{k'}\big\rangle = \mathrm{e}^{-(-1)^s\mathrm{i}\,k} H_{s,s'}\,\delta_{k,k'}. \tag{5.17}$$

For each k, we define operator $\tilde{H}_k$, the components of which are

$$\tilde{H}_{s,s'} = \mathrm{e}^{-(-1)^s\,\mathrm{i}\,k} H_{s,s'}. \tag{5.18}$$

In matrix form we have

$$\tilde{H}_k = \begin{bmatrix} \mathrm{e}^{-\mathrm{i}k} & 0 \\ 0 & \mathrm{e}^{\mathrm{i}k} \end{bmatrix} \cdot H$$
$$= \frac{1}{\sqrt{2}} \begin{bmatrix} \mathrm{e}^{-\mathrm{i}k} & \mathrm{e}^{-\mathrm{i}k} \\ \mathrm{e}^{\mathrm{i}k} & -\mathrm{e}^{\mathrm{i}k} \end{bmatrix} \tag{5.19}$$

Equation (5.17) shows that the non-diagonal part of operator U is associated with the coin space. The goal now is to diagonalize operator $\tilde{H}_k$. The tensor product of an eigenvector of $\tilde{H}_k$ with vector $|\kappa_k\rangle$ is an eigenvector of U. To check this, note that (5.16) can be written as

$$U|s\rangle|\kappa_k\rangle = \big(\tilde{H}_k|s\rangle\big)|\kappa_k\rangle. \tag{5.20}$$

The action of the shift operator S has been absorbed in $\tilde{H}_k$ when U acts in $|\kappa_k\rangle$. If $|\alpha_k\rangle$ is an eigenvector of $\tilde{H}_k$ with eigenvalue α_k, we have

$$U|\alpha_k\rangle|\kappa_k\rangle = \big(\tilde{H}_k|\alpha_k\rangle\big)|\kappa_k\rangle$$
$$= \alpha_k|\alpha_k\rangle|\kappa_k\rangle. \tag{5.21}$$

Therefore, $|\alpha_k\rangle|\kappa_k\rangle$ is the eigenvector of U associated with the eigenvalue α_k. This result shows that the diagonalization of the evolution operator reduces to the diagonalization of $\tilde{H}_k$. U is defined in an infinite dimensional Hilbert space, while $\tilde{H}_k$ is defined in a two-dimensional space.

The characteristic polynomial of $\tilde{H}_k$ is

$$\lambda^2 + \mathrm{i}\sqrt{2}\,\lambda \sin k - 1. \tag{5.22}$$

The eigenvalues are

$$\alpha_k = \mathrm{e}^{-\mathrm{i}\omega_k}, \tag{5.23}$$
$$\beta_k = \mathrm{e}^{\mathrm{i}(\pi+\omega_k)}, \tag{5.24}$$

where ω_k is an angle in the interval $[-\pi/2, \pi/2]$ that satisfies the equation

$$\sin\omega_k = \frac{1}{\sqrt{2}} \sin k. \tag{5.25}$$

The normalized eigenvectors are

$$|\alpha_k\rangle = \frac{1}{\sqrt{c^-}} \begin{bmatrix} \mathrm{e}^{-\mathrm{i}k} \\ \sqrt{2}\,\mathrm{e}^{-\mathrm{i}\omega_k} - \mathrm{e}^{-\mathrm{i}k} \end{bmatrix}, \tag{5.26}$$

$$|\beta_k\rangle = \frac{1}{\sqrt{c^+}} \begin{bmatrix} \mathrm{e}^{-\mathrm{i}k} \\ -\sqrt{2}\,\mathrm{e}^{\mathrm{i}\omega_k} - \mathrm{e}^{-\mathrm{i}k} \end{bmatrix}, \tag{5.27}$$

where

$$c^{\pm} = 2\left(1 + \cos^2 k\right) \pm 2\,\cos k\,\sqrt{1 + \cos^2 k}. \tag{5.28}$$

The spectral decomposition of U is

$$U = \int_{-\pi}^{\pi} \frac{\mathrm{d}k}{2\pi} \left(\mathrm{e}^{-\mathrm{i}\,\omega_k}\,|\alpha_k, \kappa_k\rangle\langle\alpha_k, \kappa_k| + \mathrm{e}^{\mathrm{i}\,(\pi+\omega_k)}\,|\beta_k, \kappa_k\rangle\langle\beta_k, \kappa_k|\right). \tag{5.29}$$

The t-th power of U is

$$U^t = \int_{-\pi}^{\pi} \frac{\mathrm{d}k}{2\pi} \left(\mathrm{e}^{-\mathrm{i}\,\omega_k\,t}\,|\alpha_k, \kappa_k\rangle\langle\alpha_k, \kappa_k| + \mathrm{e}^{\mathrm{i}\,(\pi+\omega_k)\,t}\,|\beta_k, \kappa_k\rangle\langle\beta_k, \kappa_k|\right). \tag{5.30}$$

5.1.3 Analytical Solution

Let us take the initial state with the particle located at the origin $n = 0$ and the coin state with *spin* up $|0\rangle$. Thus, the initial condition in the computational basis is

$$|\psi(0)\rangle = |0\rangle|n = 0\rangle. \tag{5.31}$$

Using (5.30) we obtain

$$\begin{aligned} |\psi(t)\rangle &= U^t|\psi(0)\rangle \\ &= \int_{-\pi}^{\pi} \frac{\mathrm{d}k}{2\pi} \left(\mathrm{e}^{-\mathrm{i}\,\omega_k\,t}\,|\alpha_k, \kappa_k\rangle\,\langle\alpha_k, \kappa_k|0, 0\rangle\right. \\ &\quad \left. + \mathrm{e}^{\mathrm{i}\,(\pi+\omega_k)\,t}\,|\beta_k, \kappa_k\rangle\,\langle\beta_k, \kappa_k|0, 0\rangle\right). \end{aligned} \tag{5.32}$$

Using (5.26), (5.27), and (5.12), we obtain

$$\langle\alpha_k, \kappa_k|0, 0\rangle = \frac{\mathrm{e}^{\mathrm{i}\,k}}{\sqrt{c^-}}, \tag{5.33}$$

$$\langle\beta_k, \kappa_k|0, 0\rangle = \frac{\mathrm{e}^{\mathrm{i}\,k}}{\sqrt{c^+}}. \tag{5.34}$$

Therefore,

$$|\psi(t)\rangle = \int_{-\pi}^{\pi} \frac{\mathrm{d}k}{2\pi} \left(\frac{\mathrm{e}^{-\mathrm{i}\,(\omega_k t - k)}}{\sqrt{c^-}}|\alpha_k\rangle + \frac{\mathrm{e}^{\mathrm{i}\,(\pi+\omega_k)\,t + \mathrm{i}\,k}}{\sqrt{c^+}}|\beta_k\rangle\right)|\kappa_k\rangle. \tag{5.35}$$

The state of the walk is written on the basis of eigenvectors of U. It is convenient to express the result in the computational basis. As an intermediate step, we will

express the eigenvectors $|\alpha_k\rangle$ and $|\beta_k\rangle$ in the computational basis through (5.26) and (5.27) keeping intact vectors $|\kappa_k\rangle$:

$$|\psi(t)\rangle = \int_{-\pi}^{\pi} \frac{\mathrm{d}k}{2\pi} \left(\frac{\mathrm{e}^{-\mathrm{i}\,(\omega_k t - k)}}{c^-} \begin{bmatrix} \mathrm{e}^{-\mathrm{i}\,k} \\ \sqrt{2}\,\mathrm{e}^{-\mathrm{i}\,\omega_k} - \mathrm{e}^{-\mathrm{i}\,k} \end{bmatrix} + \frac{\mathrm{e}^{\mathrm{i}\,(\pi+\omega_k)\,t + \mathrm{i}\,k}}{c^+} \begin{bmatrix} \mathrm{e}^{-\mathrm{i}\,k} \\ -\sqrt{2}\,\mathrm{e}^{\mathrm{i}\,\omega_k} - \mathrm{e}^{-\mathrm{i}\,k} \end{bmatrix} \right) |\kappa_k\rangle. \tag{5.36}$$

We can determine coefficients $\tilde{\psi}_s(k,t)$ of (5.14), which are given by

$$\tilde{\psi}_0(k,t) = \frac{\mathrm{e}^{-\mathrm{i}\omega_k t}}{c^-} + \frac{\mathrm{e}^{\mathrm{i}(\pi+\omega_k)t}}{c^+}, \tag{5.37}$$

$$\tilde{\psi}_1(k,t) = \frac{\mathrm{e}^{-\mathrm{i}\omega_k t + \mathrm{i}k} \left(\sqrt{2}\,\mathrm{e}^{-\mathrm{i}\,\omega_k} - \mathrm{e}^{-\mathrm{i}\,k} \right)}{c^-} - \frac{\mathrm{e}^{\mathrm{i}(\pi+\omega_k)t + \mathrm{i}k} \left(\sqrt{2}\,\mathrm{e}^{\mathrm{i}\,\omega_k} + \mathrm{e}^{-\mathrm{i}\,k} \right)}{c^+}. \tag{5.38}$$

To simplify these expressions, it is convenient to use the identities

$$\frac{1}{c^\pm} = \frac{1}{2} \left(1 \mp \frac{\cos k}{\sqrt{1+\cos^2 k}} \right) \tag{5.39}$$

and

$$\sqrt{2}\,\mathrm{e}^{\pm \mathrm{i}\,\omega_k} \pm \mathrm{e}^{-\mathrm{i}\,k} = \frac{c^\pm}{2\sqrt{1+\cos^2 k}}. \tag{5.40}$$

We finally obtain

$$\tilde{\psi}_0(k,t) = \frac{1}{2} \left(1 + \frac{\cos k}{\sqrt{1+\cos^2 k}} \right) \mathrm{e}^{-\mathrm{i}\,\omega_k t} + \frac{(-1)^t}{2} \left(1 - \frac{\cos k}{\sqrt{1+\cos^2 k}} \right) \mathrm{e}^{\mathrm{i}\,\omega_k t}, \tag{5.41}$$

$$\tilde{\psi}_1(k,t) = \frac{\mathrm{e}^{\mathrm{i}k}}{2\sqrt{1+\cos^2 k}} \left(\mathrm{e}^{-\mathrm{i}\,\omega_k t} - (-1)^t \mathrm{e}^{\mathrm{i}\,\omega_k t} \right). \tag{5.42}$$

Coefficients $\psi_{0,n}$ and $\psi_{1,n}$ of the *wave function* in the computational basis are given by

$$\psi_{s,n}(t) = \int_{-\pi}^{\pi} \frac{\mathrm{d}k}{2\pi}\, \mathrm{e}^{\mathrm{i}kn}\, \tilde{\psi}_s(k,t). \tag{5.43}$$

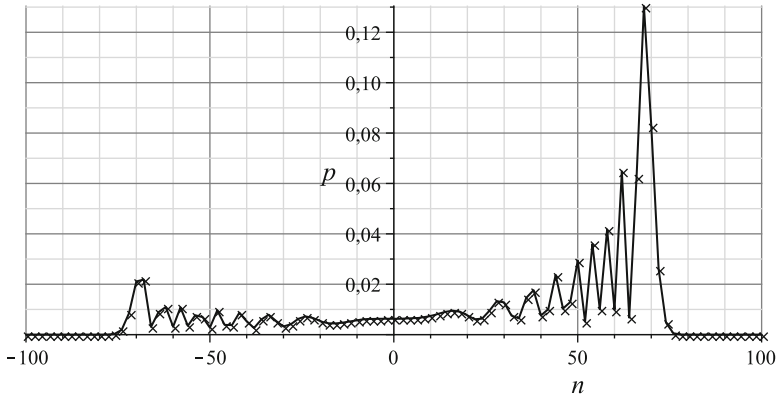

Fig. 5.1 Probability distribution of the quantum walk on the line after 100 steps from the analytical expression. The *cross-shaped points* correspond to integer values of n

When we substitute the expressions for $\tilde{\psi}_0(k,t)$ and $\tilde{\psi}_1(k,t)$ within the integral, we obtain two terms that are equal in modulus after the integration. Depending on the value of t, these terms either cancel or add up, so that at the end we have

$$\psi_{0,n}(t) = \int_{-\pi}^{\pi} \frac{\mathrm{d}k}{2\pi} \left(1 + \frac{\cos k}{\sqrt{1+\cos^2 k}}\right) \mathrm{e}^{-\mathrm{i}\,(\omega_k t - k n)}, \tag{5.44}$$

$$\psi_{1,n}(t) = \int_{-\pi}^{\pi} \frac{\mathrm{d}k}{2\pi} \frac{\mathrm{e}^{\mathrm{i}k}}{\sqrt{1+\cos^2 k}} \mathrm{e}^{-\mathrm{i}\,(\omega_k t - k n)} \tag{5.45}$$

when $n + t$ is even. When $n + t$ is odd, the coefficients are zero.

Using (5.4) we can calculate the probability distribution. The graph in Fig. 5.1 shows the distribution after 100 steps. Only the even points were displayed, since the probability is zero in odd points. This graph coincides with the graph generated numerically with the same initial condition in Sect. 3.2.

Exercise 5.3. Show that the integrals

$$(\pm 1)^t \int_{-\pi}^{\pi} \frac{\mathrm{d}k}{2\pi} \left(1 \pm \frac{\cos k}{\sqrt{1+\cos^2 k}}\right) \mathrm{e}^{-\mathrm{i}(\pm\omega_k t - k n)}$$

are real numbers and equal to each other when $n + t$ is even and have opposite signs when $n + t$ is odd. Show the same for the integrals

$$(\pm 1)^{t+1} \int_{-\pi}^{\pi} \frac{\mathrm{d}k}{2\pi} \frac{\mathrm{e}^{\mathrm{i}k}}{\sqrt{1+\cos^2 k}} \mathrm{e}^{-\mathrm{i}(\pm\omega_k t - k n)}.$$

Use these facts to obtain (5.44) and (5.45) from (5.41) and (5.42).

Exercise 5.4. Calculate analytically the *probability amplitudes* of the Hadamard quantum walk with initial condition

$$|\psi(0)\rangle = \frac{|0\rangle + \mathrm{i}|1\rangle}{\sqrt{2}}|n=0\rangle.$$

Depict the graph of the probability distribution and verify that it is symmetrical about the origin. Let $f_n(t)$ be the following function:

$$f_n(t) = \begin{cases} \frac{2}{\pi t\left(1-\frac{n^2}{t^2}\right)\sqrt{1-\frac{2n^2}{t^2}}}, & |n| \leq \frac{t}{\sqrt{2}}; \\ 0, & \frac{t}{\sqrt{2}} < |n|. \end{cases}$$

Plot the graph of $f_n(t)$ together with the probability distribution for some values of t and check that $f_n(t)$ is a good approximation, disregarding the rapid oscillation of the probability distribution.

5.1.4 Other Coins

A question that naturally arises is how general the results of the last section are. The *standard quantum walk* has an evolution operator in the form $U = S(C \otimes I)$, where the shift operator S is given by (5.1). The only degrees of freedom are (1) the choice of coin operator C and (2) the choice of the initial condition. For the quantum walk on the line, these choices are not independent. A generic coin operator, disregarding a global phase, has the form

$$C = \begin{bmatrix} \sqrt{\rho} & \sqrt{1-\rho}\,\mathrm{e}^{\mathrm{i}\theta} \\ \sqrt{1-\rho}\,\mathrm{e}^{\mathrm{i}\phi} & -\sqrt{\rho}\,\mathrm{e}^{\mathrm{i}(\theta+\phi)} \end{bmatrix}, \tag{5.46}$$

where $0 \leq \rho \leq 1$ and $0 \leq \theta, \phi \leq \pi$.

The coin state $|0\rangle$ induces a movement to the right, while $|1\rangle$, to the left. Note that

$$C|0\rangle = \sqrt{\rho}|0\rangle + \sqrt{1-\rho}\,\mathrm{e}^{\mathrm{i}\theta}|1\rangle. \tag{5.47}$$

Therefore, depending on the value of ρ, the coin can increase the probability associated with "go to right" or "go to left" . The *non-biased coin* is obtained by taking $\rho = 1/2$. Angles θ and ϕ play no role in this case. The Hadamard coin is an example of a non-biased coin, and it is the simplest one. A non-biased coin does not guarantee a *symmetric probability distribution*, because there is still freedom in the initial condition. The generic initial condition starting from the origin has the form

$$|\Psi(0)\rangle = \left(\cos\alpha\,|0\rangle + \mathrm{e}^{\mathrm{i}\beta}\,\sin\alpha\,|1\rangle\right)|0\rangle, \tag{5.48}$$

so we have two control parameters: α and β.

Considering non-biased coins and repeating the calculation of the quantum state for a generic time using the generic initial condition, we conclude that the change produced by parameters θ and ϕ can be fully achieved through appropriate choices of parameters α and β. So, if we fix the coin as the Hadamard operator, we can obtain all possible quantum walks through an appropriate choice of the initial condition. For some of these choices, the probability distribution is symmetric, assuming that the walker starts from the origin, generating a *non-biased walk*.

Exercise 5.5. Find a coin that generates a symmetrical probability distribution using the initial condition

$$|\psi(0)\rangle = \frac{|0\rangle + |1\rangle}{\sqrt{2}}|n = 0\rangle.$$

Exercise 5.6. In the classical random walk, we can have a walker on the line that can move to the left, to the right, or stay in the same position. What is the quantum version of this classical walk? Find the shift operator and use the Grover coin to calculate the first steps using the initial condition $|\Psi(0)\rangle = |\mathrm{D}\rangle|0\rangle$. Obtain the answer in the computational basis.

Exercise 5.7. Using the generic operator of (5.46) as coin, show that the coin operator $\tilde{C}_k$ associated with the Fourier space is given by

$$\tilde{C}_k = \begin{bmatrix} \sqrt{\rho}\,\mathrm{e}^{-\mathrm{i}k} & \sqrt{1-\rho}\,\mathrm{e}^{\mathrm{i}(-k+\theta)} \\ \sqrt{1-\rho}\,\mathrm{e}^{\mathrm{i}(k+\phi)} & -\sqrt{\rho}\,\mathrm{e}^{\mathrm{i}(k+\theta+\phi)} \end{bmatrix}.$$

Verify that operator (5.19) can be obtained by a suitable choice of parameters ρ, θ, and ϕ. Find the eigenvalues and eigenvectors of $\tilde{C}_k$. Show that in the Fourier space, we can write

$$\left|\tilde{\Psi}_k(t)\right\rangle = \tilde{C}_k\left|\tilde{\Psi}_k(0)\right\rangle,$$

where $\left|\tilde{\Psi}_k(0)\right\rangle$ can be obtained by calculating the Fourier transform of $|\Psi(0)\rangle)$, given by (5.48). Show that parameters θ and β only appear in the β only appear in the expression of $\left|\tilde{\Psi}_k(t)\right\rangle$ in the form $\theta + \beta$. Therefore, any choice of θ can be choice of β. Show that parameter ϕ plays the role of a global phase, and it is eliminated when we take the *inverse Fourier transform*.

5.2 Two-Dimensional Lattices

Suppose that the spatial part for the movement of the quantum walk consists of the points of an infinite two-dimensional lattice. The spatial part has an associated Hilbert space $\mathcal{H}_P$ of infinite dimension, the computational basis of which is $\{|x, y\rangle : x, y \in \mathbb{Z}\}$. If the walker is at a lattice point, it has four options to move. The coin decides which direction it takes. In a practical implementation, the particle may

have *spin* 3/2, because it has four possible spin states. Another option is to use two states with two levels each, *i.e.* two qubits. In this case, the state of the coin is the tensor product of the state of each qubit. For example, suppose that the walker is a *Hydrogen atom*. If we control the *energy level* so that the electron lives in the first two orbital layers, we have a two-level state (qubit). The other qubit is the spin of the electron. The state of the whole system spin-orbital layers has four states. The coin space $\mathcal{H}_M$ has dimension 4 and its computational basis can be denoted by $\{|i_x, i_y\rangle : 0 \leq i_x, i_y \leq 1\}$. The Hilbert space associated with the quantum walk is the coin-position space, which is given by $\mathcal{H}_M \otimes \mathcal{H}_P$.

The generic state of the walker at time t is described by

$$|\Psi(t)\rangle = \sum_{i_x,i_y=0}^{1} \sum_{x,y=-\infty}^{\infty} \psi_{i_x,i_y;x,y}(t)|i_x, i_y\rangle|x, y\rangle, \tag{5.49}$$

where the coefficients $\psi_{i_x,i_y;x,y}(t)$ are complex functions that obey the *normalization condition*

$$\sum_{i_x,i_y=0}^{1} \sum_{x,y=-\infty}^{\infty} \left|\psi_{i_x,i_y;x,y}(t)\right|^2 = 1, \tag{5.50}$$

for all time t. The probability distribution is given by

$$p_{x,y}(t) = \sum_{i_x,i_y=0}^{1} |\psi_{i_x,i_y;x,y}(t)|^2. \tag{5.51}$$

The action of the shift operator S is

$$S|i_x, i_y\rangle|x, y\rangle = |i_x, i_y\rangle|x + (-1)^{i_x}, y + (-1)^{i_y}\rangle. \tag{5.52}$$

If $i_x = 0$ and $i_y = 0$, the values of x and y are incremented by one unit, which means that if the walker leaves position $(0, 0)$, it will go to $(1, 1)$, that is, it goes through the main diagonal of the lattice. If $i_x = 0$ and $i_y = 1$, x is incremented by one unit, while y is decremented by one unit, indicating that the walker goes through the secondary diagonal to the right. Similarly, for cases $i_x = i_y = 1$ and $i_x = 1, i_y = 0$. If the values i_x and i_y are equal, the walker goes through the main diagonal. Otherwise, it goes through the secondary diagonal.

Applying the standard evolution operator

$$U = S\,(C \otimes I) \tag{5.53}$$

to the generic state, we obtain

$$
\begin{aligned}
|\Psi(t+1)\rangle &= \sum_{j_x,j_y=0}^{1} \sum_{x,y=-\infty}^{\infty} \psi_{j_x,j_y;x,y}(t)\, S\Big(C\,\big|j_x, j_y\big\rangle |x, y\rangle\Big) \\
&= \sum_{j_x,j_y=0}^{1} \sum_{x,y=-\infty}^{\infty} \psi_{j_x,j_y;x,y}(t)\, S\left(\sum_{i_x,i_y=0}^{1} C_{i_x,i_y;j_x,j_y} \big|i_x, i_y\big\rangle |x, y\rangle\right) \\
&= \sum_{i_x,i_y,j_x,j_y=0}^{1} \sum_{x,y=-\infty}^{\infty} \psi_{j_x,j_y;x,y}(t)\, C_{i_x,i_y;j_x,j_y} \\
&\qquad\qquad \big|i_x, i_y\big\rangle \big|x + (-1)^{i_x},\ y + (-1)^{i_y}\big\rangle.
\end{aligned}
$$

We can rename $x + (-1)^{i_x}$, $y + (-1)^{i_y}$ to x, y, so that

$$
\begin{aligned}
|\Psi(t+1)\rangle = &\sum_{i_x,i_y,j_x,j_y=0}^{1} \sum_{x,y=-\infty}^{\infty} C_{i_x,i_y;j_x,j_y} \\
&\times \psi_{j_x,j_y;x-(-1)^{i_x},\, y-(-1)^{i_y}}(t) \big|i_x, i_y\big\rangle |x, y\rangle. \qquad (5.54)
\end{aligned}
$$

Expanding the left hand side of the above equation in the computational basis and matching the coefficients, we obtain the walker's evolution equation

$$
\psi_{i_x,i_y;x,y}(t+1) = \sum_{j_x,j_y=0}^{1} C_{i_x,i_y;j_x,j_y}\ \psi_{j_x,j_y;x+(-1)^{i_x},\, y+(-1)^{i_y}}(t). \qquad (5.55)
$$

This equation is too complex to be solved analytically for a generic coin. In next Chapter, exact solutions are obtained using Fourier transform for the *flip-flop* quantum walk with Grover coin on *finite* two-dimensional lattices, which can be used to obtain information about the behavior on infinite lattice. The flip-flop shift operator inverts the coin direction. However, (5.55) can be analyzed numerically, providing quick results. We have to choose a coin operator. In the following sections, we describe the quantum walk evolution numerically for three important non-equivalent coins: *Hadamard*, *Fourier* and *Grover*.

Exercise 5.8. Show that if the coin operator is the tensor product of two operators $C = C_1 \otimes C_2$, then the evolution operator (5.53) can be factorized as the tensor product of two operators.

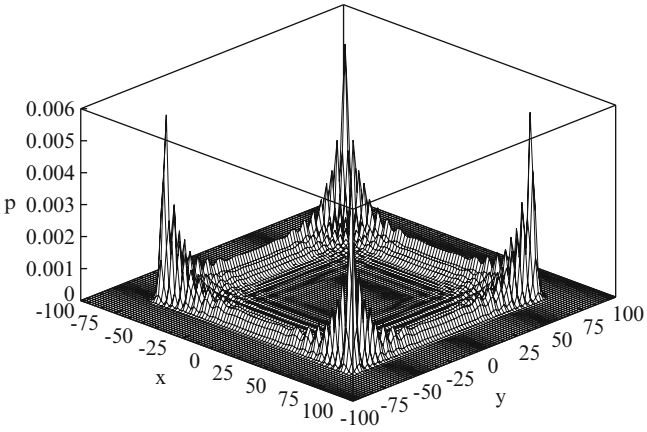

Fig. 5.2 Probability distribution of the quantum walk in the two-dimensional lattice with the Hadamard coin after 100 steps

5.2.1 The Hadamard Coin

The Hadamard coin is $C = H \otimes H$ and its matrix representation is

$$C = \frac{1}{2}\begin{bmatrix} 1 & 1 & 1 & 1 \\ 1 & -1 & 1 & -1 \\ 1 & 1 & -1 & -1 \\ 1 & -1 & -1 & 1 \end{bmatrix}. \tag{5.56}$$

Let us take the following state as initial condition:

$$|\Psi(0)\rangle = \frac{|0\rangle + \mathrm{i}|1\rangle}{\sqrt{2}} \otimes \frac{|0\rangle + \mathrm{i}|1\rangle}{\sqrt{2}} \otimes |x = 0, y = 0\rangle, \tag{5.57}$$

which is based on the initial condition used in Sect. 3.2 to obtain a symmetrical probability distribution for the Hadamard coin. The graph of the probability distribution after 100 steps is shown in Fig. 5.2.

The dynamics in this example is equivalent to two diagonal *uncoupled quantum walks*. The analytical results obtained for the one-dimensional Hadamard walk do apply in this case. A detailed analysis of Fig. 5.2 shows the characteristics of the one-dimensional walk analyzed before.

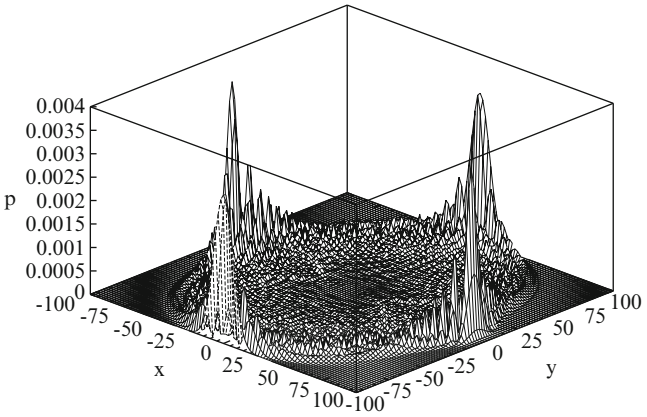

Fig. 5.3 Probability distribution of a quantum walk in the two-dimensional lattice with the Fourier coin

5.2.2 The Fourier Coin

The Fourier coin is $C = F_4$ and its matrix representation is

$$F_4 = \frac{1}{2}\begin{bmatrix} 1 & 1 & 1 & 1 \\ 1 & \mathrm{i} & -1 & -\mathrm{i} \\ 1 & -1 & 1 & -1 \\ 1 & -\mathrm{i} & -1 & \mathrm{i} \end{bmatrix}. \tag{5.58}$$

Let us take the following state as initial condition:

$$|\Psi(0)\rangle = \frac{1}{2}\left(|00\rangle + \frac{1-\mathrm{i}}{\sqrt{2}}|01\rangle + |10\rangle - \frac{1-\mathrm{i}}{\sqrt{2}}|11\rangle\right)|x = 0, y = 0\rangle. \tag{5.59}$$

The graph of the probability distribution after 100 steps is shown in Fig. 5.3.

The graph is *invariant* under rotation of 180°, but it is not invariant under rotation of 90°. The walk is symmetrical in each direction, but the evolution in the direction x is different from the evolution in y.

5.2.3 The Grover Coin

Finally, we will use the Grover coin which is given by

$$G = 2|\mathrm{D}\rangle\langle\mathrm{D}| - I, \tag{5.60}$$

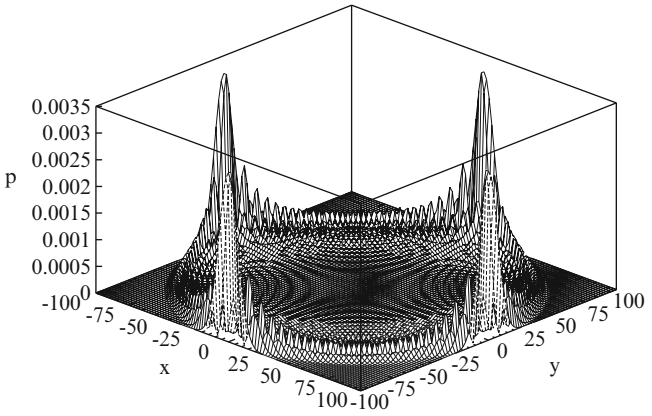

Fig. 5.4 Probability distribution of the quantum walk in the two-dimensional lattice with the Grover coin

where $|\mathrm{D}\rangle = \frac{1}{2}\sum_{i_x,i_y=0}^{1}|i_x,i_y\rangle$ is the diagonal state of $\mathcal{H}_M$. The matrix representation is

$$G = \frac{1}{2}\begin{bmatrix} -1 & 1 & 1 & 1 \\ 1 & -1 & 1 & 1 \\ 1 & 1 & -1 & 1 \\ 1 & 1 & 1 & -1 \end{bmatrix}. \tag{5.61}$$

The initial condition which has the largest standard deviation for the Grover coin is the state

$$|\Psi(0)\rangle = \frac{1}{2}\big(|00\rangle - |01\rangle - |10\rangle + |11\rangle\big)|x=0, y=0\rangle. \tag{5.62}$$

The graph of the probability distribution after 100 steps is shown in Fig. 5.4.

The graph is *invariant* under rotation of 90°, showing that the directions x and y are equivalent.

5.2.4 Standard Deviation

If we fix the evolution operator in the one-dimensional quantum walk, we can obtain all possible walks by changing the initial condition. This is not true for the two-dimensional case. The three coins that we analyzed are independent. They fall into three distinct classes, regardless of the initial conditions. The choice of initial condition can change the position standard deviation. Different from what was displayed in the examples, we can generate probability distributions strongly centered around the origin by a suitable choice of initial conditions.

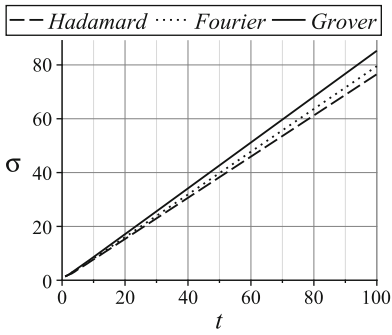

Fig. 5.5 Standard deviation of the quantum walk on the two-dimensional lattice for Hadamard, Fourier, and Grover coins

The best way to compare the coins analyzed so far is by calculating the standard deviation of the probability distribution generated by each one. The formula for the standard deviation of the position for the one-dimensional case was described in Sect. 3.2. In the two-dimensional case, the natural extension is

$$\sigma(t) = \sqrt{\sum_{x,y=-\infty}^{\infty} (x^2 + y^2)\ p_{x,y}(t)}, \tag{5.63}$$

which is valid when the *expected value* of the position is zero. The graphs in Fig. 5.5 show the standard deviation for the Hadamard (dashed line), Fourier (dotted line), and Grover (continuous line) coins. Note that the Grover coin has the largest standard deviation among the three coins.

The Grover coin has several advantages over Fourier and Hadamard coins, besides the gain in the standard deviation, which can be useful in algorithmic applications. The Grover coin can be applied in any dimension and is non-trivial for dimension greater than one. The Hadamard coin can only be used in dimensions that are power of two. The Fourier coin has a simple expression when the dimension is power of two. It is interesting to use a coin that is somehow "distant" from the identity operator. The coin of Grover has this property.

Exercise 5.9. Are Hadamard, Fourier, and Grover coins biased?

Exercise 5.10. Show that the standard deviation of the two-dimensional Hadamard walk and standard deviation of the one-dimensional Hadamard walk are equal.

5.2.5 *Program QWalk*

The graphics in this section were made from the data generated by *program QWalk*, which can be obtained from the *Computer Physics Communications* library.[1] Also

[1] http://cpc.cs.qub.ac.uk/summaries/AEAX_v1_0.html

see http://qubit.lncc.br/qwalk. The program has already implemented the evolution equation (5.55). The user must launch command `qw2d` using some input file, which must have extension `in`, *e.g.* `hadamard.in`. *Windows* users should use the command `cmd` to open the appropriate window. To generate the graph in Fig. 5.2, the input file must contain the command

```
BEGIN
 COIN HADAMARD
 STATE HADAMARD
 LATTYPE DIAGONAL
 STEPS 100
END
```

that implements the operator $H \otimes H$ and the initial condition given by (5.57). To implement other initial conditions, the option `STATE HADAMARD` should be replaced by `STATE CUSTOM` and one must add the command

```
BEGINSTATE
 jx jy x y a b
ENDSTATE
```

outside the `BEGIN` $\cdots$ `END` environment in order to implement an initial condition of type $|\Psi(0)\rangle = (a + b\,i)\big|j_x, j_y\big\rangle|x, y\rangle$. Variables `jx,jy,x,y` are integer numbers and variables `a,b` are floating-point numbers. If the initial condition is a superposition of states, new lines with the same format should be added in the command `BEGINSTATE`. Any input outside the environments `BEGIN` $\cdots$ `END` is ignored.

To implement other coins, the option `COIN HADAMARD` should be replaced by `COIN CUSTOM`. For example, to implement the coin

$$\frac{1}{\sqrt{2}}\begin{bmatrix} 1 & i \\ i & 1 \end{bmatrix},$$

the command

```
BEGINCOIN
 0.70710678  0.0       0.0 0.70710678
 0.0  0.70710678       0.70710678 0.0
ENDCOIN
```

should be added outside the environment `BEGIN` $\cdots$ `END`.

The output files have extensions `dat` and `sta`. The files with extension `plt` are *gnuplot scripts*, and can be used to generate the graph of the probability distribution in the *encapsulated postscript* format. The correct version of gnuplot must be used. Files with extension `sta` contain data about the expected value and standard deviation of the probability distribution.

Exercise 5.11. Use the program QWalk to plot the probability distribution of the two-dimensional quantum walk with the Grover coin after 100 steps with the initial condition

$$|\Psi(0)\rangle = |\mathrm{D}\rangle|x = 0, y = 0\rangle.$$

Check that the distribution is strongly centered around the origin. Plot the graph of standard deviation and show that growth is linear with time. Why is this not a contradiction?

Further Reading

The quantum walk on the line is analyzed in many papers. The seminal article is [63], which obtained (5.44) and (5.45). A thorough analysis was presented in [7, 19, 44, 45]. Reference [77] analyzes generic coins and generic initial conditions. A review of the main results of the walk on the line and additional references can be found in the review book [80].

Reference [49] was among the first to analyze walks in dimensions greater than one. Reference [77] performed thorough examination of possible coins for walks on two-dimensional lattices. Reference [56] describes *program QWalk*, which provides tools to generate numerical data to plot graphs of the probability distribution and standard deviation. The PhD thesis [82] analyzes quantum walks on two-dimensional lattices with focus on recurrence problems and contains additional references. More references on quantum walks on infinite graphs can be found in review book [80] or in [79].

Chapter 6
Quantum Walks on Finite Graphs

In this chapter, we calculate the state of quantum walks on *cycles*, *finite two-dimensional lattices*, and *hypercubes*. The cycle is the finite version of the line. The finite lattice is the two-dimensional version of the cycle with the form of a *torus*. Finally, the hypercube is a generalization of the cube to dimensions greater than three. These graphs are basic ones but have interesting properties. They can be analyzed by means of the *Fourier transform*, allowing analytical calculations, which have many useful by-products in other contexts. In particular, the spectral decomposition of the quantum-walk evolution operator can be used in *spatial search algorithms* on these graphs. The spectral decomposition is described in details in this chapter.

There are some interesting physical quantities of quantum walks on finite graphs that have different properties compared to walks on infinite graphs, such as the *limiting distribution*, the *mixing time*, and the *hitting time*. The position standard deviation, on the other hand, is less important in the finite case. The number of vertices is used as a parameter to describe bounds on the mixing time and hitting time. These topics will be addressed in subsequent chapters. The number of vertices is also used as a metric to measure the efficiency of algorithms.

6.1 Cycle

Suppose that the space on which the walker moves is the set of vertices of a N-cycle. If the walker moves N steps clockwise, it reaches the departure point. The same is true for the counterclockwise direction. The spatial part has associated an N-dimensional Hilbert space $\mathcal{H}^N$ with *computational basis* $\{|j\rangle, 0 \leq j \leq N-1\}$, where the values of j correspond to the labels of the vertices. The vertex with label j is a neighbor of vertices with labels $j-1$ and $j+1$ and only of them. The coin space has dimension 2, because the walker can move clockwise or counterclockwise. Thus, the Hilbert space associated with the quantum walk is $\mathcal{H}^2 \otimes \mathcal{H}^N$, with

R. Portugal, *Quantum Walks and Search Algorithms*, Quantum Science and Technology, DOI 10.1007/978-1-4614-6336-8_6,

computational basis $\{|s, j\rangle, 0 \leq s \leq 1, 0 \leq j \leq N-1\}$, where we set $s = 0$ as clockwise and $s = 1$ as counterclockwise. Under these conventions, the *shift operator* is

$$S|s, j\rangle = |s,\ j + (-1)^s\rangle. \tag{6.1}$$

If $s = 0$, the value of j will be incremented by one after one application of S, and if $s = 1$, j is decremented by one unit. Arithmetic operations with variable j are performed modulo N.

The generic state at time t is described by

$$|\Psi(t)\rangle = \sum_{j=0}^{N-1} \psi_{0,j}(t)|0, j\rangle + \psi_{1,j}(t)|1, j\rangle, \tag{6.2}$$

where coefficients $\psi_{0,j}(t)$ and $\psi_{1,j}(t)$ are complex functions that obey the normalization condition

$$\left|\psi_{0,j}(t)\right|^2 + \left|\psi_{1,j}(t)\right|^2 = 1, \tag{6.3}$$

for all time t.

Let us use the Hadamard coin operator

$$H = \frac{1}{\sqrt{2}}\begin{bmatrix} 1 & 1 \\ 1 & -1 \end{bmatrix}. \tag{6.4}$$

Applying the *standard evolution operator*

$$U = S\,(H \otimes I) \tag{6.5}$$

on the generic state, we obtain

$$\begin{aligned} |\Psi(t+1)\rangle &= \sum_{j=0}^{N-1} S\left(\psi_{0,j}(t)H|0\rangle|j\rangle + \psi_{1,j}(t)H|1\rangle|j\rangle\right) \\ &= \sum_{j=0}^{N-1} \frac{\psi_{0,j}(t) + \psi_{1,j}(t)}{\sqrt{2}} S|0\rangle|j\rangle + \frac{\psi_{0,j}(t) - \psi_{1,j}(t)}{\sqrt{2}} S|1\rangle|j\rangle \\ &= \sum_{j=0}^{N-1} \frac{\psi_{0,j}(t) + \psi_{1,j}(t)}{\sqrt{2}}|0, j+1\rangle + \frac{\psi_{0,j}(t) - \psi_{1,j}(t)}{\sqrt{2}}|1, j-1\rangle. \end{aligned}$$

Using (6.2) on the left-hand side of the above equation, that is, expanding the left-hand side in the computational basis, and equating with the corresponding coefficients on the right-hand side of the equation, we obtain the walker evolution equations

$$\psi_{0,j}(t+1) = \frac{\psi_{0,j-1}(t) + \psi_{1,j-1}(t)}{\sqrt{2}},$$
$$\psi_{1,j}(t+1) = \frac{\psi_{0,j+1}(t) - \psi_{1,j+1}(t)}{\sqrt{2}}.$$

These equations are very difficult to be solved in the way they stand. However, they have a form that is suitable for computational simulation, which helps us to obtain quick results and to have a general idea about the behavior of the quantum walk. What we usually do is to plot the probability distribution, which is given by

$$p_j(t) = \left|\psi_{0,j}(t)\right|^2 + \left|\psi_{1,j}(t)\right|^2. \tag{6.6}$$

6.1.1 Fourier Transform

The analytical expression for the evolution of the walk on the cycle can be obtained more easily, if we use the *Fourier transform* on the spatial part. The Fourier transform acts on the spatial part of the computational basis as follows:

$$|\kappa_k\rangle = \frac{1}{\sqrt{N}} \sum_{j=0}^{N-1} \omega_N^{jk} |j\rangle, \tag{6.7}$$

where $\omega_N = \mathrm{e}^{\frac{2\pi \mathrm{i}}{N}}$. The range of k is the same of j. The Fourier transform defines a new *orthonormal basis* $\{|\kappa_k\rangle : 0 \leq k \leq N-1\}$ called *Fourier basis*. In this new basis, the generic state of the walker is

$$|\Psi(t)\rangle = \sum_{s=0}^{1} \sum_{k=0}^{N-1} \tilde{\psi}_{s,k}(t)\, |s\rangle |\kappa_k\rangle, \tag{6.8}$$

where the coefficients are given by

$$\tilde{\psi}_{s,k} = \frac{1}{\sqrt{N}} \sum_{j=0}^{N-1} \omega_N^{-jk} \psi_{s,j}. \tag{6.9}$$

The interpretation of this last equation is that the amplitude of a state on the Fourier basis is the *Fourier transform* of the amplitudes in the computational basis.

Exercise 6.1. Show the following properties of the Fourier transform:

1. $|\kappa_0\rangle$ is the diagonal state of Hilbert space $\mathcal{H}^N$.
2. $\{|\kappa_k\rangle : 0 \leq k \leq N-1\}$ is an orthonormal basis for Hilbert space $\mathcal{H}^N$.

3. $|0\rangle = \frac{1}{\sqrt{N}} \sum_{k=0}^{N-1} |\kappa_k\rangle$.
4. $|j\rangle = \frac{1}{\sqrt{N}} \sum_{k=0}^{N-1} \omega_N^{-jk} |\kappa_k\rangle$.

Let us calculate the action of the shift operator on the spatial Fourier basis, that is, its action on $|s\rangle|\kappa_k\rangle$. Using (6.7), we have

$$\begin{aligned} S|s\rangle|\kappa_k\rangle &= \frac{1}{\sqrt{N}} \sum_{j=0}^{N-1} \omega_N^{jk} S|s, j\rangle \\ &= \frac{1}{\sqrt{N}} \sum_{j=0}^{N-1} \omega_N^{jk} |s\rangle|j + (-1)^s\rangle. \end{aligned}$$

Renaming dummy index j such that $j' = j + (-1)^s$, we obtain

$$\begin{aligned} S|s\rangle|\kappa_k\rangle &= \frac{1}{\sqrt{N}} \sum_{j'=0}^{N-1} \omega_N^{(j'-(-1)^s)k} |s\rangle|j'\rangle \\ &= \omega_N^{-(-1)^s k} |s\rangle|\kappa_k\rangle. \end{aligned} \tag{6.10}$$

This result shows that the shift operator only changes the state phase. However, this is not enough for our purposes, because we wish to *diagonalize* U, which also depends on the coin operator. The diagonalization of U allows us to find an analytical expression for the state of the quantum walk at any time.

Applying U on vector $|s'\rangle|\kappa_k\rangle$ and using (6.10), we obtain

$$\begin{aligned} U|s'\rangle|\kappa_k\rangle &= S\left(\sum_{s=0}^{1} H_{s,s'}|s\rangle|\kappa_k\rangle\right) \\ &= \sum_{s=0}^{1} \omega_N^{-(-1)^s k} H_{s,s'}|s\rangle|\kappa_k\rangle. \end{aligned}$$

The entries U in the spatial Fourier basis is

$$\langle s, \kappa_k|U|s', \kappa_{k'}\rangle = \omega_N^{-(-1)^s k} H_{s,s'} \delta_{k,k'}. \tag{6.11}$$

For each k, we define operator $\tilde{H}^{(k)}$ with entries

$$\tilde{H}^{(k)}_{s,s'} = \omega_N^{-(-1)^s k} H_{s,s'}. \tag{6.12}$$

In matrix form, we have

$$\tilde{H}^{(k)} = \begin{bmatrix} \omega_N^{-k} & 0 \\ 0 & \omega_N^{k} \end{bmatrix} \cdot H$$
$$= \frac{1}{\sqrt{2}} \begin{bmatrix} \omega_N^{-k} & \omega_N^{-k} \\ \omega_N^{k} & -\omega_N^{k} \end{bmatrix} \tag{6.13}$$

Equation (6.11) shows that the non-diagonal part of operator U is associated with the coin space. For each k, we have a *reduced evolution operator* $\tilde{H}^{(k)}$. The goal now is to diagonalize $\tilde{H}^{(k)}$. The tensor products of the eigenvectors of $\tilde{H}^{(k)}$ by vectors $|\kappa_k\rangle$ are eigenvectors of U associated with the same eigenvalues of $\tilde{H}^{(k)}$.

Exercise 6.2. Show that if $|\alpha_k\rangle$ is an eigenvector of $\tilde{H}^{(k)}$ with eigenvalue α_k, then $|\alpha_k\rangle|\kappa_k\rangle$ is the eigenvector of U associated with the same eigenvalue α_k.

The characteristic polynomial of matrix $\tilde{H}^{(k)}$ is

$$\lambda^2 + \mathrm{i}\sqrt{2}\sin\left(\frac{2\pi k}{N}\right)\lambda - 1. \tag{6.14}$$

Therefore, the eigenvalues are $\mathrm{e}^{-\mathrm{i}\theta_k}$ and $\mathrm{e}^{\mathrm{i}(\pi+\theta_k)}$, where θ_k is a solution of equation

$$\sin\theta_k = \frac{1}{\sqrt{2}}\sin\frac{2\pi k}{N}. \tag{6.15}$$

The normalized eigenvectors are

$$|\alpha_k\rangle = \frac{1}{\sqrt{c_k^-}}\left[\left(\sqrt{1+\cos^2\tilde{k}} - \cos\tilde{k}\right)\mathrm{e}^{\mathrm{i}\tilde{k}}\right], \tag{6.16}$$

$$|\beta_k\rangle = \frac{1}{\sqrt{c_k^+}}\left[-\left(\sqrt{1+\cos^2\tilde{k}} + \cos\tilde{k}\right)\mathrm{e}^{\mathrm{i}\tilde{k}}\right], \tag{6.17}$$

where

$$c_k^{\pm} = 2\sqrt{1+\cos^2\tilde{k}}\left(\sqrt{1+\cos^2\tilde{k}} \pm \cos\tilde{k}\right), \tag{6.18}$$

and

$$\tilde{k} = \frac{2\,\pi\,k}{N}. \tag{6.19}$$

The spectral decomposition of U is

$$U = \sum_{k=0}^{N-1}\left(\mathrm{e}^{-\mathrm{i}\,\theta_k}\,|\alpha_k,\kappa_k\rangle\langle\alpha_k,\kappa_k| + \mathrm{e}^{\mathrm{i}\,(\pi+\theta_k)}\,|\beta_k,\kappa_k\rangle\langle\beta_k,\kappa_k|\right). \tag{6.20}$$

The t-th power of U is

$$U^t = \sum_{k=0}^{N-1} \left(\mathrm{e}^{-\mathrm{i}\,\theta_k t}\, |\alpha_k, \kappa_k\rangle\langle\alpha_k, \kappa_k| + \mathrm{e}^{\mathrm{i}\,(\pi+\theta_k)t}\, |\beta_k, \kappa_k\rangle\langle\beta_k, \kappa_k| \right), \tag{6.21}$$

because a function f applied to U is by definition applied directly to the eigenvalues, when U is written in the basis of their eigenvectors.

Exercise 6.3. Show that $\left\{ |\alpha_k, \kappa_k\rangle,\ |\beta_k, \kappa_k\rangle \ :\ 0 \le k < N \right\}$ is an orthonormal basis of Hilbert space $\mathcal{H}^2 \otimes \mathcal{H}^N$.

6.1.2 Analytical Solutions

Let us take the initial state with the particle located at the vertex of label 0 and with coin value pointing clockwise. Thus, the initial condition in the computational basis is

$$|\psi(0)\rangle = |0\rangle|0\rangle. \tag{6.22}$$

Using (6.21), we obtain

$$\begin{aligned} |\psi(t)\rangle &= U^t |\psi(0)\rangle \\ &= \sum_{k=0}^{N-1} \left(\mathrm{e}^{-\mathrm{i}\,\theta_k t}\, |\alpha_k, \kappa_k\rangle \langle\alpha_k, \kappa_k|0, 0\rangle \right. \\ &\qquad \left. + \mathrm{e}^{\mathrm{i}\,(\pi+\theta_k)t}\, |\beta_k, \kappa_k\rangle \langle\beta_k, \kappa_k|0, 0\rangle \right). \end{aligned} \tag{6.23}$$

Using (6.16), (6.17), and (6.7), we obtain

$$\langle\alpha_k, \kappa_k|0, 0\rangle = \frac{1}{\sqrt{N\, c_k^-}}, \tag{6.24}$$

$$\langle\beta_k, \kappa_k|0, 0\rangle = \frac{1}{\sqrt{N\, c_k^+}}. \tag{6.25}$$

Therefore,

$$|\psi(t)\rangle = \frac{1}{\sqrt{N}} \sum_{k=0}^{N-1} \left(\frac{\mathrm{e}^{-\mathrm{i}\,\theta_k t}}{\sqrt{c_k^-}} |\alpha_k\rangle + \frac{(-1)^t \mathrm{e}^{\mathrm{i}\,\theta_k t}}{\sqrt{c_k^+}} |\beta_k\rangle \right) |\kappa_k\rangle. \tag{6.26}$$

To calculate the probability of finding the walker at any vertex of the cycle, we have to express the quantum state in the computational basis. Using identity

$$\frac{1}{c_k^{\pm}} = \frac{1}{2}\left(1 \mp \frac{\cos\tilde{k}}{\sqrt{1+\cos^2\tilde{k}}}\right) \tag{6.27}$$

and (6.16) and (6.17), we obtain

$$|\psi(t)\rangle = \frac{1}{\sqrt{N}} \sum_{k=0}^{N-1} \begin{bmatrix} A_k(t) \\ B_k(t) \end{bmatrix} |\kappa_k\rangle, \tag{6.28}$$

where

$$A_k(t) = \cos\theta_k t - \frac{\mathrm{i}\cos\tilde{k}\ \sin\theta_k t}{\sqrt{1+\cos^2\tilde{k}}}, \tag{6.29}$$

$$B_k(t) = -\frac{\mathrm{i}\,\mathrm{e}^{\mathrm{i}\tilde{k}}\ \sin\theta_k t}{\sqrt{1+\cos^2\tilde{k}}}, \tag{6.30}$$

which is valid when t is even. Using (6.7), we obtain

$$|\psi(t)\rangle = \frac{1}{N} \sum_{j=0}^{N-1} \begin{bmatrix} \sum_{k=0}^{N-1} A_k(t)\,\mathrm{e}^{\mathrm{i}\,j\,\tilde{k}} \\ \sum_{k=0}^{N-1} B_k(t)\,\mathrm{e}^{\mathrm{i}\,j\,\tilde{k}} \end{bmatrix} |j\rangle. \tag{6.31}$$

Using (6.6), we obtain the probability distribution

$$p_j(t) = \frac{1}{N^2}\left|\sum_{k=0}^{N-1} A_k(t)\,\mathrm{e}^{\mathrm{i}\,j\,\tilde{k}}\right|^2 + \frac{1}{N^2}\left|\sum_{k=0}^{N-1} B_k(t)\,\mathrm{e}^{\mathrm{i}\,j\,\tilde{k}}\right|^2. \tag{6.32}$$

This equation is valid for any value of N, but only for even values of t. Obtaining expressions for $A_k(t)$ and $B_k(t)$ when t is odd is oriented in Exercise 6.4. When N is even, the probability distribution is zero in vertices j such that $j + t$ is odd. When N is odd, the probability distribution is nonzero for all vertices eventually. Exercise 6.6 gives some hints to proof those facts.

If we make a shift of $(-N)$ on the values of j in the interval $[N/2, N-1]$, the probability distribution of the cycle is equal to the probability distribution of the walk on the line for $t \leq N$. This can be seen from the graph of the probability distribution in Fig. 6.1 for a cycle with $N = 200$. Note that for j in the interval $[0, N/2]$, the graph in Fig. 6.1 is equal to the one in Fig. 5.1 of Sect. 5.1.3. If the rest of the graph is shifted leftward, the graph becomes equal to the graph of the line.

In the line, the *wave fronts* go in opposite directions and they move away. In the cycle, the *wave fronts* move toward each other, they are close at $t \simeq N/\sqrt{2}$, and right after that there is a collision of the front peaks if N is even, as can be seen in Fig. 6.1. It is interesting to compare to what happens in cycles with an

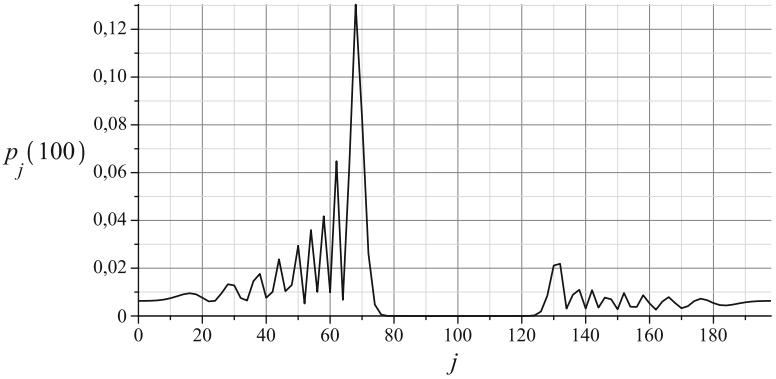

Fig. 6.1 Probability distribution of the quantum walk on cycle with $N = 200$ after 100 steps starting from initial condition $|\psi(0)\rangle = |0\rangle|0\rangle$. The points corresponding to odd values j were excluded because they have zero probability

odd number of vertices. The wave fronts do not collide at $t \simeq N/\sqrt{2}$, but they intertwine because there is an inverse relationship between the *parity* of j and the nonzero values of the probability. This fact shows that quantum walks on odd and even cycles have different behavior. A confirming evidence comes from the form of the *limiting distribution*, which is uniform for odd cycles for all initial conditions, while non-uniform and initial-condition dependent for even cycles. In terms of graph structure, even cycles are *bipartite graphs*.[1] The asymptotic behavior of *classical random walks* on bipartite graphs is different from the behavior on *non-bipartite graphs*. Part of this difference is inherited in the quantum context.

On the line, all possible quantum walks can be obtained from the Hadamard coin through a suitable choice of initial condition. In the cycle, this is true for a period of time while there is no interference of the front waves. When the wave fronts collide or reach its tail in the even and odd cycles, relative phase factors can produce constructive or destructive interference. These phase factors are introduced through evolution operators and cannot be reproduced by choosing initial conditions.

Exercise 6.4. Show that, to obtain valid expressions for $A_k(t)$ and $B_k(t)$ for odd t, we have to interchange $\cos\theta_k t$ by $-\mathrm{i}\sin\theta_k t$ in (6.29) and (6.30).

Exercise 6.5. Show that

$$\frac{1}{N}\sum_{j=0}^{N-1} \mathrm{e}^{\mathrm{i}\, j\,(\tilde{k}-\tilde{k}')} = \delta_{k\,k'}.$$

[1] A graph is bipartite if the set of vertices can be divided into two subsets A and B such that every edge connects a vertex in A with a vertex in B.

Using the above identity and (6.32), show that

$$\sum_{j=0}^{N-1} p_j(t) = 1$$

for any even number of steps t. Using Exercise 6.4, show also for odd t.

Exercise 6.6. Consider N even. If t is even, show that

$$|\psi(t)\rangle = \frac{1}{N} \sum_{j=0}^{N-1} \left(1 + (-1)^j\right) \begin{bmatrix} \sum_{k=0}^{N/2-1} A_k(t)\, \mathrm{e}^{\mathrm{i}\, j\, \tilde{k}} \\ \sum_{k=0}^{N/2-1} B_k(t)\, \mathrm{e}^{\mathrm{i}\, j\, \tilde{k}} \end{bmatrix} |j\rangle.$$

From this result, show that $p_j(t) = 0$ for odd j. Using Exercise 6.4, show that when t is odd, $p_j(t) = 0$ for even j. How can this result be interpreted in terms of the *parity* of N and the properties of the shift operator?

6.1.3 Periodic Solutions

In some cases, the evolution of a quantum walk can be periodic, that is, there is an integer T such that $|\psi(t+T)\rangle = |\psi(t)\rangle$ for any number of steps t. To obtain a periodic solution, we can use (6.21), which completely determines the state of the quantum walk at time t once given the initial condition. We must find T such that $U^T = I$. This implies that

$$\mathrm{e}^{-\mathrm{i}\theta_k T} = \mathrm{e}^{\mathrm{i}(\pi+\theta_k)T} = 1, \tag{6.33}$$

for all k. Therefore, T must be even and

$$\cos\theta_k T = 1,$$
$$\sin\theta_k T = 0,$$

that is, $\theta_k T = 2\pi j_k$, where each j_k must be an integer. Using (6.15), we obtain

$$\sin\frac{2\pi j_k}{T} = \frac{1}{\sqrt{2}} \sin\frac{2\pi k}{N}, \tag{6.34}$$

which must be valid for $0 \le k \le N-1$. This equation can be solved by exhaustive search and we quickly find solutions for $N = 2$ and $T = 2$; $N = 4$ and $T = 8$; $N = 8$ and $T = 24$.

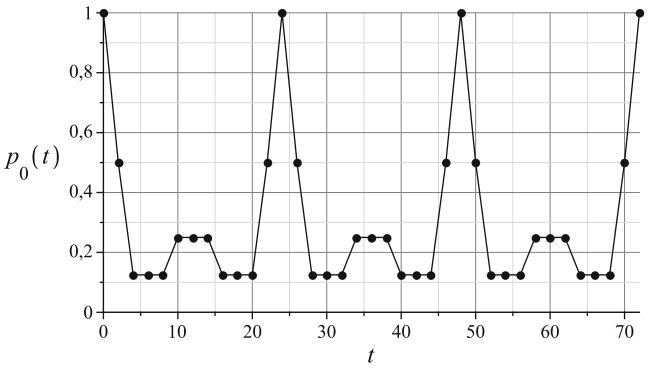

Fig. 6.2 Graph of the probability at vertex $v = 0$ as a function of time for a cycle with $N = 8$. The graph has period $T = 24$. The plot shows only the probability at even values of t

Figure 6.2 shows the plot of the probability at vertex $v = 0$ as a function of time for a cycle with eight vertices. Note that the graph is periodic. The same holds for any other vertex.

6.2 Finite Two-Dimensional Lattice

Suppose that N is a perfect square and consider a $\sqrt{N} \times \sqrt{N}$ lattice with *periodic boundary conditions*, that is, a lattice with the shape of *torus*. If the walker moves $\sqrt{N}$ steps toward x-direction, it returns to original position. The same holds for the y-direction. The vectors of the computational basis of the spatial part have the form of $|x, y\rangle$, where $x, y \in \{0, \ldots, \sqrt{N} - 1\}$. The coin space has dimension 4. The vectors of the computational basis of the coin space have the form of $|d, s\rangle$, with $0 \leq d, s \leq 1$, where d determines the direction of movement: $d = 0$ stands for x-direction and $d = 1$ stands for y-direction, and s determines the direction sign: $s = 0$ stands for positive direction and $s = 1$ stands for negative direction.

Under these conventions, we write the *shift operator* as

$$S|d, s\rangle|x, y\rangle = |d, s \oplus 1\rangle|x + (-1)^s \delta_{d0}, y + (-1)^s \delta_{d1}\rangle. \tag{6.35}$$

If $d = 0$ and $s = 0$, x will be incremented by one unit, and y remain unchanged. When x changes, y remains unchanged, and vice versa. Note that the coin state changes from $|d, s\rangle$ to $|d, s \oplus 1\rangle$, that is, the direction is inverted after the shift. This inversion in the coin value is important for speeding up search algorithms in the two-dimensional lattice. This issue will be addressed in Sect. 8.3. Shift operators that invert the coin are called *flip–flop*. Arithmetic operations with variables x and y are performed modulo $\sqrt{N}$.

We use the *Grover coin*, which is given by

$$G = 2|\mathrm{D}\rangle\langle\mathrm{D}| - I, \tag{6.36}$$

where $|\mathrm{D}\rangle = \frac{1}{2}\sum_{d,s=0}^{1}|d,s\rangle$ is the *diagonal state* of $\mathcal{H}^2 \otimes \mathcal{H}^2$. The *matrix representation* of G is

$$G = \frac{1}{2}\begin{bmatrix} -1 & 1 & 1 & 1 \\ 1 & -1 & 1 & 1 \\ 1 & 1 & -1 & 1 \\ 1 & 1 & 1 & -1 \end{bmatrix}. \tag{6.37}$$

The generic state of the walker at time t is described by

$$|\Psi(t)\rangle = \sum_{d,s=0}^{1}\sum_{x,y=0}^{\sqrt{N}-1}\psi_{d,s;x,y}(t)|d,s\rangle|x,y\rangle, \tag{6.38}$$

where coefficients $\psi_{d,s;x,y}(t)$ are complex functions that obey the normalization condition

$$\sum_{d,s=0}^{1}\sum_{x,y=0}^{\sqrt{N}-1}\left|\psi_{d,s;x,y}(t)\right|^2 = 1, \tag{6.39}$$

for all time t.

Applying the *standard evolution operator*

$$U = S\,(G \otimes I) \tag{6.40}$$

on the generic state, we obtain

$$\begin{aligned}
|\Psi(t+1)\rangle &= \sum_{d',s'=0}^{1}\sum_{x,y=0}^{\sqrt{N}-1}\psi_{d',s';x,y}(t)\,S\Big(G\big|d',s'\big\rangle|x,y\rangle\Big) \\
&= \sum_{d',s'=0}^{1}\sum_{x,y=0}^{\sqrt{N}-1}\psi_{d',s';x,y}(t)\,S\left(\sum_{d,s=0}^{1}G_{d,s;d',s'}|d,s\rangle|x,y\rangle\right) \\
&= \sum_{d,s,d',s'=0}^{1}\sum_{x,y=0}^{\sqrt{N}-1}\psi_{d',s';x,y}(t)\,G_{d,s;d',s'} \\
&\qquad |d,s\oplus 1\rangle|x+(-1)^s\delta_{d0},\ y+(-1)^s\delta_{d1}\rangle.
\end{aligned}$$

We can rename the dummy indices of the sum from $x+(-1)^s\delta_{d0}$, $y+(-1)^s\delta_{d1}$, $s\oplus 1$ to x, y, s. Then,

$$|\Psi(t+1)\rangle = \sum_{d,s,d',s'=0}^{1} \sum_{x,y=0}^{\sqrt{N}-1} G_{d,s\oplus 1;\,d',s'} \times \psi_{d',s';\,x-(-1)^{s\oplus 1}\delta_{d0},\,y-(-1)^{s\oplus 1}\delta_{d1}}(t)|d,s\rangle|x,y\rangle. \quad (6.41)$$

Expanding the left-hand side of the above equation in the computational basis and equating coefficients alike, we obtain the *evolution equation* of walker

$$\psi_{d,s;\,x,y}(t+1) = \sum_{d',s'=0}^{1} G_{d,s\oplus 1;\,d',s'}\, \psi_{d',s';\,x+(-1)^{s}\delta_{d0},\,y+(-1)^{s}\delta_{d1}}(t). \quad (6.42)$$

This equation is too complex to be solved the way it is written. In one-dimensional case, we have learned that by taking the Fourier transform on the spatial part, we can diagonalize the shift operator. This allowed us to find analytically the state of the quantum walk at any time instant. The same technique works here.

6.2.1 Fourier Transform

The Fourier transform acts on the spatial part of the computational basis in the following form:

$$\left|\kappa_{k_x,k_y}\right\rangle = \frac{1}{\sqrt{N}} \sum_{x,y=0}^{\sqrt{N}-1} \omega_{\sqrt{N}}^{xk_x+yk_y} |x,y\rangle, \quad (6.43)$$

where $\omega_{\sqrt{N}} = \mathrm{e}^{\frac{2\pi \mathrm{i}}{\sqrt{N}}}$. The Fourier transform is the tensor product of the Fourier transform at each coordinate. The range of variables k_x and k_y is the same of x and y. For each value of k_x and k_y, $\left|\kappa_{k_x,k_y}\right\rangle$ is a vector written in the computational basis. The Fourier transform defines a new orthonormal basis $\left\{\left|\kappa_{k_x,k_y}\right\rangle : 0 \le k_x, k_y \le \sqrt{N}-1\right\}$ called *Fourier basis*. In this new basis, the generic state of the walker is

$$|\Psi(t)\rangle = \sum_{d,s=0}^{1} \sum_{k_x,k_y=0}^{\sqrt{N}-1} \tilde{\psi}_{d,s;\,k_x,k_y}(t)\, |d,s\rangle \left|\kappa_{k_x,k_y}\right\rangle, \quad (6.44)$$

where the coefficients are given by

$$\tilde{\psi}_{d,s;\,k_x,k_y} = \frac{1}{\sqrt{N}} \sum_{x,y=0}^{\sqrt{N}-1} \omega_{\sqrt{N}}^{-(xk_x+yk_y)} \psi_{d,s;\,x,y}. \quad (6.45)$$

The interpretation of this last equation is that the amplitudes of a state on the Fourier basis is the *Fourier transform* of the amplitudes in the computational basis.

Exercise 6.7. Show the following properties of the Fourier transform:

1. $|\kappa_{0,0}\rangle$ is the diagonal state of Hilbert space $\mathcal{H}^{\sqrt{N}} \otimes \mathcal{H}^{\sqrt{N}}$.
2. $\left\{\left|\kappa_{k_x,k_y}\right\rangle : 0 \leq k_x, k_y \leq \sqrt{N}-1\right\}$ is an orthonormal basis for Hilbert space $\mathcal{H}^{\sqrt{N}} \otimes \mathcal{H}^{\sqrt{N}}$.
3. $|0,0\rangle = \frac{1}{\sqrt{N}} \sum_{k_x,k_y=0}^{\sqrt{N}-1} \left|\kappa_{k_x,k_y}\right\rangle$.

Let us calculate the action of the shift operator on the spatial Fourier basis, that is, its action on $|d,s\rangle\left|\kappa_{k_x,k_y}\right\rangle$. Using (6.43), we have

$$\begin{aligned} S|d,s\rangle\left|\kappa_{k_x,k_y}\right\rangle &= \frac{1}{\sqrt{N}} \sum_{x,y=0}^{\sqrt{N}-1} \omega_{\sqrt{N}}^{xk_x+yk_y} S|d,s\rangle|x,y\rangle \\ &= \frac{1}{\sqrt{N}} \sum_{x,y=0}^{\sqrt{N}-1} \omega_{\sqrt{N}}^{xk_x+yk_y} |d,s\oplus 1\rangle \otimes \\ &\qquad |x+(-1)^s\delta_{d0}, y+(-1)^s\delta_{d1}\rangle. \end{aligned}$$

To simplify the last equation, we rename the dummy indices such that $x' = x + (-1)^s\delta_{d0}$ and $y' = y + (-1)^s\delta_{d1}$. Then,

$$\begin{aligned} S|d,s\rangle\left|\kappa_{k_x,k_y}\right\rangle &= \frac{1}{\sqrt{N}} \sum_{x',y'=0}^{\sqrt{N}-1} \omega_{\sqrt{N}}^{(x'-(-1)^s\delta_{d0})k_x+(y'-(-1)^s\delta_{d1})k_y} \\ &\qquad \times |d,s\oplus 1\rangle\left|x',y'\right\rangle \\ &= \omega_{\sqrt{N}}^{-(-1)^s(\delta_{d0}k_x+\delta_{d1}k_y)} |d,s\oplus 1\rangle\left|\kappa_{k_x,k_y}\right\rangle. \end{aligned} \tag{6.46}$$

This result is useful to diagonalize the evolution operator.

Applying U on vector $|d',s'\rangle\left|\kappa_{k_x,k_y}\right\rangle$ and using (6.46), we obtain

$$\begin{aligned} U\left|d',s'\right\rangle\left|\kappa_{k_x,k_y}\right\rangle &= S\left(\sum_{d,s=0}^{1} G_{d,s;d',s'}|d,s\rangle\left|\kappa_{k_x,k_y}\right\rangle\right) \\ &= \sum_{d,s=0}^{1} \omega_{\sqrt{N}}^{-(-1)^s(\delta_{d0}k_x+\delta_{d1}k_y)} G_{d,s;d',s'}|d,s\oplus 1\rangle\left|\kappa_{k_x,k_y}\right\rangle \\ &= \sum_{d,s=0}^{1} \omega_{\sqrt{N}}^{(-1)^s(\delta_{d0}k_x+\delta_{d1}k_y)} G_{d,s\oplus 1;d',s'}|d,s\rangle\left|\kappa_{k_x,k_y}\right\rangle. \end{aligned}$$

The entries of U on the spatial Fourier basis are

$$\left\langle d, s, \kappa_{k'_x,k'_y} \middle| U \middle| d', s', \kappa_{k_x,k_y} \right\rangle = \frac{\omega^{(-1)^s(\delta_{d0}k_x+\delta_{d1}k_y)}}{\sqrt{N}} G_{d,s\oplus 1;\, d',s'}\, \delta_{k_x,k'_x}\delta_{k_y,k'_y}. \quad (6.47)$$

For each k_x and k_y, we define operator $\tilde{G}$ with entries

$$\tilde{G}_{d,s;\,d',s'} = \frac{\omega^{(-1)^s(\delta_{d0}k_x+\delta_{d1}k_y)}}{\sqrt{N}} G_{d,s\oplus 1;\, d',s'}. \quad (6.48)$$

The matrix representation is

$$\tilde{G} = \begin{bmatrix} 0 & \frac{\omega^{k_x}}{\sqrt{N}} & 0 & 0 \\ \frac{\omega^{-k_x}}{\sqrt{N}} & 0 & 0 & 0 \\ 0 & 0 & 0 & \frac{\omega^{k_y}}{\sqrt{N}} \\ 0 & 0 & \frac{\omega^{-k_y}}{\sqrt{N}} & 0 \end{bmatrix} \cdot G. \quad (6.49)$$

Equation (6.47) shows that the non-diagonal part of operator U is associated with the coin space. The goal now is to diagonalize operator $\tilde{G}$. The tensor products of eigenvectors of $\tilde{G}$ with vector $\left|\kappa_{k_x,k_y}\right\rangle$ are eigenvectors of U associated with the same eigenvalues of $\tilde{G}$.

If $k_x = 0$ and $k_y = 0$, matrix $\tilde{G}$ reduces to

$$\tilde{G}_{(k_x=0,k_y=0)} = \frac{1}{2}\begin{bmatrix} 1 & -1 & 1 & 1 \\ -1 & 1 & 1 & 1 \\ 1 & 1 & 1 & -1 \\ 1 & 1 & -1 & 1 \end{bmatrix}. \quad (6.50)$$

The determinant $\left|\tilde{G}_{(k_x=0,k_y=0)} - \lambda I\right|$ is $(\lambda-1)^3(\lambda+1)$. Therefore, the eigenvalues are $+1$ with multiplicity 3 and -1 with multiplicity 1. The eigenvectors associated with eigenvalue $+1$ are

$$\left|\nu^{1a}_{0,0}\right\rangle = \frac{1}{2}\begin{bmatrix} 1 \\ 1 \\ 1 \\ 1 \end{bmatrix}, \left|\nu^{1b}_{0,0}\right\rangle = \frac{1}{\sqrt{2}}\begin{bmatrix} 1 \\ -1 \\ 0 \\ 0 \end{bmatrix}, \left|\nu^{1c}_{0,0}\right\rangle = \frac{1}{\sqrt{2}}\begin{bmatrix} 0 \\ 0 \\ 1 \\ -1 \end{bmatrix}. \quad (6.51)$$

The eigenvector associated with eigenvalue -1 is

$$\left|\nu^{-1}_{0,0}\right\rangle = \frac{1}{2}\begin{bmatrix} 1 \\ 1 \\ -1 \\ -1 \end{bmatrix}. \quad (6.52)$$

Note that $\left|v_{0,0}^{1a}\right\rangle = |\mathrm{D}\rangle$. The set of these eigenvectors is an orthonormal basis.

If $k_x \neq 0$ or $k_y \neq 0$, the determinant of $\tilde{G} - \lambda I$ is

$$\left|\tilde{G} - \lambda I\right| = \left(\lambda^2 - 1\right)\left(\lambda^2 - \left(\cos\frac{2\pi k_x}{\sqrt{N}} + \cos\frac{2\pi k_y}{\sqrt{N}}\right)\lambda + 1\right). \tag{6.53}$$

Therefore, the eigenvalues of $\tilde{G}$ are

$$\lambda = \begin{cases} \pm 1, \\ \mathrm{e}^{\pm \mathrm{i}\theta(k_x,k_y)}, \end{cases} \tag{6.54}$$

where

$$\cos\theta(k_x,k_y) = \frac{1}{2}\left(\cos\frac{2\pi k_x}{\sqrt{N}} + \cos\frac{2\pi k_y}{\sqrt{N}}\right). \tag{6.55}$$

Eigenvectors $|v\rangle = (a,b,c,d)$ are found as follows: We calculate vector $(\tilde{G} - \lambda I)|v\rangle$ and equate each entry to zero. We have a system of four equations in variables a,b,c,d. We eliminate one of the equations, for example, the last one, and solve the system of equations in the three variables a,b,c. After that, choose the value d that normalizes the vector. This procedure for eigenvalue $+1$ results in eigenvector

$$\left|v_{k_x,k_y}^{+1}\right\rangle = \frac{1}{n^{(+1)}}\begin{bmatrix} \omega^{k_x}\left(\omega^{k_y}-1\right) \\ 1-\omega^{k_y} \\ \omega^{k_y}\left(1-\omega^{k_x}\right) \\ \omega^{k_x}-1 \end{bmatrix}. \tag{6.56}$$

For eigenvalue -1, we have

$$\left|v_{k_x,k_y}^{-1}\right\rangle = \frac{1}{n^{(-1)}}\begin{bmatrix} -\omega^{k_x}\left(1+\omega^{k_y}\right) \\ -\left(1+\omega^{k_y}\right) \\ \omega^{k_y}\left(1+\omega^{k_x}\right) \\ 1+\omega^{k_x} \end{bmatrix}. \tag{6.57}$$

In these expressions we are taking $\omega = \omega_{\sqrt{N}}$. Variables $n^{(\pm 1)}$ are normalization constants. For eigenvalues $\pm\theta(k_x,k_y)$, we denote the eigenvectors by $\left|v_{k_x,k_y}^{\pm\theta}\right\rangle$. Let us show the expression for the positive case:

$$\left|v_{k_x,k_y}^{+\theta}\right\rangle = \frac{\mathrm{i}}{2\sqrt{2}\sin\theta}\begin{bmatrix} \mathrm{e}^{-\mathrm{i}\theta} - \omega^{k_x} \\ \mathrm{e}^{-\mathrm{i}\theta} - \omega^{-k_x} \\ \mathrm{e}^{-\mathrm{i}\theta} - \omega^{k_y} \\ \mathrm{e}^{-\mathrm{i}\theta} - \omega^{-k_y} \end{bmatrix}. \tag{6.58}$$

To obtain the fourth eigenvector, we replace θ by $-\theta$. Remember that θ depends on k_x and k_y. The expression for $\sin\theta$ can be obtained from (6.55).

If $k_x = k_y$ or $k_x = \sqrt{N} - k_y$, the eigenvectors simplify to the following expressions:

$$\left|v^{+\theta}_{k_x,k_x}\right\rangle = \frac{1}{\sqrt{2}}\begin{bmatrix}1\\0\\1\\0\end{bmatrix},\quad \left|v^{-\theta}_{k_x,k_x}\right\rangle = \frac{1}{\sqrt{2}}\begin{bmatrix}0\\1\\0\\1\end{bmatrix}, \tag{6.59}$$

$$\left|v^{+\theta}_{k_x,\sqrt{N}-k_x}\right\rangle = \frac{1}{\sqrt{2}}\begin{bmatrix}1\\0\\0\\1\end{bmatrix},\quad \left|v^{-\theta}_{k_x,\sqrt{N}-k_x}\right\rangle = \frac{1}{\sqrt{2}}\begin{bmatrix}0\\1\\1\\0\end{bmatrix}. \tag{6.60}$$

Note that if $\sqrt{N}$ is even and $k_x = k_y = \frac{\sqrt{N}}{2}$, (6.55) implies that $\theta = \pi$. In this case, the eigenvectors of (6.59) have eigenvalue -1. The basis is complete when we take the eigenvectors of (6.56) and (6.57). The eigenvalue -1 has multiplicity 3 and eigenvalue 1 has multiplicity 1. Matrix $\tilde{G}$ is the negative of the matrix described in (6.50).

The union of sets $\left\{|v^{1a}_{0,0}\rangle|\kappa_{0,0}\rangle,\ |v^{1b}_{0,0}\rangle|\kappa_{0,0}\rangle,\ |v^{1c}_{0,0}\rangle|\kappa_{0,0}\rangle,\ |v^{-1}_{0,0}\rangle|\kappa_{0,0}\rangle\right\}$ and $\left\{\left|v^{+1}_{k_x,k_y}\right\rangle|\kappa_{k_x,k_y}\rangle,\ \left|v^{-1}_{k_x,k_y}\right\rangle|\kappa_{k_x,k_y}\rangle,\ \left|v^{\pm\theta}_{k_x,k_y}\right\rangle|\kappa_{k_x,k_y}\rangle : 0 \le k_x, k_y < \sqrt{N},\ (k_x,k_y) \ne (0,0)\right\}$ is an orthonormal basis of eigenvectors of U for Hilbert space $\mathcal{H}^2 \otimes \mathcal{H}^2 \otimes \mathcal{H}^{\sqrt{N}} \otimes \mathcal{H}^{\sqrt{N}}$. The associated eigenvalues are ± 1 and $e^{\pm i\theta(k_x,k_y)}$.

Exercise 6.8. Show that the norm of $\left|v^{\pm 1}_{k_x,k_y}\right\rangle$ is

$$n^{(\pm 1)} = 2\sqrt{2}\left(1 \mp \cos\theta\right)^{\frac{1}{2}}.$$

Obtain expressions $n^{(+1)} = 4\sin\frac{\theta}{2}$ and $n^{(-1)} = 4\cos\frac{\theta}{2}$.

Exercise 6.9. Show that $\left|v^{1a}_{0,0}\right\rangle$ is orthogonal to $\left|v^{\pm 1}_{k_x,k_y}\right\rangle$.

Exercise 6.10. Verify that $\left|v^{+\theta}_{k_x,k_y}\right\rangle$ given by (6.58) is a unit vector. Show that $\left|v^{+\theta}_{k_x,k_y}\right\rangle$ is an eigenvector of $\tilde{G}$ associated with eigenvalue $e^{i\theta}$.

Exercise 6.11. Vector $\left|v^{-\theta}_{k_x,k_y}\right\rangle$ is the complex conjugate of $\left|v^{\theta}_{k_x,k_y}\right\rangle$?

Exercise 6.12. Show that

1. $|\mathrm{D}\rangle = \frac{\left|v^{\theta}_{k_x,k_y}\right\rangle + \left|v^{-\theta}_{k_x,k_y}\right\rangle}{\sqrt{2}}$,
2. $\left\langle v^{\pm\theta}_{k_x,k_y}|\mathrm{D}\right\rangle = \frac{1}{\sqrt{2}}$,
3. $\langle \mathrm{D}|\tilde{G}|\mathrm{D}\rangle = \cos\theta$.

6.2.2 Analytical Solutions

Let us calculate the state of the quantum walk at a generic time instant. Let us take as initial condition state

$$|\Psi(0)\rangle = |\mathrm{D}\rangle|0,0\rangle, \tag{6.61}$$

that is, a walker located at the vertex $(0,0)$ with the diagonal state of the coin space.

Let us use the following notation for the eigenvalues and eigenvectors of U: $\left|\nu^j_{k_x,k_y}\right\rangle|\kappa_{k_x,k_y}\rangle$, where the eigenvalues have the form $\nu^j_{k_x,k_y}$ and $1 \leq j \leq 4$. Then,

$$U = \sum_{j=1}^{4} \sum_{k_x,k_y=0}^{\sqrt{N}-1} \nu^j_{k_x,k_y} \left|\nu^j_{k_x,k_y}, \kappa_{k_x,k_y}\right\rangle\left\langle\nu^j_{k_x,k_y}, \kappa_{k_x,k_y}\right|. \tag{6.62}$$

At time t, the state of the quantum walk will be given by

$$\begin{aligned}|\Psi(t)\rangle &= U^t|\Psi(0)\rangle \\ &= \sum_{j=1}^{4} \sum_{k_x,k_y=0}^{\sqrt{N}-1} (\nu^j_{k_x,k_y})^t \left\langle\nu^j_{k_x,k_y}, \kappa_{k_x,k_y}\middle|\Psi(0)\right\rangle \\ &\quad \times \left|\nu^j_{k_x,k_y}\right\rangle|\kappa_{k_x,k_y}\rangle,\end{aligned} \tag{6.63}$$

The state of the quantum walk at time t can be calculated explicitly. The task is reduced to calculate the entries of the initial condition in the basis of eigenvectors of U and, after that, to calculate the t-th power of the eigenvalues. We have already obtained explicit expressions for the eigenvalues and eigenvectors of U.

Using (6.63), we obtain

$$|\Psi(t)\rangle = \sum_{j=1}^{4} \sum_{k_x,k_y=0}^{\sqrt{N}-1} (\nu^j_{k_x,k_y})^t \left\langle\nu^j_{k_x,k_y}\middle|\mathrm{D}\right\rangle\langle\kappa_{k_x,k_y}|0,0\rangle \left|\nu^j_{k_x,k_y}\right\rangle|\kappa_{k_x,k_y}\rangle. \tag{6.64}$$

Using (6.43), we have $\langle\kappa_{k_x,k_y}|0,0\rangle = 1/\sqrt{N}$. Among all eigenvectors of $\tilde{G}$, only $\left|\nu^{1a}_{0,0}\right\rangle$ and $\left|\nu^{\pm\theta}_{k_x,k_y}\right\rangle$ are not orthogonal to $|\mathrm{D}\rangle$. Therefore, the above equation reduces to

$$\begin{aligned}|\Psi(t)\rangle &= \frac{(+1)^t}{\sqrt{N}} \left|\nu^{1a}_{0,0}\right\rangle|\kappa_{0,0}\rangle \\ &\quad + \frac{1}{\sqrt{N}} \sum_{\substack{k_x,k_y=0 \\ (k_x,k_y)\neq(0,0)}}^{\sqrt{N}-1} (\mathrm{e}^{\mathrm{i}\theta})^t \left\langle\nu^{\theta}_{k_x,k_y}\middle|\mathrm{D}\right\rangle \left|\nu^{\theta}_{k_x,k_y}\right\rangle|\kappa_{k_x,k_y}\rangle \\ &\quad + (\mathrm{e}^{-\mathrm{i}\theta})^t \left\langle\nu^{-\theta}_{k_x,k_y}\middle|\mathrm{D}\right\rangle \left|\nu^{-\theta}_{k_x,k_y}\right\rangle|\kappa_{k_x,k_y}\rangle.\end{aligned} \tag{6.65}$$

Since $\left\langle \nu^{\pm\theta}_{k_x,k_y} \middle| \mathrm{D} \right\rangle = 1/\sqrt{2}$, it follows that the state of the quantum walk at time t is

$$|\Psi(t)\rangle = \frac{1}{\sqrt{N}} |\mathrm{D}\rangle|\mathrm{D}\rangle + \frac{1}{\sqrt{2N}} \sum_{\substack{k_x,k_y=0 \\ (k_x,k_y)\neq(0,0)}}^{\sqrt{N}-1} \left(\mathrm{e}^{\mathrm{i}\theta t} \left| \nu^{\theta}_{k_x,k_y} \right\rangle + \mathrm{e}^{-\mathrm{i}\theta t} \left| \nu^{-\theta}_{k_x,k_y} \right\rangle \right) |\kappa_{k_x,k_y}\rangle, \quad (6.66)$$

where $|\kappa_{k_x,k_y}\rangle$, θ, and $\left| \nu^{\pm\theta}_{k_x,k_y} \right\rangle$ are given by (6.43), (6.55), and (6.58), respectively.

Exercise 6.13. Show that (6.66) reduces to (6.61) when $t = 0$.

Exercise 6.14. The purpose of this exercise is to analyze the quantum walk on a finite-dimensional lattice with a *shift operator* that does not invert the coin.

1. Obtain the shift operator analogous to (6.46) without inverting the direction of the coin.
2. Show that the matrix $\tilde{G}$, analogous to (6.48), is

$$\tilde{G} = \begin{bmatrix} \omega^{k_x}_{\sqrt{N}} & 0 & 0 & 0 \\ 0 & \omega^{-k_x}_{\sqrt{N}} & 0 & 0 \\ 0 & 0 & \omega^{k_y}_{\sqrt{N}} & 0 \\ 0 & 0 & 0 & \omega^{-k_y}_{\sqrt{N}} \end{bmatrix} \cdot G. \quad (6.67)$$

3. Obtain the eigenvalues and eigenvectors of this new matrix $\tilde{G}$.
4. Use (6.61) as initial condition. Find the state of the quantum walk $|\Psi(t)\rangle$ at time t, analogous to (6.66).

6.3 Hypercube

The *hypercube* is an n-dimensional *regular graph* of *degree* n with $N = 2^n$ vertices. The labels of the vertices are binary n-tuples. Two vertices are *adjacent* if and only if their corresponding n-tuples differ only by one bit, that is, their *Hamming distance* is equal to 1. The edges also have labels, which specify the entry of the tuples that has different bits, that is, if two vertices differ in the a-th entry, the label of the edge connecting these vertices is a. The Hilbert space associated with a quantum walk on the hypercube is $\mathcal{H} = \mathcal{H}^n \otimes \mathcal{H}^{2^n}$. Vectors of the form $|a\rangle|\vec{v}\rangle$, where $1 \leq a \leq n$ and $\vec{v}$ are binary n-tuples, form the computational basis of $\mathcal{H}$. Vector $|a\rangle$ is a coin state associated with the edge of label a, specifying the direction of movement. In this

section, we use vector $|1\rangle$ as the first vector of the computational basis of the coin space. Vector $|\vec{v}\rangle$ is in the computational basis of $\mathcal{H}^{2^n}$ and specifies in which vertex the walker is.

Exercise 6.15. Make a sketch of a 3-dimensional hypercube and label all vertices and all edges.

The *shift operator* should move the walker from state $|a\rangle|\vec{v}\rangle$ to $|a\rangle|\vec{v} \oplus \vec{e}_a\rangle$, where $\vec{e}_a$ is the binary n-tuple with all entries zero except the a-th entry, the value of which is 1. Operation $\oplus$ is the *binary sum* (*bitwise xor*). This shift has the following meaning: if the coin value is a and the walker position is $\vec{v}$, the walker will move through edge a to the adjacent vertex $|\vec{v} \oplus \vec{e}_a\rangle$. The coin is unchanged after the shift, characterizing a *flip–flop shift*, because in binary arithmetic the inverse of a is a ($a \oplus a = 0$). So,

$$S|a\rangle|\vec{v}\rangle = |a\rangle|\vec{v} \oplus \vec{e}_a\rangle. \tag{6.68}$$

An equivalent way of writing the shift operator is

$$S = \sum_{a=1}^{n} \sum_{\vec{v}=0}^{2^n-1} |a, \vec{v} \oplus \vec{e}_a\rangle\langle a, \vec{v}|. \tag{6.69}$$

The range of variable $\vec{v}$ (in the sum) is written in decimal base. For example, the notation $\vec{v} = 2^n - 1$ means $\vec{v} = (1, \ldots, 1)$. We will use this notation if its meaning is clear from the context.

We will use the *Grover coin*, which is

$$G = 2|\mathrm{D}\rangle\langle\mathrm{D}| - I, \tag{6.70}$$

where $|\mathrm{D}\rangle$ is the *diagonal state* of the coin space. The matrix representation is

$$G = \begin{bmatrix} \frac{2}{n} - 1 & \frac{2}{n} & \cdots & \frac{2}{n} \\ \frac{2}{n} & \frac{2}{n} - 1 & \cdots & \frac{2}{n} \\ \vdots & \vdots & \ddots & \vdots \\ \frac{2}{n} & \frac{2}{n} & \cdots & \frac{2}{n} - 1 \end{bmatrix}. \tag{6.71}$$

The entries of G are $G_{ij} = \frac{2}{n} - \delta_{ij}$. The Grover coin is invariant under permutation of directions. That is, if the labels of edges were interchanged (keeping the labels of the vertices), the Grover coin would drive the walker to follow the same path. This is equivalent to keep the labels and to swap the rows and columns of G corresponding to the permutation of labels. The *Grover matrix* is unchanged by simultaneous permutation of rows and columns.

A generic state of the walker at time t is described by

$$|\Psi(t)\rangle = \sum_{a=1}^{n} \sum_{\vec{v}=0}^{2^n-1} \psi_{a,\vec{v}}(t) \big|a, \vec{v}\big\rangle, \tag{6.72}$$

where coefficients $\psi_{a,\vec{v}}(t)$ are complex functions that obey the *normalization condition*

$$\sum_{a=1}^{n} \sum_{\vec{v}=0}^{2^n-1} \big|\psi_{a,\vec{v}}(t)\big|^2 = 1. \tag{6.73}$$

Applying the *standard evolution operator*

$$U = S\ (G \otimes I) \tag{6.74}$$

to the generic state, we obtain

$$\begin{aligned} |\Psi(t+1)\rangle &= \sum_{b=1}^{n} \sum_{\vec{v}=0}^{2^n-1} \psi_{b,\vec{v}}(t)\ S\Big(G|b\rangle\big|\vec{v}\big\rangle\Big) \\ &= \sum_{b=1}^{n} \sum_{\vec{v}=0}^{2^n-1} \psi_{b,\vec{v}}(t)\ S\Big(\sum_{a=1}^{n} G_{ab}|a\rangle\big|\vec{v}\big\rangle\Big) \\ &= \sum_{a,b=1}^{n} \sum_{\vec{v}=0}^{2^n-1} \psi_{b,\vec{v}}(t)\ G_{ab}|a\rangle\big|\vec{v} \oplus \vec{e}_a\big\rangle. \end{aligned}$$

We can rename the dummy index $\vec{v}$ to $\vec{v} \oplus \vec{e}_a$. So,

$$|\Psi(t+1)\rangle = \sum_{a,b=1}^{n} \sum_{\vec{v}=0}^{2^n-1} G_{ab}\ \psi_{b,\vec{v}\oplus\vec{e}_a}(t)\ |a\rangle\big|\vec{v}\big\rangle. \tag{6.75}$$

Expanding the left-hand side of the above equation on computational basis and equating coefficients alike, we obtain the evolution equation

$$\psi_{a,\vec{v}}(t+1) = \sum_{b=1}^{n} G_{ab}\ \psi_{b,\vec{v}\oplus\vec{e}_a}(t). \tag{6.76}$$

This equation is too complex to be solved the way it is written. For the cycle and the finite two-dimensional lattice, we have learned that we can diagonalize the shift operator by taking the Fourier transform on the spatial part. This technique has allowed us to analytically solve the evolution equation. The same technique works here.

6.3.1 Fourier Transform

The *Fourier transform* acts on the computational basis as follows:

$$\left|\beta_{\vec{k}}\right\rangle \equiv \frac{1}{\sqrt{2^n}} \sum_{\vec{v}=0}^{2^n-1} (-1)^{\vec{k}\cdot\vec{v}} \left|\vec{v}\right\rangle, \tag{6.77}$$

where $\vec{k}\cdot\vec{v}$ is the inner product between *binary vectors* $\vec{k}$ and $\vec{v}$. The range of variable $\vec{k}$ is the same of variable $\vec{v}$. As before, the Fourier transform defines a new orthonormal basis $\left\{\left|\beta_{\vec{k}}\right\rangle : 0 \leq \vec{k} \leq 2^n - 1\right\}$ called *Fourier basis*. In this new basis, the generic state of the walker is

$$|\Psi(t)\rangle = \sum_{a=1}^{n} \sum_{\vec{k}=0}^{2^n-1} \tilde{\psi}_{a,\vec{k}}(t) \left|a\right\rangle \left|\beta_{\vec{k}}\right\rangle, \tag{6.78}$$

where coefficients $\tilde{\psi}_{a,\vec{k}}(t)$ are given by

$$\tilde{\psi}_{a,\vec{k}} = \frac{1}{\sqrt{2^n}} \sum_{\vec{v}=0}^{2^n-1} (-1)^{\vec{k}\cdot\vec{v}} \psi_{a,\vec{v}}. \tag{6.79}$$

The interpretation of this last equation is that the amplitudes of a state on the Fourier basis is the *Fourier transform* of the amplitudes in the computational basis.

Exercise 6.16. Show the following properties of the Fourier transform:

1. $\left|\beta_{\vec{0}}\right\rangle$ is the diagonal state of Hilbert space $\mathcal{H}^{2^n}$.
2. $\left\{\left|\beta_{\vec{k}}\right\rangle : 0 \leq \vec{k} \leq 2^n - 1\right\}$ is an orthonormal basis for the Hilbert space $\mathcal{H}^{2^n}$.
3. $\left|\vec{0}\right\rangle = \frac{1}{\sqrt{2^n}} \sum_{\vec{k}=0}^{2^n-1} \left|\beta_{\vec{k}}\right\rangle$.

We will show that the shift operator is diagonal in basis $\left\{\left|a\right\rangle \left|\beta_{\vec{k}}\right\rangle : 1 \leq a \leq n,\right.$ $\left. 0 \leq \vec{k} \leq 2^n - 1\right\}$, that is, we show that $\left|a\right\rangle \left|\beta_{\vec{k}}\right\rangle$ is an eigenvector of S. In fact, using (6.77), we have

$$\begin{aligned} S\left|a\right\rangle \left|\beta_{\vec{k}}\right\rangle &= \frac{1}{\sqrt{2^n}} \sum_{\vec{v}=0}^{2^n-1} (-1)^{\vec{k}\cdot\vec{v}} S\left|a,\vec{v}\right\rangle \\ &= \frac{1}{\sqrt{2^n}} \sum_{\vec{v}=0}^{2^n-1} (-1)^{\vec{k}\cdot\vec{v}} \left|a,\vec{v}\oplus\vec{e}_a\right\rangle \end{aligned}$$

$$= \frac{1}{\sqrt{2^n}} \sum_{\vec{v}=0}^{2^n-1} (-1)^{\vec{k}\cdot(\vec{v}\oplus\vec{e}_a)} \left|a, \vec{v}\right\rangle$$

$$= (-1)^{\vec{k}\cdot\vec{e}_a} |a\rangle \left|\beta_{\vec{k}}\right\rangle. \tag{6.80}$$

The inner product $\vec{k}\cdot\vec{e}_a$ is the a-th entry of $\vec{k}$, which we denote by k_a. Therefore, $(-1)^{k_a}$ is the eigenvalue associated with eigenvector $|a\rangle\left|\beta_{\vec{k}}\right\rangle$.

We have showed that S is a diagonal operator in the new basis, but this does not imply that the evolution operator is diagonal. If the coin operator is not diagonal, the evolution operator is not diagonal too. However, we want to diagonalize the evolution operator to explicitly calculate the state of the quantum walk at generic time t. Despite being a hard-working task, we explicitly calculate expressions for the eigenvalues and eigenvectors of U.

Applying U on vector $|b\rangle\left|\beta_{\vec{k}}\right\rangle$ and using (6.80), we obtain

$$U|b\rangle\left|\beta_{\vec{k}}\right\rangle = S\left(\sum_{a=1}^{n} G_{ab}\,|a\rangle\left|\beta_{\vec{k}}\right\rangle\right)$$

$$= \sum_{a=1}^{n} (-1)^{k_a} G_{ab}\,|a\rangle\left|\beta_{\vec{k}}\right\rangle. \tag{6.81}$$

The entries of U on the spatial Fourier basis is

$$\left\langle a, \beta_{\vec{k}'}\right| U \left|b, \beta_{\vec{k}}\right\rangle = (-1)^{k_a} G_{ab}\,\delta_{\vec{k},\vec{k}'}. \tag{6.82}$$

Let us define operator $\tilde{G}$ with entries $\tilde{G}_{ab} = (-1)^{k_a} G_{ab}$ for generic vectors $\vec{k}$ and $\vec{k}'$.

The goal now is to diagonalize operator $\tilde{G}$. Let us start with the simplest case, which is $\vec{k} = \vec{0} = (0, \cdots, 0)$. In this case, operator $\tilde{G}$ is reduced to the Grover operator G. First, note that $G^2 = I$. So, the eigenvalues are ± 1. We know that $|\mathrm{D}\rangle$ is an eigenvector of G associated with eigenvalue 1. Let us focus now on the eigenvectors associated with eigenvalue -1. We must look for vectors $|\alpha\rangle$ such that $(G + I)|\alpha\rangle = 0$. Using (6.70), we conclude that $G + I$ is a matrix with all entries equal to $2/n$. It follows that any vector of the form

$$\left|\alpha_a^{\vec{0}}\right\rangle = \frac{1}{\sqrt{2}} \left(|1\rangle - |a\rangle\right), \tag{6.83}$$

where $1 < a \leq n$, is an eigenvector of G associated with eigenvalue -1. Counting the number of vectors, it follows that set $\left\{\left|\alpha_a^{\vec{0}}\right\rangle : 1 \leq a \leq n\right\}$, where $\left|\alpha_1^{\vec{0}}\right\rangle = |\mathrm{D}\rangle$, is a non-orthogonal basis of eigenvectors of G of Hilbert space $\mathcal{H}^n$.

Let us calculate the spectral decomposition when $\vec{k} = (1, \ldots, 1)$. In this case, we have $\tilde{G} = -G$ and the eigenvectors of G associated with eigenvalue -1 are eigenvectors of $\tilde{G}$ associated with eigenvalue $+1$ and vice versa. In summary, eigenvectors

$$\left|\alpha_a^{\vec{1}}\right\rangle = \frac{1}{\sqrt{2}}\left(|a\rangle - |n\rangle\right), \tag{6.84}$$

where $1 \leq a \leq n-1$, are associated with eigenvalue $+1$ and $\left|\alpha_n^{\vec{1}}\right\rangle = |\mathrm{D}\rangle$ is associated with eigenvalue -1.

Now let us consider a vector $\vec{k}$ with *Hamming weight* $0 < k < n$, that is, with k entries equal to 1 and $n-k$ equal to 0. Matrix $\tilde{G}$ is obtained from G by inverting the signs of the rows corresponding to the entries of $\vec{k}$ that are equal to 1. Therefore, k rows of $\tilde{G}$ invert signs compared to G. To find the eigenvectors associated with eigenvalues ± 1, we see the Hilbert space as a sum of two vector spaces, the first associated with the rows that have not inverted the sign and the second associated with the rows that have inverted the signs. By permutating rows and columns, matrix $\tilde{G}$ assumes the following form:

$$\tilde{G} = \left[\begin{array}{ccc|ccc} \frac{2}{n}-1 & \frac{2}{n} & \cdots & & & \\ \frac{2}{n} & \frac{2}{n}-1 & & & \frac{2}{n} & \\ \vdots & & \ddots & & & \\ \hline & & & -\frac{2}{n}+1 & -\frac{2}{n} & \cdots \\ & -\frac{2}{n} & & -\frac{2}{n} & -\frac{2}{n}+1 & \\ & & & \vdots & & \ddots \end{array}\right], \tag{6.85}$$

where the first diagonal block is a $(n-k)$-square matrix and the second block is a k-square matrix. To find the eigenvalues associated with eigenvalue 1, we look for vectors $|\alpha\rangle$ such that $(\tilde{G} - I)|\alpha\rangle = 0$. Note that

$$\tilde{G} - I = \left[\begin{array}{ccc|c} \frac{2}{n}-2 & \frac{2}{n} & \cdots & \\ \frac{2}{n} & \frac{2}{n}-2 & & \frac{2}{n} \\ \vdots & & \ddots & \\ \hline & -\frac{2}{n} & & -\frac{2}{n} \end{array}\right]. \tag{6.86}$$

Therefore, a vector of the form[2] $|\alpha\rangle = (0,\ldots,0 \mid 1,-1,0,\ldots,0)/\sqrt{2}$ is an eigenvector of eigenvalue 1. Vector $|\alpha\rangle$ has zero entries except at two positions corresponding to the rows that inverted the sign, the first position with value $+1$ and the second with value -1. We can build $k-1$ vectors in this way. Following the same method, we conclude that we can find $n-k-1$ eigenvectors with zero entries except for two positions corresponding to the rows that have not inverted sign, with values $+1$ and -1 too. The total number of eigenvectors found so far is $(k-1)+(n-k-1)=n-2$. Therefore, it is missing two eigenvectors associated with the complex non-real eigenvalues.

The remaining two eigenvectors can be found as follows: If a matrix has the property that the sum of the entries of a row is invariant for all rows, the vector with entries equal to 1 is an eigenvector with eigenvalue 1. In the case of matrix $\tilde{G}$, this property is valid in two blocks. The first block consists of the first $n-k$ rows and second of k remaining rows. Therefore, the form of the eigenvector should be $|\alpha\rangle = (a,\ldots,a \mid b,\ldots,b)$, that is, the first $n-k$ entries must have some value a, and the k remaining entries must have some value b. Without loss of generality, we take $b=1$. Let $\mathrm{e}^{\mathrm{i}\omega_k}$ be the corresponding eigenvalue. Note that the eigenvalue depends on k (the Hamming weight of $\vec{k}$), but it does not depend explicitly on $\vec{k}$. We solve the matrix equation

$$\left[\begin{array}{ccc|ccc} \frac{2}{n}-1-\mathrm{e}^{\mathrm{i}\omega_k} & \frac{2}{n} & \cdots & & & \\ \frac{2}{n} & \frac{2}{n}-1-\mathrm{e}^{\mathrm{i}\omega_k} & & & \frac{2}{n} & \\ \vdots & & \ddots & & & \\ \hline & & & -\frac{2}{n}+1-\mathrm{e}^{\mathrm{i}\omega_k} & -\frac{2}{n} & \cdots \\ & -\frac{2}{n} & & -\frac{2}{n}+1-\mathrm{e}^{\mathrm{i}\omega_k} & -\frac{2}{n} & \\ & & & \vdots & & \ddots \end{array}\right] \left[\begin{array}{c} a \\ \\ \vdots \\ \\ a \\ \hline 1 \\ \vdots \\ 1 \end{array}\right] = 0,$$

which reduces to

$$\begin{cases} \left(1-\frac{2k}{n}-\mathrm{e}^{\mathrm{i}\omega_k}\right)a+\frac{2k}{n}=0, \\ -2\left(1-\frac{k}{n}\right)a+1-\frac{2k}{n}-\mathrm{e}^{\mathrm{i}\omega_k}=0. \end{cases} \tag{6.87}$$

Solving this system of equations, we obtain

[2] The vertical bar separates the first $n-k$ entries from the last k entries.

$$\begin{cases} a = \pm \mathrm{i} \frac{\sqrt{\frac{k}{n}}}{\sqrt{1-\frac{k}{n}}}, \\ \\ \mathrm{e}^{\mathrm{i}\omega_k} = 1 - \frac{2k}{n} \mp 2\mathrm{i}\sqrt{\frac{k}{n}\left(1-\frac{k}{n}\right)}. \end{cases} \tag{6.88}$$

Then,

$$\begin{cases} \cos\omega_k = 1 - \frac{2k}{n}, \\ \\ \sin\omega_k = \mp 2\sqrt{\frac{k}{n}\left(1-\frac{k}{n}\right)}. \end{cases} \tag{6.89}$$

We have found the two remaining eigenvectors. Normalizing, the eigenvector associated with eigenvalue $\mathrm{e}^{\mathrm{i}\omega_k}$ is written as

$$\left|\alpha_1^{\vec{k}}\right\rangle = \frac{1}{\sqrt{2}} \begin{bmatrix} \frac{-\mathrm{i}}{\sqrt{n-k}} \\ \vdots \\ \frac{-\mathrm{i}}{\sqrt{n-k}} \\ \hline \\ \frac{1}{\sqrt{k}} \\ \vdots \\ \frac{1}{\sqrt{k}} \end{bmatrix}, \tag{6.90}$$

and eigenvector $\left|\alpha_n^{\vec{k}}\right\rangle$ associated with eigenvalue $\mathrm{e}^{-\mathrm{i}\omega_k}$ is the complex conjugate of vector $\left|\alpha_1^{\vec{k}}\right\rangle$.

These eigenvectors were described by separating the rows that inverted sign from the rows that have remained unchanged. We must permute the entries of the eigenvectors to match the rows in their original positions. The variable that points out which rows have inverted sign is $\vec{k}$. If entry k_a is zero, it means that there was no sign inversion in the a-th row, and if $k_a = 1$, then there was an inversion. The eigenvectors $\left|\alpha_1^{\vec{k}}\right\rangle$ and $\left|\alpha_n^{\vec{k}}\right\rangle$ associated with eigenvalues $\mathrm{e}^{\pm\mathrm{i}\omega_k}$ are written in the original basis as

$$\left|\alpha_1^{\vec{k}}\right\rangle = \frac{1}{\sqrt{2}} \sum_{a=1}^{n} \left(\frac{k_a}{\sqrt{k}} - \mathrm{i}\frac{1-k_a}{\sqrt{n-k}} \right) |a\rangle, \tag{6.91}$$

$$\left|\alpha_n^{\vec{k}}\right\rangle = \frac{1}{\sqrt{2}} \sum_{a=1}^{n} \left(\frac{k_a}{\sqrt{k}} + \mathrm{i}\frac{1-k_a}{\sqrt{n-k}} \right) |a\rangle, \tag{6.92}$$

for $0 < k < n$.

We conclude that set $\left\{\left|\phi_{a,\vec{k}}\right\rangle := \left|\alpha_a^{\vec{k}}\right\rangle\left|\beta_{\vec{k}}\right\rangle : 1 \leq a \leq n,\ 0 \leq \vec{k} \leq 2^n - 1\right\}$ is a non-orthogonal basis of eigenvectors of U for the Hilbert space $\mathcal{H}^n \otimes \mathcal{H}^{2^n}$. The eigenvalues are ± 1 and $e^{\pm i\omega_k}$. Expressions $\left|\alpha_a^{\vec{k}}\right\rangle$ in the computational basis are given by (6.83), (6.84) for $k = 0$ and $k = n$; and $\left|\alpha_1^{\vec{0}}\right\rangle = \left|\alpha_n^{\vec{1}}\right\rangle = |\mathrm{D}\rangle$ are particular cases. For $0 < k < n$, $a = 1$ or $a = n$, $\left|\alpha_a^{\vec{k}}\right\rangle$ are given by (6.91) and (6.92). Vectors $\left|\beta_{\vec{k}}\right\rangle$) are given by (6.77).

Exercise 6.17. Obtain explicit expressions for eigenvectors $\left|\alpha_a^{\vec{k}}\right\rangle$ when $0 < k < n$ and $0 < a < n$ associated with eigenvalues $e^{\pm i\omega_k}$.

Exercise 6.18. Show explicitly that the eigenvectors associated with eigenvalues $e^{\pm i\omega_k}$ are mutually orthogonal and orthogonal to the other eigenvectors.

Exercise 6.19. Show that the eigenvectors of (6.91) and (6.92) are unit vectors.

Exercise 6.20. Let $\phi_{a,\vec{k}}$ be the eigenvalue associated with eigenvector $\left|\phi_{a,\vec{k}}\right\rangle$. Make a table of all values $\phi_{a,\vec{k}}$ for all a and $\vec{k}$.

6.3.2 *Analytical Solutions*

Now we calculate the state of the quantum walk in a generic time instant. Let us use state

$$|\Psi(0)\rangle = |\mathrm{D}\rangle\left|\vec{0}\right\rangle, \tag{6.93}$$

as initial condition, that is, initially the walker is located at vertex $\vec{v} = \vec{0}$ with the *diagonal state* in the *coin space*. This initial condition is invariant under permutation of edges. Suppose that $\phi_{a,\vec{k}}$ is an eigenvalue associated with eigenvector $\left|\phi_{a,\vec{k}}\right\rangle$. Using the *spectral decomposition* of U, we have

$$U = \sum_{a,\vec{k}} \phi_{a,\vec{k}} \left|\phi_{a,\vec{k}}\right\rangle\left\langle\phi_{a,\vec{k}}\right|. \tag{6.94}$$

At time t, the state of the quantum walk will be given by

$$\begin{aligned} |\Psi(t)\rangle &= U^t|\Psi(0)\rangle \\ &= \sum_{a,\vec{k}} \left(\phi_{a,\vec{k}}^t \left\langle\phi_{a,\vec{k}}|\Psi(0)\right\rangle\right) \left|\phi_{a,\vec{k}}\right\rangle, \end{aligned} \tag{6.95}$$

Using the above equation, we have

$$
\begin{aligned}
|\Psi(t)\rangle &= \sum_{a,\vec{k}} (\phi_{a,\vec{k}})^t \left\langle \phi_{a,\vec{k}} | \Psi(0) \right\rangle \left| \phi_{a,\vec{k}} \right\rangle \\
&= \sum_{a,\vec{k}} (\phi_{a,\vec{k}})^t \left\langle \alpha_a^{\vec{k}} | \mathrm{D} \right\rangle \left\langle \beta_{\vec{k}} | \vec{0} \right\rangle \left| \alpha_a^{\vec{k}} \right\rangle | \beta_{\vec{k}} \rangle \\
&= \frac{1}{\sqrt{2^n}} \sum_{a,\vec{k}} (\phi_{a,\vec{k}})^t \left\langle \alpha_a^{\vec{k}} | \mathrm{D} \right\rangle \left| \alpha_a^{\vec{k}} \right\rangle | \beta_{\vec{k}} \rangle . \qquad (6.96)
\end{aligned}
$$

In the last formula, we have used (6.77) to simplify $\left\langle \beta_{\vec{k}} | \vec{0} \right\rangle$. Only eigenvectors $\left| \alpha_1^{\vec{0}} \right\rangle = |\mathrm{D}\rangle$, $\left| \alpha_n^{\vec{1}} \right\rangle = |\mathrm{D}\rangle$, and associated with eigenvalues $+1$ and -1, and eigenvectors of the type $\left| \alpha_1^{\vec{k}} \right\rangle$ and $\left| \alpha_n^{\vec{k}} \right\rangle$ for $0 < k < 2^n - 1$ associated with eigenvalues $\mathrm{e}^{\pm \mathrm{i}\omega_k}$ are not orthogonal to vector $|\mathrm{D}\rangle$. Therefore, (6.96) reduces to

$$
\begin{aligned}
|\Psi(t)\rangle = \frac{1}{\sqrt{2^n}} \Big(& (1)^t \left| \alpha_1^{\vec{0}} \right\rangle | \beta_{\vec{0}} \rangle + (-1)^t \left| \alpha_n^{\vec{1}} \right\rangle | \beta_{\vec{1}} \rangle \\
& + \sum_{\vec{k}=1}^{2^n-2} (\mathrm{e}^{\mathrm{i}\omega_k})^t \left\langle \alpha_1^{\vec{k}} | \mathrm{D} \right\rangle \left| \alpha_1^{\vec{k}} \right\rangle | \beta_{\vec{k}} \rangle \\
& + \sum_{\vec{k}=1}^{2^n-2} (\mathrm{e}^{-\mathrm{i}\omega_k})^t \left\langle \alpha_n^{\vec{k}} | \mathrm{D} \right\rangle \left| \alpha_n^{\vec{k}} \right\rangle | \beta_{\vec{k}} \rangle \Big) . \qquad (6.97)
\end{aligned}
$$

Using (6.91), we have

$$
\left\langle \alpha_1^{\vec{k}} | \mathrm{D} \right\rangle = \frac{1}{\sqrt{2}} \left(\sqrt{\frac{k}{n}} + \mathrm{i} \sqrt{1 - \frac{k}{n}} \right) , \qquad (6.98)
$$

$$
\left\langle \alpha_n^{\vec{k}} | \mathrm{D} \right\rangle = \frac{1}{\sqrt{2}} \left(\sqrt{\frac{k}{n}} - \mathrm{i} \sqrt{1 - \frac{k}{n}} \right) , \qquad (6.99)
$$

for $1 < k < n$. The state of the quantum walk on the hypercube at time t is

$$
\begin{aligned}
|\Psi(t)\rangle = \frac{1}{\sqrt{2^n}} & \Big(|\mathrm{D}\rangle | \beta_{\vec{0}} \rangle + (-1)^t |\mathrm{D}\rangle | \beta_{\vec{1}} \rangle \Big) \\
& + \frac{1}{\sqrt{2^{n+1}}} \sum_{\vec{k}=1}^{2^n-2} \mathrm{e}^{\mathrm{i}\omega_k t} \left(\sqrt{\frac{k}{n}} + \mathrm{i} \sqrt{1 - \frac{k}{n}} \right) \left| \alpha_1^{\vec{k}} \right\rangle | \beta_{\vec{k}} \rangle \\
& + \frac{1}{\sqrt{2^{n+1}}} \sum_{\vec{k}=1}^{2^n-2} \mathrm{e}^{-\mathrm{i}\omega_k t} \left(\sqrt{\frac{k}{n}} - \mathrm{i} \sqrt{1 - \frac{k}{n}} \right) \left| \alpha_n^{\vec{k}} \right\rangle | \beta_{\vec{k}} \rangle . \qquad (6.100)
\end{aligned}
$$

It is remarkable that we obtain an analytical expression for the quantum state at any time. This result allows us to obtain several other results such as the *limiting distribution* and the *mixing time* on the hypercube. The analytical result was obtained, because we have used the Fourier transform. Note that only the eigenvectors that are non-orthogonal to $|\mathrm{D}\rangle \otimes I$ are used to obtain the expression of $|\Psi(t)\rangle$. This fact depends on the choice of initial condition. If the initial condition is in a subspace spanned by some of the eigenvectors of U, the state will remain in this subspace during the evolution. In the case of $|\Psi(t)\rangle$, the dimension of the subspace is $2^{n+1}-2$ and is spanned by an orthonormal basis given by $\left\{\left|\alpha_1^{\vec{k}}\right\rangle|\beta_{\vec{k}}\rangle : 0 \leq \vec{k} < 2^n - 1, \left|\alpha_n^{\vec{k}}\right\rangle|\beta_{\vec{k}}\rangle : 0 < \vec{k} \leq 2^n - 1\right\}$. We will show in the next section that the evolution of the quantum walk with initial condition $|\mathrm{D}\rangle\left|\vec{0}\right\rangle$ uses a much smaller subspace.

Before ending this section, we obtain a simpler expression for $|\Psi(t)\rangle$, which will be useful in future applications. Note that expression

$$\sqrt{\frac{k}{n}} + \mathrm{i}\sqrt{1-\frac{k}{n}}$$

is a complex number of modulus 1. Let us define eigenvectors

$$\left|\tilde{\alpha}_1^{\vec{k}}\right\rangle = \left(\sqrt{\frac{k}{n}} + \mathrm{i}\sqrt{1-\frac{k}{n}}\right)\left|\alpha_1^{\vec{k}}\right\rangle, \tag{6.101}$$

$$\left|\tilde{\alpha}_n^{\vec{k}}\right\rangle = \left(\sqrt{\frac{k}{n}} - \mathrm{i}\sqrt{1-\frac{k}{n}}\right)\left|\alpha_n^{\vec{k}}\right\rangle, \tag{6.102}$$

for $0 < k < n$. Eigenvectors $\left|\tilde{\alpha}_1^{\vec{k}}\right\rangle$ and $\left|\tilde{\alpha}_n^{\vec{k}}\right\rangle$ are unit vectors and obey the same properties that $\left|\alpha_1^{\vec{k}}\right\rangle$ and $\left|\alpha_n^{\vec{k}}\right\rangle$ obey. However, the inner product of these new eigenvectors with $|\mathrm{D}\rangle$ is $1/\sqrt{2}$ and the expression of $|\Psi(t)\rangle$ reduces to

$$\begin{aligned}|\Psi(t)\rangle = {} & \frac{1}{\sqrt{2^n}}\left(|\mathrm{D}\rangle|\beta_{\vec{0}}\rangle + (-1)^t|\mathrm{D}\rangle|\beta_{\vec{1}}\rangle\right) \\ & + \frac{1}{\sqrt{2^{n+1}}}\sum_{\vec{k}=1}^{2^n-2}\left(\mathrm{e}^{\mathrm{i}\omega_k t}\left|\tilde{\alpha}_1^{\vec{k}}\right\rangle|\beta_{\vec{k}}\rangle + \mathrm{e}^{-\mathrm{i}\omega_k t}\left|\tilde{\alpha}_n^{\vec{k}}\right\rangle|\beta_{\vec{k}}\rangle\right).\end{aligned} \tag{6.103}$$

6.3.3 Reducing the Hypercube to a Line

Note the walker starts in vertex $\vec{0}$ with the diagonal state in the coin space. After the first step, the state is

$$\begin{aligned}|\Psi(1)\rangle &= S\,(G\otimes I)|\mathrm{D}\rangle\left|\vec{0}\right\rangle \\ &= \frac{1}{\sqrt{n}}\sum_{a=1}^{n}|a\rangle\left|\vec{e}_a\right\rangle \\ &= \frac{1}{\sqrt{n}}\Big(|1\rangle|1,0,\ldots,0\rangle+\cdots+|n\rangle|0,\ldots,0,1\rangle\Big).\end{aligned} \tag{6.104}$$

The quantum walk is described by a state that has the same amplitude for the vertices with the same *Hamming weight*. Since the *Grover coin* is not biased, it is interesting to ask whether the amplitudes corresponding to the vertices of the same weight will remain the same in the next steps. Applying U on $|\Psi(1)\rangle$, we obtain

$$|\Psi(2)\rangle = \frac{2-n}{n}|\mathrm{D}\rangle\left|\vec{0}\right\rangle+\frac{2}{n\sqrt{n}}\sum_{\substack{a,b=1\\a\neq b}}^{n}|a\rangle\left|\vec{e}_a\oplus\vec{e}_b\right\rangle. \tag{6.105}$$

The terms with Hamming weight equal to zero have coefficient $(2-n)/n$. The terms with Hamming weight 2 have coefficient $2/n\sqrt{n}$. Again, the amplitudes are equal for the vertices with the same Hamming weight. However, in the next step we obtain

$$\begin{aligned}|\Psi(3)\rangle = \frac{2-n}{n\sqrt{n}}\sum_{a=1}^{n}|a\rangle\left|\vec{e}_a\right\rangle+\frac{2(4-n)}{n^2\sqrt{n}}\sum_{\substack{a,b=1\\a\neq b}}^{n}|a\rangle\left|\vec{e}_b\right\rangle \\ +\frac{4}{n^2\sqrt{n}}\sum_{\substack{a,b,c=1\\a\neq b\neq c\neq a}}^{n}|c\rangle\left|\vec{e}_a\oplus\vec{e}_b\oplus\vec{e}_c\right\rangle.\end{aligned} \tag{6.106}$$

The terms with Hamming weight 3 have coefficient $4/n^2\sqrt{n}$, and the terms with Hamming weight 1 are divided into two blocks, the first with coefficient $(2-n)/n\sqrt{n}$ corresponding to terms with vertices that satisfy $v_a = 1$ and with coefficient $2(4-n)/n^2\sqrt{n}$ corresponding to terms that satisfy $v_a = 0$. Since the hypercube and the evolution operator are symmetric under permutation of edges, it is interesting to ask again if the amplitudes corresponding to vertices $|a\rangle\left|\vec{v}\right\rangle$ with the same Hamming weight belonging to the block $v_a = 0$ will remain equal to each other in the next steps and the same regarding the amplitudes corresponding to the terms belonging to the block $v_a = 1$.

A formal way of showing that $|\Psi(t)\rangle$ has the symmetry above described is to consider the following permutation operation: a generic vector in the computational

basis has the form $|a\rangle|v_1,\ldots,v_n\rangle$, where $1 \le a \le n$, and $\vec{v} = (v_1,\ldots,v_n)$ is a binary vector. The permutation of i with j is defined as follows: it converts vector $|a\rangle|v_1,\ldots,v_i,\ldots,v_j,\ldots,v_n\rangle$ into vector $|a\rangle|v_1,\ldots,v_j,\ldots,v_i,\ldots,v_n\rangle$ and vice versa, if $a \neq i$ and $a \neq j$. If a is equal to i or j, a should also be permuted. If $|\Psi(t)\rangle$ is invariant under such a permutation for all i and j, then the coefficients in block $v_a = 0$ are equal and the same is true for the coefficients in block $v_a = 1$. Vice versa: If the coefficients are equal, $|\Psi(t)\rangle$ is invariant under such permutations for all i and j. In other words, this kind of permutation preserves the blocks, that is, a vector of a block does not move to another block and vice versa. Take, for example, these two states for $n = 2$:

$$|\psi\rangle = \frac{1}{\sqrt{2}}\big(|1\rangle|1,0\rangle + |2\rangle|0,1\rangle\big),$$
$$|\phi\rangle = \frac{1}{\sqrt{2}}\big(|1\rangle|0,1\rangle + |1\rangle|1,0\rangle\big).$$

State $|\psi\rangle$ is invariant. On the other hand, $|\phi\rangle$ is not invariant, since the permutation of 1 with 2 converts $|\phi\rangle$ into $\big(|2\rangle|1,0\rangle + |2\rangle|0,1\rangle\big)/\sqrt{2}$.

Let us define a basis of invariant vectors under those permutations. This basis will span an invariant subspace $\mathcal{H}_{\text{inv}} \subset \mathcal{H}$. The basis of $\mathcal{H}_{\text{inv}}$ is obtained as follows: Select an arbitrary vector in the computational basis of Hilbert space $\mathcal{H}$, for example vector $|1\rangle|1,0,0\rangle$, which is associated with a 3-dimensional hypercube. Apply all allowed permutations on $|1\rangle|1,0,0\rangle$. The resulting set is $\Big\{|1\rangle|1,0,0\rangle,\ |2\rangle|0,1,0\rangle$ $|3\rangle|0,0,1\rangle\Big\}$. Add up all these vectors and normalize. The result is

$$|\lambda_1\rangle = \frac{1}{\sqrt{3}}\Big(|1\rangle|1,0,0\rangle + |2\rangle|0,1,0\rangle + |3\rangle|0,0,1\rangle\Big). \tag{6.107}$$

By construction, vector $|\lambda_1\rangle$ is invariant under the permutation operations. Now select another vector in the computational basis of $\mathcal{H}$ that is not in the previous set and repeat the process over until you have exhausted all possibilities. The resulting set is an invariant basis of $\mathcal{H}_{\text{inv}}$. This basis has vectors $|\rho_0\rangle$, …, $|\rho_{n-1}\rangle$ and vectors $|\lambda_1\rangle$, …, $|\lambda_n\rangle$, defined by

$$|\rho_v\rangle = \frac{1}{\sqrt{(n-v)\binom{n}{v}}} \sum_{\substack{a,\vec{v} \\ |\vec{v}|=v \\ v_a=0}} |a,\vec{v}\rangle, \tag{6.108}$$

$$|\lambda_v\rangle = \frac{1}{\sqrt{v\binom{n}{v}}} \sum_{\substack{a,\vec{v} \\ |\vec{v}|=v \\ v_a=1}} |a,\vec{v}\rangle, \tag{6.109}$$

where the sum runs over the vertices of the same Hamming weight v with the following constraint: $|a,\vec{v}\rangle$ is in $|\rho_v\rangle$ is a-th entry of $\vec{v}$ is 0, otherwise it is in $|\lambda_v\rangle$. As

usual, $\binom{n}{v}$ is the binomial expression $n!/(n-v)!v!$. The basis described by (6.108) and (6.109) is orthonormal and has $2n$ elements, which shows that the dimension of $\mathcal{H}_{\text{inv}}$ is $2n$.

Exercise 6.21. Obtain expressions (6.105) and (6.106) by applying $U = S(G \otimes I)$ on $|\Psi(1)\rangle$.

Exercise 6.22. Obtain all vectors invariant under the permutations in a 3-dimensional hypercube following the method used to obtain (6.107). Divide the set of vectors into two blocks *right* and *left*. Vectors $|a\rangle|\vec{v}\rangle$ in block *right* have the property $v_a = 0$ and vectors in block *left* have the property $v_a = 1$. The names of the vectors should use ρ for vectors in block *right*, λ in block *left*, and the Hamming weight of the vertices v as a sub-index. Verify the results of this process with vectors of (6.108) and (6.109).

Exercise 6.23. Show that:

1. $|\rho_0\rangle = |\mathrm{D}\rangle|\vec{0}\rangle$.
2. $|\lambda_n\rangle = |\mathrm{D}\rangle|\vec{1}\rangle$.
3. Vectors $|\rho_v\rangle$, $0 \le v \le n-1$, and $|\lambda_v\rangle$, $1 \le v \le n$ are orthonormal.

The initial condition $|\mathrm{D}\rangle|\vec{0}\rangle$ is in the vector space spanned by $|\rho_v\rangle$ and $|\lambda_v\rangle$, because $|\mathrm{D}\rangle|\vec{0}\rangle$ is equal to $|\rho_0\rangle$. One way to show that the state of the quantum walk remains on the space spanned by $|\rho_v\rangle$ and $|\lambda_v\rangle$ during the evolution is to show that the *evolution operator* can be written only in terms of $|\rho_v\rangle$ and $|\lambda_v\rangle$. First we show that the shift operator can be written in this basis. Let us calculate the action of S on vector $|\rho_v\rangle$. Using (6.108), we have

$$\begin{aligned} S|\rho_v\rangle &= \frac{1}{\sqrt{(n-v)\binom{n}{v}}} \sum_{\substack{a,\vec{v} \\ |\vec{v}|=v \\ v_a=0}} S|a,\vec{v}\rangle \\ &= \frac{1}{\sqrt{(n-v)\binom{n}{v}}} \sum_{\substack{a,\vec{v} \\ |\vec{v}|=v+1 \\ v_a=1}} |a,\vec{v}\rangle \end{aligned}$$

Note that the action of S on $|a,\vec{v}\rangle$ replace a-th entry of $\vec{v}$ from 0 to 1. Therefore, the Hamming weight of this vertex increases one unit. Using the binomial expression, we show that $(n-v)\binom{n}{v} = (v+1)\binom{n}{v+1}$. Using this equation, we obtain

$$S|\rho_v\rangle = \frac{1}{\sqrt{(v+1)\binom{n}{v+1}}} \sum_{\substack{a,\vec{v} \\ |\vec{v}|=v+1 \\ v_a=1}} |a,\vec{v}\rangle$$

$$= |\lambda_{v+1}\rangle. \tag{6.110}$$

Similarly, we obtain

$$S|\lambda_v\rangle = |\rho_{v-1}\rangle. \tag{6.111}$$

Therefore, the shift operator can be written as

$$S = \sum_{v=0}^{n-1} |\lambda_{v+1}\rangle\langle\rho_v| + \sum_{v=1}^{n} |\rho_{v-1}\rangle\langle\lambda_v|. \tag{6.112}$$

The physical interpretation of the shift operator shows that the quantum walk takes place in a one-dimensional lattice with $n+1$ vertices, with the position being specified by v. The *chirality* is specified by ρ and λ and it determines the direction of the movement. Operator S shifts $|\rho_v\rangle$ rightward and inverts the chirality and it shifts $|\lambda_v\rangle$ leftward also inverting the chirality. The boundary conditions are reflective, since in $v = 0$ the walker has no overlap with $|\lambda_0\rangle$ and in $v = n$ it has no overlap with $|\rho_n\rangle$.

The coin operator can also be expressed in terms of basis $|\rho_v\rangle$ and $|\lambda_v\rangle$. Actually, the following results are valid:

$$G \otimes I\, |\rho_v\rangle = \cos\omega_v|\rho_v\rangle + \sin\omega_v|\lambda_v\rangle, \tag{6.113}$$

$$G \otimes I\, |\lambda_v\rangle = \sin\omega_v|\rho_v\rangle - \cos\omega_v|\lambda_v\rangle, \tag{6.114}$$

where

$$\cos\omega_v = 1 - \frac{2v}{n} \tag{6.115}$$

$$\sin\omega_v = 2\sqrt{\frac{v}{n}\left(1 - \frac{v}{n}\right)}. \tag{6.116}$$

The proof of this result is oriented in Exercise 6.25. Equations (6.113) and (6.114) show that the action of the coin operator on the quantum walk in the one-dimensional lattice is a rotation of angle ω_v, which depends on point v. This is different from the standard quantum walk.

Exercise 6.24. Show that (6.111) is true.

Exercise 6.25. The purpose of this exercise is to prove that the action of the Grover coin on basis $|\rho_v\rangle$ and $|\lambda_v\rangle$ is the one described in (6.113) and (6.114).

Show that

$$\sum_{\substack{a,\vec{v} \\ |\vec{v}|=v_0 \\ v_a=0}} \left\langle \mathrm{D}, \vec{v}' | a, \vec{v} \right\rangle = \frac{(n - v_0)}{\sqrt{n}} \delta_{v_0 v'}.$$

[Hint: Show that if $|\vec{v'}| \neq v_0$, the result is zero. Fix a transposed vector $\left\langle \mathrm{D}, \vec{v'} \right|$ with $|\vec{v'}| = v_0$ and expand the sum. Show that there are $n - v_0$ values of a satisfying $v_a = 0$ for a fixed vector such that $|\vec{v}\rangle\,|\vec{v}\rangle = \left|\vec{v'}\right\rangle$.] Use this result to show that

$$\left\langle \mathrm{D}, \vec{v'} | \rho_v \right\rangle = \sqrt{\frac{n-v}{n\binom{n}{v}}}\,\delta_{v,v'}.$$

Show also that

$$|\mathrm{D}\rangle \sum_{|\vec{v}|=v} |\vec{v}\rangle = \sqrt{\frac{n-v}{n}\binom{n}{v}}|\rho_v\rangle + \sqrt{\frac{v}{n}\binom{n}{v}}|\lambda_v\rangle.$$

Use expressions $G = 2|\mathrm{D}\rangle\langle\mathrm{D}| - I_n$ and $I_{2^n} = \sum_{\vec{v'}} \left|\vec{v'}\right\rangle\left\langle\vec{v'}\right|$ to calculate $G \otimes I_{2^n}|\rho_v\rangle$ and compare the result with (6.113). Use the previous identities.

Using a similar procedure, show that (6.114) is true.

Exercise 6.26. From (6.113) and (6.114), obtain an expression for $G \otimes I$. Can this expression be factored in $\mathcal{H}_{\text{inv}}$? Define the computational basis of $\mathcal{H}_{\text{inv}}$ as $\{|0, v\rangle, |1, v\rangle,\ 0 \leq v \leq n\}$, where $\{|0\rangle, |1\rangle\} \in \mathcal{H}^2$ and $|v\rangle \in \mathcal{H}^n$ such that $|0, v\rangle = |\rho_v\rangle$, $|1, v\rangle = |\lambda_v\rangle$. Obtain operator $C_v \in \mathcal{H}^2$ such that the coin operator has the form $\sum_{v=0}^{n} C_v \otimes |v\rangle\langle v|$. Give a physical interpretation for the action of the coin operator on this expression.

Using (6.112)–(6.114), we obtain the following expression for the evolution operator in basis $|\rho_v\rangle$ and $|\lambda_v\rangle$:

$$\begin{aligned} U &= S(G \otimes I) \\ &= \sum_{v=0}^{n-1} -\cos\omega_{v+1}|\rho_v\rangle\langle\lambda_{v+1}| + \sin\omega_{v+1}|\rho_v\rangle\langle\rho_{v+1}| \\ &\quad + \sum_{v=1}^{n} \sin\omega_{v-1}|\lambda_v\rangle\langle\lambda_{v-1}| + \cos\omega_{v-1}|\lambda_v\rangle\langle\rho_{v-1}|. \end{aligned} \tag{6.117}$$

Therefore, $\mathcal{H}_{\text{inv}}$ is an invariant subspace under the action of U. Since the initial condition $|\rho_0\rangle = |\mathrm{D}\rangle\left|\vec{0}\right\rangle$ belongs to $\mathcal{H}_{\text{inv}}$, the state of the quantum walk $|\Psi(t)\rangle$ will be in $\mathcal{H}_{\text{inv}}$ during the evolution. The orthonormal basis $|\rho_v\rangle$, $|\lambda_v\rangle$ allows us to interpret physically the quantum walk on a hypercube as a quantum walk on the points of a finite line. From the state vector on the line, we can recover the state vector on the hypercube. However, the basis $|\rho_v\rangle$, $|\lambda_v\rangle$ is not the best one to obtain the evolution of the quantum walk, because $|\rho_v\rangle$ and $|\lambda_v\rangle$ are not eigenvectors of the *reduced evolution operator*.

The strategy now is to find the spectral decomposition of U in $\mathcal{H}_{\text{inv}}$. The goal is to find $2n$ linearly independent eigenvectors of U that are in the reduced space $\mathcal{H}_{\text{inv}}$. We know that $\left\{\left|\tilde{\alpha}_1^{\vec{k}}\right\rangle|\beta_{\vec{k}}\rangle,\ \left|\tilde{\alpha}_n^{\vec{k}}\right\rangle|\beta_{\vec{k}}\rangle : 0 < \vec{k} \leq 2^n - 1\right\}$ is an eigenbasis of U for a subspace where the quantum walk is, as shown in (6.103). The associated eigenvalues are $\left\{e^{i\omega_k}, e^{-i\omega_k}\right\}$, where ω_k satisfies

$$\cos\omega_k = 1 - \frac{2k}{n}.$$

Eigenvectors $|\mathrm{D}\rangle\left|\beta_{\vec{0}}\right\rangle$ and $|\mathrm{D}\rangle\left|\beta_{\vec{1}}\right\rangle$ are in the space spanned by $|\lambda_v\rangle$ and $|\rho_v\rangle$ (see Exercises 6.27 and 6.28). However, the remaining eigenvectors are not. For example, $\left|\tilde{\alpha}_1^{\vec{k}}\right\rangle|\beta_{\vec{k}}\rangle$ explicitly depends on $\vec{k}$, and thus is not invariant by the permutations of the entries of $\vec{k}$, as the ones described at the beginning of this section. Note that all eigenvectors of the kind $\left|\tilde{\alpha}_1^{\vec{k}}\right\rangle|\beta_{\vec{k}}\rangle$ with the same Hamming weight k have the same eigenvalue $e^{i\omega_k}$. Since the sum of the eigenvectors with the same Hamming weight is also an eigenvector, we can generate a new eigenvector, which is invariant under permutation of the entries of $\vec{k}$ and, therefore, it will be in the subspace spanned by $|\rho_v\rangle$ and $|\lambda_v\rangle$. So, we define

$$\left|\omega_k^+\right\rangle = \frac{1}{\sqrt{\binom{n}{k}}} \sum_{|\vec{k}|=k} \left|\tilde{\alpha}_1^{\vec{k}}\right\rangle|\beta_{\vec{k}}\rangle, \tag{6.118}$$

for $0 \leq k < n$. Similarly, we define

$$\left|\omega_k^-\right\rangle = \frac{1}{\sqrt{\binom{n}{k}}} \sum_{|\vec{k}|=k} \left|\tilde{\alpha}_n^{\vec{k}}\right\rangle|\beta_{\vec{k}}\rangle, \tag{6.119}$$

for $0 < k \leq n$ associated with eigenvalue $e^{-i\omega_k}$. These eigenvectors are in $\mathcal{H}_{\text{inv}}$. The number of eigenvectors coincides with the dimension of $\mathcal{H}_{\text{inv}}$. Thus, set $\left\{\left|\omega_k^+\right\rangle : 0 \leq k \leq n-1, \left|\omega_k^-\right\rangle : 1 \leq k \leq n\right\}$ is an orthonormal basis of eigenvectors of U for $\mathcal{H}_{\text{inv}}$ associated with eigenvalues $\left\{e^{i\omega_k}, e^{-i\omega_k}\right\}$.

The initial condition $|\mathrm{D}\rangle\left|\vec{0}\right\rangle$ can be expressed in this new basis of eigenvectors, if there are coefficients a_k and b_k such that

$$|\mathrm{D}\rangle\left|\vec{0}\right\rangle = \sum_{k=0}^{n-1} a_k \left|\omega_k^+\right\rangle + \sum_{k=1}^{n} b_k |\omega_k^-\rangle. \tag{6.120}$$

Since the eigenbasis is orthonormal, it follows that

$$a_k = \left\langle \omega_k^+ \middle| \mathrm{D}, \vec{0} \right\rangle,$$
$$b_k = \left\langle \omega_k^- \middle| \mathrm{D}, \vec{0} \right\rangle.$$

Using that $\left\langle \tilde{\alpha}_1^k \middle| \mathrm{D} \right\rangle = \left\langle \tilde{\alpha}_n^k \middle| \mathrm{D} \right\rangle = 1/\sqrt{2}$, (6.118) and (6.119), we obtain

$$a_k = \sqrt{\frac{1}{2^{n+1}} \binom{n}{k}},$$
$$b_k = \sqrt{\frac{1}{2^{n+1}} \binom{n}{k}},$$

for $0 < k < n$. Using (6.98) and (6.99), we obtain $a_0 = b_n = 1/\sqrt{2^n}$. So,

$$|\Psi(0)\rangle = \frac{1}{\sqrt{2^n}} \left(\left| \omega_0^+ \right\rangle + |\omega_n^-\rangle \right) + \frac{1}{\sqrt{2^{n+1}}} \sum_{k=1}^{n-1} \sqrt{\binom{n}{k}} \left(\left| \omega_k^+ \right\rangle + |\omega_k^-\rangle \right). \tag{6.121}$$

Then, the state of the quantum walk at time t is

$$|\Psi(t)\rangle = \frac{1}{\sqrt{2^n}} \left(\left| \omega_0^+ \right\rangle + (-1)^t |\omega_n^-\rangle \right) + \frac{1}{\sqrt{2^{n+1}}} \sum_{k=1}^{n-1} \sqrt{\binom{n}{k}} \left(\mathrm{e}^{\mathrm{i}\omega_k t} \left| \omega_k^+ \right\rangle + \mathrm{e}^{-\mathrm{i}\omega_k t} |\omega_k^-\rangle \right). \tag{6.122}$$

Exercise 6.27. Show that

$$\left| \alpha_1^{\vec{0}} \right\rangle \left| \beta_{\vec{0}} \right\rangle = |\mathrm{D}\rangle \otimes \frac{1}{\sqrt{2^n}} \sum_{\vec{v}=0}^{2^n-1} |\vec{v}\rangle = \frac{1}{\sqrt{2^n}} \left(\sum_{v=0}^{n-1} \sqrt{\binom{n-1}{v}} |\rho_v\rangle + \sum_{v=1}^{n} \sqrt{\binom{n-1}{v-1}} |\lambda_v\rangle \right).$$

Exercise 6.28. Show that

$$\left|\alpha_n^{\vec{1}}\right\rangle\left|\beta_{\vec{1}}\right\rangle = |\mathrm{D}\rangle \otimes \frac{1}{\sqrt{2^n}} \sum_{\vec{v}=0}^{2^n-1} (-1)^v |\vec{v}\rangle$$

$$= \frac{1}{\sqrt{2^n}} \left(\sum_{v=0}^{n-1} (-1)^v \sqrt{\binom{n-1}{v}} |\rho_v\rangle + \sum_{v=1}^{n} (-1)^v \sqrt{\binom{n-1}{v-1}} |\lambda_v\rangle \right).$$

[Hint: Use the first identity of Exercise 6.25.]

Exercise 6.29. Show that $\left\{ \left|\omega_k^+\right\rangle : 0 \leq k \leq n-1, \left|\omega_k^-\right\rangle : 1 \leq k \leq n \right\}$ is an orthonormal basis of $\mathcal{H}_{\mathrm{inv}}$ with eigenvalues $\mathrm{e}^{\pm \mathrm{i}\omega_k}$.

Further Reading

The quantum walk on the cycle was analyzed in [3], which is a seminal paper in the area. References [13, 14, 77] are also useful. Periodic solutions were obtained in [76, 77]. The quantum walk on two-dimensional lattices was analyzed in [49, 77]. Periodic solutions can also be found on two-dimensional lattice, see [77, 81]. One of the first paper analyzing quantum walks on the hypercube is [59]. Reference [43] showed that the quantum hitting time between two opposite vertices of the hypercube is exponentially smaller than the classical hitting time. More references about quantum walks in finite graphs can be found in Venegas–Andraca's review book [80].

Chapter 7
Limiting Distribution and Mixing Time

In this chapter, we use the notion of quantum walks on *finite regular graphs* with the goal of analyzing the *limiting probability distribution* and the *mixing time*. In finite quantum systems, there is a *quasi-periodic* pattern in the time evolution, preventing the convergence to a limiting distribution. The quasi-periodic behavior of the quantum state can be obtained from the expression of the eigenvalues of the evolution operator. A possible way to obtain limiting configurations is to define a new distribution called *average probability distribution*, which evolves stochastically and does not have the quasi-periodic behavior.

We obtain the limiting distribution for *cycles*, *finite lattices*, and *hypercubes* using the evolution operators and the initial conditions studied in previous chapters.

We define the concept of distance between probability distributions, which paves the way for the definition of the *mixing time*. The mixing time captures the notion of how quickly the average probability distribution approaches to the limiting distribution.

7.1 Quantum Walks on Graphs

Consider a finite *regular graph*[1] of *degree* d with N vertices. The Hilbert space associated with a quantum walk on this graph is $\mathcal{H} = \mathcal{H}^d \otimes \mathcal{H}^N$, where $\mathcal{H}^d$ is the coin space and $\mathcal{H}^N$ is the position space. The computational basis of $\mathcal{H}$ is the set of vectors $\{|a, v\rangle,\ 0 \leq a \leq d-1,\ 0 \leq v \leq N-1\}$. Labels v for the *vertices* indicate the possible places the walker can visit and labels a for the *edges* indicate the possible directions that the walker can take departing from vertex v. Label a refers to a directed edge from v to some neighbor vertex w, since we can consider an

[1] A regular graph is a graph where each vertex has the same number of neighbors (each vertex have the same degree).

R. Portugal, *Quantum Walks and Search Algorithms*, Quantum Science and Technology, DOI 10.1007/978-1-4614-6336-8_7,

undirected edge as two opposite directed edges. The directed edge from w to v may have another label. Disregarding the edge labels, the graphs we are considering are *undirected*.

The *evolution operator* of the *standard quantum walk* is

$$U = S(C \otimes I), \tag{7.1}$$

where C is the *coin operator*, which must be unitary, and S is the *shift operator*, which is usually defined as

$$S|a, v\rangle = |a, w\rangle, \tag{7.2}$$

where w is the vertex *adjacent* to v through the edge of label a. The interpretation of this action is: The walker leaves vertex v, takes direction a, and arrives in vertex w. It is tempting to say that if the shift operator is applied again without using the coin, the walker will go in the same direction, leaving vertex w this time. However, the labels of the edges leaving vertex w can be chosen in any order, and thus the result of this second hypothetical application of S must be specified and can move the walker back to v.

Usually, we consider the graph embedded in a larger space, where we define directions for the movement. For example, we use the label 0 on the line representing "move rightward" and 1 representing "move leftward" and in the cycle, we use 0 for clockwise and 1 for counterclockwise. For the line, there is no m such that $S^m = I$, and for the N-cycle, the smallest value of m such that $S^m = I$ is $m = N$. Therefore, successive applications of S (without the application of coin) moves the walker away who never returns for the walk on the line, and returns after N steps on the cycle.

Equation (7.2) can be modified to

$$S|a, v\rangle = |b, w\rangle, \tag{7.3}$$

where b may be different from a defining a second kind of shift operator. One of the most interesting kinds of shift operator for search algorithms is called *flip–flop*. If the walker leaves vertex v and goes to vertex w through the edge of label a, the next value of the edge (b in (7.3)) can be chosen in such way that forces the walker to go from w to v. In this case we $S^2 = I$. We have used this kind of shift operator in the analysis of quantum walks on *finite two-dimensional lattices* and *hypercubes*. It improves the *time complexity* of search algorithms, making them faster than the algorithms based on the walks of the first kind. The reason for this difference is well understood and is related to the degeneracy of the eigenvalues of the subspace containing the initial condition, as discussed in Sect. 8.1.

Instead of assuming that the graph is embedded in a larger space, we can define the labels of the edges using an intrinsic method. If an edge is incident to vertices v and w, we can give the same label a for both the edge from v to w and as from w to v. However, this convention is only possible if the *chromatic index*

(*edge chromatic number*)[2] is d. The colors can be used as labels. The shift operator is defined by (7.2) and is a flip–flop shift operator. If the walker is at vertex v and the coin value is a, it goes to the vertex connected to v by edge a. The coin value is not modified, so a new application of S (without applying the coin) moves the walker back to vertex v. Therefore, $S^2 = I$. Not all graphs have a compatible chromatic index. A counter-example, where the chromatic index is different from d, is the cycle with odd number of vertices. The cycle is a regular graph of degree 2. If N is odd, the cycle has chromatic index 3. For example, for $N = 3$ all edges are adjacent, so we need three different colors. We can still define the flip–flop shift operator on those graphs, but the expression for the shift operator will be the one given in (7.3).

Equation (7.1) can be generalized such that the coin may depend on the vertex, as in the *abstract search algorithm* analyzed in Sect. 8.1. In this case, the evolution operator is $U = S\,C'$, where C' is an operator of the composite Hilbert space.

In the most general case, we can remove any restriction in the form of the evolution operator U and simply require that U follows the graph structure (being unitary). That is, the walker should leave v and go to an adjacent vertex or remain in v. So, $U|a, v\rangle$ should be written as a linear combination of vectors of the form $|b, w\rangle$, where w is adjacent to the v or is v itself and b assumes values in the edge set. Some of the results of this chapter are valid in this more general situation. It is possible to define quantum walks on non-regular graphs, but we do not address this issue in this book.

7.2 Limiting Probability Distribution

Classical random walks in connected *non-bipartite* graphs have a *limiting* or *stationary distribution* that does not depend on the initial condition. In the quantum context, it is interesting to ask whether there is a stationary probability distribution or if there is a stationary quantum state when the quantum walk evolves up to $t \to \infty$. If there is, how does the limiting distribution depend on the *initial condition*?

Suppose that the initial condition of a quantum walk is $|\Psi(0)\rangle$. The state of the walker at time t is

$$|\Psi(t)\rangle = U^t|\Psi(0)\rangle,$$

where U is the evolution operator. Suppose that $\left\{|\lambda_{a,k}\rangle : 0 \leq a \leq d-1\ 0 \leq k \leq N-1\right\}$ is an orthonormal basis of eigenvectors of U associated with eigenvalues $\mathrm{e}^{2\pi \mathrm{i}\lambda_{a,k}}$. The *spectral decomposition* of U is

[2]The chromatic index is the smallest number of colors needed for an edge coloring of a graph so that no vertex is incident to two edges of the same color.

$$U = \sum_{a=0}^{d-1} \sum_{k=0}^{N-1} \mathrm{e}^{2\pi \mathrm{i} \lambda_{a,k}} |\lambda_{a,k}\rangle\langle\lambda_{a,k}|, \tag{7.4}$$

where $0 \leq \lambda_{a,k} < 1$. The initial state can be written in the basis of eigenvectors of U as follows:

$$|\Psi(0)\rangle = \sum_{a=0}^{d-1} \sum_{k=0}^{N-1} c_{a,k} |\lambda_{a,k}\rangle, \tag{7.5}$$

where $c_{a,k} = \langle \lambda_{a,k} | \Psi(0) \rangle$. Then,

$$|\Psi(t)\rangle = \sum_{a=0}^{d-1} \sum_{k=0}^{N-1} c_{a,k} \mathrm{e}^{2\pi \mathrm{i} \lambda_{a,k} t} |\lambda_{a,k}\rangle. \tag{7.6}$$

One may wonder if state $|\Psi(t)\rangle$ tends to a stationary state when $t \to \infty$, that is, does $\lim_{t\to\infty} |\Psi(t)\rangle$ exist? We can easily show that this limit does not exist, because the norm $\| \, |\Psi(t+1)\rangle - |\Psi(t)\rangle \, \|$ is constant for all t, in fact,

$$\begin{aligned} \frac{1}{2} \| \, |\Psi(t+1)\rangle - |\Psi(t)\rangle \, \|^2 &= \frac{1}{2} \| U^t (U - I) |\Psi(0)\rangle \|^2 \\ &= 1 - \Re\big(\langle \Psi(0) | U | \Psi(0) \rangle\big). \end{aligned}$$

Note that the dependence on t disappears, because operator U is unitary. Since the real part of $\langle \Psi(0)|U|\Psi(0)\rangle$ is fixed, once given the evolution operator and the initial condition, the norm is nonzero and constant, if $U \neq I$. If $|\Psi(t)\rangle$ tended toward a stationary value, the above norm would tend to zero.

The probability of finding the walker in vertex v is given by

$$p_v(t) = \sum_{a=0}^{d-1} \big| \langle a, v | \Psi(t) \rangle \big|^2 . \tag{7.7}$$

When we consider the set of vertices of the graph, we have a probability distribution $p_v(t)$ that satisfies

$$\sum_{v=0}^{N-1} p_v(t) = 1.$$

The probability distribution depends on the initial condition. We may again ask ourselves if there is a limiting probability distribution in the general case, since the argument of the preceding paragraph does not directly exclude this possibility.

Both state $|\Psi(t)\rangle$ and the probability distribution contain terms of the type $\mathrm{e}^{2\pi \mathrm{i} \lambda t}$, which generate a *quasi-periodic* evolution, that is, for any positive value of ϵ there is an infinite number of values of t such that $\big| \langle \Psi(t) | \Psi(0) \rangle \big| \geq 1 - \epsilon$. When the evolution is periodic, this inequality is true when we take $\epsilon = 0$. In the general case,

the statement is true, if it is possible to find values of t such that all eigenvalues to power t are arbitrarily close to 1 simultaneously. To show this, let us start showing how to find an infinite number of values of t such that $e^{i\theta t}$ is arbitrarily close to 1 for a fixed θ. Let $\epsilon > 0$ be the desired accuracy. If θ is a rational multiple 2π, simply take t as integer multiples of the denominator of $\theta/2\pi$. To show the statement when θ is an irrational multiple of 2π, take an integer n greater than $2\pi/\epsilon$ and define $0 \leq \theta_j < 2\pi$ such that $j\ \theta \equiv \theta_j \mod 2\pi$.[3] There will always be two values j_2 and j_1 smaller than n such that $|\theta_{j_1} - \theta_{j_2}| \leq 2\pi/n < \epsilon$, because if we divide the unit circle into identical sections such that each sector has angle ϵ and taking n values j, there will be a sector with more than one θ_j. Suppose that $j_2 > j_1$, then $|\theta_{j_2-j_1}| < \epsilon$. Since θ is an irrational multiple of 2π, we know that $\theta_{j_2-j_1} \neq 0$. Therefore, when l varies, sequence $\theta_{l(j_2-j_1)}$ is a partition of the unit circle such that the angles are smaller than ϵ. Therefore, the time instant $t = j_2 - j_1$ obeys $\theta_t < \epsilon$ and $e^{i\theta t}$ is close to 1, as desired. We can repeat the process taking $\epsilon = \theta_t$ to obtain a second value of t greater than the first with the desired properties. This process can be repeated an infinite number of times.

To obtain a value of t such that both $e^{i\theta_1 t}$ and $e^{i\theta_2 t}$ are close to 1, we use the following procedure: Suppose that $\theta_2 > \theta_1$, $\lambda_1 = \theta_2 - \theta_1$, and ϵ is the desired accuracy. We use the method described in the preceding paragraph to find time t_1 such that $\lambda_1 t_1 < \epsilon^2$ modulo 2π. Then, we find $0 \leq \lambda_2 < 2\pi$ such that $\theta_1 t_1 \equiv \lambda_2 \mod 2\pi$ and determine the value of t_2 such that $\lambda_2 t_2 < \epsilon$ modulo 2π. The desired time is $t_1 t_2$. When the number of eigenvalues is greater than 2, to find time t such that all eigenvalues become arbitrarily close to 1, we use the described procedure recursively. The procedure works correctly for two eigenvalues because in the first step, we obtain $t_1 = O(1/\epsilon^2)$ such that $|\theta_2 - \theta_1| t_1 \leq \epsilon^2$ modulo 2π. The geometrical interpretation is that $e^{i\theta_1 t_1}$ and $e^{i\theta_2 t_1}$ are very close, but need not to be close to 1. In the second step, we obtain $t_2 = O(1/\epsilon)$ such that $\theta_1 t_1 t_2 \leq \epsilon$ modulo 2π. Therefore, these inequalities imply that $\theta_2 t_1 t_2 \leq O(\epsilon)$ modulo 2π. Thus, $t = t_1 t_2$ is the time instant we are looking for such that $e^{i\theta_1 t}$ and $e^{i\theta_2 t}$ are close to 1 within the error margin. This process can be repeated over, and we take smaller values of ϵ to obtain the next values of t.

Figure 7.1 shows the probability of finding the walker in the initial vertex as a function of the number of steps of a quantum walk in the cycle with ten vertices using the Hadamard coin. Note that in some moments the probability approaches 1, in particular, at time $t = 264$. Note that the procedure described in the previous paragraph does not necessarily find the first time such that the state of the walk approaches the initial state. When the number of vertices increases, the frequency to return to its original state decreases, because it takes longer for the powers of the eigenvalues to collide.

We have showed that there is a time $t > 0$ such that $|\Psi(t)\rangle$ is arbitrarily close to the initial condition. Due to the cyclic nature of the evolution, the same procedure

[3] The notation $a \equiv b \mod 2\pi$ means that b (which can be an irrational number) is the remainder of the division of a by an integer multiple of 2π.

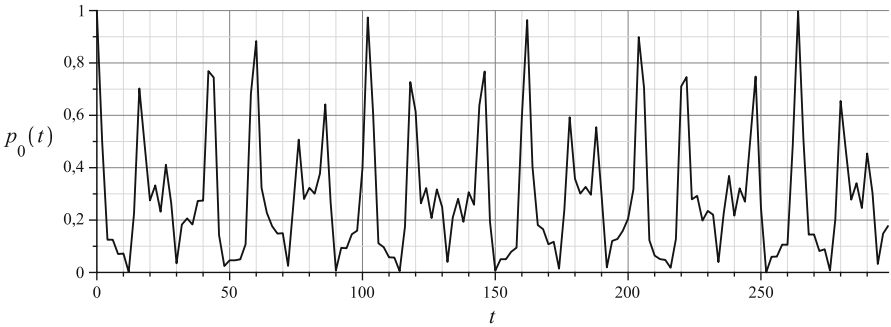

Fig. 7.1 Probability of finding the walker in the initial vertex for a quantum walk in a cycle with ten vertices. The probabilities for odd t are not shown, because they are always equal to zero

can be used to find an infinite number of times such that the quantum state is close to the initial condition. Since this is a general characteristic of quantum mechanics in finite systems, we can ask ourselves if there is some way to define limiting distributions in the context of quantum walks.

The *average probability distribution* in time is given by

$$\bar{p}_v(T) = \frac{1}{T}\sum_{t=0}^{T-1} p_v(t). \tag{7.8}$$

Note that $\bar{p}_v(T)$ is a probability distribution, because

$$\sum_{v=0}^{N-1} \bar{p}_v(T) = 1$$

for all T. We can give a physical interpretation for $\bar{p}_v(T)$ as follows: Take an integer value of t *randomly* distributed between 0 and $T-1$. Let the quantum walk evolve from the initial condition until that time t. Measure in the computational basis to determine in what vertex the walker is. Keeping T fixed, repeat the process a large number of times. Analyzing the results, we can determine how many times the walker is in each vertex. Dividing these values by the total number of repetitions, we obtain a probability distribution close to $\bar{p}_v(T)$. Greater the number of repetitions, better the approximation.

The interpretation of $\bar{p}_v(T)$ uses *projective measurements*. Therefore, $\bar{p}_v(T)$ evolves *stochastically*. Now we have a good reason to believe that $\bar{p}_v(T)$ converges to a limiting distribution when T tends to infinity. Define

$$\pi(v) = \lim_{T\to\infty} \bar{p}_v(T). \tag{7.9}$$

This limit exists and can be explicitly calculated once given the initial condition. We can obtain a useful formula for calculating the limiting distribution and at the same time prove its existence.

Using (7.7) and (7.8), we obtain

$$\bar{p}_v(T) = \frac{1}{T}\sum_{t=0}^{T-1}\sum_{b=0}^{d-1}\left|\langle b, v|\Psi(t)\rangle\right|^2.$$

Using (7.6), we obtain

$$\bar{p}_v(T) = \frac{1}{T}\sum_{t=0}^{T-1}\sum_{b=0}^{d-1}\left|\sum_{a=0}^{d-1}\sum_{k=0}^{N-1} c_{a,k}\mathrm{e}^{2\pi\mathrm{i}\lambda_{a,k}t}\,\langle b, v|\lambda_{a,k}\rangle\right|^2.$$

Using that $|c|^2 = c\,c^*$ and switching the sums with the limit, we obtain

$$\begin{aligned}\bar{p}_v(T) = &\sum_{a,a',b=0}^{d-1}\sum_{k,k'=0}^{N-1} c_{a,k}c^*_{a',k'}\,\langle b, v|\lambda_{a,k}\rangle\langle\lambda_{a',k'}|b, v\rangle\\ &\times\frac{1}{T}\sum_{t=0}^{T-1}\mathrm{e}^{2\pi\mathrm{i}(\lambda_{a,k}-\lambda_{a',k'})t}.\end{aligned} \tag{7.10}$$

To obtain the limiting distribution, we have to calculate the limit

$$\lim_{T\to\infty}\frac{1}{T}\sum_{t=0}^{T-1}\left(\mathrm{e}^{2\pi\mathrm{i}(\lambda_{a,k}-\lambda_{a',k'})}\right)^t.$$

Using the formula for the sum of a geometric sequence, we obtain

$$\frac{1}{T}\sum_{t=0}^{T-1}\left(\mathrm{e}^{2\pi\mathrm{i}(\lambda_{a,k}-\lambda_{a',k'})}\right)^t = \begin{cases}\frac{\mathrm{e}^{2\pi\mathrm{i}(\lambda_{a,k}-\lambda_{a',k'})T}-1}{T\left(\mathrm{e}^{2\pi\mathrm{i}(\lambda_{a,k}-\lambda_{a',k'})}-1\right)}, & \text{if } \lambda_{a,k}\neq\lambda_{a',k'};\\ 1, & \text{if } \lambda_{a,k}=\lambda_{a',k'}.\end{cases} \tag{7.11}$$

If $\lambda_{a,k} \neq \lambda_{a',k'}$, the result is a *complex number* the *modulus* of which obeys the following inequality:

$$\begin{aligned}\left|\frac{\mathrm{e}^{2\pi\mathrm{i}(\lambda_{a,k}-\lambda_{a',k'})T}-1}{T\left(\mathrm{e}^{2\pi\mathrm{i}(\lambda_{a,k}-\lambda_{a',k'})}-1\right)}\right|^2 &= \frac{1}{T^2}\,\frac{1-\cos 2\pi(\lambda_{a,k}-\lambda_{a',k'})T}{1-\cos 2\pi(\lambda_{a,k}-\lambda_{a',k'})}\\ &\leq \frac{1}{T^2}\,\frac{1}{1-\cos 2\pi(\lambda_{a,k}-\lambda_{a',k'})}.\end{aligned}$$

Taking the limit $T \to \infty$, we obtain that the modulus of this complex number is zero. Then,

$$\lim_{T\to\infty} \frac{1}{T} \sum_{t=0}^{T-1} \left(e^{2\pi i(\lambda_{a,k}-\lambda_{a',k'})} \right)^t = \begin{cases} 0, \text{ if } \lambda_{a,k} \neq \lambda_{a',k'}; \\ 1, \text{ if } \lambda_{a,k} = \lambda_{a',k'}. \end{cases} \tag{7.12}$$

Substituting the above result for (7.10), we obtain the following expression for the limiting distribution:

$$\pi(v) = \sum_{a,a'=0}^{d-1} \sum_{\substack{k,k'=0 \\ \lambda_{a,k}=\lambda_{a',k'}}}^{N-1} c_{a,k} c^*_{a',k'} \sum_{b=0}^{d-1} \langle b, v|\lambda_{a,k}\rangle \langle \lambda_{a',k'}|b, v\rangle . \tag{7.13}$$

The sum should run over the pairs of indices (a, k) and (a', k') that correspond to equal eigenvalues $\lambda_{a,k} = \lambda_{a',k'}$. If all eigenvalues are different, that is, $\lambda_{a,k} \neq \lambda_{a',k'}$ for all (a, k) and (a', k'), the expression of the limiting distribution simplifies to

$$\pi(v) = \sum_{a=0}^{d-1} \sum_{k=0}^{N-1} |c_{a,k}|^2 \, p_{a,k}(v), \tag{7.14}$$

where

$$p_{a,k}(v) = \sum_{b=0}^{d-1} \left| \langle b, v|\lambda_{a,k}\rangle \right|^2 . \tag{7.15}$$

Note that the limiting distribution depends on $c_{a,k}$, which are the coefficients of the initial state in the basis of eigenvectors of U. Therefore, the limiting distribution depends on the initial condition in the general case.

Exercise 7.1. Let U be the evolution operator of a quantum walk as discussed in Sect. 7.1. Suppose that the limiting distribution is the same for any initial condition of type $|a, v\rangle$. Show that the limiting distribution is uniform on the vertices of the graph.

7.2.1 Limiting Distribution in the Fourier Basis

We have analyzed quantum walks in many graphs using the *Fourier basis* of the Hilbert space associated with the vertices. Let us denote this basis by $\{|\kappa_{\vec{k}}\rangle\}$, where $\vec{k}$ is the index of the vector basis, the size of which is equal to the number of vertices of the graph. We use the notation $\vec{k}$ (as a vector) to include cases where the dimension is greater than one, such as the *two-dimensional lattice* and the *hypercube*. The evolution operator can be written using a *reduced operator*, which depends on $\vec{k}$,

acting on the coin space. If $\left\{\left|\alpha_{a,\vec{k}}\right\rangle,\ 0 \leq a \leq d-1\right\}$ is an orthonormal basis of eigenvectors with eigenvalues $\alpha_{a,\vec{k}}$ of the reduced space, then $\left\{\left|\alpha_{a,\vec{k}}, \kappa_{\vec{k}}\right\rangle,\ 0 \leq a \leq d-1,\ 0 \leq \vec{k} \leq N-1\right\}$ is an orthonormal basis of eigenvectors of the evolution operator, which replaces $|\lambda_{a,k}\rangle$ in (7.4) until (7.6). The notation $\vec{k} = n$, where n is a decimal number, means that the decimal number must be converted into a vector with the corresponding number of entries. The eigenvalues of the evolution operator are the same eigenvalues $\alpha_{a,\vec{k}}$ of the reduced operator, because $|s\rangle\left|\kappa_{\vec{k}}\right\rangle$ is an eigenvector of the shift operator, where $|s\rangle$ is in the computational basis of the coin space.

In the Fourier basis, the expression for the limiting distribution is simpler. When all eigenvalues are different, (7.15) reduces to

$$p_{a,\vec{k}}(v) = \sum_{b=0}^{d-1} \left|\left\langle b\middle|\alpha_{a,\vec{k}}\right\rangle\right|^2 \left|\langle v|\kappa_{\vec{k}}\rangle\right|^2. \tag{7.16}$$

Term $\left|\langle v|\kappa_{\vec{k}}\rangle\right|^2$ is equal to $1/N$, since the coefficients of vector $\left|\kappa_{\vec{k}}\right\rangle$ are roots of unity divided by $\sqrt{N}$. This is true when the graph is a *Cayley graph*[4] of an *abelian group*, which includes cycles ($\mathbb{Z}_N$), two-dimensional lattices ($\mathbb{Z}^2_{\sqrt{N}}$), and hypercubes ($\mathbb{Z}_2^n$). Since vectors $\left|\alpha_{a,\vec{k}}\right\rangle$ have unit norm, it follows that

$$\sum_{b=0}^{d-1} \left|\left\langle b\middle|\alpha_{a,\vec{k}}\right\rangle\right|^2 = 1.$$

Therefore, $p_{a,\vec{k}}(v) = 1/N$ for all v. Substituting for (7.14) and using that the initial condition has unit norm, we obtain the uniform distribution

$$\pi(v) = \frac{1}{N}. \tag{7.17}$$

Among the graphs we have analyzed in Chap. 6, only cycles with odd number of vertices have different eigenvalues, as we shall see. Therefore, the limiting distribution is uniform in cycles with odd number of vertices, regardless of the initial condition.

Let us return to (7.13), which is valid in the general case in the Fourier basis. Renaming the original eigenvectors, we obtain

$$\pi(v) = \sum_{a,a'=0}^{d-1} \sum_{\substack{\vec{k},\vec{k}'=0 \\ \alpha_{a,\vec{k}}=\alpha_{a',\vec{k}'}}}^{N-1} c_{a,\vec{k}}\, c^*_{a',\vec{k}'} \sum_{b=0}^{d-1} \left\langle \alpha_{a',\vec{k}'}\middle|b\right\rangle \left\langle b\middle|\alpha_{a,\vec{k}}\right\rangle \langle v|\kappa_{\vec{k}}\rangle \langle \kappa_{\vec{k}'}|v\rangle. \tag{7.18}$$

[4] A Cayley graph is a directed graph which encodes the structure of a discrete group. The graph depends on the choice of a *generating set* S, which can be symmetric in the sense that if $g \in S$ then $g^{-1} \in S$. In this case, the Cayley graph is a regular undirected graph. If the group is abelian, the Fourier transform is defined using the *group character*.

Using the *completeness relation*, we obtain

$$\pi(v) = \sum_{a,a'=0}^{d-1} \sum_{\substack{\vec{k},\vec{k}'=0 \\ \alpha_{a,\vec{k}}=\alpha_{a',\vec{k}'}}}^{N-1} c_{a,\vec{k}}\, c^*_{a',\vec{k}'} \left\langle \alpha_{a',\vec{k}'} \middle| \alpha_{a,\vec{k}} \right\rangle \langle v|\kappa_{\vec{k}}\rangle \langle \kappa_{\vec{k}'}|v\rangle . \tag{7.19}$$

We will use this last equation to calculate the limiting distribution in even cycles, two-dimensional lattices, and hypercubes.

Exercise 7.2. Show that the expression of $\pi(v)$ in (7.19) satisfies

$$\sum_{v=0}^{N-1} \pi(v) = 1.$$

7.3 Limiting Distribution in Cycles

In this section, we compute the limiting distribution in cycles. We need the expressions of the eigenvalues and eigenvectors of the evolution operator to use (7.19). We need also to convert the notation. For the Hadamard coin, the eigenvalues are

$$\alpha_{0,\vec{k}} = \mathrm{e}^{-\mathrm{i}\theta_k}, \tag{7.20}$$

$$\alpha_{1,\vec{k}} = \mathrm{e}^{\mathrm{i}(\pi+\theta_k)} = -\mathrm{e}^{\mathrm{i}\theta_k}, \tag{7.21}$$

where θ_k is a solution of equation

$$\sin\theta_k = \frac{1}{\sqrt{2}} \sin\frac{2\pi k}{N}, \tag{7.22}$$

as described in Sect. 6.1.1. The analysis of eigenvalue collisions for different values of k plays an important role for determining the sum describing $\pi(v)$.

Figure 7.2 shows the eigenvalues for cycles with $N = 13$ and $N = 14$. The eigenvalues are confined to two regions of the unit circle. In fact, from (7.22), we have

$$|\sin\theta_k| \leq \frac{1}{\sqrt{2}}.$$

Then, $\theta_k \in [-\frac{\pi}{4}, \frac{\pi}{4}]$ or $\theta_k \in [\frac{3\pi}{4}, \frac{5\pi}{4}]$. If $-\theta_k$ is a solution of (7.22), then $\pi + \theta_k$ also is, since $\sin(\pi+\theta_k) = \sin(-\theta_k)$. Each eigenvalue of the form $\mathrm{e}^{-\mathrm{i}\theta_k}$ in the first sector $[-\frac{\pi}{4}, \frac{\pi}{4}]$ matches another (different) eigenvalue of the form $\mathrm{e}^{\mathrm{i}(\pi+\theta_k)}$ symmetrically opposite in the second sector.

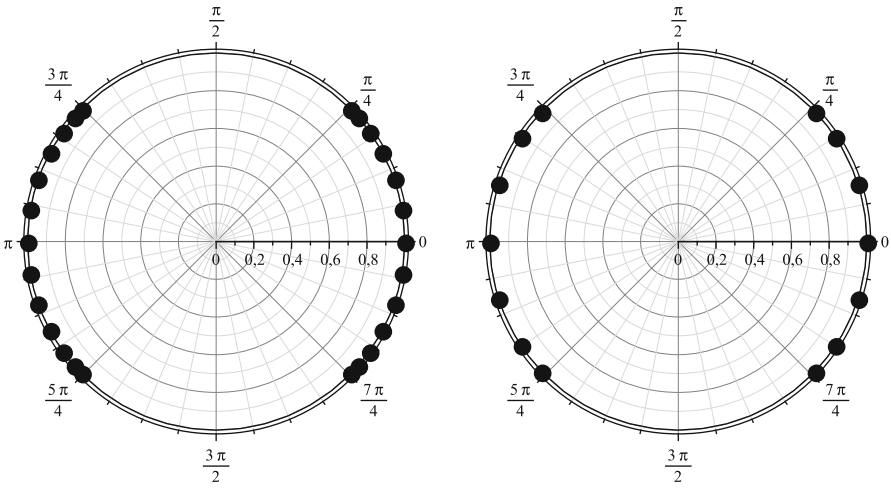

Fig. 7.2 Eigenvalues of the evolution operator for cycles with $N = 13$ and $N = 14$

The behavior of the eigenvalues depends on the parity of N. Two eigenvalues are equal if

$$\sin\frac{2\pi k}{N} = \sin\frac{2\pi k'}{N}.$$

This equation implies that $k = k'$ or $k + k' = \frac{N}{2}$ or $k + k' = \frac{3N}{2}$. If N is odd, only the first of these equations is satisfied and hence all eigenvalues are different. If N is even, there are 2 equal eigenvalues with different k's, unless $k = N/4$ or $k = 3N/4$, that only occur when 4 divides N.

Since all eigenvalues are different for cycles with odd number of vertices, the limiting distribution is uniform for any initial condition. In the rest of this section, we address the case N even.

The eigenvectors of the reduced operator are $\left|\alpha_{0,\vec{k}}\right\rangle = |\alpha_k\rangle$ and $\left|\alpha_{1,\vec{k}}\right\rangle = |\beta_k\rangle$, which are given by (6.16) and (6.17), respectively. Using the value of $|\kappa_k\rangle$ given by (6.7), we obtain

$$\left\langle v|\kappa_{\vec{k}}\right\rangle\left\langle\kappa_{\vec{k}'}|v\right\rangle = \frac{\omega_N^{v(k-k')}}{N}.$$

To adapt (7.19) for the cycle, we must take $d = 2$. Expanding the sum in variables a and a', we obtain

$$\pi(v) = \frac{1}{N}\sum_{\substack{k,k'=0\\ \mathrm{e}^{-\mathrm{i}\theta_k}=\mathrm{e}^{-\mathrm{i}\theta_{k'}}}}^{N-1} c_{0,k}\, c_{0,k'}^*\, \left\langle\alpha_{k'}|\alpha_k\right\rangle \omega_N^{v(k-k')}$$

$$+\frac{1}{N}\sum_{\substack{k,k'=0\\ \mathrm{e}^{\mathrm{i}(\pi+\theta_k)}=\mathrm{e}^{\mathrm{i}(\pi+\theta_{k'})}}}^{N-1} c_{1,k}\, c_{1,k'}^*\, \left\langle\beta_{k'}|\beta_k\right\rangle \omega_N^{v(k-k')}. \tag{7.23}$$

The cross terms $a = 0$, $a' = 1$, and vice versa do not contribute to any term, because the eigenvalues $e^{-i\theta_k}$ and $e^{i(\pi+\theta_k)}$ are never the same for any values of k and k', since $e^{-i\theta_k}$ is either in quadrant I or quadrant IV, as we can see in Fig. 7.2, while $e^{i(\pi+\theta_{k'})}$ is quadrant II or quadrant III. On the other hand, $e^{-i\theta_k}$ is equal to $e^{-i\theta_{k'}}$, if $k' = k$ or $k' = N/2 - k$, as discussed in Sect. 6.1.1. Therefore, the double sums in $\pi(v)$ reduces to simple sums each generating three terms: $k' = k$, $k' = N/2 - k \mod N$, and $k = N/2 - k' \mod N$. When $k' = k$, the sums can be easily calculated, using that $|\alpha_k\rangle$, $|\beta_k\rangle$, and $|\Psi(0)\rangle$ are unit vectors, generating term $1/N$ in (7.24). The sums under the constraints $k' = N/2 - k \mod N$ and $k = N/2 - k' \mod N$ are complex conjugate to each other. They can be simplified using the symmetries of the eigenvalues. Moreover, we can always take an initial condition such that $c_{0,k}$ and $c_{1,k}$ are real numbers, because the phases of $c_{0,k}$ and $c_{1,k}$ can be absorbed in the eigenvectors. Eventually, (7.23) reduces to

$$\pi(v) = \frac{1}{N} + \frac{1}{N}\,\Re\left(\sum_{\substack{k=0\\ k\neq \frac{N}{4},\frac{3N}{4}}}^{N-1} c_{0,k}\, c_{0,\frac{N}{2}-k}\left\langle \alpha_{\frac{N}{2}-k}\middle|\alpha_k\right\rangle \omega_N^{v\left(2k-\frac{N}{2}\right)}\right) + \frac{1}{N}\,\Re\left(\sum_{\substack{k=0\\ k\neq \frac{N}{4},\frac{3N}{4}}}^{N-1} c_{1,k}\, c_{1,\frac{N}{2}-k}\left\langle \beta_{\frac{N}{2}-k}\middle|\beta_k\right\rangle \omega_N^{v\left(2k-\frac{N}{2}\right)}\right), \tag{7.24}$$

where $\Re(\,)$ is the real part and the sub-indices must be evaluated modulo N to include case $k > N/2$. Note that if 4 divides N, we delete the terms $k = N/4$ and $k = 3N/4$, since the eigenvalue is unique for these values of k.

Using that $\omega_N = \exp(2\pi i/N)$, we obtain

$$\omega_N^{v\left(2k-\frac{N}{2}\right)} = (-1)^v e^{\frac{4\pi i k v}{N}}. \tag{7.25}$$

Using (6.16) and (6.17), we obtain

$$\left\langle \alpha_{\frac{N}{2}-k}\middle|\alpha_k\right\rangle = \left\langle \beta_{\frac{N}{2}-k}\middle|\beta_k\right\rangle = \frac{1 - e^{\frac{4\pi i k}{N}}}{2\sqrt{1+\cos^2\frac{2\pi k}{N}}}. \tag{7.26}$$

Substituting for (7.24), we obtain the limiting distribution in the cycle with generic (real) initial conditions

$$\pi(v) = \frac{1}{N} + \frac{(-1)^v}{2N}\sum_{\substack{k=0\\ k\neq \frac{N}{4},\frac{3N}{4}}}^{N-1}\left(c_{0,k}\, c_{0,\frac{N}{2}-k} + c_{1,k}\, c_{1,\frac{N}{2}-k}\right) \times \frac{\cos\frac{4\pi k v}{N} - \cos\frac{4\pi k (v+1)}{N}}{\sqrt{1+\cos^2\frac{2\pi k}{N}}}. \tag{7.27}$$

This expression is generic in the sense that any limiting distribution in the cycle with the Hadamard coin can be obtained from it. The sub-indices are evaluated modulo N.

The last step is to find coefficients $c_{0,k}$ and $c_{1,k}$ of the initial condition in the basis of eigenvectors of the evolution operator. Taking $t = 0$ in (6.26), we obtain

$$|\Psi(0)\rangle = \sum_{k=0}^{N-1} \left(\frac{1}{\sqrt{N c_k^-}} |\alpha_k\rangle |\kappa_k\rangle + \frac{1}{\sqrt{N c_k^+}} |\beta_k\rangle |\kappa_k\rangle \right). \tag{7.28}$$

Therefore,

$$c_{0,k} = \frac{1}{\sqrt{N c_k^-}},$$
$$c_{1,k} = \frac{1}{\sqrt{N c_k^+}}.$$

Using (6.18), we obtain

$$c_{0,k}\, c_{0,\frac{N}{2}-k} + c_{1,k}\, c_{1,\frac{N}{2}-k} = \frac{1}{N\sqrt{1+\cos^2\frac{2\pi k}{N}}}. \tag{7.29}$$

Therefore, the limiting distribution in the cycle with the Hadamard coin and initial condition $|\Psi(0)\rangle = |0\rangle|0\rangle$ is

$$\pi(v) = \frac{1}{N} + \frac{(-1)^v}{2N^2} \sum_{\substack{k=0 \\ k \neq \frac{N}{4}, \frac{3N}{4}}}^{N-1} \frac{\cos\frac{4\pi k v}{N} - \cos\frac{4\pi k (v+1)}{N}}{1+\cos^2\frac{2\pi k}{N}}. \tag{7.30}$$

Figure 7.3 shows the limiting probability distribution $\pi(v)$ of a cycle with $N = 102$. The central peak pointing downward is typical for even values of N, that are non-divisible by 4. When N is divisible by 4, the peak points upward.

Exercise 7.3. Show that

$$\cos\frac{4\pi k v}{N} - \cos\frac{4\pi k\,(v+1)}{N} = 2\sin\frac{2\pi k}{N}\sin\frac{2\pi k}{N}(2v+1).$$

From this equality, obtain an equivalent expression for $\pi(v)$.

Exercise 7.4. Show that the expression of $\pi(v)$ in (7.30) satisfies

$$\sum_{v=0}^{N-1} \pi(v) = 1.$$

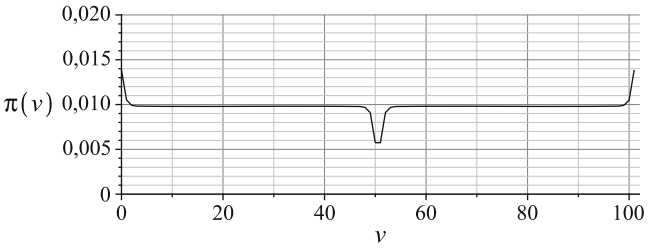

Fig. 7.3 Limiting probability distribution in a cycle with $N = 102$ using the Hadamard coin and initial condition $|\Psi(0)\rangle = |0\rangle|0\rangle$

Exercise 7.5. Show that

$$\pi(0) \simeq \frac{\sqrt{2}}{N},$$

when $N \gg 1$.

Exercise 7.6. Show that

$$\pi(v) \simeq \frac{c_1(v)\sqrt{2} - c_2(v)}{N},$$

when $v \ll N$ and $1 \ll N$, where

$$c_1(v) = \frac{2+\sqrt{2}}{4}(d_+)^v + \frac{2-\sqrt{2}}{4}(d_-)^v,$$

$$c_2(v) = \frac{3\,(d_+)^{2v} + 1 + \sqrt{2}}{2\sqrt{2}\,(d_+)^v} - \frac{3\,(d_-)^{2v} + 1 - \sqrt{2}}{2\sqrt{2}\,(d_-)^v} - 1,$$

and $d_\pm = 3 \pm 2\sqrt{2}$.

7.4 Limiting Distribution in Hypercubes

The spectral decomposition of the evolution operator for the hypercube is described in Sect. 6.3. If the initial condition is

$$|\Psi(0)\rangle = |\mathrm{D}\rangle\big|\vec{v} = 0\big\rangle,$$

the state of the quantum walk at time t is given by (6.103). Replacing $t = 0$ into this equation, we obtain the initial condition in the basis of the eigenvectors of the evolution operator

$$|\Psi(0)\rangle = \frac{1}{\sqrt{2^n}}\Big(|\mathrm{D}\rangle|\beta_{\vec{0}}\rangle + |\mathrm{D}\rangle|\beta_{\vec{1}}\rangle\Big) + \frac{1}{\sqrt{2^{n+1}}}\sum_{\vec{k}=1}^{2^n-2}\left(\left|\widetilde{\alpha}_1^{\vec{k}}\right\rangle|\beta_{\vec{k}}\rangle + \left|\widetilde{\alpha}_n^{\vec{k}}\right\rangle|\beta_{\vec{k}}\rangle\right). \tag{7.31}$$

Therefore,

$$c_{1,\vec{k}} = c_{n,\vec{k}} = \begin{cases} \frac{1}{\sqrt{2^n}}, & \vec{k} = 0,\ \vec{k} = n; \\ \frac{1}{\sqrt{2^{n+1}}}, & 0 < \vec{k} < n, \end{cases} \tag{7.32}$$

and all other values are zero. Equation (7.19) assumes the form

$$\pi(\vec{v}) = \sum_{\substack{\vec{k},\vec{k}'=0 \\ k=k'}}^{N-1} c_{1,\vec{k}}c_{1,\vec{k}'}\left\langle\widetilde{\alpha}_1^{\vec{k}'}\middle|\widetilde{\alpha}_1^{\vec{k}}\right\rangle\langle\vec{v}|\beta_{\vec{k}}\rangle\langle\beta_{\vec{k}'}|\vec{v}\rangle + \sum_{\substack{\vec{k},\vec{k}'=0 \\ k=k'}}^{N-1} c_{n,\vec{k}}c_{n,\vec{k}'}\left\langle\widetilde{\alpha}_n^{\vec{k}'}\middle|\widetilde{\alpha}_n^{\vec{k}}\right\rangle\langle\vec{v}|\beta_{\vec{k}}\rangle\langle\beta_{\vec{k}'}|\vec{v}\rangle. \tag{7.33}$$

Note that parameter a starts at 1 and goes up to n in the convention used in the description of the hypercube in Sect. 6.3. The cross terms do not appear because $\left\langle\widetilde{\alpha}_n^{\vec{k}'}\middle|\widetilde{\alpha}_1^{\vec{k}}\right\rangle = 0$. The collision between the eigenvectors is guaranteed by restricting $k = k'$ in the sum, where k is *Hamming weight* of $\vec{k}$.

Using (6.101) and (6.102) along with (6.91) and (6.92), we obtain

$$\left\langle\widetilde{\alpha}_1^{\vec{k}'}\middle|\widetilde{\alpha}_1^{\vec{k}}\right\rangle = \left\langle\widetilde{\alpha}_n^{\vec{k}'}\middle|\widetilde{\alpha}_n^{\vec{k}}\right\rangle = \frac{n\,(\vec{k}\cdot\vec{k}') + k(n-2k)}{2k(n-k)}. \tag{7.34}$$

Using (6.77), we obtain

$$\langle\vec{v}|\beta_{\vec{k}}\rangle = \frac{1}{\sqrt{2^n}}(-1)^{\vec{k}\cdot\vec{v}}. \tag{7.35}$$

Substituting these results for (7.33), we obtain

$$\pi(\vec{v}) = \frac{2}{2^{2n}} + \frac{1}{2^{2n}}\sum_{\substack{\vec{k},\vec{k}'=0 \\ (k=k'\neq 0,n)}}^{2^n-1}(-1)^{(\vec{k}+\vec{k}')\cdot\vec{v}}\,\frac{n\,(\vec{k}\cdot\vec{k}') + k(n-2k)}{2k(n-k)}. \tag{7.36}$$

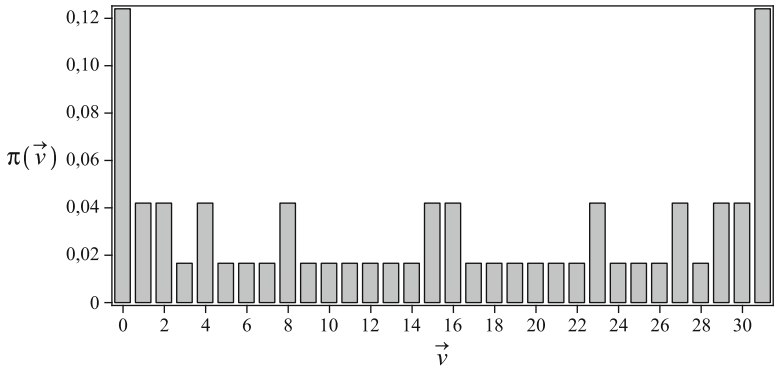

Fig. 7.4 Limiting distribution on the hypercube with $N = 2^5$. The labels of the vertices are in the decimal notation

The graph in Fig. 7.4 shows the limiting distribution on the hypercube with $N = 32$ vertices, obtained from (7.36). Note that the distribution has the same value for different vertices. In particular, the distribution is equal for all vertices of the same Hamming weight. This suggests that π depends only on the Hamming weight of $\vec{v}$. We can see that the graph is symmetric with respect to central vertical axis. This suggests that the limiting distribution has the following invariance: $\pi(v) = \pi(2^n - 1 - v)$, which can be confirmed with all points on the graph.

Since the limiting distribution depends only on the Hamming weight of the vertices, we can define a new probability distribution for a walk on the line. The new expression is

$$\pi(v) = \binom{n}{v} \pi(\vec{v}). \tag{7.37}$$

The binomial coefficient gives the number of vertices that have the same Hamming weight. The new distribution satisfies

$$\sum_{v=0}^{n} \pi(v) = 1.$$

The graph of Fig. 7.5 shows this distribution for a hypercube with 2^{32} vertices.

Exercise 7.7. Show that

$$\begin{aligned} \pi\,(0) &= \frac{1}{4^n} + \frac{\Gamma\left(n + \frac{1}{2}\right)}{2\sqrt{\pi}\, n\, \Gamma(n)} \\ &= \frac{1}{4^n}\left(1 + \frac{(2n)!}{2(n!)^2}\right) \end{aligned}$$

where Γ is the *gamma function*, which is an extension of the *factorial function*.

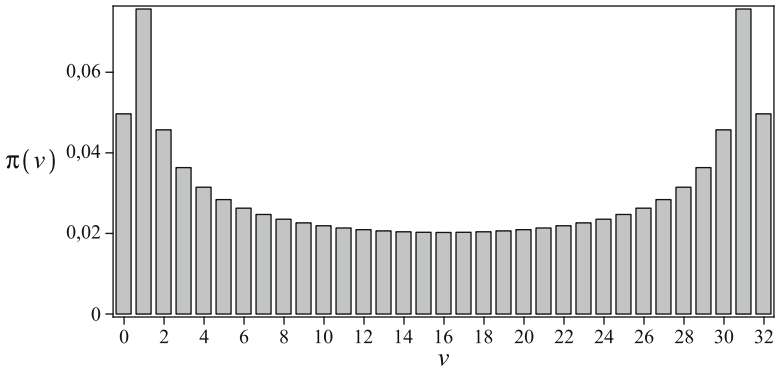

Fig. 7.5 Limiting distribution as function of the Hamming weight for a hypercube with $N = 2^{32}$, given by (7.37)

7.5 Limiting Distribution in Finite Lattices

The two-dimensional finite lattice is an interesting example where the limiting distribution can be found analytically. The details of the calculation of the spectral decomposition of the evolution operator are presented in Sect. 6.2. If the initial condition is

$$|\Psi(0)\rangle = |\mathrm{D}\rangle|x = 0, y = 0\rangle,$$

the state of the quantum walk at time t in the basis of the eigenvectors of the evolution operator is

$$|\Psi(t)\rangle = \frac{1}{\sqrt{N}}|\mathrm{D}\rangle|\mathrm{D}\rangle + \frac{1}{\sqrt{2N}} \sum_{\substack{k_x,k_y=0 \\ (k_x,k_y)\neq(0,0)}}^{\sqrt{N}-1} \left(\mathrm{e}^{\mathrm{i}\theta t}\left|\nu^{\theta}_{k_x,k_y}\right\rangle + \mathrm{e}^{-\mathrm{i}\theta t}\left|\nu^{-\theta}_{k_x,k_y}\right\rangle\right)|\kappa_{k_x,k_y}\rangle.$$

From this expression we can see that the eigenvectors of U that generate the subspace where the quantum walk evolves are $|\mathrm{D}\rangle|\mathrm{D}\rangle$, $\left|\nu^{\pm\theta}_{k_x,k_y}\right\rangle|\kappa_{k_x,k_y}\rangle$, $0 \leq k_x, k_y \leq \sqrt{N}-1$, $(k_x, k_y) \neq (0,0)$.

Equation (7.13) assumes the form

$$\pi(x,y) = |c_{0,0}|^2 \left(\sum_{d,s=0}^{1} \left|\langle d,s|\mathrm{D}\rangle\right|^2 \right) \left|\langle x,y|\mathrm{D}\rangle\right|^2$$
$$+ \sum_{\substack{k_x,k_y=0 \\ (k_x,k_y)\neq(0,0)}}^{\sqrt{N}-1} \sum_{\substack{k'_x,k'_y=0 \\ (k'_x,k'_y)\neq(0,0) \\ \theta=\theta'}}^{\sqrt{N}-1} c^{+}_{k_x,k_y} \left(c^{+}_{k'_x,k'_y}\right)^*$$
$$\times \sum_{d,s=0}^{1} \left\langle d,s|v^{\theta}_{k_x,k_y}\right\rangle \left\langle v^{\theta'}_{k'_x,k'_y}|d,s\right\rangle \langle x,y|\kappa_{k_x,k_y}\rangle \left\langle \kappa_{k'_x,k'_y}|x,y\right\rangle$$
$$+ c^{-}_{k_x,k_y} \left(c^{-}_{k'_x,k'_y}\right)^*$$
$$\times \sum_{d,s=0}^{1} \left\langle d,s|v^{-\theta}_{k_x,k_y}\right\rangle \left\langle v^{-\theta'}_{k'_x,k'_y}|d,s\right\rangle \langle x,y|\kappa_{k_x,k_y}\rangle \left\langle \kappa_{k'_x,k'_y}|x,y\right\rangle, \quad (7.38)$$

where $\theta' = \theta(k'_x, k'_y)$. Note that we have simply rewritten the terms of (7.13) without performing simplifications. The label a in (7.13) is converted to d, s. The index k of eigenvectors is converted to k_x, k_y. The sum in the new indices is restricted to terms with nonzero c_{k_x,k_y}. Coefficients c_{k_x,k_y} are obtained by taking $t = 0$ in the equation of $|\Psi(t)\rangle$, because for $t = 0$ we have the decomposition of the initial condition in the basis of the eigenvectors of the evolution operator. Then, we obtain

$$c_{0,0} = \tfrac{1}{\sqrt{N}}, \quad (7.39)$$
$$c^{+}_{k_x,k_y} = c^{-}_{k_x,k_y} = \tfrac{1}{\sqrt{2N}}. \quad (7.40)$$

Using the completeness relation $I_4 = \sum_{d,s=0}^{1} |d,s\rangle\langle d,s|$, we obtain

$$\sum_{d,s=0}^{1} \left\langle d,s|v^{\pm\theta}_{k_x,k_y}\right\rangle \left\langle v^{\pm\theta'}_{k'_x,k'_y}|d,s\right\rangle = \left\langle v^{\pm\theta'}_{k'_x,k'_y}|v^{\pm\theta}_{k_x,k_y}\right\rangle. \quad (7.41)$$

Using (6.43), we obtain

$$\langle x,y|\kappa_{k_x,k_y}\rangle = \frac{1}{\sqrt{N}}\, \omega^{xk_x+yk_y}, \quad (7.42)$$

where $\omega = \mathrm{e}^{\frac{2\pi \mathrm{i}}{\sqrt{N}}}$.

Substituting these partial results for (7.38) and simplifying, we obtain

$$\pi(x,y) = \frac{1}{N^2} + \frac{1}{N^2} \sum_{\substack{k_x,k_y=0 \\ (k_x,k_y)\neq(0,0)}}^{\sqrt{N}-1} \sum_{\substack{k'_x,k'_y=0 \\ (k'_x,k'_y)\neq(0,0) \\ \theta(k'_x,k'_y)=\theta(k_x,k_y)}}^{\sqrt{N}-1} \left\langle \nu^{\theta'}_{k'_x,k'_y} \middle| \nu^{\theta}_{k_x,k_y} \right\rangle$$

$$\times \ \mathrm{e}^{\frac{2\pi \mathrm{i}}{\sqrt{N}}\left(x(k_x-k'_x)+y(k_y-k'_y)\right)}. \tag{7.43}$$

We use $\left\langle \nu^{\theta'}_{k'_x,k'_y} \middle| \nu^{\theta}_{k_x,k_y} \right\rangle = \left\langle \nu^{-\theta'}_{k'_x,k'_y} \middle| \nu^{-\theta}_{k_x,k_y} \right\rangle$, which can be verified using (6.58). The first term is absorbed in the sum. In the double sum, values (k_x, k_y) need not be equal to (k'_x, k'_y), but the combination of values must be such that $\theta' = \theta$. Using that $\cos\theta' = \cos\theta$, we obtain

$$\left\langle \nu^{\theta'}_{k'_x,k'_y} \middle| \nu^{\theta}_{k_x,k_y} \right\rangle = \frac{1 - 2\cos^2\theta(k_x,k_y) + \cos\theta(k_x - k'_x, k_y - k'_y)}{2\sin^2\theta(k_x,k_y)}. \tag{7.44}$$

The simplification of this equation requires detailed knowledge of the collisions of the eigenvalues, that is, the relations about k'_x, k'_y such that $\theta(k'_x, k'_y) = \theta(k_x, k_y)$.

7.6 Distance Between Distributions

If we have more than one probability distribution on a graph with N vertices, it is interesting to define the notion of closeness between them. To use terms *close* or *far*, we have to define a metric. Let p and q be two probability distributions, that is, $0 \leq p_v \leq 1$, $0 \leq q_v \leq 1$, and

$$\sum_{v=1}^{N} p_v = \sum_{v=1}^{N} q_v = 1. \tag{7.45}$$

The definition that is usually used for *distance* is

$$D(p,q) = \frac{1}{2} \sum_{v=1}^{N} |p_v - q_v|, \tag{7.46}$$

known as *total variation distance* or L_1 distance, because the power of the terms inside the sum has degree 1. This definition satisfies

1. $0 \leq D(p,q) \leq 1$,
2. $D(p,q) = 0$ if and only if $p = q$,
3. $D(p,q) = D(q,p)$,
4. $D(p,q) \leq D(p,r) + D(r,q)$.

The last two properties are called *symmetrical* and *triangle inequality*, respectively.

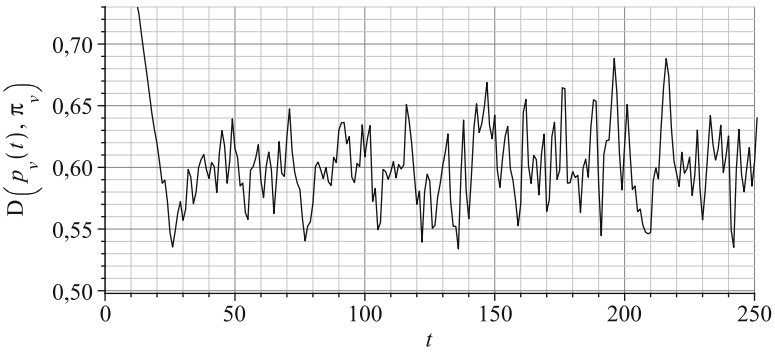

Fig. 7.6 Distance between the distribution $p_v(t)$ and the limiting distribution π_v as a function of time for a cycle with 102 vertices. The graph has a quasi-periodic pattern

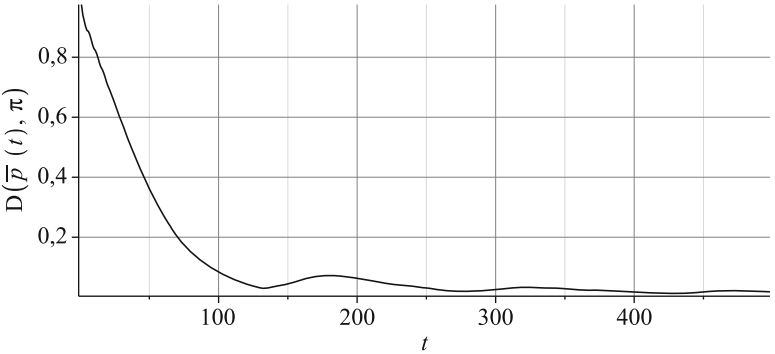

Fig. 7.7 Distance between the average distribution $\bar{p}_v(t)$ and the limiting distribution π_v as a function of time for a cycle with 102 vertices

We can better understand the characteristics of the unitary evolution by analyzing the distance between distribution $p_v(t)$ and the limiting distribution π_v. Figure 7.6 shows the typical behavior of this distance as a function of time for the even cycle with 102 vertices and initial condition $|\psi(0)\rangle = |0\rangle|0\rangle$. The graph shows the *quasi-periodic* behavior discussed in Sect. 7.2 manifesting in the distance between the instantaneous and the limiting distribution.

It is much more interesting to analyze the distance between the *average distribution* $\bar{p}_v(t)$ and the *limiting distribution* π_v as a function of time, because we have a notion of convergence, since the limiting distribution is reached from the average distribution in the limit $t \to \infty$. Figure 7.7 shows $D(\bar{p}(t), \pi)$ as a function of time for a cycle with 102 vertices using the Hadamard coin and initial condition $|\psi(0)\rangle = |0\rangle|0\rangle$. The curve does not have a quasi-periodic pattern, in fact, disregarding the oscillation, we have the impression that the curve obeys a power law such as $1/t^a$, where a is a positive number. This kind of conjecture can be

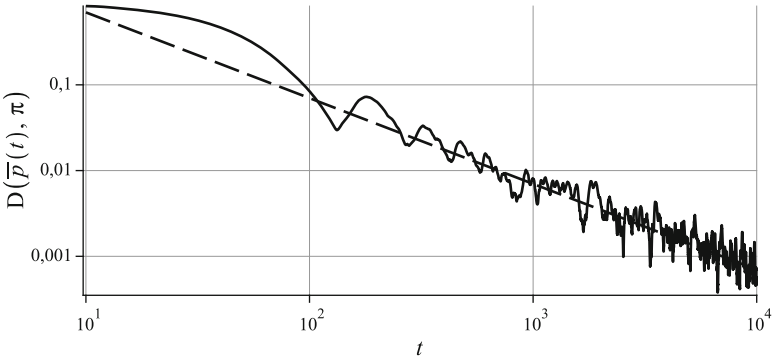

Fig. 7.8 Loglog plot of the distance between the average distribution $\bar{p}_v(t)$ and the limiting distribution π_v as a function of time for the cycle with 102 vertices up to $t = 10^4$. The equation of the *dashed line* is $7.0/t$

checked by plotting the curve using the axes in a log scale. If the result is a straight line, the slope is a. Suppose that

$$D(\bar{p}(t), \pi) = \frac{b}{t^a}$$

for some b. Taking the logarithm of both sides, we obtain

$$\log D(\bar{p}(t), \pi) = -a \log t + \log b.$$

If the conjecture is true and we plot $\log D(\bar{p}(t), \pi)$ as a function of $\log t$, we obtain a straight line with negative slope. The base of the logarithm plays no role if we want to check the conjecture. It is only relevant when we wish to obtain the value of b. Figure 7.8 show the loglog plot of $D(\bar{p}(t), \pi)$ as a function of t. It seems that the curve oscillates around a straight line. To find the line equation we select the extremum points, which are around $(10, 0.7)$ and $(10^4, 0.0007)$. Then,

$$\begin{aligned} a &\simeq -\frac{\log 0.0007 - \log 0.7}{\log 10^4 - \log 10} \\ &\simeq 1.0, \end{aligned}$$

and b can be easily found. The line equation is $7.0/t$.

In the nontrivial cases, we can analytically show that $D(\bar{p}(t), \pi)$ has a dominant inverse power law behavior for a generic graph. Using (7.10) and (7.12), we obtain

$$\begin{aligned} \bar{p}_v(t) - \pi(v) = \sum_{a,a',b=0}^{d-1} \sum_{k,k'=0}^{N-1} & c_{a,k} c^*_{a',k'} \left\langle b, v \middle| \lambda_{a,k} \right\rangle \left\langle \lambda_{a',k'} \middle| b, v \right\rangle \\ & \times \left(\frac{1}{t} \sum_{t=0}^{t-1} \mathrm{e}^{2\pi \mathrm{i} (\lambda_{a,k} - \lambda_{a',k'})t} - \delta_{\lambda_{a,k}, \lambda_{a',k'}} \right). \end{aligned}$$

The terms of the sum corresponding to $\lambda_{a,k} = \lambda_{a',k'}$ vanish. Using (7.11) and (7.46), we obtain

$$D(\bar{p}(t),\pi) = \frac{1}{2t}\sum_{v=1}^{N}\left|\sum_{a,a'=0}^{d-1}\sum_{\substack{k,k'=0\\ \lambda_{a,k}\neq\lambda_{a',k'}}}^{N-1} c_{a,k}c^{*}_{a',k'}\,\frac{\mathrm{e}^{2\pi\mathrm{i}(\lambda_{a,k}-\lambda_{a',k'})t}-1}{\mathrm{e}^{2\pi\mathrm{i}(\lambda_{a,k}-\lambda_{a',k'})}-1}\right.$$
$$\left.\times\sum_{b=0}^{d-1}\langle\lambda_{a',k'}|b,v\rangle\langle b,v|\lambda_{a,k}\rangle\right|. \tag{7.47}$$

The factor $1/t$ is responsible for the inverse power law. The only term that depends on t in the sum is $\mathrm{e}^{2\pi\mathrm{i}(\lambda_{a,k}-\lambda_{a',k'})t}-1$, the modulus of which is a bounded periodic function. The linear combination of terms of this kind produces the oscillatory pattern around the straight line showed in Fig. 7.8.

Exercise 7.8. Show that in odd cycles, the distance between the limiting distribution and the initial distribution starting from any vertex is

$$D\big(p(0),\pi\big) = 1-\frac{1}{N}. \tag{7.48}$$

Note that when $N \gg 1$ this distance is close to the maximum distance.

Exercise 7.9. Simplify (7.47) for walks that can be analyzed in the Fourier basis.

Exercise 7.10. Obtain an explicit expression for (7.47) for walks on (odd and even) cycles with the Hadamard coin using the initial condition $|\psi(t)\rangle = |0\rangle|0\rangle$. Reproduce Fig. 7.7 using the analytical result.

7.7 Mixing Time

We have learned that the *average distribution* $\bar{p}_v(t)$ tends to the *limiting distribution* π_v. Usually, the approach is not monotonic, but there is a moment, that we denote by τ_ϵ, such that the distance between the distributions is smaller than or equal to the threshold ϵ and does not become larger.

Formally, the *quantum mixing time* is defined as

$$\tau_\epsilon = \min\big\{T \mid \forall t \geq T,\ D\big(\bar{p}_v(t),\pi_v\big) \leq \epsilon\big\}, \tag{7.49}$$

which can be interpreted as the number of steps it takes for the probability distribution to approach its final configuration. The quantum mixing time depends on the initial condition in general.

Table 7.1 Quantum and classical mixing times for the N-cycle, the two-dimensional lattice, and the hypercube with N vertices

τ_ϵ	N-cycle	2d lattice	Hypercube
Quantum	$O\left(\frac{N \log N}{\epsilon}\right)$	$O\left(\frac{\sqrt{N} \log N}{\epsilon}\right)$	$O\left(\frac{\log N}{\epsilon}\right)$
Classical	$O\left(N^2 \log \frac{1}{\epsilon}\right)$	$O\left(N \log \frac{1}{\epsilon}\right)$	$O\left(\log N \log \frac{\log N}{\epsilon}\right)$

The mixing time captures the notion of the velocity in which the limiting distribution is reached. A small mixing time means that the limiting distribution is quickly reached. The mixing time τ_ϵ depends on parameter ϵ. If $D\left(\bar{p}_v(t), \pi_v\right)$ obeys an inverse power law as a function of time, then τ_ϵ obeys an inverse power law as a function of ϵ. Parameter ϵ is not the only one. In finite graphs, the number of vertices is a key parameter to assess the characteristics of the mixing time. It is interesting to compare the *quantum mixing time* with the *classical mixing time* of a *classical random walk* on the same graph. The definition of the classical mixing time is the same—(7.49), but instead of using the average probability distribution of the quantum walk the definition employs the probability distribution of the classical random walk.

In general, it is not possible to obtain closed analytical expressions for the mixing time in terms of the number of vertices. We can obtain upper or lower *bounds* or we can analyze numerically. Table 7.1 summarizes some results about quantum and classical mixing times for comparison. The quantum mixing times were obtained using numerical methods. The N-cycle with even N, the $(\sqrt{N} \times \sqrt{N})$-lattice with even $\sqrt{N}$, and hypercubes are bipartite graphs. The classical random walk in those cases must be the *lazy random walk*, which is defined in such way that the walker moves to one of its nearest neighbors or stays fixed with equal probability. This guarantees that there is a classical limiting distribution, which is uniform for those graphs.

The logarithm term in the classical mixing time shows that the limiting distribution is reached surprisingly rapidly by the classical random walk for a fixed N. On the other hand, the scaling with the graph size for cycles and lattices is smaller for the quantum mixing time.

Further Reading

The study of quantum walks on graphs received a boost after [3], which has provided a definition of the *limiting distribution* and the *quantum mixing time*. This reference also analyzes the quantum walk on odd cycles. The limiting distribution on even cycles was calculated in [13, 14], on hypercubes in [55], and on two-dimensional lattices in [54]. The mixing time in cycles was analyzed in [3], in hypercubes in [55, 59]. Classical mixing times are analyzed in [60], which has a detailed study of the classical mixing time of random walks on hypercubes.

Chapter 8
Spatial Search Algorithms

An interesting problem in the area of algorithms is the *spatial search problem*, which consists of finding one or more specific points in a physical region that can be modelled by a *two-dimensional lattice*, so that the vertices are the places one can search and the edges are the directions to which one can move. The quantum version of this problem was analyzed by *Benioff* in a very concrete way. He imagined a *quantum robot* that moves to adjacent nodes in a unit time. The position of the robot can be in superposition of a finite number of places. How many steps will the robot take to find a marked node with high probability?

If we consider n consecutive sites in a line, the quantum motion of the robot from one end to the other will take $n - 1$ time units with no possibility of gain in complexity compared to a classical robot. However, if the sites form a two-dimensional lattice with the *topology* of a *torus*, the quantum robot can find a marked site more quickly. A direct application of *Grover's algorithm* to this problem in two-dimensional lattices does not improve the time complexity compared to searching using a *classical robot* that moves at random.

The quantum robot will be faster than the classical one if a strategy known as *abstract search algorithm* is used. In this chapter, we describe how this algorithm works and we analyze its time complexity in details. The two-dimensional lattice is used as a concrete example. At the end, we show that Grover's algorithm can be seen as a spatial search problem in the *complete graph*.

8.1 Abstract Search Algorithm

The *abstract search algorithm* in a finite *regular graph* is based on a modification of the *standard quantum walk*. Consider a quantum walk driven by

$$U = S(C \otimes I), \tag{8.1}$$

R. Portugal, *Quantum Walks and Search Algorithms*, Quantum Science and Technology, DOI 10.1007/978-1-4614-6336-8_8,

where S is the shift operator and C is the coin operator. The computational basis of the Hilbert space is $\{|a\rangle|v\rangle, 0 \leq a \leq d-1, 0 \leq v \leq N-1\}$, where d is the degree of the graph and N is the number of vertices. The state of a generic edge is represented by $|a\rangle$ and a generic vertex by $|v\rangle$. The Grover coin is given by

$$G = 2|\mathrm{D}\rangle\langle\mathrm{D}| - I, \tag{8.2}$$

where $|\mathrm{D}\rangle$ is the diagonal state, the coin space. Operator S moves the walker from one vertex to its neighbor. The next neighbor is determined by the coin value.

In the *standard quantum walk*, the coin operator does not change from vertex to vertex. The coin operator used in all the vertices is, for example, the Grover operator. In the abstract search algorithm, we must somehow mark the vertex by using an operator which distinguishes between *searched* and *non-searched vertices*. A generalized coin operator can make this distinction. Consider the following coin operator:

$$C' = -I \otimes |v_0\rangle\langle v_0| + G \otimes (I - |v_0\rangle\langle v_0|), \tag{8.3}$$

where v_0 is the searched vertex. It is easy to verify that

$$C'|a\rangle|v\rangle = \begin{cases} -|a\rangle|v_0\rangle, & \text{if } v = v_0; \\ (G|a\rangle)|v\rangle, & \text{if } v \neq v_0. \end{cases} \tag{8.4}$$

The above equation shows that the action of C' is equivalent to operator $-I$, if the associated vertex is v_0, and is equivalent to Grover's operator, if the vertex is not v_0. C' is the operator that marks vertex v_0. It acts on the combined coin-vertex space, yet it is called a coin operator.

We now have a new evolution operator

$$U' = SC'. \tag{8.5}$$

U' can be written as the product of the unmodified original operator U by a *reflection operator*. To show this, we use (8.3) and then (8.2).

$$\begin{aligned} U' &= S\left(-I \otimes |v_0\rangle\langle v_0| + G \otimes (I - |v_0\rangle\langle v_0|)\right) \\ &= S\left(G \otimes I - (I + G) \otimes |v_0\rangle\langle v_0|\right) \\ &= U - 2\,S\left(|\mathrm{D}\rangle\langle\mathrm{D}| \otimes |v_0\rangle\langle v_0|\right) \end{aligned}$$

Note that $|\mathrm{D}\rangle$ is an eigenvector of operator G with eigenvalue 1, that is, $|\mathrm{D}\rangle = G|\mathrm{D}\rangle$. So,

$$\begin{aligned} U' &= U - 2\,S\,(G \otimes I)\left(|\mathrm{D}\rangle\langle\mathrm{D}| \otimes |v_0\rangle\langle v_0|\right) \\ &= U\left(I - 2|\mathrm{D}\rangle\langle\mathrm{D}| \otimes |v_0\rangle\langle v_0|\right) \\ &= U\,R, \end{aligned}$$

where

$$R = I - 2|\mathrm{D}, v_0\rangle\langle \mathrm{D}, v_0|. \tag{8.6}$$

R is a *reflection operator* around the hyperplane orthogonal to vector $|\mathrm{D}\rangle|v_0\rangle$. To check this fact note that

$$R|\psi\rangle|v\rangle = \begin{cases} -|\mathrm{D}\rangle|v_0\rangle, \text{ if } |\psi\rangle = |\mathrm{D}\rangle \text{ and } v = v_0; \\ +|\psi\rangle|v\rangle, \text{ if } |\psi\rangle = |\mathrm{D}\rangle^{\perp} \text{ or } v \neq v_0. \end{cases} \tag{8.7}$$

That is, any vector $|\psi\rangle|v\rangle$ orthogonal to $|\mathrm{D}\rangle|v_0\rangle$ is invariant under the action of R. The linear combination of these vectors forms the hyperplane orthogonal to $|\mathrm{D}\rangle|v_0\rangle$. On the other hand, vector $|\mathrm{D}\rangle|v_0\rangle$ inverts the sign under the action of R. What happens to a generic vector under the action of R can be seen by decomposing the generic vector as the sum of a vector in the vector space spanned by $|\mathrm{D}\rangle|v_0\rangle$ and another vector in the orthogonal hyperplane. Vector $|\mathrm{D}\rangle|v_0\rangle$ is called *target state* because the goal of the algorithm is to drive the quantum computer to a state that has high fidelity to $|\mathrm{D}\rangle|v_0\rangle$. In this case, the measurement of the second register in the computational basis will provide v_0 with high probability.

The initial state of the abstract search algorithm is

$$|\Psi_0\rangle = |\mathrm{D_C}\rangle|\mathrm{D_V}\rangle, \tag{8.8}$$

where $|\mathrm{D_C}\rangle$ is the diagonal state of the coin space and $|\mathrm{D_V}\rangle$ is the diagonal state of the vertex space. It is important that the initial state can be efficiently generated. If the quantum walk is simulated in a quantum computer, the diagonal state will be efficiently generated by applying Hadamard operators. However, the goal is to implement the abstract search algorithm directly on a device built specifically for quantum walks, that is, a device that implements the shift operator S and coin operators C and C'. Thus, $|\Psi_0\rangle$ must be efficiently generated with operators S and C.

Similar to Grover's algorithm described in Sect. 4.1, the abstract search algorithm is iterative, that is, operator U' must be applied successively until the probability of finding the marked vertex is considerable. The number of applications of U' is used for calculating the time complexity of the algorithm. We have to find t_f such that $(U')^{t_f}|\Psi_0\rangle$ has high fidelity to $|\mathrm{D}\rangle|v_0\rangle$. The value of t_f is the algorithm runtime and the success probability is

$$p = \sum_a |\langle a, v_0|(U')^{t_f}|\Psi_0\rangle|^2. \tag{8.9}$$

To determine t_f, it is convenient to use the spectral decomposition of U'. Suppose that its eigenvectors and eigenvalues are $|\alpha_k\rangle$ and α_k, respectively. Then,

$$U' = \sum_k \alpha_k |\alpha_k\rangle\langle\alpha_k|. \tag{8.10}$$

At the final time t_f, the state of the walk is given by

$$(U')^{t_f}|\Psi_0\rangle = \sum_k (\alpha_k)^{t_f} |\alpha_k\rangle \langle\alpha_k|\Psi_0\rangle, \tag{8.11}$$

since a function f applied to U' is by definition $\sum_k f(\alpha_k)|\alpha_k\rangle\langle\alpha_k|$. The calculation of the eigenvalues and eigenvectors of an operator is usually a hard-working task. In the case of operator U', the calculation of the spectral decomposition is not doable even in the simplest graphs, where the search problem is nontrivial, such as in finite two-dimensional lattices and hypercubes. Analytical results can be obtained without calculating the complete spectral decomposition of U', because the evolution of the walk can be obtained from the eigenvectors and eigenvalues of operator U associated with the original unmodified walk. In the case of finite-dimensional lattices and hypercubes, the spectral decomposition of U is known. However, there is a price to pay. In this type of analysis, the results are approximations. From the spectral decomposition of U, we obtain two complex conjugate eigenvectors of U', which are associated with the complex eigenvalues with the smallest argument. The abstract search algorithm approximately evolves in the two-dimensional vector space spanned by these eigenvectors. It is notable that the algorithm evolves in a real subspace of the Hilbert space (because all operators involved are real), but its analysis is performed using two non-real eigenvectors of U' associated with non-real eigenvalues. This analysis is similar to the analysis of Grover's algorithm presented in Sect. 4.1.2.

The eigenvalues of U' have the form $\exp(\pm i\theta)$, $0 \leq \theta \leq \pi$, because U' is a unitary operator. Among all eigenvalues different from 1, we select the eigenvalue with the smallest argument θ. Let us denote this eigenvalue by $\exp(i\alpha)$ and the associated unit eigenvector by $|\alpha^+\rangle$. Because U' is real, $\exp(-i\alpha)$ is also an eigenvalue. Let $|\alpha^-\rangle$ be the associated unit eigenvector. Eigenvectors $|\alpha^+\rangle$ and $|\alpha^-\rangle$ are associated with different eigenvalues; therefore, they are orthogonal. Moreover, they are complex conjugates. Those eigenvectors of U' can be calculated from the eigenvectors of U, as we shall see.

Using $|\alpha^+\rangle$ and $|\alpha^-\rangle$, we define two key vectors for describing the evolution of the abstract search algorithm, which are

$$|\beta^+\rangle = \frac{1}{\sqrt{2}}\left(|\alpha^+\rangle + |\alpha^-\rangle\right), \tag{8.12}$$

$$|\beta^-\rangle = \frac{1}{\sqrt{2}}\left(|\alpha^+\rangle - |\alpha^-\rangle\right). \tag{8.13}$$

Vectors $|\beta^+\rangle$ and $|\beta^-\rangle$ are orthonormal and define a plane where the abstract search algorithm evolves. Let us obtain what are the conditions that guarantee the success of the algorithm. To begin, we must show that the initial condition has high *fidelity* with that plane. In fact, we require that the initial condition should have high fidelity to $|\beta^-\rangle$, that is, the first condition is

$$|\langle\Psi_0|\beta^-\rangle| \approx 1, \tag{8.14}$$

where $|\Psi_0\rangle$ is given by (8.8).

If the first condition is true, vector $|\beta^-\rangle$ can be used as initial condition for the analysis of the abstract search algorithm. The analysis using $|\beta^-\rangle$ is simpler than the one using $|\Psi_0\rangle$, because we know the expression of $|\beta^-\rangle$ as a linear combination of eigenvectors of U'. Suppose t_f is the algorithm runtime, the final state will be approximately

$$\begin{aligned}\left|\Psi_f\right\rangle &\approx (U')^{t_f}|\beta^-\rangle \\ &\approx \frac{1}{\sqrt{2}}\left(\mathrm{e}^{\mathrm{i}\alpha t_f}\left|\alpha^+\right\rangle - \mathrm{e}^{-\mathrm{i}\alpha t_f}|\alpha^-\rangle\right).\end{aligned} \tag{8.15}$$

If we take $t_f = \lfloor \pi/2\alpha \rfloor$, then $\left|\Psi_f\right\rangle \approx \mathrm{i}\left|\beta^+\right\rangle$. This choice seems appropriate, because the initial state rotates around 90 degrees, as in Grover's algorithm. We want a final state with high fidelity to vector $|\mathrm{D}\rangle|v_0\rangle$ associated with the marked vertex, in which case the success probability of the algorithm would be high. So, the second condition that guarantees that the algorithm is successful is

$$\left|\left\langle \mathrm{D}, v_0 \middle| \beta^+ \right\rangle\right| \approx 1. \tag{8.16}$$

Summing up, the initial condition of the algorithm is $|\Psi_0\rangle = |\mathrm{D_C}\rangle|\mathrm{D_V}\rangle$. We apply $(U')^{\lfloor \pi/2\alpha \rfloor}$ to the initial state and measure the register associated with the vertices in the computational basis. The analysis of the algorithm is as follows. If the first condition is true, the final state will have high fidelity to $\mathrm{i}\left|\beta^+\right\rangle$. If the second condition is true, the success probability will be close to 1. Time complexity of the algorithm cannot be determined in general, because it depends on angle α. If α is small, the number of applications of U' will be large. The parameter used to measure the time complexity is the number of vertices N. For example, if α is of the order of $1/\sqrt{N}$, the time complexity of the algorithm will be around $\sqrt{N}$.

If the second condition is not true, the algorithm must be modified in order to increase the success probability. A solution without creativity is to repeat the algorithm $1/p$ times, where

$$p = \left|\left\langle \mathrm{D}, v_0 \middle| \beta^+ \right\rangle\right|^2. \tag{8.17}$$

This is the usual method of probability amplification of the success probability of *randomized algorithms* with independent repetitions, which can be applied to both the classical and quantum cases. If p does not depend on N, repeating the algorithm $1/p$ times does not change its time complexity. Each time the algorithm is executed, we check if the resulting vertex is the searched one. This check is not expensive, because it requires one application of the modified coin operator. The runtime is increased by the factor $1/p$.

If p depends on N, factor $1/p$ can significantly change the time complexity. In this case, it is interesting to change the strategy. In Sect. 4.4, we have described the method of *amplitude amplification*, which is useful for search algorithms and when we want to find a marked point in the domain of a Boolean function. The

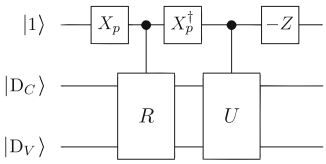

Fig. 8.1 Circuit that describes a new evolution operator designed to increase the success probability maintaining the number of iterations

purpose of the method is as follows: Let $f : \{0,1\}^n \to \{0,1\}$ be an oracle and U_f be a unitary operator that implements function f. Suppose that we know a unitary operator A such that a measurement of the register in state $A|0\rangle^{\otimes n}$ outputs x such that $f(x) = 1$ with known probability p. Then, we can define a quantum circuit that determines x with high probability with $O(1/\sqrt{p})$ applications of U_f.

If the second condition is not satisfied and the success probability depends on N, it is necessary to apply the method of amplitude amplification. If p can be explicitly found from the expression of (8.17), we find the marked element with high probability with $O(1/\sqrt{p})$ applications of $(U')^{t_f}$. The implementation details should follow the description given in Sect. 4.4.

There is another way to avoid the second condition. The strategy is to use a new evolution operator described in Fig. 8.1, where $-Z$ is the negative of the Pauli matrix Z and matrix X_p is given by

$$X_p = \begin{pmatrix} \cos\sqrt{p} & \sin\sqrt{p} \\ -\sin\sqrt{p} & \cos\sqrt{p} \end{pmatrix}. \tag{8.18}$$

The addition of a new control qubit, the state of which is rotated by a convenient angle, increases the success probability. For the abstract search algorithm in two-dimensional lattices, the probability p depends on the inverse of $\log N$. Using the algorithm in Fig. 8.1, the success probability is constant. In this case, there is no need to apply the method of amplitude amplification.

As shown in Fig. 8.1, the initial condition of this new version of the algorithm is

$$|\Psi_0\rangle = |1\rangle|\mathrm{D_C}\rangle|\mathrm{D_V}\rangle. \tag{8.19}$$

The evolution operator is

$$U'' = (-Z \otimes I) \cdot C(U) \cdot (X_p^\dagger \otimes I) \cdot C(R) \cdot (X_p \otimes I), \tag{8.20}$$

where $C(U)$ and $C(R)$ are controlled operators as shown in Fig. 8.1. The target state is $|p_1\rangle|\mathrm{D_C}\rangle|v_0\rangle$, where

$$|p_1\rangle \equiv X_p^\dagger|1\rangle = -\sin\sqrt{p}\,|0\rangle + \cos\sqrt{p}\,|1\rangle. \tag{8.21}$$

The calculation of the stopping time and the success probability follows the rules of the abstract search algorithm, see Exercise 8.3.

Exercise 8.1.

1. Use the measurement postulate with projectors $P_v = I \otimes |v\rangle\langle v|$ to show that p given by (8.9) is the success probability if t_f is the runtime of the abstract search algorithm.
2. Show that

$$p \geq |\langle \mathrm{D}, v_0 | (U')^{t_f} | \Psi_0 \rangle|^2.$$

Exercise 8.2. Let U' be a real unitary operator.

1. Show that the eigenvalues are complex conjugate pairs.
2. Show that the unit eigenvectors associated with a pair of conjugate eigenvalues are complex conjugate.
3. Show that there is a basis of real eigenvectors for the eigenspaces associated with eigenvalues ± 1.

Exercise 8.3. Show that operator U'' of (8.20) can be written as

$$U'' = U_c \cdot R_c,$$

where R_c is a reflection operator around the hyperplane orthogonal to the target vector $|p_1\rangle|\mathrm{D_C}\rangle|v_0\rangle$. Find the expression for U_c and show that the initial condition $|\Psi_0\rangle$ given by (8.19) is invariant under this operator. How can we calculate the stopping time and the conditions which guarantee the success of the algorithm that uses U'' as evolution operator?

8.2 Analysis of the Evolution

The abstract search algorithm as a generic method is useful only if it is possible to obtain the expressions of $|\alpha^{\pm}\rangle$ in terms of the eigenvalues and eigenvectors of the original operator U. From these expressions, we can explicitly calculate $|\beta^{\pm}\rangle$, $|\langle \Psi_0 | \beta^- \rangle|$, and $|\langle \mathrm{D}, v_0 | \beta^+ \rangle|$. We also need to obtain an expression for α in terms of the eigenvalues and eigenvectors of U. From the expressions of α, $|\langle \Psi_0 | \beta^- \rangle|$, and $|\langle \mathrm{D}, v_0 | \beta^+ \rangle|$, we can find out what is the functional dependence of these expressions on N and we can obtain the time complexity of the algorithm.

The initial condition of the algorithm is vector $|\Psi_0\rangle = |\mathrm{D_C}\rangle|\mathrm{D_V}\rangle$, which is an eigenvector of U with eigenvalue 1. $|\Psi_0\rangle$ is invariant under the action of U, but it is not invariant under the action of U'. Therefore, the multiplicity of eigenvalue 1 of U is greater than or equal to 1.

Exercise 8.4. Show that the vector $|\Psi_0\rangle = |\mathrm{D_C}\rangle|\mathrm{D_V}\rangle$ is an eigenvector of U with eigenvalue 1. Show that $|\Psi_0\rangle$ is not an eigenvector of U'.

Suppose that the spectral decomposition of the original operator U is known. Let us denote:

1. $|\Phi_0\rangle$ as the normalized eigenvector with eigenvalue 1. This eigenvector is equal to the initial condition.
2. $\left|\Phi_j^{\pm}\right\rangle$ as the eigenvectors with eigenvalues $e^{\pm i\theta_j}$, where $0 < \theta_j < \pi$.
3. $\left|\Phi_{-1}^{(k)}\right\rangle$ as the orthonormal eigenvectors with eigenvalue -1. Eigenvalue -1 may have multiplicity greater than 1. The eigenvectors are real and are indexed by k.

These eigenvectors form an orthonormal basis for the Hilbert space.

Let us start by decomposing the target vector $|D\rangle|v_0\rangle$ in the basis of eigenvectors of U.

$$|D\rangle|v_0\rangle = a_0|\Phi_0\rangle + \sum_j a_j \left(\left|\Phi_j^+\right\rangle + \left|\Phi_j^-\right\rangle\right) + \sum_k a_k \left|\Phi_{-1}^{(k)}\right\rangle. \tag{8.22}$$

The coefficients are given by expressions

$$\begin{aligned} a_0 &= \left\langle \Phi_0 \middle| D, v_0 \right\rangle, \\ a_j &= \left\langle \Phi_j^+ \middle| D, v_0 \right\rangle = \left\langle \Phi_j^- \middle| D, v_0 \right\rangle, \\ a_k &= \left\langle \Phi_{-1}^{(k)} \middle| D, v_0 \right\rangle. \end{aligned} \tag{8.23}$$

Coefficients a_0 and a_k are real, because $|D, v_0\rangle$, $|\Phi_0\rangle$, and $\left|\Phi_{-1}^{(k)}\right\rangle$ are real. By choosing appropriately eigenvectors $\left|\Phi_j^{\pm}\right\rangle$, coefficients a_j are real numbers.

Exercise 8.5. Suppose that the decomposition of $|D\rangle|v_0\rangle$ in the eigenspace associated with eigenvalues $e^{\pm i\theta_j}$ has the form $\sum_j \left(a_j^+ \left|\Phi_j^+\right\rangle + a_j^- \left|\Phi_j^-\right\rangle\right)$. Show that $\left|\Phi_j^{\pm}\right\rangle$ can be redefined such that $a_j^+ = a_j^- = a_j$, where a_j are real numbers. Show that after this redefinition the sum $\left|\Phi_j^+\right\rangle + \left|\Phi_j^-\right\rangle$ is a real vector.

Let us define vector $|\omega_\alpha\rangle$ as follows:

$$\begin{aligned} |\omega_\alpha\rangle = {} & a_0 \cot\frac{\alpha}{2} |\Phi_0\rangle \\ & + \sum_j a_j \left(\cot\frac{\alpha - \theta_j}{2} \left|\Phi_j^+\right\rangle + \cot\frac{\alpha + \theta_j}{2} \left|\Phi_j^-\right\rangle\right) \\ & - \tan\frac{\alpha}{2} \sum_k a_k \left|\Phi_{-1}^{(k)}\right\rangle. \end{aligned} \tag{8.24}$$

Vector $|\omega_\alpha\rangle$ is not a unit vector. It is useful for defining other vectors, which are unit vectors. Let c be the norm of $|\omega_\alpha\rangle$, that is,

$$c = \sqrt{\langle\omega_\alpha|\omega_\alpha\rangle}. \tag{8.25}$$

Angle α is the smallest argument of the eigenvalues of U' different from 1. That is, the eigenvalues of U' different from 1 have the form $\mathrm{e}^{\pm \mathrm{i}\theta'_i}$, $0 < \theta'_i \leq \pi/2$, and $\alpha = \min\{\theta'_1, \theta'_2, \ldots\}$.

Using $|\omega_\alpha\rangle$, we define $|\alpha^\pm\rangle$ as follows:

$$\begin{aligned} |\alpha^+\rangle &= \frac{1}{\sqrt{1+c^2}}\Big(|\mathrm{D}, v_0\rangle + \mathrm{i}|\omega_\alpha\rangle\Big) \\ |\alpha^-\rangle &= \frac{1}{\sqrt{1+c^2}}\Big(|\mathrm{D}, v_0\rangle + \mathrm{i}|\omega_{-\alpha}\rangle\Big), \end{aligned} \tag{8.26}$$

where $|\omega_{-\alpha}\rangle$ is obtained from (8.24) by replacing α by $-\alpha$. Vectors $|\alpha^\pm\rangle$ are not necessarily eigenvectors of U' as we wish. We must impose the restrictions

$$\langle \mathrm{D}, v_0|\omega_{\pm\alpha}\rangle = 0. \tag{8.27}$$

Actually, the following result is true:

$$\langle \mathrm{D}, v_0|\omega_{\pm\alpha}\rangle = 0 \quad \Leftrightarrow \quad U'|\alpha^\pm\rangle = \mathrm{e}^{\pm \mathrm{i}\alpha}|\alpha^\pm\rangle, \tag{8.28}$$

the proof of which is oriented in Exercise 8.6.

Using (8.22), (8.24), and the trigonometric relations

$$\cot a + \cot b = \frac{-2\sin(a+b)}{\cos(a+b) - \cos(a-b)}, \tag{8.29}$$

we obtain that restriction (8.27) is equivalent to

$$a_0^2 \cot\frac{\alpha}{2} - 2\sin\alpha \sum_j \frac{a_j^2}{\cos\alpha - \cos\theta_j} - \tan\frac{\alpha}{2}\sum_k a_k^2 = 0. \tag{8.30}$$

We can obtain angle α from (8.30), which is too complex to be exactly solved. For two-dimensional lattices and hypercubes, when the number of vertices grows, α tends to zero. In these cases, we use the following approximations:

$$\begin{aligned} \sin\alpha &\approx \tan\alpha \approx \alpha, \\ \cot\alpha &\approx \frac{1}{\alpha}, \\ \cos\alpha &\approx 1. \end{aligned} \tag{8.31}$$

Equation (8.30) reduces asymptotically to

$$\alpha \approx \frac{a_0}{\sqrt{\sum_j \frac{a_j^2}{1-\cos\theta_j} + \frac{1}{4}\sum_k a_k^2}}. \tag{8.32}$$

Note that α is given in terms of the eigenvalues of U and coefficients of the expansion of $|\mathrm{D}\rangle|v_0\rangle$ in the basis of eigenvectors of U. If we know α, we can estimate the number of steps of the algorithm, because the stopping time is $t_f = \pi/2\alpha$.

Exercise 8.6. The purpose of this exercise is to prove proposition (8.28). First show that the left-hand side implies the right-hand side, that is, start assuming that $\langle \mathrm{D}, v_0 | \omega_\alpha \rangle = 0$.

1. Show that
$$U' |\alpha^+\rangle = U \frac{-|\mathrm{D}, v_0\rangle + \mathrm{i}|\omega_\alpha\rangle}{\sqrt{2}}.$$
2. Replace U by UI in the previous equation and use the completeness relation
$$I = |\Phi_0\rangle\langle\Phi_0| + \sum_j \left(\left|\Phi_j^+\right\rangle\left\langle\Phi_j^+\right| + \left|\Phi_j^-\right\rangle\left\langle\Phi_j^-\right| \right) + \sum_k \left|\Phi_{-1}^{(k)}\right\rangle\left\langle\Phi_{-1}^{(k)}\right|$$
to evaluate explicitly the right-hand side.
3. Show that
$$\mathrm{e}^{\mathrm{i}\theta}\left(-1 + \mathrm{i}\cot\frac{\alpha-\theta}{2}\right) = \mathrm{e}^{\mathrm{i}\alpha}\left(1 + i\cot\frac{\alpha-\theta}{2}\right)$$
for any angle θ and use this fact to simplify the final result.
4. Show that the right-hand side implies the left-hand side.

Exercise 8.7. Using (8.24), show that if the orthogonality relation (8.30) is true, then $\langle \omega_{-\alpha} | \omega_\alpha \rangle = -1$. You may use formula

$$\cot\frac{a+b}{2}\cot\frac{a-b}{2} = -\frac{\cos(a)+\cos(b)}{\cos(a)-\cos(b)}.$$

Using (8.26) and the previous result, show that $\langle \alpha^- | \alpha^+ \rangle = 0$. This is expected, because $|\alpha^+\rangle$ and $|\alpha^-\rangle$ are eigenvectors of a unitary operator associated with different eigenvalues.

Vectors $|\beta^+\rangle$ and $|\beta^-\rangle$ of (8.12) and (8.13) define a plane where the abstract search algorithm approximately evolves as long as conditions (8.14) and (8.16) are satisfied. Let us analyze when the first condition is valid. Using (8.13) and (8.26), we obtain

$$|\beta^-\rangle = \frac{\mathrm{i}}{\sqrt{2}\sqrt{1+c^2}}\Big(|\omega_\alpha\rangle - |\omega_{-\alpha}\rangle\Big). \tag{8.33}$$

Up a global phase, we can rewrite $|\beta^-\rangle$ as follows:

$$|\beta^-\rangle = \frac{1}{\Big\| |\omega_\alpha\rangle - |\omega_{-\alpha}\rangle \Big\|} \Big(|\omega_\alpha\rangle - |\omega_{-\alpha}\rangle \Big). \tag{8.34}$$

This last expression is better to evaluate $\big|\langle \Phi_0 | \beta^- \rangle\big|$. In fact, using (8.24) and the formula (8.29) for the sum of cotangents, we obtain

$$\begin{aligned} \big|\langle \Phi_0 | \beta^- \rangle\big| &= \frac{2a_0 \cot \frac{\alpha}{2}}{\sqrt{4a_0^2 \cot^2 \frac{\alpha}{2} + 8 \sin^2 \alpha \sum_j \frac{a_j^2}{(\cos\alpha - \cos\theta_j)^2} + 4 \tan^2 \frac{\alpha}{2} \sum_k a_k^2}} \\ &= \left(1 + \frac{8 \sin^4 \frac{\alpha}{2}}{a_0^2} \sum_j \frac{a_j^2}{(\cos\alpha - \cos\theta_j)^2} + \frac{\tan^4 \frac{\alpha}{2}}{a_0^2} \sum_k a_k^2 \right)^{-1/2} \end{aligned} \tag{8.35}$$

If angle α tends to zero when we increase the number of vertices, we will show that the first condition is satisfied asymptotically. In fact, using approximations (8.31) and formula $(1+\epsilon)^{-1/2} \approx 1 - \frac{\epsilon}{2}$, which is valid when $\epsilon \ll 1$, we obtain

$$\big|\langle \Phi_0 | \beta^- \rangle\big| \approx 1 - \alpha^4 \left(\frac{1}{4a_0^2} \sum_j \frac{a_j^2}{(1-\cos\theta_j)^2} + \frac{1}{32 a_0^2} \sum_k a_k^2 \right). \tag{8.36}$$

We now consider the second condition. Using again (8.12), (8.13), and (8.26), we obtain

$$|\beta^+\rangle = \frac{1}{\sqrt{2}\sqrt{1+c^2}} \Big(2|\mathrm{D}, v_0\rangle + \mathrm{i}|\omega_\alpha\rangle + \mathrm{i}|\omega_{-\alpha}\rangle \Big). \tag{8.37}$$

Again, we can rewrite $|\beta^+\rangle$ such that the normalization is easier to calculate. Using that $|\mathrm{D}, v_0\rangle$ is a unit vector and orthogonal to $|\omega_{\pm\alpha}\rangle$, we have

$$|\beta^+\rangle = \frac{1}{\sqrt{4 + \Big\| |\omega_\alpha\rangle + |\omega_{-\alpha}\rangle \Big\|^2}} \Big(2|\mathrm{D}, v_0\rangle + \mathrm{i}|\omega_\alpha\rangle + \mathrm{i}|\omega_{-\alpha}\rangle \Big). \tag{8.38}$$

Using (8.24), we obtain

$$\Big\| |\omega_\alpha\rangle + |\omega_{-\alpha}\rangle \Big\|^2 = 2 \sum_j a_j^2 \left(\cot \frac{\alpha - \theta_j}{2} - \cot \frac{\alpha + \theta_j}{2} \right)^2. \tag{8.39}$$

Using again that $|\mathrm{D}, v_0\rangle$ is a unit vector orthogonal to $|\omega_{\pm\alpha}\rangle$, we obtain

$$\left|\left\langle \mathrm{D}, v_0 \middle| \beta^+ \right\rangle\right| = \frac{1}{\sqrt{1 + \sum_j a_j^2 \left(\cot\frac{\alpha-\theta_j}{2} - \cot\frac{\alpha+\theta_j}{2}\right)^2}}. \tag{8.40}$$

The expression of $\left|\left\langle \mathrm{D}, v_0 \middle| \beta^+ \right\rangle\right|$ is not as favorable as the expression $\left|\left\langle \Phi_0 \middle| \beta^- \right\rangle\right|$. Note that the second condition is not satisfied automatically when α tends to zero. Expanding expression (8.40) in Taylor series in terms of variable α and selecting the first term, we obtain

$$\left|\left\langle \mathrm{D}, v_0 \middle| \beta^+ \right\rangle\right| \approx \frac{1}{\sqrt{1 + 4\sum_j a_j^2 \cot^2\frac{\theta_j}{2}}}. \tag{8.41}$$

As we have discussed before, the second condition is to be relaxed. Any value of $\left|\left\langle \mathrm{D}, v_0 \middle| \beta^+ \right\rangle\right|$, which does not depend on the number of vertices, is satisfactory. We will see, later on, that the validity of the second condition may depend on judicious choices of the shift operator of the quantum walk.

8.3 Finite Two-Dimensional Lattice

As an application of the abstract search algorithm, we analyze the search for a marked vertex in a two-dimensional lattice with periodic boundary conditions, that is, a torus-shaped lattice. The standard quantum walk in this type of graph is analyzed in Sect. 6.2, where we list an orthonormal basis of eigenvectors of U. Here we are only interested in the eigenvectors that generate the smallest subspace containing the initial condition $|\Psi_0\rangle = |\mathrm{D_C}\rangle|\mathrm{D_V}\rangle$ and the marked vertex $|\mathrm{D}\rangle|x_0, y_0\rangle$. Therefore, we will list only the eigenvectors that are not orthogonal to $|\mathrm{D_C}\rangle$. The only eigenvector with eigenvalue 1 is $\left|\nu_{0,0}^{1a}\right\rangle|\kappa_{0,0}\rangle$, which is equal to the initial condition. The remaining eigenvectors are $\left|\nu_{k_x,k_y}^{\pm\theta}\right\rangle\left|\kappa_{k_x,k_y}\right\rangle$ and are associated with eigenvalues $\mathrm{e}^{\pm\mathrm{i}\theta}$, where θ depends on k_x and k_y and is given by

$$\cos\theta(k_x, k_y) = \frac{1}{2}\left(\cos\frac{2\pi k_x}{\sqrt{N}} + \cos\frac{2\pi k_y}{\sqrt{N}}\right). \tag{8.42}$$

The first task is to determine the coefficients of the expansion of $|\mathrm{D}\rangle|x_0, y_0\rangle$ is the basis of eigenvectors of U, that is, to determine coefficients a_0, a_j, and a_k defined in (8.23). The searched vertex is $|v_0\rangle = |x_0, y_0\rangle$. Equation (8.22) assumes the form

$$\begin{aligned}|\mathrm{D}\rangle|x_0, y_0\rangle &= a_{0,0}^{1a}|\mathrm{D}\rangle|\mathrm{D}\rangle \\ &+ \sum_{\substack{k_x,k_y=0 \\ (k_x,k_y)\neq(0,0)}}^{\sqrt{N}-1} \left(a_{k_x,k_y}^{+\theta}\left|\nu_{k_x,k_y}^{\theta}\right\rangle + a_{k_x,k_y}^{-\theta}\left|\nu_{k_x,k_y}^{-\theta}\right\rangle\right)\left|\kappa_{k_x,k_y}\right\rangle. \end{aligned} \tag{8.43}$$

Using (6.43) on Page 6.43 and Exercise 6.12 on Page 6.12, we obtain

$$\begin{aligned} a_{0,0}^{1a} &= \langle \mathrm{D}|\mathrm{D}\rangle \langle \kappa_{0,0}|x_0, y_0\rangle \\ &= \frac{1}{\sqrt{N}}, \\ a_{k_x,k_y}^{+\theta} &= \left\langle \nu_{k_x,k_y}^{+\theta}|\mathrm{D}\right\rangle \langle \kappa_{k_x,k_y}|x_0, y_0\rangle \\ &= \frac{1}{\sqrt{2N}}\omega^{-x_0k_x-y_0k_y}, \\ a_{k_x,k_y}^{-\theta} &= \left\langle \nu_{k_x,k_y}^{-\theta}|\mathrm{D}\right\rangle \langle \kappa_{k_x,k_y}|x_0, y_0\rangle \\ &= \frac{1}{\sqrt{2N}}\omega^{-x_0k_x-y_0k_y}. \end{aligned} \tag{8.44}$$

These coefficients correspond to a_0 and a_j in (8.23). Note that $a_{k_x,k_y}^{+\theta} = a_{k_x,k_y}^{-\theta}$. This is the result of a proper choice of the eigenvectors $\left|\nu_{k_x,k_y}^{\pm\theta}\right\rangle$ in (6.58) on Page. 6.58. The phases of these eigenvectors are chosen such that $\left\langle \nu_{k_x,k_y}^{\pm\theta}|\mathrm{D}\right\rangle$ are real (see Exercise 8.5). Note also that the coefficient a_k is zero because the two eigenvectors associated with eigenvalue -1, which are not orthogonal to the initial condition, have already been included. These two eigenvectors play some role only when $\sqrt{N}$ is even and $k_x = k_y = \sqrt{N}/2$.

We will calculate angle α using (8.32). The number of steps of the algorithm is $\pi/2\alpha$. Equation (8.32) reduces to

$$\frac{1}{\alpha} \approx \frac{1}{a_{0,0}^{1a}} \sqrt{\sum_{\substack{k_x,k_y=0 \\ (k_x,k_y)\neq(0,0)}}^{\sqrt{N}-1} \frac{\left(a_{k_x,k_y}^{+\theta}\right)^2}{1-\cos\theta(k_x,k_y)}}. \tag{8.45}$$

Using (8.44), we obtain

$$\frac{1}{\alpha} \approx \sqrt{\frac{1}{2}\sum_{\substack{k_x,k_y=0 \\ (k_x,k_y)\neq(0,0)}}^{\sqrt{N}-1} \frac{1}{1-\cos\theta(k_x,k_y)}}. \tag{8.46}$$

Our goal is to determine how α depends on N. The above expression is too complex to be exactly evaluated. We define upper and lower bounds for α, which are more tractable algebraically. The main inequality that we use is

$$1-\frac{\theta^2}{2} \leq \cos\theta \leq 1-\frac{2\theta^2}{\pi^2}, \tag{8.47}$$

which can be checked in Fig. 8.2 for the range $0 \leq \theta \leq \pi$ showing the functions of θ involved in the inequalities.

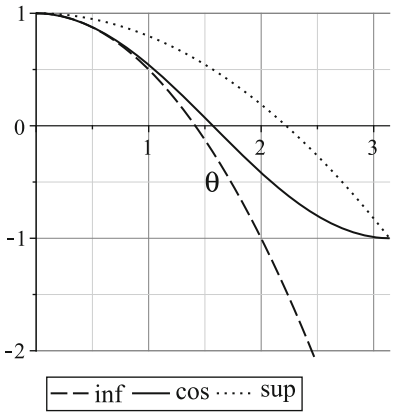

Fig. 8.2 The cosine function between an upper and a lower bounds given by inequalities (8.47)

To continue the analysis, we assume that $\sqrt{N}$ is even. Inequalities (8.47) can only be used to evaluate the right-hand side of (8.42) if $0 \le k_x, k_y \le \sqrt{N}/2 - 1$. We separate the sum of (8.46) into two parts as follows:

$$\frac{\sqrt{2}}{\alpha} \approx \sqrt{\sum_{\substack{k_x,k_y=0 \\ (k_x,k_y)\neq(0,0)}}^{\frac{\sqrt{N}}{2}-1} \frac{1}{1-\cos\theta(k_x,k_y)} + \sum_{k_x,k_y=\frac{\sqrt{N}}{2}}^{\sqrt{N}-1} \frac{1}{1-\cos\theta(k_x,k_y)}}. \tag{8.48}$$

The second term within the root contributes with a value close to the first term. The detailed analysis is oriented in Exercise 8.8. Let us analyze the first term.

Using inequalities (8.47), we obtain

$$1 - \frac{2\pi^2 k_x^2}{N} \le \cos\frac{2\pi k_x}{\sqrt{N}} \le 1 - \frac{8k_x^2}{N}. \tag{8.49}$$

We have similar inequalities for the variable k_y. Adding up these inequalities, dividing by 2, and using (8.42), we obtain

$$1 - \frac{\pi^2(k_x^2+k_y^2)}{N} \le \cos\theta \le 1 - \frac{4(k_x^2+k_y^2)}{N}. \tag{8.50}$$

Subtracting 1 and inverting, we obtain

$$\sum_{k_x,k_y} \frac{N}{\pi^2(k_x^2+k_y^2)} \le \sum_{k_x,k_y} \frac{1}{1-\cos\theta} \le \sum_{k_x,k_y} \frac{N}{4(k_x^2+k_y^2)}. \tag{8.51}$$

We have to evaluate the sum

$$S = \sum_{\substack{k_x,k_y=0 \\ (k_x,k_y)\neq(0,0)}}^{\frac{\sqrt{N}}{2}-1} \frac{1}{k_x^2 + k_y^2}. \tag{8.52}$$

Again we are faced with a complex expression. Since our goal is to determine the functional dependence with variable N, we use the following approach: Consider a $\sqrt{N}$-by-$\sqrt{N}$ square lattice such that vertex $(0, 0)$ is in the center. Each vertex can be labeled by (k_x, k_y). The sum uses all the lattice vertices except the origin. Now draw circles of integer radius $r = 1, \ldots, \sqrt{N}/2$. The points that lie on a circle of radius r satisfy $k_x^2 + k_y^2 = r^2$. To determine the contribution of these points, we calculate how many of them are on the circumference. Let $p(r)$ be this number of points. The sum will be approximately

$$S \approx \sum_{r=1}^{\frac{\sqrt{N}}{2}} \frac{p(r)}{r^2}.$$

Each lattice point represents a cell of unit area. The number of cells that a circle of radius r cuts is approximately given by the perimeter, that is, $p(r) \approx 2\pi r$. The sum is approximately

$$\begin{aligned} S &\approx 2\,\pi \sum_{r=1}^{\frac{\sqrt{N}}{2}} \frac{1}{r} \\ &= 2\,\pi\,\Psi\left(\frac{\sqrt{N}}{2} + 1\right) + 2\,\pi\,\gamma, \end{aligned}$$

where Ψ is the *digamma function* and γ is the *Euler number*. Selecting the dominant term of the *asymptotic expansion* of the digamma function and neglecting additive constants, we obtain asymptotically

$$S \approx \pi \log N. \tag{8.53}$$

Substituting this result for inequalities (8.51), we obtain

$$\frac{1}{\pi} N \log N \leq \sum_{k_x,k_y} \frac{1}{1 - \cos\theta} \leq \frac{\pi}{4} N \log N. \tag{8.54}$$

Thus, the functional dependence of the inverse of α with N is

$$\frac{1}{\alpha} = O\left(\sqrt{N \log N}\right). \tag{8.55}$$

The above expression describes the time complexity of the algorithm, since the number of times we apply the evolution operator is $\pi/2\alpha$. Next step is the analysis of the success probability.

The success probability is determined by the value of $\left|\langle \mathrm{D}, v_0 | \beta^+ \rangle\right|^2$, which can be obtained from (8.41), assuming that the first condition is satisfied. The proof of the validity of the first condition is proposed as an exercise. For finite lattices, (8.41) reduces to

$$\left|\langle \mathrm{D}, x_0, y_0 | \beta^+ \rangle\right| \approx \frac{1}{\sqrt{1 + 4 \sum_{\substack{k_x,k_y=0 \\ (k_x,k_y)\neq(0,0)}}^{\sqrt{N}-1} (a_{k_x,k_y}^{+\theta})^2 \cot^2 \frac{\theta(k_x,k_y)}{2}}}. \tag{8.56}$$

Using the trigonometric identity

$$\cot^2 \frac{\theta}{2} = \frac{1+\cos\theta}{1-\cos\theta} \tag{8.57}$$

and the expression for coefficients $a_{k_x,k_y}^{+\theta}$, we obtain

$$\left|\langle \mathrm{D}, x_0, y_0 | \beta^+ \rangle\right|^2 \approx \frac{1}{1 + \frac{1}{N} \sum_{\substack{k_x,k_y=0 \\ (k_x,k_y)\neq(0,0)}}^{\sqrt{N}-1} \frac{1+\cos\theta}{1-\cos\theta}}. \tag{8.58}$$

Assuming that the term $1 + \cos\theta$ is constant and using inequality (8.54), we obtain

$$\left|\langle \mathrm{D}, x_0, y_0 | \beta^+ \rangle\right|^2 = O\left(\frac{1}{\log N}\right). \tag{8.59}$$

This result shows that the success probability tends to zero as N increases. This is a negative result, which contributes to the total cost of the algorithm. If the success probability is p, we use the method of amplitude amplification, which multiplies the factor $\pi/4\sqrt{p}$ to the original time complexity. Since the time complexity of the original algorithm is given by (8.55), the total cost of the algorithm applying the method of amplitude amplification is $O\left(\sqrt{N}\log N\right)$.

Exercise 8.8. Show that the second term within the root in (8.48) is equivalent to

$$\sum_{k_x,k_y=0}^{\frac{\sqrt{N}}{2}-1} \frac{1}{1+\cos\theta}.$$

Using inequality $1 - \cos\theta \leq 1 + \cos\theta$, show that this term is positive and is less than or equal to the first term within the root. If $1/\alpha_0$ is the value without the second term, show that $1/\alpha_0 \leq 1/\alpha \leq 2/\alpha_0$.

Exercise 8.9. Show that the inner product between the initial condition $|\mathrm{D_C}\rangle|\mathrm{D_V}\rangle$ and $|\beta^-\rangle$ given by (8.36) is

$$\langle \mathrm{D}|\beta^-\rangle = 1 - O\left(\frac{1}{\log^2 N}\right).$$

Is the first condition described by (8.14) asymptotically satisfied?

8.4 Grover's Algorithm as an Abstract Search Algorithm

Grover's algorithm can be seen as an abstract search algorithm in a *complete graph* with N vertices. In the complete graph, all vertices are connected by undirected edges. Suppose that each vertex has a directed *loop* (an edge that connects to the same vertex at both ends). In this case, each vertex has incident N edges with labels 1 to N. The choice of these labels should be as natural as possible: All edges incident to vertex v have label number v, including the loop. The basis of the Hilbert space is $\{|a\rangle|v\rangle, 1 \leq a \leq N, 1 \leq v \leq N\}$, where $|a\rangle$ is the coin state and $|v\rangle$ is the position state. The shift operator is given by

$$S|a\rangle|v\rangle = |v\rangle|a\rangle. \tag{8.60}$$

Note that if the walker is at vertex v and the coin value is a, it should go to the vertex a, since the label of the edge incident to vertex a coming from vertex v is a and vice versa, the label of the edge incident to vertex v coming from vertex a is v.

Exercise 8.10. Why the shift operator of (8.60) was not defined preserving the coin state?

A small modification must be made in the general method described in Sect. 8.1. In (8.3), we have learned that the modified coin operator applies operator $-I$ on the coin state of the searched vertex and applies the Grover coin on the other vertices. This is equivalent to applying operator $U' = UR$, where U is the evolution operator of original quantum walk and R is a reflection operator. There is another way to obtain the same result, which is used to show that Grover's algorithm can be seen as an abstract search algorithm. Consider the following coin operator:

$$C'_G = -G \otimes |v_0\rangle\langle v_0| + G \otimes (I - |v_0\rangle\langle v_0|). \tag{8.61}$$

The difference from the modified coin operator C' defined in (8.3) is that operator C'_G applies $-G$ instead of $-I$ on the searched state. The evolution operator in this case is given by

$$U' = S(G \otimes R), \tag{8.62}$$

where $R = I - 2|v_0\rangle\langle v_0|$. R is a reflection operator around the hyperplane orthogonal to vector $|v_0\rangle$.

Operator R is the same one used in the original Grover's algorithm, which applies $(GR)^t$ on the initial state $|\mathrm{D}\rangle$, where $t = \left\lfloor \frac{\pi}{4}\sqrt{N} \right\rfloor$. The state of the quantum computer immediately before the measurement is $(GR)^{\lfloor \frac{\pi}{4}\sqrt{N} \rfloor}|\mathrm{D}\rangle$.

The evolution operator in the abstract search algorithm uses the tensor product $G \otimes R$. Operator U' must be applied $\left\lfloor \frac{\pi}{2}\sqrt{N} \right\rfloor$ times, that is, twice the value used in the original algorithm. The initial state in this case should be $|\Phi_0\rangle = |\mathrm{D_C}\rangle|\mathrm{D_V}\rangle$. Let us follow step-by-step the evolution of the quantum computer:

$$\begin{aligned} U'|\Phi_0\rangle = &= S(G|\mathrm{D}\rangle \otimes R|\mathrm{D}\rangle) \\ &= S(|\mathrm{D}\rangle \otimes R|\mathrm{D}\rangle) \\ &= R|\mathrm{D}\rangle \otimes |\mathrm{D}\rangle \end{aligned} \tag{8.63}$$

To obtain the last equality, we use (8.60). The next application of U' yields

$$\begin{aligned} (U')^2|\Phi_0\rangle = &= S(G \otimes R)(R|\mathrm{D}\rangle \otimes |\mathrm{D}\rangle) \\ &= S(GR|\mathrm{D}\rangle \otimes R|\mathrm{D}\rangle) \\ &= R|\mathrm{D}\rangle \otimes GR|\mathrm{D}\rangle. \end{aligned} \tag{8.64}$$

Repeating this process, we easily convince ourselves that

$$(U')^{\lfloor \frac{\pi}{2}\sqrt{N} \rfloor}|\Phi_0\rangle = R(GR)^{\lfloor \frac{\pi}{4}\sqrt{N} \rfloor - 1}|\mathrm{D}\rangle \otimes (GR)^{\lfloor \frac{\pi}{4}\sqrt{N} \rfloor}|\mathrm{D}\rangle. \tag{8.65}$$

Measuring the register associated with the position state in the computational basis, we obtain the same result of the original Grover's algorithm.

Exercise 8.11. Consider the quantum walk with the original Grover coin and with the shift operator given by (8.60). Take as initial condition a walker located at a vertex with the diagonal state in the coin space. Show that one can obtain the same result of the original Grover's algorithm. At what time must the quantum computer be measured?

Exercise 8.12. Consider the quantum walk with the original Grover coin and with the shift operator given by (8.60). Take as initial condition a walker located at a vertex with the diagonal state in the coin space. Show that at time $t = 4$ the walk returns to the initial condition. Exercise 8.13 suggests another form of solving this problem.

Exercise 8.13. Consider the quantum walk with the original Grover coin and with the shift operator given by (8.60).

1. Show that $U^4 = I$.
2. From the previous item, obtain the eigenvalues of U.

8.5 Generalization

We have showed that the abstract search algorithm is obtained by modifying the coin of the standard quantum walk. The evolution operator of the abstract search algorithm is $U' = UR$, where U is the evolution operator of the original standard quantum walk and R is a reflection operator around the hyperplane orthogonal to vector $|\mathrm{D}, v_0\rangle$, where v_0 is the marked vertex. The abstract search algorithm can be generalized, without being linked to a quantum walk. In its most general form, the abstract search algorithm consists of two unitary operators U_1 and U_2 and two states $|\psi_1\rangle$ and $|\psi_2\rangle$ satisfying the following conditions:

1. $U_2 = I - 2|\psi_2\rangle\langle\psi_2|$.
2. $U_1|\psi_1\rangle = |\psi_1\rangle$ and there is no other eigenvector with eigenvalue 1.
3. U_1 and $|\psi_1\rangle$ are real.

The evolution operator of the abstract search algorithm is $U' = U_1U_2$. The initial state is $|\psi_1\rangle$. Under certain constraints, the final state $(U_1U_2)^{t_f}|\psi_1\rangle$ will have high fidelity to state $|\psi_2\rangle$, which has the searched information.

Further Reading

The idea of space search algorithms started with *Benioff* in [15], who showed that a direct application of Grover's algorithm does not provide an improvement in the time complexity for searching a marked vertex in lattices. A more efficient algorithm was presented in [1]. The *abstract search algorithm* originated in [71], which describes a search algorithm on hypercubes. The formalization of the method is described in [10], which analyzes the search for a marked vertex in two-dimensional lattices with time complexity $O\left(\sqrt{N}\log N\right)$. Using the same general method, *Tulsi* described a more efficient algorithm in [78], achieving an algorithm with time complexity $O\left(\sqrt{N\log N}\right)$. Reference [8] does not use the amplitude–amplification method for searching in the two-dimensional lattice. The abstract search algorithm was analyzed with more detail and has been applied on several other graphs generating more efficient algorithms than their classical analogues [2, 28, 35].

Chapter 9
Hitting Time

In this chapter we define a new model of *discrete-time quantum walks* on graphs without using an explicit coin operator. Instead, the model uses an auxiliary space by duplicating the original graph and forcing the walker to jump systematically from the original graph to the copy and vice versa. The graph and its copy form a *bipartite graph*. At the end, the copy is discarded. This model has many advantages over the *standard quantum walk model* and it allows to define the *quantum hitting time* in a natural and elegant way.

As usual, before entering the quantum context, we present the relevant classical notions. The focus of this chapter is the *hitting time*; hence, we restrict ourselves to the basic theory of classical *Markov chains*. The most known formula for calculating the *classical hitting time* in graphs uses the *stationary distribution*. However, there is an alternative formula that does not rely on the stationary distribution and requires the definition of an associated directed graph. This process can be generalized to the quantum context. Using the original graph, we define an associated bipartite graph, and then a directed bipartite graph. To define the *quantum hitting time* in the original graph, the quantum walk takes place in the directed bipartite graph. We show how the evolution operator is obtained from the *stochastic matrix* of the original graph and we exemplify the process in the complete graph.

9.1 Classical Hitting Time

Consider a connected, non-directed, and non-bipartite *graph* $\Gamma(X, E)$, where $X = \{x_1, \ldots, x_n\}$ is the vertex set and E is the edge set. The *hitting time* of a *classical random walk* in this graph is the *expected time* for the walker to reach a marked vertex for the first time, once given the initial conditions. We may have more than one marked vertex forming a subset M of the vertex set X. In this case, the hitting time is the expected time for the walker to reach a vertex in M for the first time. It does not matter which the vertex is, but it must be the first vertex in M to be visited.

R. Portugal, *Quantum Walks and Search Algorithms*, Quantum Science and Technology, DOI 10.1007/978-1-4614-6336-8_9,

If $p_{x\,x'}(t)$ is the probability of the walker to reach x' for the first time at time t having left x at $t = 0$, the hitting time from vertex x to x' is

$$H_{x\,x'} = \sum_{t=0}^{\infty} t\; p_{x\,x'}(t). \tag{9.1}$$

Define $H_{x\,x} = 0$ when the departure and arrival vertices are the same.

For example, the probability $p_{x\,x'}(t)$ at time $t = 1$ when $x \neq x'$ for the *complete graph* with n vertices is $1/(n-1)$, because the walker has $n-1$ possible vertices to go in the first step. To arrive in vertex x' at time $t = 2$ for the first time, the walker must visit one of $n-2$ vertices different from x and x'. The probability is $(n-2)/(n-1)$. After this visit, it must go directly to vertex x', which occurs with probability $1/(n-1)$. Therefore, $p_{x\,x'}(2) = (n-2)/(n-1)^2$. Generalizing this argument, we obtain $p_{x\,x'}(t) = (n-2)^{t-1}/(n-1)^t$. Then,

$$H_{x\,x'} = \sum_{t=0}^{\infty} t\; \frac{(n-2)^{t-1}}{(n-1)^t}.$$

Using the identity $\sum_{t=0}^{\infty} t\alpha^t = 1/(1-\alpha)^2$, which is valid for $0 < \alpha < 1$, we obtain

$$H_{x\,x'} = n - 1. \tag{9.2}$$

Usually, the hitting time depends on x and x', but in the complete graph the departure and arrival vertices are equivalent. In the general case, $H_{x\,x'}$ can be different from $H_{x'x}$.

The notion of hitting time from a vertex to a subset can be formalized as follows: suppose that M is a non-empty subset of X with cardinality m and let $p_{xM}(t)$ be the probability that the walker reaches any of the vertices in M for the first time at time t having left x at $t = 0$. The hitting time from x to M is

$$H_{xM} = \sum_{t=0}^{\infty} t\; p_{xM}(t). \tag{9.3}$$

Again, we define $H_{xM} = 0$ if $x \in M$.

Let us use an extended notion of hitting time when the walker starts from a probability distribution. In the former case, the probability to depart from vertex x is 1 and the probability to depart from any other vertex is 0. Suppose that the walker starts in a distribution σ, that is, at the initial time the probability of the walker to be at vertex x is σ_x. The most used initial distributions are the *uniform distribution* $\sigma_x = 1/n$ and the *stationary distribution*, which will be defined ahead. In any case, the initial distribution must satisfy $\sum_{x\in X} \sigma_x = 1$. The hitting time from σ to M is

$$H_{\sigma M} = \sum_{x\in X} \sigma_x\, H_{xM}. \tag{9.4}$$

That is, $H_{\sigma M}$ is the *expected value* of the hitting time H_{xM} from x to M weighted with distribution σ.

Exercise 9.1. Show that for the complete graph

$$H_{xM} = \frac{n-1}{m}$$

if $x \notin M$.

Exercise 9.2. Show that for the complete graph

$$H_{\sigma M} = \frac{(n-m)(n-1)}{mn}$$

if σ is the uniform distribution. Why $H_{\sigma M} \approx H_{xM}$ for $n \gg m$?

9.1.1 Hitting Time Using the Stationary Distribution

Equations (9.1) and (9.3) are unpleasant for the practical calculation of the hitting time in graphs. Fortunately, there are alternative methods. The best-known method uses a recursive reasoning. Let us illustrate this method using the complete graph. We want to calculate $H_{x\,x'}$. The walker departs from x, moves directly to x' with probability $1/(n-1)$ taking one time unit. With probability $(n-2)/(n-1)$, the walker moves to vertex x'' different from x' and therefore will take one time unit plus the expected time to go from x'' to x', which is $H_{x\,x'}$. Thus, we establish the following recursive equation:

$$H_{x\,x'} = \frac{1}{n-1} + \frac{n-2}{n-1}\left(1 + H_{x\,x'}\right), \tag{9.5}$$

the solution of which is equal to (9.2).

This method works for a generic graph. If V_x is the *neighborhood* of x, the cardinality of V_x is the degree of x denoted by d_x. To help this calculation, we assume that the distance between x and x' is greater than 1. So, the walker will depart from x and will move to the neighboring vertex x'' with probability $1/d_x$ taking one time unit. Now, we must add this result by the expected time to move from x'' to x'. This has to be done for all vertices x'' that are neighbors of vertex x. We obtain

$$H_{x\,x'} = \frac{1}{d_x}\sum_{x'' \in V_x}\left(1 + H_{x''\,x'}\right). \tag{9.6}$$

Equation (9.5) is a special case of (9.6), because for the complete graph $d_x = n-1$ and $H_{x''\,x'} = H_{x\,x'}$ unless $x'' = x'$. The case $x'' = x'$ generates the first term in (9.5). The remaining $n-2$ cases generate the second term. This shows that (9.6) is general and the distance between x and x' need not be greater than 1. However, we cannot take $x = x'$ (distance 0), since the left-hand side is zero and the right-hand side is not.

The goal now is to solve (9.6) in terms of the hitting time $H_{x\,x'}$. This task is facilitated if (9.6) is converted to the matrix form. If H is an $n \times n$-matrix with entries $H_{x\,x'}$, the left-hand side will be converted into H and the right-hand side must be expanded. Using that

$$p_{x\,x'} = \begin{cases} \frac{1}{d_x}, & \text{if } x' \text{ is adjacent to } x; \\ 0, & \text{otherwise,} \end{cases} \tag{9.7}$$

we obtain the following matrix equation:

$$H = J + PH + D, \tag{9.8}$$

where J is a matrix with all entries equal to 1, P is the *right stochastic matrix*, and D is a diagonal matrix that should be introduced to validate the matrix equation for the diagonal elements. P is also called by the *transition matrix* or the *probability matrix*, as we have discussed in Chap. 3.

The diagonal matrix D can be calculated using the *stationary distribution* π, which is the distribution that satisfies equation $\pi^T \cdot P = \pi^T$. It is also called *limiting* or *equilibrium distribution*. For graphs $\Gamma(X, E)$ described in the beginning of this section, there is always a limiting distribution. Multiplying (9.8) by π^T from the left side, we obtain

$$D_{x\,x} = -\frac{1}{\pi_x},$$

where π_x is the x-th entry of π.

Equation (9.8) can be written as $(I - P)H = J + D$. When we try to find H using this equation, we deal with the fact that $I - P$ is a non-invertible matrix, because $I - P$ has the eigenvalue 0 associated with an eigenvector with all entries equal to 1, which we denote by $\mathbf{1}$. This means that equation $(I - P)X = J + D$ has more than one solution X. In fact, if matrix X is a solution, then $X + \mathbf{1} \cdot v^T$ is also a solution for any vector v. However, having at hand a solution X of this equation does not guarantee that we have found H. There is a way to verify whether X is a correct solution by using that $H_{x\,x}$ must be zero for all x. A solution of equation $(I - P)X = J + D$ is

$$X = (I - P + \mathbf{1} \cdot \pi^T)^{-1}(J + D), \tag{9.9}$$

as can be checked by solving Exercise 9.3. Now we add a term of type $\mathbf{1} \cdot v^T$ to cancel out the diagonal entries of X, and we obtain

$$H = X - \mathbf{1} \cdot v^T, \tag{9.10}$$

where the entries of vector v is the diagonal entries of X, that is, $v_x = X_{x\,x}$.

Exercise 9.3. Let

$$M = I - P + \mathbf{1} \cdot \pi^T.$$

1. Show that M is invertible.
2. Using equations $\pi^T \cdot P = \pi^T$, $P \cdot \mathbf{1} = \mathbf{1}$, and

$$M^{-1} = \sum_{t=0}^{\infty} (I - M)^t,$$

show that

$$M^{-1} = \sum_{t=0}^{\infty} P^t - \mathbf{1} \cdot \pi^T.$$

3. Show that solution (9.9) satisfies equation $(I - P)X = J + D$.
4. Show that matrix H given by (9.10) satisfies $H_{xx} = 0$.

Exercise 9.4. Find the stochastic matrix of the complete graph with n vertices. Using the fact that the stationary distribution is uniform in this graph, find matrix X using (9.9) and then find matrix H using (9.10). Check out the results with (9.2).

9.1.2 Hitting Time Without Using the Stationary Distribution

There is an alternative method for calculating the hitting time that does not use the stationary distribution. We will use definition (9.4) to describe the method for $H_{\sigma M}$. The vertices in M are called *marked vertices*. We define a *modified directed graph* from the original undirected graph $\Gamma(X, E)$. Each edge of an undirected graph can be viewed as two opposite directed edges, that is, the directed edges are fused to form the non-directed edge. The *modified directed graph* is obtained by converting all directed edges leaving the marked vertices into *loops*, while maintaining unchanged the incoming directed edges. This means that if the walker reaches a marked vertex, the walker will be imprisoned in the steps following. To calculate the hitting time, the original undirected graph and the modified directed graph are equivalent. However, the probability matrices are different. Let us denote the stochastic matrix of the modified graph by P'. The entries of P' are

$$p'_{xy} = \begin{cases} p_{xy}, & x \notin M; \\ \delta_{xy}, & x \in M. \end{cases} \tag{9.11}$$

What is the probability of finding the walker in $X \setminus M$ at time t before visiting M? Let $\sigma^{(0)}$ be the initial probability distribution on the vertices of the original graph viewed as a row vector. Then, the distribution after t steps is

$$\sigma^{(t)} = \sigma^{(0)} \cdot P^t. \tag{9.12}$$

Let $\mathbf{1}$ be the column n-vector with all entries equal to 1. Define $\mathbf{1}_{X \setminus M}$ as the column n-vector with $n - m$ entries equal to 1 corresponding to the vertices that are in $X \setminus M$

and m entries equal to zero corresponding to the vertices are in M. The probability of finding the walker in $X \backslash M$ at time t is $\sigma^{(t)} \cdot \mathbf{1}_{X \backslash M}$. However, this expression is not useful for calculating the hitting time, because the walker has already visited M. We want to find the probability of the walker being in $X \backslash M$ at time t having not visited M. This result is obtained if we use matrix P' instead of P in (9.12). In fact, if the evolution is driven by matrix P' and the walker has visited M, it remains imprisoned in M in the steps following. Therefore, if the walker is found in $X \backslash M$, it has certainly not visited M. The probability of finding the walker in $X \backslash M$ at time t without having visited M is $\sigma^{(0)} \cdot (P')^t \cdot \mathbf{1}_{X \backslash M}$.

In (9.3), we have calculated the average time to reach a marked vertex for the first time employing the usual formula for calculating weighted averages. When the variable t assumes nonnegative integer values, there is an alternative formula for calculating this average. This formula applies in this context, because time t is the number of steps. Let T be the number of steps to reach a marked vertex for the first time and let $p(T \geq t)$ be the probability of reaching M for the first time for any number of steps T equal to or greater than t. If the initial condition is distribution σ, the hitting time can be equivalently defined by formula

$$H_{\sigma M} = \sum_{t=1}^{\infty} p(T \geq t). \tag{9.13}$$

To verify the equivalence of this new formula with the previous one, note that

$$p(T \geq t) = \sum_{j=t}^{\infty} p(T = j), \tag{9.14}$$

where $p(T = t)$ is the probability of reaching M for the first time with exactly t steps. Substituting (9.14) for (9.13) and inverting the sum order, we obtain

$$\begin{aligned} H_{\sigma M} &= \sum_{j=1}^{\infty} \sum_{t=1}^{j} p(T = j) \\ &= \sum_{j=1}^{\infty} j \, p(T = j). \end{aligned} \tag{9.15}$$

This last equation is equivalent to (9.3).

We can give another interpretation for probability $p(T \geq t)$. If the walker reaches M at $T \geq t$, then in the first $t - 1$ steps it will still be in $X \backslash M$, that is, it will be in one of the unmarked vertices without having visited M. We have learned in a previous paragraph that the probability of the walker being in $X \backslash M$ at time t without having visited M is $\sigma^{(0)} \cdot (P')^{t-1} \cdot \mathbf{1}_{X \backslash M}$. Then,

$$p(T \geq t) = \sigma^{(0)} \cdot (P')^{t-1} \cdot \mathbf{1}_{X \backslash M}. \tag{9.16}$$

Define $P_{\overline{M}}$ as a square $(n - m)$-matrix obtained from P by deleting the rows and columns corresponding to vertices of M. Define $\sigma_{\overline{M}}$ and $\mathbf{1}_{\overline{M}}$ using the same procedure. Analyzing the entries that do not vanish after multiplying the matrices in the right-hand side of (9.16), we conclude that

$$p(T \geq t) = \sigma_{\overline{M}}^{(0)} \cdot P_{\overline{M}}^{t-1} \cdot \mathbf{1}_{\overline{M}}. \tag{9.17}$$

Substituting the above equation for (9.13), we obtain

$$\begin{aligned} H_{\sigma M} &= \sigma_{\overline{M}}^{(0)} \cdot \left(\sum_{t=0}^{\infty} P_{\overline{M}}^{t} \right) \cdot \mathbf{1}_{\overline{M}} \\ &= \sigma_{\overline{M}}^{(0)} \cdot \left(I - P_{\overline{M}} \right)^{-1} \cdot \mathbf{1}_{\overline{M}}. \end{aligned} \tag{9.18}$$

Matrix $I - P_{\overline{M}}$ is always invertible for connected, non-directed, and non-bipartite graphs. This result follows from the fact that $\mathbf{1}$ is not an eigenvector of $P_{\overline{M}}$, and hence $I - P_{\overline{M}}$ has no eigenvalue equal to 0.

Among the results presented here, the most important one is the strategy that was used to generate (9.18), because it will be also used to define the *quantum hitting time*, which is the main topic of the next sections.

Exercise 9.5. Use (9.18) to find the hitting time in the complete graph with n vertices and compare the results with Exercises 9.1 and 9.2.

9.2 Reflection Operators in a Bipartite Graph

To define the *quantum hitting time*, we use a duplication process in order to obtain a *bipartite graph* associated with the original graph, as will be explained in details in Sect. 9.6. At the moment, we define the quantum operators in the bipartite graph. Using these operators we will define the quantum hitting time in the original graph in Sect. 9.6.

Consider a bipartite graph with sets X and Y of equal cardinalities. Let x and y be generic vertices of X and Y, respectively. Define p_{xy} as the inverse of the outdegree of vertex x, if y is *adjacent* to x, otherwise $p_{xy} = 0$. For example, if x is adjacent to only two vertices y_1 and y_2 in set Y, then $p_{xy_1} = p_{xy_2} = 1/2$. Analogously, we define q_{yx} as the inverse of the outdegree of vertex y. Variables p_{xy} and q_{yx} satisfy

$$\sum_{y \in Y} p_{xy} = 1 \quad \forall x \in X, \tag{9.19}$$

$$\sum_{x \in X} q_{yx} = 1 \quad \forall y \in Y. \tag{9.20}$$

The quantum walk on the bipartite graph has an associated Hilbert space $\mathcal{H}^{n^2} = \mathcal{H}^n \otimes \mathcal{H}^n$, where $n = |X| = |Y|$. The computational basis of the first factor is $\{|x\rangle : x \in X\}$ and of the second is $\{|y\rangle : y \in Y\}$. The computational basis of $\mathcal{H}^{n^2}$ is $\{|x, y\rangle : x \in X, y \in Y\}$. Instead of using probability matrices P and Q of the classical random walk, the entries of which are p_{xy} and q_{yx}, we define operators $A : \mathcal{H}^n \to \mathcal{H}^{n^2}$ and $B : \mathcal{H}^n \to \mathcal{H}^{n^2}$ as follows:

$$A = \sum_{x \in X} |\alpha_x\rangle\langle x|, \tag{9.21}$$

$$B = \sum_{y \in Y} |\beta_y\rangle\langle y|, \tag{9.22}$$

where

$$|\alpha_x\rangle = |x\rangle \otimes \left(\sum_{y \in Y} \sqrt{p_{xy}}\, |y\rangle \right), \tag{9.23}$$

$$|\beta_y\rangle = \left(\sum_{x \in X} \sqrt{q_{yx}}\, |x\rangle \right) \otimes |y\rangle. \tag{9.24}$$

The dimensions of A and B are $n^2 \times n$. Another way to write (9.21) and (9.22) is

$$A|x\rangle = |\alpha_x\rangle, \tag{9.25}$$

$$B|y\rangle = |\beta_y\rangle, \tag{9.26}$$

the interpretation of which is that the result of multiplying matrix A by the x-th vector in the computational basis of $\mathcal{H}^n$ is the x-th column of A. Therefore, the columns of matrix A are the vectors $|\alpha_x\rangle$ and the columns of matrix B are the vectors $|\beta_y\rangle$. Using (9.23) and (9.24) along with (9.19) and (9.20), we obtain

$$\langle \alpha_x | \alpha_{x'} \rangle = \delta_{x,x'}, \tag{9.27}$$

$$\langle \beta_y | \beta'_y \rangle = \delta_{y,y'}. \tag{9.28}$$

Then, we have

$$A^{\mathrm{T}} A = I_n, \tag{9.29}$$

$$B^{\mathrm{T}} B = I_n. \tag{9.30}$$

These equations imply that the actions of A and B preserve the norm of vectors. So, if $|\mu\rangle$ is a unit vector in $\mathcal{H}^n$, then $A|\mu\rangle$ is a unit vector in $\mathcal{H}^{n^2}$. The same regarding B.

It is natural to investigate the product in the reverse order. Using (9.21) and (9.22), we obtain

$$AA^{\mathrm{T}} = \sum_{x \in X} |\alpha_x\rangle\langle\alpha_x|, \tag{9.31}$$

$$BB^{\mathrm{T}} = \sum_{y \in Y} |\beta_y\rangle\langle\beta_y|. \tag{9.32}$$

Using (9.29) and (9.30), we have $(AA^{\mathrm{T}})^2 = AA^{\mathrm{T}}$ and $(BB^{\mathrm{T}})^2 = BB^{\mathrm{T}}$. So, let us define the projectors

$$\Pi_A = AA^{\mathrm{T}}, \tag{9.33}$$

$$\Pi_B = BB^{\mathrm{T}}. \tag{9.34}$$

Equations (9.31) and (9.32) show that Π_A projects a generic vector in $\mathcal{H}^{n^2}$ in subspace $\mathcal{H}_A$ spanned by $\{|\alpha_x\rangle : x \in X\}$ and Π_B projects in subspace $\mathcal{H}_B$ spanned by $\{|\beta_y\rangle : y \in Y\}$.

After obtaining the projectors, we can define the associated *reflection operators*, which are

$$\mathcal{R}_A = 2\,\Pi_A - I_{n^2}, \tag{9.35}$$

$$\mathcal{R}_B = 2\,\Pi_B - I_{n^2}. \tag{9.36}$$

$\mathcal{R}_A$ reflects a generic vector in $\mathcal{H}^{n^2}$ around subspace $\mathcal{H}_A$. We can check this in the following way: $\mathcal{R}_A$ leaves invariant any vector in $\mathcal{H}_A$, that is, if $|\psi\rangle \in \mathcal{H}_A$, then $\mathcal{R}_A|\psi\rangle = |\psi\rangle$, as can be confirmed by (9.35). On the other hand, $\mathcal{R}_A$ inverts the sign of any vector orthogonal to $\mathcal{H}_A$, that is, if $|\psi\rangle \in \mathcal{H}_A^{\perp}$, then $\mathcal{R}_A|\psi\rangle = -|\psi\rangle$. A generic vector in $\mathcal{H}^{n^2}$ can be written as a linear combination of a vector in $\mathcal{H}_A$ with one in $\mathcal{H}_A^{\perp}$. The action of $\mathcal{R}_A$ leaves the component in $\mathcal{H}_A$ unchanged and inverts the sign of the component in $\mathcal{H}_A^{\perp}$. Geometrically, this is a *reflection* around $\mathcal{H}_A$, as if $\mathcal{H}_A$ is the mirror and $\mathcal{R}_A|\psi\rangle$ is the image of $|\psi\rangle$. The same is true for $\mathcal{R}_B$ with respect to subspace $\mathcal{H}_B$.

Now let us analyze the relation between subspaces $\mathcal{H}_A$ and $\mathcal{H}_B$. The best way is to analyze the angles between vectors in basis $\{|\alpha_x\rangle : x \in X\}$ and vectors in $\{|\beta_y\rangle : y \in Y\}$. Define the *inner product matrix* C such that $C_{xy} = \langle\alpha_x|\beta_y\rangle$. Using (9.23) and (9.24), we can express the entries of C in terms of the transition probabilities as $C_{xy} = \sqrt{p_{xy}q_{yx}}$. In matrix form, we write

$$C = A^{\mathrm{T}}B, \tag{9.37}$$

which can be obtained from (9.21) and (9.22). C is an n-dimensional matrix called *discriminant*. It provides essential information about the quantum walk that we will define on the bipartite graph. C is not a *normal matrix* in general, and the

eigenvalues and eigenvectors do not play an important role in this context. We will analyze its *singular values and vectors*, which are quantities conceptually close to eigenvalues and eigenvectors.

Exercise 9.6. Consider the *complete bipartite graph* with sets X and Y both with cardinality 2. Find the vectors $|\alpha_x\rangle$ and $|\beta_y\rangle$. Eliminating the last entry, these vectors can be represented in $\mathbb{R}^3$. Sketch a cube with a vertex in the origin, the opposite vertex in point $(1, 1, 1)$, and with three edges on axis x, y, and z. Show that the real vector space $\mathbb{R}^3_A$ spanned by the columns of A is a vertical plane containing axis z and cutting the cube in half. Show that the real vector space $\mathbb{R}^3_B$ spanned by the columns of B is a 45° tilted plane containing axis y and also cutting the cube in half. Show that the intersection of these vector spaces is spanned by vector

$$|\mu\rangle = \frac{1}{\sqrt{3}} \begin{bmatrix} 1 \\ 1 \\ 1 \end{bmatrix}.$$

Find a vector $|\psi_A\rangle$ orthogonal to $|\mu\rangle$ belonging to $\mathbb{R}^3_A$. Find a vector $|\psi_B\rangle$ orthogonal to $|\mu\rangle$ belonging to $\mathbb{R}^3_B$. What is the angle between $|\psi_A\rangle$ and $|\psi_B\rangle$? Let $|\psi\rangle$ be a vector orthogonal to $|\mu\rangle$ belonging to $\mathbb{R}^3$. Show that $\mathcal{R}_B\mathcal{R}_A$ rotates vector $|\psi\rangle$ of $2\pi/3$ radians in the plane orthogonal to $|\mu\rangle$.

Exercise 9.7. The purpose of this exercise is to generalize the formulas of this section when the cardinality of set X is different from the cardinality of set Y. Let $|X| = m$ and $|Y| = n$. What are the dimensions of matrices A, B, and C in this case? What formulas of this section explicitly change?

Exercise 9.8. Consider the complete bipartite graph when X has a single element and Y has two elements. Show that $\mathcal{R}_A$ is the Pauli matrix σ_x and $\mathcal{R}_B$ is the identity matrix I_2.

9.3 Quantum Evolution Operator

We are now ready to define a quantum walk on the bipartite graph. Let us define the *evolution operator* as

$$U_P := \mathcal{R}_B \, \mathcal{R}_A, \tag{9.38}$$

where $\mathcal{R}_A$ and $\mathcal{R}_B$ are the reflection operators given by (9.35) and (9.36). At time t, the state of the quantum walk is U_P^t applied to the initial state. Note that the structure of this walk is different from the structure of the *standard quantum walk*, which employs a coin and a shift operator. The new definition has some advantages. In particular, the *quantum hitting time* can be naturally defined as a generalization of the *classical hitting time*. It can be shown using general arguments that the quantum hitting time for this quantum walk on a finite graph is at least quadratically smaller than the classical hitting time of a random walk on the same graph.

The analysis of the evolution of the quantum walk can be performed from the *spectral decomposition* of U_P, which simplifies the calculation of U^t. The spectral decomposition associated with the nontrivial eigenvalues can be calculated from the *singular values and vectors* of matrix C defined by (9.37), as discussed in the following sections.

The definition of U_P is different from the *standard quantum walk*, but it is similar to the evolution operator of Grover's algorithm. In Sect. 4.1, we have showed that the evolution operator of *Grover's algorithm* is the product of two reflections. In the context of discrete-time quantum walks, the fact that U_P does not explicitly use a coin is an interesting property.

Exercise 9.9. The objective of this exercise is to determine under what conditions state

$$|\psi(0)\rangle = \frac{1}{\sqrt{n}} \sum_{\substack{x \in X \\ y \in Y}} \sqrt{p_{xy}} |x, y\rangle$$

is an eigenvector of U_P associated with eigenvalue 1. Show that the action of $\mathcal{R}_A$ leaves $|\psi(0)\rangle$ invariant. Does the action of $\mathcal{R}_B$ leave $|\psi(0)\rangle$ invariant? Under what conditions?

9.4 Singular Values and Vectors

The *singular value decomposition theorem* states that there are unitary matrices U and V such that

$$C = UDV^\dagger, \tag{9.39}$$

where D is an n-dimensional diagonal matrix with nonnegative real entries. Usually the diagonal elements are sorted with the largest element occupying the first position. These elements are called singular values and are uniquely determined once given matrix C. In the general case, matrices U and V are not uniquely determined. They can be determined by applying the spectral theorem on matrix $C^\dagger C$. $C^\dagger C$ is a positive semidefinite Hermitian matrix, that is, its eigenvalues are nonnegative real numbers. Then, $C^\dagger C$ admits a spectral decomposition and the square root $\sqrt{C^\dagger C}$ is well defined. Written in the basis of eigenvectors of $C^\dagger C$, $\sqrt{C^\dagger C}$ is a diagonal matrix where each diagonal element is the square root of corresponding eigenvalue of $C^\dagger C$.

Let λ_i^2 and $|v_i\rangle$ be the *eigenvalues* and *eigenvectors* of $C^\dagger C$. Then,

$$C^\dagger C = \sum_{i=1}^{n} \lambda_i^2 \, |v_i\rangle\langle v_i| \tag{9.40}$$

hence

$$\sqrt{C^\dagger C} = \sum_{i=1}^{n} \lambda_i \, |v_i\rangle\langle v_i|. \tag{9.41}$$

We will show how to find U and V. For each i such that $\lambda_i > 0$, define

$$|\mu_i\rangle = \frac{1}{\lambda_i} C\,|v_i\rangle. \tag{9.42}$$

Since $\{|v_i\rangle : 1 \leq i \leq n\}$ is an orthonormal basis, it follows that

$$\langle \mu_i | \mu_j \rangle = \delta_{ij}, \tag{9.43}$$

for all i, j such that λ_i and λ_j are positive. For the eigenvectors in the *kernel* of $\sqrt{C^\dagger C}$, define $\left|\mu'_j\right\rangle = |v_j\rangle$. However, with this extension we generally lose the orthogonality between vectors $|\mu_i\rangle$ and $\left|\mu'_j\right\rangle$. We can apply the *Gram–Schmidt procedure* to redefine vectors $\left|\mu'_j\right\rangle$ such that they are orthogonal to the vectors that do not belong to the kernel and we shall call them $\left|\mu_j\right\rangle$. At the end, we can obtain a complete set satisfying orthonormality condition (9.43). With vectors $|v_i\rangle$ and $|\mu_i\rangle$, we obtain U and V using equations

$$U = \sum_{i=1}^{n} |\mu_i\rangle\langle i|, \tag{9.44}$$

$$V = \sum_{i=1}^{n} |v_i\rangle\langle i|. \tag{9.45}$$

$|v_i\rangle$ and $|\mu_i\rangle$ are the singular vectors and λ_i are the corresponding singular values. They obey the following equations:

$$C\,|v_i\rangle = \lambda_i \, |\mu_i\rangle, \tag{9.46}$$

$$C^{\mathrm{T}}|\mu_i\rangle = \lambda_i \, |v_i\rangle, \tag{9.47}$$

for $1 \leq i \leq n$. Note that $|\mu_i\rangle$ and $|v_i\rangle$ have a dual behavior. In fact, they are called the *left* and *right singular vectors*, respectively.

By left multiplying (9.46) by A and (9.47) by B, we obtain

$$\Pi_A \, B|v_i\rangle = \lambda_i \, A|\mu_i\rangle, \tag{9.48}$$

$$\Pi_B \, A|\mu_i\rangle = \lambda_i \, B|v_i\rangle. \tag{9.49}$$

We have learned earlier that the action of operators A and B preserves the norm of the vectors. Since $|\mu_i\rangle$ and $|v_i\rangle$ are unit vectors, $A|\mu_i\rangle$ and $B|v_i\rangle$ are also unit

vectors. The action of projectors either decreases the norm of vectors or maintains it invariant. Using (9.48), we conclude that the singular values satisfy inequalities $0 \leq \lambda_i \leq 1$. Therefore, λ_i can be written as $\lambda_i = \cos\theta_i$, where $0 \leq \theta_i \leq \pi/2$. The geometric interpretation of θ_i is the angle between vectors $A|\mu_i\rangle$ and $B|\nu_i\rangle$. In fact, using (9.37) and (9.46) we obtain that the inner product between $A|\mu_i\rangle$ and $B|\nu_i\rangle$ is

$$\cos\theta_i = \langle\mu_i|A^{\mathrm{T}}\, B|\nu_i\rangle. \tag{9.50}$$

Exercise 9.10. Show that U and V given by (9.44) and (9.45) are unitary. Show that (9.39) is satisfied for these U and V.

Exercise 9.11. Show that if $\lambda_i \neq \lambda_j$ then the vector space spanned by $A|\mu_i\rangle$ and $B|\nu_i\rangle$ is orthogonal to the vector space spanned by $A\big|\mu_j\big\rangle$ and $B\big|\nu_j\big\rangle$.

Exercise 9.12. The objective of this exercise is to use matrix $CC^\dagger$ instead of $C^\dagger C$ to obtain the singular values and vectors of C.

1. Show that if $|\nu\rangle$ is an eigenvector of $C^\dagger C$ associated with the eigenvalue λ^2, then $C|\nu\rangle$ is an eigenvector of $CC^\dagger$ with the same eigenvalue.
2. Use $C^\dagger$ to define vectors $|\mu_i\rangle$ in (9.42) and interchange the roles of $|\mu_i\rangle$ and $|\nu_i\rangle$ to define U and V.
3. Show that the new matrices U and V are unitary and satisfy (9.39).

Exercise 9.13. Calculate the singular values and vectors of C associated with Exercise 9.6. Calculate vectors $A|\mu_i\rangle$ and $B|\nu_i\rangle$ and show that they play a key role in the geometric interpretation used in Exercise 9.6.

9.5 Spectral Decomposition of the Evolution Operator

Equations (9.48) and (9.49) show that the projectors Π_A and Π_B have a symmetric action on vectors $A\big|\mu_j\big\rangle$ and $B\big|\nu_j\big\rangle$ for each j. It is expected that the action of the reflection operators $\mathcal{R}_A$ and $\mathcal{R}_B$ on a linear combination of vectors $A\big|\mu_j\big\rangle$ and $B\big|\nu_j\big\rangle$ outputs a vector in the plane spanned by $A\big|\mu_j\big\rangle$ and $B\big|\nu_j\big\rangle$. That is, this plane is invariant under the action of U_P. So, let us try the following *Ansatz* to obtain the eigenvectors of U_P:

$$U\big(a\, A\big|\mu_j\big\rangle + b\, B\big|\nu_j\big\rangle\big) = \lambda'_j\big(a\, A\big|\mu_j\big\rangle + b\, B\big|\nu_j\big\rangle\big). \tag{9.51}$$

The goal is to find a, b, and λ'_j obeying (9.51). Using (9.38), (9.35), and (9.36), we obtain

$$(2\,\Pi_B - I)(2\,\Pi_A - I)\big(a\, A\big|\mu_j\big\rangle + b\, B\big|\nu_j\big\rangle\big) = \lambda'_j\big(a\, A\big|\mu_j\big\rangle + b\, B\big|\nu_j\big\rangle\big). \tag{9.52}$$

Using (9.48) and (9.49), we obtain the equations

$$\lambda'_j\, a = \; -a \; - \; 2\lambda_j b, \tag{9.53}$$

$$\lambda'_j\, b = 2\lambda_j a + (4\lambda_j^2 - 1)b, \tag{9.54}$$

when $A\big|\mu_j\big\rangle$ and $B\big|\nu_j\big\rangle$ are linearly independent, that is, *non-collinear*. It follows that $\theta_j \neq 0$, since θ_j is the angle between $A\big|\mu_j\big\rangle$ and $B\big|\nu_j\big\rangle$—see (9.50). Using $\lambda_j = \cos\theta_j$, the above system of equations requires that

$$\lambda'_j = \mathrm{e}^{\pm 2\mathrm{i}\theta_j}. \tag{9.55}$$

Using (9.53), we obtain

$$\begin{aligned} \frac{b}{a} &= -\frac{1 + \mathrm{e}^{\pm 2\,\mathrm{i}\theta_j}}{2\cos\left(\theta_j\right)} \\ &= -\mathrm{e}^{\pm\,\mathrm{i}\theta_j}. \end{aligned} \tag{9.56}$$

Therefore, vectors

$$\left|\theta_j^{\pm}\right\rangle = \frac{A\big|\mu_j\big\rangle - \mathrm{e}^{\pm\,\mathrm{i}\theta_j} B\big|\nu_j\big\rangle}{\sqrt{2}\sin\theta_j} \tag{9.57}$$

are normalized eigenvectors of U_P associated with eigenvalues $\mathrm{e}^{\pm 2\mathrm{i}\theta_j}$, when $0 < \theta_j \leq \pi/2$.

Vectors $A\big|\mu_j\big\rangle$ and $B\big|\nu_j\big\rangle$ are linearly independent only if $\lambda_j \neq 1$. When $A\big|\mu_j\big\rangle$ and $B\big|\nu_j\big\rangle$ are *collinear*, (9.57) does not provide the expression for the eigenvectors associated with $\lambda_j = 1$. However, since $A\big|\mu_j\big\rangle$ is invariant under the action of Π_A, $B\big|\nu_j\big\rangle$ also is. And vice versa, since $B\big|\nu_j\big\rangle$ is invariant under Π_B, $A\big|\mu_j\big\rangle$ also is. Therefore, $A\big|\mu_j\big\rangle$ and $B\big|\nu_j\big\rangle$ are invariant under the action of $\mathcal{R}_B$ and $\mathcal{R}_A$ and are eigenvectors of U_P with eigenvalue 1. The number of eigenvectors with eigenvalue 1 that we can find using this method will depend on the multiplicity (k) of the singular value 1. Table 9.1 summarizes the results of the spectral decomposition of U_P obtained so far. We have already found $2n - k$ eigenvectors of U_P, where the first $2(n-k)$ are associated with the eigenvalues $\mathrm{e}^{\pm 2\mathrm{i}\theta_j}$ and the k remaining eigenvectors are associated with the eigenvalue 1.

$\mathcal{H}_A$ and $\mathcal{H}_B$ are the vector spaces spanned by the columns of matrix A and B, respectively, that is, $\mathcal{H}_A$ is spanned by vectors $|\alpha_x\rangle$, where $x \in X$, and $\mathcal{H}_B$ is spanned by vectors $\big|\beta_y\big\rangle$, $y \in Y$. Both spaces $\mathcal{H}_A$ and $\mathcal{H}_B$ are n-dimensional subspaces of $\mathcal{H}^{n^2}$. Let $\mathcal{H}_{A,B}$ be the vector space spanned by vectors $|\alpha_x\rangle$ and $\big|\beta_y\big\rangle$. The dimension of $\mathcal{H}_{A,B}$ is at most $2n$. The dimension of $\mathcal{H}_{A,B}$ will be exactly $2n$, if $A\big|\mu_j\big\rangle$ and $B\big|\nu_j\big\rangle$ are linearly independent for all j. For each j such that $\lambda_j = 1$, the dimension of $\mathcal{H}_{A,B}$ is reduced by 1. On the other hand, the dimension of $\mathcal{H}_{A,B}$ is

Table 9.1 Eigenvalues and normalized eigenvectors of U_P obtained from the singular values and vectors of C, where k is the multiplicity of the singular value 1 of C and n is the dimension of C

Eigenvalue	Eigenvector	Range
$e^{\pm 2i\theta_j}$	$\left\|\theta_j^{\pm}\right\rangle = \frac{A\|\mu_j\rangle - e^{\pm i\theta_j} B\|\nu_j\rangle}{\sqrt{2}\sin\theta_j}$	$1 \leq j \leq n-k$
1	$\|\theta_j\rangle = A\|\mu_j\rangle$	$n-k+1 \leq j \leq n$
1	$\|\theta_j\rangle =$ no expr.	$2n-k+1 \leq j \leq n^2$

Angles θ_j are obtained from the singular values λ_j through formula $\cos\theta_j = \lambda_j$. The eigenvectors $\left|\theta_j\right\rangle$, for $2n-k+1 \leq j \leq n^2$, cannot be obtained by the method described in this section, but we know that they are associated with eigenvalue 1

$2n$ minus the dimension of $\mathcal{H}_A \cap \mathcal{H}_B$. Therefore, the eigenvectors $\left|\theta_j\right\rangle$, $1 \leq j \leq k$, span the subspace $\mathcal{H}_A \cap \mathcal{H}_B$, and $\left|\theta_j^{\pm}\right\rangle$, $k+1 \leq j \leq n$, span the space orthogonal to $\mathcal{H}_A \cap \mathcal{H}_B$ in $\mathcal{H}_{A,B}$.

The set of eigenvectors found so far does not form a *basis*, since $n^2 - 2n + k$ eigenvectors belonging to the vector space orthogonal to $\mathcal{H}_{A,B}$ ($\mathcal{H}_A^{\perp} \cap \mathcal{H}_B^{\perp}$) are missing. These eigenvectors are associated with the eigenvalue 1, because projectors Π_A and Π_B cancel a vector $|\psi\rangle$ that is in the space orthogonal to both $\mathcal{H}_A$ and $\mathcal{H}_B$. Therefore, $\mathcal{R}_A|\psi\rangle = -|\psi\rangle$ and $\mathcal{R}_B|\psi\rangle = -|\psi\rangle$. Since $U = \mathcal{R}_B\mathcal{R}_A$, it follows that $U|\psi\rangle = |\psi\rangle$. A basis of orthonormal vectors for space $\mathcal{H}_A^{\perp} \cap \mathcal{H}_B^{\perp}$ completes the spectral decomposition of U_P. The method of singular values and vectors cannot be used to calculate these remaining eigenvectors. However, we show later on that only the eigenvectors associated with eigenvalues other than 1 contribute to the calculation of the hitting time.

Exercise 9.14. Show that if the singular value λ_j is equal to 0, then $A\left|\mu_j\right\rangle$ and $B\left|\nu_j\right\rangle$ are orthonormal eigenvectors of U_P associated with the eigenvalue -1.

Exercise 9.15. Using the eigenvectors in Table 9.1, compute a basis of eigenvectors of the evolution operator U_P associated with the graph of Exercise 9.6 for the subspace $\mathcal{H}_{A,B}$. Find a basis for $\mathcal{H}_{A,B}^{\perp}$ and check whether this basis is formed by eigenvectors of U_P associated with the eigenvalue 1. Check whether any eigenvalue has multiplicity greater than 1 and completely characterize the eigenvectors of U_P.

Exercise 9.16. Suppose that sets X and Y have two vertices each. Consider the complete bipartite graph. Use Table 9.1 to calculate a basis of eigenvectors of the evolution operator U_P associated with this graph for space $\mathcal{H}_{A,B}$. Find a basis for $\mathcal{H}_{A,B}^{\perp}$, the searched vector being orthogonal to the basis vectors of $\mathcal{H}_{A,B}$. Check which eigenvalues have multiplicity greater than 1 and completely characterize the eigenvectors of U_P.

9.6 Quantum Hitting Time

Let us define the *quantum hitting time* in a connected, non-directed, and non-bipartite *graph* $\Gamma(X, E)$ as a natural generalization of the classical concept. We define an associated bipartite graph using a process of duplication. Let X and Y be the sets of vertices of the same cardinality of the bipartite graph. Each edge $\{x_i, x_j\}$ in set E of the original graph, which connects the adjacent vertices x_i and x_j, corresponds to two edges $\{x_i, y_j\}$ and $\{y_i, x_j\}$ in the bipartite graph. Figure 9.1 shows an example of an undirected graph (first graph) and its *associated bipartite graph* (second graph). Using the notation of Sect. 9.2, we have $p_{xy} = q_{xy}$ and $p_{xy} = p_{yx}$, since the bipartite graph is undirected and there is an identification between X and Y.

The quantum walk in the bipartite graph is defined by the evolution operator U_P given by (9.38). In the bipartite graph, one application of U_P corresponds to two steps of the quantum walk, from X to Y and from Y to X. We have to take the partial trace over the space associated with Y to obtain the state of the quantum walk in X.

To define the quantum hitting time, we use a second evolution operator associated with a *directed bipartite graph* modified from the original bipartite graph. This process is similar to the method used to calculate the *classical hitting time* without using the classical stationary distribution described in Sect. 9.1.2. The modified directed graph is obtained from the original bipartite graph converting all directed edges leaving the marked vertices into loops, but keeping the incoming directed edges unchanged. The third graph in Fig. 9.1 is an example in which set $M = \{x_3\}$ has a single element (the loops were omitted). Note that if x_3 is a marked vertex, y_3 will also be marked by the duplication process. All edges leaving x_3 and y_3 were removed. This means that if the walker reaches a marked vertex, the walker will be stuck in this marked vertex in the steps following.

We have learned in Sect. 9.1.2 that the original undirected graph and the modified directed graph are equivalent to calculate the classical hitting time. In the quantum case, to define the hitting time in the original graph, the quantum walk evolves in

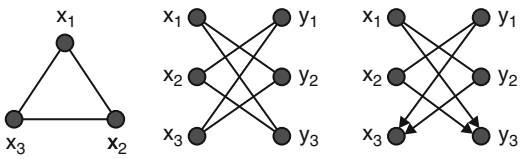

Fig. 9.1 Example of a connected graph with three vertices, its bipartite graph generated by the duplication process, and the directed bipartite graph assuming that x_3 is the only marked vertex. The quantum hitting time is defined in the first graph, but the quantum walk evolves in the third graph

the modified directed graph driven by the evolution operator $U_{P'}$, where P' is the modified stochastic matrix given by

$$p'_{xy} = \begin{cases} p_{xy}, & x \notin M; \\ \delta_{xy}, & x \in M, \end{cases} \tag{9.58}$$

where p_{xy} are the entries of the stochastic matrix P of the undirected bipartite graph. When we use operator $U_{P'}$ of the directed graph, the probabilities associated with the marked vertices increase periodically. To find a marked vertex, we must measure the position of the walker as soon as the probability of being in M is high. The hitting time is a good metric for quantifying at what time we must perform a measurement to find the walker's position.

The initial condition of the quantum walk is

$$|\psi(0)\rangle = \frac{1}{\sqrt{n}} \sum_{\substack{x \in X \\ y \in Y}} \sqrt{p_{xy}} |x, y\rangle. \tag{9.59}$$

Note that $|\psi(0)\rangle$ is defined using the stochastic matrix of the original graph and it is invariant under the action of U_P associated with the original graph, when the probability distribution p_{xy} is symmetric, that is, $|\psi(0)\rangle$ is an eigenvector of U_P associated with the eigenvalue 1. However, $|\psi(0)\rangle$ is not an eigenvector of $U_{P'}$ in general. Now let us define the quantum hitting time.

Definition 9.17 (Quantum Hitting Time). The *quantum hitting time* $H_{P,M}$ of a quantum walk on a graph with the associated evolution operator U_P starting from the initial condition $|\psi(0)\rangle$ is defined as the smallest number of steps T such that

$$F(T) \geq 1 - \frac{m}{n},$$

where m is the number of marked vertices, n is the number of vertices of the original graph, and

$$F(T) = \frac{1}{T+1} \sum_{t=0}^{T} \Big\| |\psi(t)\rangle - |\psi(0)\rangle \Big\|^2, \tag{9.60}$$

where $|\psi(t)\rangle$ is the quantum state at step t of the quantum walk in the modified directed bipartite graph with the stochastic matrix P', that is, $|\psi(t)\rangle = (U_{P'})^t |\psi(0)\rangle$.

Value $1 - m/n$ is taken as reference because it is the distance between the uniform probability distribution and the uniform probability distribution on the marked vertices. This distance can be confirmed by using (7.46) of Sect. 7.6.

The hitting time depends only on the eigenspace of $U_{P'}$ that is associated with eigenvalues different from 1. Or, similarly, the hitting time depends only on the singular values of C different from 1. We will show this fact. Table 9.1 summarizes

the results of the eigenvalues and eigenvectors of the evolution operator. Using the notation of this table, we can write the initial condition of the quantum walk in the basis of eigenvectors as follows:

$$|\psi(0)\rangle = \sum_{j=1}^{n-k} \left(c_j^+ \left|\theta_j^+\right\rangle + c_j^- \left|\theta_j^-\right\rangle\right) + \sum_{j=n-k+1}^{n^2-n+k} c_j \left|\theta_j\right\rangle, \tag{9.61}$$

where coefficients $c_j^{\pm}$ are given by

$$c_j^{\pm} = \left\langle \theta_j^{\pm} | \psi(0) \right\rangle, \tag{9.62}$$

and satisfy the constraint

$$\sum_{j=1}^{n-k} \left(\left|c_j^+\right|^2 + \left|c_j^-\right|^2\right) + \sum_{j=n-k+1}^{n^2-n+k} \left|c_j\right|^2 = 1. \tag{9.63}$$

Applying $U_{P'}^t$ on $|\psi(0)\rangle$, we obtain

$$|\psi(t)\rangle = \sum_{j=1}^{n-k} \left(c_j^+ \mathrm{e}^{2\mathrm{i}\theta_j t} \left|\theta_j^+\right\rangle + c_j^- \mathrm{e}^{-2\mathrm{i}\theta_j t} \left|\theta_j^-\right\rangle\right) + \sum_{j=n-k+1}^{n^2-n+k} c_j \left|\theta_j\right\rangle. \tag{9.64}$$

When we take the difference $|\psi(t)\rangle - |\psi(0)\rangle$, the terms associated with the eigenvalue 1 are eliminated.

Since vectors $\left|\theta_j^{\pm}\right\rangle$ are complex conjugates and $|\psi(0)\rangle$ is real, it follows from (9.62) that $\left|c_j^+\right|^2 = \left|c_j^-\right|^2$. We will denote both $\left|c_j^+\right|^2$ and $\left|c_j^-\right|^2$ by $\left|c_j\right|^2$ such that the value of the sub-index j characterizes the coefficient. Using (9.61) and (9.64), we obtain

$$\left\| |\psi(t)\rangle - |\psi(0)\rangle \right\|^2 = 4 \sum_{j=1}^{n-k} \left|c_j\right|^2 \left(1 - T_{2t}(\cos\theta_j)\right), \tag{9.65}$$

where T_n is the n-th *Chebyshev polynomial of the first kind* defined by $T_n(\cos\theta) = \cos n\theta$. $F(T)$ defined in (9.60) can be explicitly calculated. The result is

$$F(T) = \frac{2}{T+1} \sum_{j=1}^{n-k} \left|c_j\right|^2 \Big(2\,T + 1 - U_{2T}(\cos\theta_j)\Big), \tag{9.66}$$

where U_n are the *Chebyshev polynomials of the second kind* defined by

$$U_n(\cos\theta) = \frac{\sin(n+1)\theta}{\sin\theta}.$$

Function $F(T)$ is continuous, and we can select a range $[0, T]$ containing point $1 - m/n$ where $F(T)$ can be inverted to obtain the quantum hitting time by employing the following equation:

$$H_{P,M} = \left\lceil F^{-1}\left(1 - \frac{m}{n}\right)\right\rceil. \tag{9.67}$$

In principle, it is not necessary to define the hitting time as an integer value, since it is an average. If we remove the *ceiling function* from the above equation, we have a valid definition. In the example of the complete graph given below, we use this alternative definition.

9.7 Probability of Finding a Marked Element

The quantum walk defined by the evolution operator $U_{P'}$ was designed such that the probability of finding a marked element increases during some time. Since the evolution is unitary, the probability of finding a marked element will have an oscillatory pattern. Then, determining the *stopping time* (execution time) of the algorithm is crucial. If the measurement is delayed, the success probability may be very low. The hitting time must be close to the time $t_{\max}$ where the probability reaches the maximum for the first time.

In order to determine $t_{\max}$ and calculate the success probability, we need to find the analytical expression of $|\psi(t)\rangle$. Subtracting (9.64) of (9.61), we obtain

$$|\psi(t)\rangle = |\psi(0)\rangle + \sum_{j=1}^{n-k}\left(c_j^+\left(\mathrm{e}^{2\mathrm{i}\theta_j t} - 1\right)\left|\theta_j^+\right\rangle + c_j^-\left(\mathrm{e}^{-2\mathrm{i}\theta_j t} - 1\right)\left|\theta_j^-\right\rangle\right). \tag{9.68}$$

The probability of finding a marked element is calculated with the *projector* on the vector space spanned by the marked elements, which is

$$\begin{aligned}\mathcal{P}_M &= \sum_{x\in M}|x\rangle\langle x| \otimes I \\ &= \sum_{x\in M}\sum_{y}|x, y\rangle\langle x, y|.\end{aligned} \tag{9.69}$$

The probability at time t is given by $\langle\psi(t)|\mathcal{P}_M|\psi(t)\rangle$.

In this context, we highlight: (1) the problem of determining whether the set of the marked elements is empty, called *detection problem* and (2) the problem of finding an explicit marked element, called *finding problem*. In the general case, the detection problem is simpler than the finding problem, since it does not require calculating the probability of finding a marked element. The detection problem only requires the calculation of the hitting time. The calculation of the probability of

finding a marked element requires the knowledge of $|\psi(t)\rangle$, while the calculation of the hitting time requires knowledge of $|\psi(t)\rangle - |\psi(0)\rangle$. In the latter case, we need not calculate the eigenvectors associated with the eigenvalue 1.

9.8 Quantum Hitting Time in the Complete Graph

The purpose of this section is to calculate the quantum hitting time in the *complete graph*. Let n be the number of vertices. All vertices are adjacent in the complete graph. If the walker is in one vertex, it can go to $n-1$ vertices. Therefore, the stochastic matrix is

$$P = \frac{1}{n-1}\begin{bmatrix} 0 & 1 & 1 & \cdots & 1 \\ 1 & 0 & 1 & \cdots & 1 \\ 1 & 1 & 0 & \cdots & 1 \\ \vdots & \vdots & \vdots & \ddots & \vdots \\ 1 & 1 & 1 & \cdots & 0 \end{bmatrix}. \tag{9.70}$$

Multiplying P by $(n-1)$, we obtain a matrix with all entries equal to 1 minus the identity matrix. Therefore, we can write P as follows:

$$P = \frac{1}{n-1}\left(n\left|u^{(n)}\right\rangle\left\langle u^{(n)}\right| - I_n\right), \tag{9.71}$$

where $\left|u^{(j)}\right\rangle$ is defined by

$$\left|u^{(j)}\right\rangle = \frac{1}{\sqrt{j}}\sum_{i=1}^{j}|i\rangle. \tag{9.72}$$

We number the vertices from 1 to n, such that in this section the computational basis of the Hilbert space $\mathcal{H}^n$ is $\{|1\rangle, \ldots, |n\rangle\}$. We suppose that the marked vertices are the last m vertices, that is, $x \in M$ if and only if $n-m < x \leq n$.

In the definition of the quantum hitting time, the evolution operator uses the modified stochastic matrix P' defined in (9.58) instead of the original matrix P. The entries of matrix P' are

$$p'_{xy} = \begin{cases} \frac{1-\delta_{xy}}{n-1}, & 1 \leq x \leq n-m; \\ \delta_{xy}, & n-m < x \leq n. \end{cases} \tag{9.73}$$

All vectors and operators in Sect. 9.2 must be calculated using P'. Operator C in (9.37) is important because their singular values and vectors are used to calculate some eigenvectors of the evolution operator $U_{P'}$. In Sect. 9.2, we have learned that the entries C_{xy} are given by $\sqrt{p'_{xy}q_{yx}}$. Here we are setting $q_{yx} = p'_{yx}$. In the

complete graph, we have $p_{xy} = p_{yx}$. However, $p'_{xy} \neq p'_{yx}$, if x and y are in M. Using (9.73) and analyzing the values of the entries of C, we conclude that

$$C = \begin{bmatrix} P_{\overline{M}} & 0 \\ 0 & I_m \end{bmatrix}, \tag{9.74}$$

where $P_{\overline{M}}$ is the matrix obtained from P by eliminating m rows and m columns corresponding to the marked vertices. We find the singular values and vectors of C through the spectral decomposition of $P_{\overline{M}}$.

The algebraic expression of $P_{\overline{M}}$ is

$$P_{\overline{M}} = \frac{1}{n-1}\left((n-m)\left|u^{(n-m)}\right\rangle\left\langle u^{(n-m)}\right| - I_{n-m}\right), \tag{9.75}$$

where $\left|u^{(n-m)}\right\rangle$ is obtained from (9.72). Its characteristic polynomial is

$$\det(P_{\overline{M}} - \lambda I) = \left(\lambda - \frac{n-m-1}{n-1}\right)\left(\lambda + \frac{1}{n-1}\right)^{n-m-1}. \tag{9.76}$$

The eigenvalues are $\frac{n-m-1}{n-1}$ with multiplicity 1 and $\frac{-1}{n-1}$ with multiplicity $n-m-1$. Note that if $m \geq 1$, then 1 is not an eigenvalue of $P_{\overline{M}}$. The eigenvector associated with eigenvalue $\frac{n-m-1}{n-1}$ is

$$|v_{n-m}\rangle := \left|u^{(n-m)}\right\rangle \tag{9.77}$$

and the eigenvectors associated with the eigenvalue $\frac{-1}{n-1}$ are

$$|v_i\rangle := \frac{1}{\sqrt{i+1}}\left(\left|u^{(i)}\right\rangle - \sqrt{i}\,|i+1\rangle\right), \tag{9.78}$$

where $1 \leq i \leq n-m-1$. The set $\left\{|v_i\rangle, 1 \leq i \leq n-m\right\}$ is an orthonormal basis of eigenvectors of $P_{\overline{M}}$. The verification is oriented in Exercise 9.18.

Exercise 9.18. The objective of this exercise is to explicitly check the orthonormality of the spectral decomposition of $P_{\overline{M}}$.

1. Use (9.75) to verify that $P_{\overline{M}}|u^{n-m}\rangle = \frac{n-m-1}{n-1}|u^{n-m}\rangle$.
2. Show that $\left\langle u^{(n-m)}\middle|v_i\right\rangle = 0$, for $1 \leq i \leq n-m-1$. Use this fact and (9.75) to verify that $P_{\overline{M}}|v_i\rangle = \frac{-1}{n-1}|v_i\rangle$.
3. Show that $\left\langle u^{(i)}\middle|i+1\right\rangle = 0$ and conclude that $\left\langle u^{(i)}\middle|u^{(i)}\right\rangle = 1$, for $1 \leq i \leq n-m-1$. Use this fact to show that $\left\langle v_i\middle|v_i\right\rangle = 1$.
4. Suppose that $i < j$. Show that $\left\langle u^{(i)}\middle|u^{(j)}\right\rangle = \sqrt{\frac{i}{j}}$ and $\left\langle u^{(i)}\middle|j+1\right\rangle = 0$. Use these facts to show that $\left\langle v_i\middle|v_j\right\rangle = 0$.

Table 9.2 Right and left singular values and vectors of matrix C

Singular value	Right singular vector	Left singular vector	Range
$\cos\theta_1 = \frac{1}{n-1}$	$\lvert v_j\rangle$	$-\lvert v_j\rangle$	$1 \le j \le n-m-1$
$\cos\theta_2 = \frac{n-m-1}{n-1}$	$\lvert v_{n-m}\rangle$	$\lvert v_{n-m}\rangle$	$j = n-m$
$\cos\theta_3 = 1$	$\lvert j\rangle$	$\lvert j\rangle$	$n-m+1 \le j \le n$

Vectors $\lvert v_{n-m}\rangle$ and $\lvert v_i\rangle$ are given by (9.77) and (9.78). Angles θ_1, θ_2, and θ_3 are defined from the singular values

Table 9.3 Eigenvalues and normalized eigenvectors of $U_{P'}$ obtained from the singular values and vectors of C

Eigenvalue	Eigenvector	Range
$e^{\pm 2i\theta_1}$	$\left\lvert\theta_j^{\pm}\right\rangle = \frac{-\left(A+e^{\pm i\theta_1}B\right)\lvert v_j\rangle}{\sqrt{2}\sin\theta_1}$	$1 \le j \le n-m-1$
$e^{\pm 2i\theta_2}$	$\left\lvert\theta_{n-m}^{\pm}\right\rangle = \frac{\left(A-e^{\pm i\theta_2}B\right)\lvert v_{n-m}\rangle}{\sqrt{2}\sin\theta_2}$	$j = n-m$
1	$\lvert\theta_j\rangle = A\lvert j\rangle$	$n-m+1 \le j \le n$

Matrix C is Hermitian. Therefore, the nontrivial singular values λ_i of C defined in (9.41) are obtained by taking the modulus of the eigenvalues of $P_{\overline{M}}$. The right singular vectors $\lvert v_i\rangle$ are the eigenvectors of $P_{\overline{M}}$ and the left singular vectors are obtained from (9.42). If an eigenvalue of $P_{\overline{M}}$ is negative, the left singular vector is the negative of the corresponding eigenvector of $P_{\overline{M}}$. These vectors must be augmented with m zeros to have the dimension compatible with C. Finally, submatrix I_m in (9.74) adds to the list the singular value 1 with multiplicity m and the associated singular vectors $\lvert j\rangle$, where $n-m+1 \le j \le n$. Table 9.2 summarizes these results.

Eigenvalues and eigenvectors of $U_{P'}$ that can be obtained from the singular values and vectors of C are given in Table 9.1. Table 9.3 reproduces these results for the complete graph. It is still missing $n^2 - 2n + m$ eigenvectors associated with eigenvalue 1.

The initial condition is given by (9.59), which reduces to

$$\lvert\psi(0)\rangle = \frac{1}{\sqrt{n(n-1)}} \sum_{x,y=1}^{n} (1-\delta_{xy})\lvert x\rangle\lvert y\rangle. \tag{9.79}$$

Just the eigenvectors of $U_{P'}$ that are not orthogonal to the initial condition $\lvert\psi(0)\rangle$ are involved in the dynamics. Exercise 9.19 guides the proof that the eigenvectors $\left\lvert\theta_j\right\rangle$, $n-m+1 \le j \le n$, are orthogonal to the initial condition. Exercise 9.20 guides the proof that the eigenvectors $\left\lvert\theta_j^{\pm}\right\rangle$, $1 \le j \le n-m-1$, are also orthogonal

to the initial condition. The remaining eigenvectors are $|\theta^{\pm}_{n-m}\rangle$, associated with the positive eigenvalue of $P_{\overline{M}}$, and the eigenvectors associated with eigenvalue 1, which has not been addressed yet. Therefore, the initial condition $|\psi(0)\rangle$ can be written as

$$|\psi(0)\rangle = c^{+}|\theta^{+}_{n-m}\rangle + c^{-}|\theta^{-}_{n-m}\rangle + |\beta\rangle, \tag{9.80}$$

where coefficients $c^{\pm}$ are given by (see Exercise 9.21)

$$c^{\pm} = \frac{\sqrt{n-m}\left(1 - \mathrm{e}^{\mp \mathrm{i}\theta_2}\right)}{\sqrt{2n}\,\sin\theta_2}, \tag{9.81}$$

where θ_2 is defined by

$$\cos\theta_2 = \frac{n-m-1}{n-1}. \tag{9.82}$$

Vector $|\beta\rangle$ is the component of $|\psi(0)\rangle$ in the eigenspace associated with eigenvalue 1. The calculation of a basis of eigenvectors for this eigenspace is hard-working, we postpone this calculation for now.

Exercise 9.19. To show that $\langle\theta_j|\psi(0)\rangle = 0$ when $n-m+1 \leq j \leq n$, use the expression for A given by (9.21) and the expression for $|\alpha_x\rangle$ given by (9.23), where p_{xy} and q_{xy} are given by (9.73). Show that

$$\langle\theta_j|\psi(0)\rangle = \sum_{x\in M}\langle\alpha_x|\psi(0)\rangle.$$

Use (9.79) to show that $\langle\alpha_x|\psi(0)\rangle = 0$ if $x \in M$.

Exercise 9.20. To show that $\left\langle\theta^{\pm}_j|\psi(0)\right\rangle = 0$, for $1 \leq j \leq n-m-1$, use the expressions of A and B given by (9.21) and (9.22), and the expressions for $|\alpha_x\rangle$ and $|\beta_y\rangle$ given by (9.23) and (9.24), where p_{xy} and q_{xy} are given by (9.73). Equation (9.78) and Exercise 9.18 must also be used. The expression of $|\psi(0)\rangle$ is given by (9.79).

Exercise 9.21. The purpose of this exercise is to guide the calculation of coefficients $c^{\pm}$ in (9.80), which are defined by

$$c^{\pm} = \langle\theta^{\pm}_{n-m}|\psi(0)\rangle.$$

Using (9.79) and (9.88), cancel out the orthogonal terms and simplify the result.

Applying $U_{P'}^t$ on $|\psi(0)\rangle$—given by (9.80)—using that $\left|\theta_{n-m}^{\pm}\right\rangle$ are eigenvectors associated with eigenvalues $\mathrm{e}^{\pm 2\mathrm{i}\theta_2}$, and $|\beta\rangle$ is in the eigenspace associated with the eigenvalue 1, we obtain

$$\begin{aligned}|\psi(t)\rangle &= U_{P'}^t|\psi(0)\rangle \\ &= c^+\mathrm{e}^{2\mathrm{i}\theta_2 t}\left|\theta_{n-m}^+\right\rangle + c^-\mathrm{e}^{-2\mathrm{i}\theta_2 t}|\theta_{n-m}^-\rangle + |\beta\rangle,\end{aligned} \tag{9.83}$$

Using the expression of $|\psi(t)\rangle$ and (9.60), we can calculate $F(T)$. The difference $|\psi(t)\rangle - |\psi(0)\rangle$ can be calculated as follows: using (9.80) and (9.83), we obtain

$$|\psi(t)\rangle - |\psi(0)\rangle = c^+(\mathrm{e}^{2\mathrm{i}\theta_2 t} - 1)\left|\theta_{n-m}^+\right\rangle + c^-(\mathrm{e}^{-2\mathrm{i}\theta_2 t} - 1)|\theta_{n-m}^-\rangle \tag{9.84}$$

and using (9.81), we obtain

$$\begin{aligned}\left\||\psi(t)\rangle - |\psi(0)\rangle\right\|^2 &= \left|c^+(\mathrm{e}^{2\mathrm{i}\theta_2 t} - 1)\right|^2 + \left|c^-(\mathrm{e}^{-2\mathrm{i}\theta_2 t} - 1)\right|^2 \\ &= \frac{4(n-1)(n-m)}{n(2n-m-2)}\left(1 - T_{2t}\left(\frac{n-m-1}{n-1}\right)\right),\end{aligned}$$

where T_n are the *Chebyshev polynomials of the first kind*. Taking the average and using

$$\sum_{t=0}^{T} T_{2t}\left(\frac{n-m-1}{n-1}\right) = \frac{1}{2} + \frac{1}{2}U_{2T}\left(\frac{n-m-1}{n-1}\right) \tag{9.85}$$

we obtain

$$F(T) = \frac{2\,(n-1)\,(n-m)\left(2\,T + 1 - U_{2T}\left(\frac{n-m-1}{n-1}\right)\right)}{n\,(2\,n-m-2)\,(T+1)}, \tag{9.86}$$

where U_n are the *Chebyshev polynomials of the second kind*. The graph in Fig. 9.2 shows the behavior of function $F(T)$. $F(T)$ grows rapidly passing through the dashed line, which represents value $1 - m/n$, and oscillates around the limiting value $\frac{4(n-1)(n-m)}{n(2n-m-2)}$.

For $n \gg m$, we obtain the hitting time $H_{P,M}$ by inverting the *Laurent series* of the equation $F(T) = 1 - \frac{m}{n}$. The first terms are

$$H_{P,M} = \frac{j_0^{-1}\left(\frac{1}{2}\right)}{2}\sqrt{\frac{n}{2\,m}} - \frac{\sqrt{1 - \frac{1}{4}\,j_0^{-1}\left(\frac{1}{2}\right)^2}}{1 + 2\sqrt{1 - \frac{1}{4}\,j_0^{-1}\left(\frac{1}{2}\right)^2}} + O\left(\frac{1}{\sqrt{n}}\right), \tag{9.87}$$

where j_0 is a *spherical Bessel function of the first kind* or the *unnormalized sync function*. The value of $j_0^{-1}\left(\frac{1}{2}\right)$ is approximately 1.9.

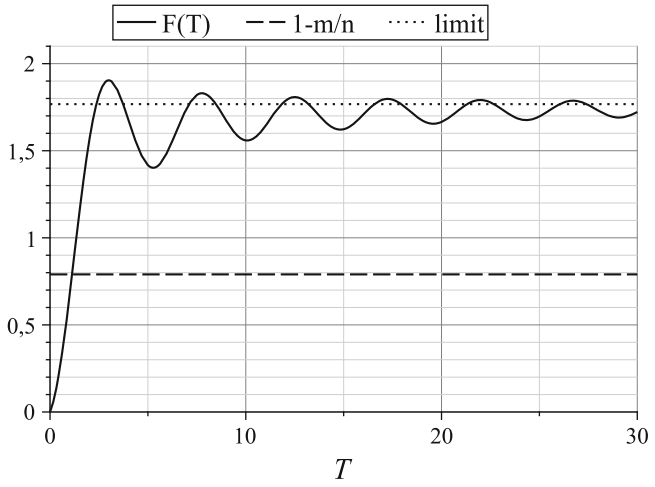

Fig. 9.2 Graph of function $F(T)$ (*solid line*), the line $1-\frac{m}{n}$ (*dashed line*), and the line $\frac{4(n-1)(n-m)}{n(2n-m-2)}$ (*dotted line*) for $n = 100$ and $m = 21$. The hitting time is the time T such that $F(T) = 1 - \frac{m}{n}$, which is around 1.13

Exercise 9.22. The purpose of this exercise is to obtain (9.85). Use the trigonometric representation of T_n and convert the cosine into a sum of exponentials of complex arguments. Use the formula for geometric sequence $\sum_{t=0}^{T} a^t = \frac{a^{T+1}-1}{a-1}$ to simplify the sum. Convert the result to the form of Chebyshev polynomials of the second kind.

9.8.1 Probability of Finding a Marked Element

The hitting time is used in search algorithms as the stopping time. It is important to calculate the success probability when we use the hitting time. The calculation of the probability of finding a marked element as a function of time is more elaborated than the calculation of the hitting time because we explicitly calculate $|\psi(t)\rangle$, that is, we calculate the vectors $\left|\theta^{\pm}_{n-m}\right\rangle$ and $|\beta\rangle$ that appear in (9.83).

Using (9.21) and (9.22), we obtain

$$\begin{aligned}\left|\theta^{\pm}_{n-m}\right\rangle &= \frac{1}{\sqrt{2}\sin\theta_2}\left(A - \mathrm{e}^{\pm \mathrm{i}\theta_2} B\right)\left|u^{(n-m)}\right\rangle \\ &= \frac{1}{\sqrt{2(n-m)}\sin\theta_2}\left(\sum_{x=1}^{n-m}|\alpha_x\rangle - \mathrm{e}^{\pm \mathrm{i}\theta_2}\sum_{y=1}^{n-m}|\beta_y\rangle\right).\end{aligned}$$

Using (9.23), (9.24), and (9.73), we obtain

$$\left|\theta_{n-m}^{\pm}\right\rangle = \frac{1}{\sqrt{2(n-1)(n-m)}\,\sin\theta_2}\left(\left(1-\mathrm{e}^{\pm\mathrm{i}\theta_2}\right)\sum_{x,y=1}^{n-m}\left(1-\delta_{xy}\right)|x\rangle|y\rangle\right.$$
$$\left.+\sum_{x=1}^{n-m}\sum_{y=n-m+1}^{n}|x\rangle|y\rangle-\mathrm{e}^{\pm\mathrm{i}\theta_2}\sum_{x=n-m+1}^{n}\sum_{y=1}^{n-m}|x\rangle|y\rangle\right). \tag{9.88}$$

Using (9.81) and (9.82), the expression for the quantum state at time t reduces to

$$|\psi(t)\rangle = \frac{1}{\sqrt{n(n-1)}}\left(\frac{2(n-1)T_{2t}\left(\frac{n-m-1}{n-1}\right)}{2n-m-2}\sum_{x,y=1}^{n-m}\left(1-\delta_{xy}\right)|x\rangle|y\rangle\right.$$
$$+\left(\frac{(n-1)T_{2t}\left(\frac{n-m-1}{n-1}\right)}{2n-m-2}-U_{2t-1}\left(\frac{n-m-1}{n-1}\right)\right)\sum_{x=1}^{n-m}\sum_{y=n-m+1}^{n}|x\rangle|y\rangle$$
$$\left.+\left(\frac{(n-1)T_{2t}\left(\frac{n-m-1}{n-1}\right)}{2n-m-2}+U_{2t-1}\left(\frac{n-m-1}{n-1}\right)\right)\sum_{x=n-m+1}^{n}\sum_{y=1}^{n-m}|x\rangle|y\rangle\right)$$
$$+|\beta\rangle. \tag{9.89}$$

Vector $|\beta\rangle$ can be determined from (9.80), since we know $|\psi(0)\rangle$ and $\left|\theta_{n-m}^{\pm}\right\rangle$. The result is

$$|\beta\rangle = \frac{1}{\sqrt{n(n-1)}}\left(\frac{-m}{2n-m-2}\sum_{x,y=1}^{n-m}\left(1-\delta_{xy}\right)|x\rangle|y\rangle\right.$$
$$+\frac{n-m-1}{2n-m-2}\sum_{x=1}^{n-m}\sum_{y=n-m+1}^{n}\left(|x\rangle|y\rangle+|y\rangle|x\rangle\right)$$
$$\left.+\sum_{x,y=n-m+1}^{n}\left(1-\delta_{xy}\right)|x\rangle|y\rangle\right). \tag{9.90}$$

The probability of finding a marked element $p_M(t)$ after performing a measurement with projectors $\mathcal{P}_M$ and $I-\mathcal{P}_M$, where $\mathcal{P}_M$ is the projector on the vector space spanned by the marked elements

$$\mathcal{P}_M = \sum_{x=n-m+1}^{n}|x\rangle\langle x|\otimes I$$
$$= \sum_{x=n-m+1}^{n}\sum_{y=1}^{n}|x,y\rangle\langle x,y|, \tag{9.91}$$

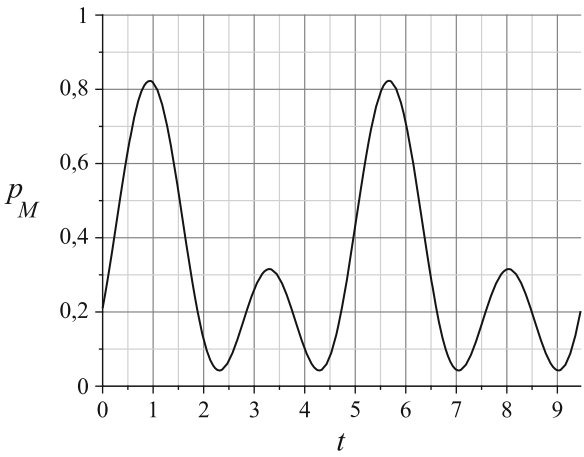

Fig. 9.3 Graph of the probability of finding a marked vertex as a function of time for $n = 100$ and $m = 21$. The initial value is $\frac{m}{n}$ and the probability has period $\frac{\pi}{\theta_2}$

is given by $\langle\psi(t)|\mathcal{P}_M|\psi(t)\rangle$. Using (9.89), we obtain

$$p_M(t) = \frac{m(m-1)}{n(n-1)} + \frac{m(n-m)}{n(n-1)}\left(\frac{n-1}{2n-m-2}T_{2t}\left(\frac{n-m-1}{n-1}\right)\right.$$
$$\left. + U_{2t-1}\left(\frac{n-m-1}{n-1}\right) + \frac{n-m-1}{2n-m-2}\right)^2 \tag{9.92}$$

the graph of which is shown in Fig. 9.3 for $n = 100$ and $m = 21$.

We can determine the critical points of $p_M(t)$ by differentiating with respect to time. The first maximum point occurs at time

$$t_{\max} = \frac{\arctan\left(\frac{\sqrt{2n-m-2}}{\sqrt{m}}\right)}{2\arccos\left(\frac{n-m-1}{n-1}\right)}, \tag{9.93}$$

the asymptotic expansion of which is

$$t_{\max} = \frac{\pi}{4}\sqrt{\frac{n}{2m}} - \frac{1}{4} + O\left(\sqrt{\frac{m}{n}}\right). \tag{9.94}$$

Substituting for the expression of the probability, we obtain

$$p_M(t_{\max}) = \frac{1}{2} + \sqrt{\frac{m}{2n}} + O\left(\frac{m}{n}\right). \tag{9.95}$$

For any values n and m, the probability of finding the marked vertex is greater than $\frac{1}{2}$ if the measurement is performed at time $t_{\max}$. The time $t_{\max}$ is less than the hitting time—see (9.87), because $\frac{\pi}{4\sqrt{2}} \approx 0.56$ and $\frac{j_0^{-1}\left(\frac{1}{2}\right)}{2\sqrt{2}} \approx 0.67$. The value of the success probability in an algorithm that uses the hitting time as the stopping time will be smaller than the probability at time $t_{\max}$. Evaluating p_M at time $H_{P,M}$ and taking the asymptotic expansion, we obtain

$$p_M(H_{P,M}) = \frac{1}{8}\, j_0^{-1}\left(\frac{1}{2}\right)^2 + O\left(\frac{1}{\sqrt{n}}\right). \tag{9.96}$$

The first term is around 0.45 and does not depend on n or m. This shows that the hitting time in the complete graph is a good parameter for the stopping time of searching algorithm.

Exercise 9.23. Using (9.92), show that

1. $p_M(0) = \frac{m}{n}$.
2. $p_M(t)$ is a periodic function with period $\frac{\pi}{\theta_2}$.
3. the maximum points for $t \geq 0$ are given by

$$t_j = \frac{1}{2\theta_2} \arctan\left(\frac{1+\cos\theta_2}{\sin\theta_2}\right) + \frac{j\pi}{2\theta_2},$$

where $j = 0, 1, \ldots$.

Exercise 9.24. Show that in the asymptotic limit $n \gg m$, the expression of the success probability is

$$p_M(t) = \frac{1}{2}\sin^2 2t\theta_2 + O\left(\frac{1}{\sqrt{n}}\right).$$

Further Reading

The theory of classical Markov chains can be found in [6, 47, 58, 62]. The last chapter of [58] describes in detail the *Perron–Frobenius theorem* that is important in the context of this chapter. The definition of the *quantum hitting time* presented in Sect. 9.6 was based on [74]. Reference [75] is also useful. The quantum walk model described in this chapter was defined by *Mario Szegedy* in [74] and was inspired by the algorithm for *element distinctness* developed by *Andris Ambainis* [9]. An extension of Szegedy's model for ergodic Markov chains was introduced in [46, 51, 52]. The main problem that these references are addressing is to show that the *hitting time* is of the order of the *detection time*. Reference [51] uses *Tulsi's* algorithm [78] to amplify the probability of finding a marked element, but can only be used for symmetrical ergodic Markov chains. Reference [46] proposed a more general algorithm which is able to find a marked element with a quadratic speedup.

Szegedy's ideas helped the development of new quantum algorithms faster than their classical counterparts. Reference [53] presents an algorithm for finding triangles in a graph. Reference [50] presents an algorithm to test the commutativity of *black box groups*. The calculation of the hitting time in the complete graph was presented in [70]. Master's thesis [40] presents an overview of the Szegedy's hitting time and the algorithm to test the commutativity of groups.

Appendix A
Linear Algebra for Quantum Computation

The purpose of this appendix is to compile the definitions, notations, and facts of linear algebra that are important for this book. This appendix also serves as a quick reference for the main operations in vector spaces, for instance, the *inner* and *tensor products*. Quantum computation inherited linear algebra from quantum mechanics as the supporting language for describing this area. Therefore, it is essential to have a solid knowledge of the basic results of linear algebra to understand quantum computation and quantum algorithms. If the reader does not have this base knowledge, we suggest reading some of the basic references recommended at the end of this appendix.

A.1 Vector Spaces

A *vector space* V over the field of complex numbers $\mathbb{C}$ is a non-empty set of elements called vectors. In V, it is defined the operations of vector addition and multiplication of a vector by a scalar in $\mathbb{C}$. The addition operation is associative and commutative. It also obeys properties

- There is an element $\mathbf{0} \in V$, such that, for each $\mathbf{v} \in V$, $\mathbf{v} + \mathbf{0} = \mathbf{0} + \mathbf{v} = \mathbf{v}$ (existence of neutral element)
- For each $\mathbf{v} \in V$, there exists $\mathbf{u} = (-1)\mathbf{v}$ in V such that $\mathbf{v} + \mathbf{u} = \mathbf{0}$ (existence of inverse element)

$\mathbf{0}$ is called zero vector. The scalar multiplication operation obeys properties

- $a.(b.\mathbf{v}) = (a.b).\mathbf{v}$ (associativity)
- $1.\mathbf{v} = \mathbf{v}$ (1 is the neutral element of multiplication)
- $(a + b).\mathbf{v} = a.\mathbf{v} + b.\mathbf{v}$ (distributivity of sum of scalars)
- $a.(\mathbf{v} + \mathbf{w}) = a.\mathbf{v} + a.\mathbf{w}$ (distributivity in V)

where $\mathbf{v}, \mathbf{w} \in V$ and $a, b \in \mathbb{C}$.

R. Portugal, *Quantum Walks and Search Algorithms*, Quantum Science and Technology, DOI 10.1007/978-1-4614-6336-8,

A vector space can be infinite, but in most applications in *quantum computation*, *finite vector spaces* are used and are denoted by $\mathbb{C}^n$. In this case, the vectors have n complex entries. In this book, we rarely use infinite spaces, and in these few cases, we are interested only in finite subspaces. In the context of *quantum mechanics*, *infinite vector spaces* are used more frequently than finite spaces.

A *basis* for $\mathbb{C}^n$ consists of exactly n linearly independent vectors. If $\{\mathbf{v}_1, \ldots, \mathbf{v}_n\}$ is a basis for $\mathbb{C}^n$, then a generic vector $\mathbf{v}$ can be written as

$$\mathbf{v} = \sum_{i=1}^{n} a_i \mathbf{v}_i,$$

where coefficients a_i are complex numbers. The *dimension* of a vector space is the number of basis vectors.

A.2 Inner Product

The *inner product* is a binary operation $(\cdot, \cdot) : V \times V \mapsto \mathbb{C}$, which obeys the following properties:

1. $(\cdot, \cdot)$ is linear in the second argument

$$\left(\mathbf{v}, \sum_{i=1}^{n} a_i \mathbf{v}_i\right) = \sum_{i=1}^{n} a_i \, (\mathbf{v}, \mathbf{v}_i).$$

2. $(\mathbf{v}_1, \mathbf{v}_2) = (\mathbf{v}_2, \mathbf{v}_1)^*$.
3. $(\mathbf{v}, \mathbf{v}) \geq 0$. The equality holds if and only if $\mathbf{v} = \mathbf{0}$.

In general, the inner product is not linear in the first argument. The property in question is called *conjugate-linear*.

There is more than one way to define an inner product on a vector space. In $\mathbb{C}^n$, the most used inner product is defined as follows: If

$$\mathbf{v} = \begin{bmatrix} a_1 \\ \vdots \\ a_n \end{bmatrix}, \quad \mathbf{w} = \begin{bmatrix} b_1 \\ \vdots \\ b_n \end{bmatrix},$$

then

$$(\mathbf{v}, \mathbf{w}) = \sum_{i=1}^{n} a_i^* b_i.$$

This expression is equivalent to the matrix product of the transpose-conjugate vector, which is usually denoted by $\mathbf{v}^\dagger$, by $\mathbf{w}$.

If an inner product is introduced in a vector space, we can define the notion of orthogonality. Two vectors are *orthogonal* if the inner product is zero. We also introduce the notion of *norm* using the inner product. The norm of $\mathbf{v}$, denoted by $\|\mathbf{v}\|$, is defined as

$$\|\mathbf{v}\| = \sqrt{(\mathbf{v}, \mathbf{v})}.$$

A *normalized vector* or *unit vector* is a vector whose norm is equal to 1. A basis is said *orthonormal* if all vectors are normalized and mutually orthogonal.

A finite vector space with an inner product is called a *Hilbert space*. In order to an infinite vector space be a Hilbert space, it must obey additional properties besides having an inner product. Since we will deal primarily with finite vector spaces, we use the term *Hilbert space* as a synonym for *vector space with an inner product*. A *subspace* W of a finite Hilbert space V is also a Hilbert space. The set of vectors orthogonal to all vectors of W is the Hilbert space $W^{\perp}$ called *orthogonal complement*. V is the direct sum of W and $W^{\perp}$, that is, $V = W \oplus W^{\perp}$. An N-dimensional Hilbert space will be denoted by $\mathcal{H}^N$ to highlight its dimension. A Hilbert space associated with a system A will be denoted by $\mathcal{H}_A$.

A.3 The Dirac Notation

In this review of linear algebra, we will systematically be using the *Dirac* or *bra-ket notation*, which was introduced by the English physicist Paul Dirac in the context of quantum mechanics to aid algebraic manipulations. This notation is very simple. Several notations are used for vectors, such as $\mathbf{v}$ and $\vec{v}$. The Dirac notation uses

$$\mathbf{v} \equiv |v\rangle.$$

Up to this point, instead of using bold or putting an arrow over letter v, we put letter v between a vertical bar and a right angle bracket. If we have an indexed basis, that is, $\{\mathbf{v}_1, \ldots, \mathbf{v}_n\}$, in the Dirac notation we use the form $\{|v_1\rangle, \ldots, |v_n\rangle\}$ or $\{|1\rangle, \ldots, |n\rangle\}$. Note that if we are using a single basis, letter $\mathbf{v}$ is unnecessary in principle. Computer scientists usually start counting from 0. So, the first basis vector is usually called $\mathbf{v}_0$. In the Dirac notation we have

$$\mathbf{v}_0 \equiv |0\rangle.$$

Vector $|0\rangle$ is not the zero vector, it is only the first vector in a collection of vectors. In the Dirac notation, the zero vector is an exception, whose notation is not modified. Here we use the notation $\mathbf{0}$.

Suppose that vector $|v\rangle$ has the following entries in a basis

$$|v\rangle = \begin{bmatrix} a_1 \\ \vdots \\ a_n \end{bmatrix}.$$

The dual vector is denoted by $\langle v|$ and is defined by

$$\langle v| = \left[a_1^* \cdots a_n^*\right].$$

Usual vectors and their duals can be seen as column and row matrices, respectively, for algebraic manipulation. The matrix product of $\langle v|$ by $|v\rangle$ is denoted by $\langle v|v\rangle$ and its value in terms of their entries is

$$\langle v|v\rangle = \sum_{i=1}^{n} a_i^* a_i \,.$$

This is an example of an inner product, which is naturally defined via the Dirac notation. If $\{|v_1\rangle, \ldots, |v_n\rangle\}$ is an orthonormal basis, then

$$\langle v_i | v_j \rangle = \delta_{ij} \,,$$

where δ_{ij} is the *Kronecker delta*. The norm of a vector in this notation is

$$\| |v\rangle \| = \sqrt{\langle v|v\rangle}.$$

We use the terminology *ket* for vector $|v\rangle$ and *bra* for dual vector $\langle v|$. Keeping consistency, we use the terminology *bra-ket* for $\langle v|v\rangle$.

It is also very common to meet the matrix product of $|v\rangle$ by $\langle v|$, denoted by $|v\rangle\langle v|$, known as the *outer product*, whose result is an $n \times n$ matrix

$$\begin{aligned} |v\rangle\langle v| &= \begin{bmatrix} a_1 \\ \vdots \\ a_n \end{bmatrix} \cdot \left[a_1^* \cdots a_n^*\right] \\ &= \begin{bmatrix} a_1 a_1^* & \cdots & a_1 a_n^* \\ & \ddots & \\ a_n a_1^* & \cdots & a_n a_n^* \end{bmatrix}. \end{aligned}$$

The key to the Dirac notation is to always view *kets* as column matrices, *bras* as row matrices, and recognize that a sequence of *bras* and *kets* is a matrix product, hence associative, but non-commutative.

A.4 Computational Basis

The *computational basis* of $\mathbb{C}^n$, denoted by $\{|0\rangle, \ldots, |n-1\rangle\}$, is given by

$$|0\rangle = \begin{bmatrix} 1 \\ 0 \\ \vdots \\ 0 \end{bmatrix}, \quad \ldots, \quad |n-1\rangle = \begin{bmatrix} 0 \\ 0 \\ \vdots \\ 1 \end{bmatrix}.$$

This basis is also known as *canonical basis*. A few times we will use the numbering of the computational basis beginning with $|1\rangle$ and ending with $|n\rangle$. In this book, when we use a small-caption *Latin letter* within a *ket* or *bra*, we are referring to the computational basis. Then, the following expression will always be valid

$$\langle i | j \rangle = \delta_{ij}.$$

The normalized sum of all computational basis vectors defines vector

$$|\mathrm{D}\rangle = \frac{1}{\sqrt{n}} \sum_{i=0}^{n-1} |i\rangle,$$

which we will call *diagonal state*. When $n = 2$, the diagonal state is given by $|\mathrm{D}\rangle = |+\rangle$ where

$$|+\rangle = \frac{|0\rangle + |1\rangle}{\sqrt{2}}.$$

Exercise A.1. Explicitly calculate the values of $|i\rangle\langle j|$ and

$$\sum_{i=0}^{n-1} |i\rangle\langle i|$$

in $\mathbb{C}^3$.

A.5 Qubit and the Bloch Sphere

The *qubit* is a *unit vector* in vector space $\mathbb{C}^2$. A generic qubit $|\psi\rangle$ is represented by

$$|\psi\rangle = \alpha\,|0\rangle + \beta\,|1\rangle,$$

where coefficients α and β are complex numbers and obey the constraint

$$|\alpha|^2 + |\beta|^2 = 1.$$

The set $\{|0\rangle,\ |1\rangle\}$ is the computational basis of $\mathbb{C}^2$ and $\alpha,\ \beta$ are called amplitudes of state $|\psi\rangle$. The term *state* (or *state vector*) is used as a synonym for *unit vector in a Hilbert space*.

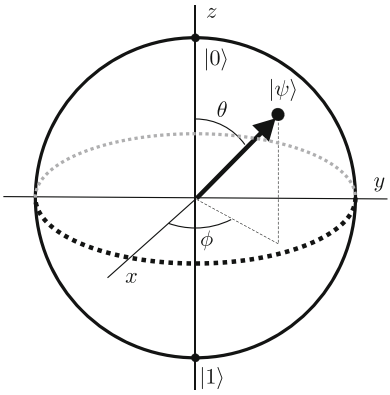

Fig. A.1 Bloch Sphere. The state $|\psi\rangle$ of a qubit is represented by a point on the sphere

In principle, we need four real numbers to describe a qubit, two for α and two for β. The constraint $|\alpha|^2 + |\beta|^2 = 1$ reduces to three numbers. In quantum mechanics, two vectors that differ from a *global phase factor* are considered equivalent. A global phase factor is a complex number of unit modulus multiplying the state. By eliminating this factor, a qubit can be described by two real numbers θ and ϕ as follows:

$$|\psi\rangle = \cos\frac{\theta}{2}|0\rangle + \mathrm{e}^{\mathrm{i}\phi}\sin\frac{\theta}{2}|1\rangle,$$

where $0 \leq \theta \leq \pi$ and $0 \leq \phi < 2\pi$. In the above notation, state $|\psi\rangle$ can be represented by a point on the surface of a sphere of unit radius, called *Bloch sphere*. Numbers θ and ϕ are spherical angles that locate the point that describes $|\psi\rangle$, as shown in Fig. A.1. The vector showed there is given by

$$\begin{bmatrix} \sin\theta\cos\phi \\ \sin\theta\sin\phi \\ \cos\theta \end{bmatrix}.$$

When we disregard global phase factors, there is a one-to-one correspondence between the quantum states of a qubit and the points on the Bloch sphere. State $|0\rangle$ is in the *north pole* of the sphere, because it is obtained by taking $\theta = 0$. State $|1\rangle$ is in the *south pole*. States

$$|\pm\rangle = \frac{|0\rangle \pm |1\rangle}{\sqrt{2}}$$

are the intersection points of the x-axis and the sphere, and states $(|0\rangle \pm \mathrm{i}|1\rangle)/\sqrt{2}$ are the intersection points of the y-axis with the sphere.

The representation of *classical bits* in this context is given by the poles of the Bloch sphere and the representation of the *probabilistic classical bit*, that is, 0 with probability p and 1 with probability $1 - p$, is given by the point in z-axis with coordinate $2p - 1$. The interior of the Bloch sphere is used to describe the states of a qubit in the presence of *decoherence*.

Exercise A.2. Using the Dirac notation, show that opposite points in the Bloch sphere correspond to orthogonal states.

Exercise A.3. Suppose you know that a qubit is either is in state $|+\rangle$ with probability p or in state $|-\rangle$ with probability $1 - p$. If this is the best you know about the qubit's state, where in the Bloch sphere would you represent this qubit?

Exercise A.4. Does the outside of Bloch sphere play any role?

A.6 Linear Operators

Let V and W be vector spaces, $\{|v_1\rangle, \ldots, |v_n\rangle\}$ a basis for V, and $\mathcal{A}$ a function $\mathcal{A} : V \mapsto W$ that satisfies

$$\mathcal{A}\left(\sum_i a_i |v_i\rangle\right) = \sum_i a_i \mathcal{A}(|v_i\rangle),$$

for any complex numbers a_i. $\mathcal{A}$ is called a *linear operator* from V to W. The term *linear operator in* V means that both the domain and codomain of $\mathcal{A}$ is V. The composition of linear operators $\mathcal{A} : V_1 \mapsto V_2$ and $\mathcal{B} : V_2 \mapsto V_3$ is also a linear operator $\mathcal{C} : V_1 \mapsto V_3$ obtained through the composition of their functions: $\mathcal{C}(|v\rangle) = \mathcal{B}(\mathcal{A}(|v\rangle))$. The sum of two linear operators, both from V to W, is naturally defined by formula $(\mathcal{A} + \mathcal{B})(|v\rangle) = \mathcal{A}(|v\rangle) + \mathcal{B}(|v\rangle)$.

The identity operator $\mathcal{I}$ in V is a linear operator such that $\mathcal{I}(|v\rangle) = |v\rangle$ for all $|v\rangle \in V$. The null operator $\mathcal{O}$ in V is a linear operator such that $\mathcal{O}(|v\rangle) = \mathbf{0}$ for all $|v\rangle \in V$.

The *rank* of a linear operator $\mathcal{A}$ in V is the dimension of the image of $\mathcal{A}$. The *kernel* or *nullspace* of a linear operator $\mathcal{A}$ in V is the set of all vectors $|v\rangle$ for which $\mathcal{A}(|v\rangle) = \mathbf{0}$. The dimension of the kernel is called the *nullity* of the operator. The *rank-nullity theorem* states that rank $\mathcal{A}$ + nullity $\mathcal{A}$ = dim V.

Fact

If we specify the action of a linear operator on a basis of vector space V, its action on any vector in V can be straightforwardly determined.

A.7 Matrix Representation

Linear operators can be represented by matrices. Let $\mathcal{A} : V \mapsto W$ be a linear operator, $\{|v_1\rangle, \ldots, |v_n\rangle\}$ and $\{|w_1\rangle, \ldots, |w_m\rangle\}$ orthonormal bases for V and W, respectively. A *matrix representation* of $\mathcal{A}$ is obtained by applying $\mathcal{A}$ to every vector in the basis of V and expressing the result as a linear combination of basis vectors of W, as follows:

$$\mathcal{A}\left(|v_j\rangle\right) = \sum_{i=1}^{m} a_{ij}\,|w_i\rangle,$$

where index j run from 1 to n. Therefore, a_{ij} are entries of an $m \times n$ matrix, which we call A. In this case, expression $\mathcal{A}\left(|v_j\rangle\right)$, which means function $\mathcal{A}$ applied to argument $|v_j\rangle$, is equivalent to the matrix product $A|v_j\rangle$. Using the outer product notation, we have

$$A = \sum_{i=1}^{m}\sum_{j=1}^{n} a_{ij}\,|w_i\rangle\langle v_j|.$$

Using the above equation and the fact that the basis of V is orthonormal, we can verify that the matrix product of A by $|v_j\rangle$ is equal to $\mathcal{A}\left(|v_j\rangle\right)$. The key to this calculation is to use the associativity of matrix multiplication:

$$\begin{aligned}\left(|w_i\rangle\langle v_j|\right)|v_k\rangle &= |w_i\rangle\left(\langle v_j|v_k\rangle\right)\\ &= \delta_{jk}|w_i\rangle.\end{aligned}$$

In particular, the matrix representation of the identity operator $\mathcal{I}$ in any orthonormal basis is the identity matrix I and the matrix representation of the null operator $\mathcal{O}$ in any orthonormal basis is the *zero matrix*.

If the linear operator $\mathcal{C}$ is the composition of the linear operators $\mathcal{B}$ and $\mathcal{A}$, the matrix representation of $\mathcal{C}$ will be obtained by multiplying the matrix representation of $\mathcal{B}$ with that of $\mathcal{A}$, that is, $C = BA$.

When we fix orthonormal bases for the vector spaces, there is a one-to-one correspondence between linear operators and matrices. In $\mathbb{C}^n$, we use the computational basis as a reference basis, so the terms *linear operator* and *matrix* are taken as synonyms. We will also use the term *operator* as a synonym for *linear operator*.

Exercise A.5. Suppose B is an operator whose action on the computational basis of the n-dimensional vector space V is

$$B|j\rangle = |\psi_j\rangle,$$

where $|\psi_j\rangle$ are vectors in V for all j.

1. Obtain the expression of B using the outer product.
2. Show that $|\psi_j\rangle$ is the j-th column in the matrix representation of B.

3. Suppose that B is the Hadamard operator

$$H = \frac{1}{\sqrt{2}} \begin{bmatrix} 1 & 1 \\ 1 & -1 \end{bmatrix}.$$

Redo the previous items using operator H.

A.8 Diagonal Representation

Let $\mathcal{O}$ be an operator in V. If there exists an orthonormal basis $\{|v_1\rangle, \ldots, |v_n\rangle\}$ of V such that

$$O = \sum_{i=1}^{n} \lambda_i |v_i\rangle\langle v_i|,$$

we say that $\mathcal{O}$ admits a *diagonal representation* or, equivalently, $\mathcal{O}$ is *diagonalizable*. The complex numbers λ_i are the *eigenvalues* of $\mathcal{O}$ and $|v_i\rangle$ are the corresponding *eigenvectors*. Any multiple of an eigenvector is also an eigenvector. If two eigenvectors are associated with the same eigenvalue, then any linear combination of these eigenvectors is an eigenvector. The number of linearly independent eigenvectors associated with the same eigenvalue is the *multiplicity* of that eigenvalue.

If there are eigenvalues with multiplicity greater than one, the diagonal representation can be factored out as follows:

$$O = \sum_{\lambda} \lambda P_\lambda,$$

where index λ runs only on the distinct eigenvalues and P_λ is the projector on the eigenspace of $\mathcal{O}$ associated with eigenvalue λ. If λ has multiplicity 1, $P_\lambda = |v\rangle\langle v|$, where $|v\rangle$ is the unit eigenvector associated with λ. If λ has multiplicity 2 and $|v_1\rangle, |v_2\rangle$ are linearly independent unit eigenvectors associated with λ, $P_\lambda = |v_1\rangle\langle v_1| + |v_2\rangle\langle v_2|$ and so on. The projectors P_λ satisfy

$$\sum_{\lambda} P_\lambda = I.$$

An alternative way to define a diagonalizable operator is by requiring that O is *similar* to a diagonal matrix. Matrices O and O' are similar if $O' = M^{-1}OM$ for some invertible matrix M. We have interest only in the case when M is a unitary matrix. The term *diagonalizable* we use here is narrower than the one used in the literature, because we are demanding that M be a unitary matrix.

Exercise A.6. Suppose that O is a diagonalizable operator with eigenvalues ± 1. Show that

$$P_{\pm 1} = \frac{I \pm O}{2}.$$

A.9 Completeness Relation

The *completeness relation* is so useful that it deserves to be highlighted. Let $\{|v_1\rangle, \ldots, |v_n\rangle\}$ be an orthonormal basis of V. Then,

$$I = \sum_{i=1}^{n} |v_i\rangle\langle v_i|.$$

The completeness relation is the diagonal representation of the identity matrix.

Exercise A.7. If $\{|v_1\rangle, \ldots, |v_n\rangle\}$ is an orthonormal basis, it is straightforward to verify the validity of equations

$$A|v_j\rangle = \sum_{i=1}^{m} a_{ij}|w_i\rangle$$

from equation

$$A = \sum_{i=1}^{m}\sum_{j=1}^{n} a_{ij}|w_i\rangle\langle v_j|.$$

Verify in the reverse direction using the completeness relation, that is, assuming that expressions $A|v_j\rangle$ are given for all $1 \leq j \leq n$, obtain A.

A.10 Cauchy–Schwarz Inequality

Let V be a Hilbert space and $|v\rangle, |w\rangle \in V$. Then,

$$|\langle v|w\rangle| \leq \sqrt{\langle v|v\rangle\langle w|w\rangle}.$$

A more explicit way of presenting the Cauchy–Schwarz inequality is

$$\left|\sum_i v_i w_i\right|^2 \leq \left(\sum_i |v_i|^2\right)\left(\sum_i |w_i|^2\right),$$

which is obtained when we take $|v\rangle = \sum_i v_i^*|i\rangle$ and $|w\rangle = \sum_i w_i|i\rangle$.

A.11 Special Operators

Let A be a linear operator in Hilbert space V. Then, there exists a unique linear operator $A^\dagger$ in V, called *adjoint operator*, that satisfies

$$(|v\rangle, A|w\rangle) = \left(A^\dagger|v\rangle, |w\rangle\right),$$

for all $|v\rangle, |w\rangle \in V$.

The matrix representation of $A^\dagger$ is the transpose-conjugate matrix $(A^*)^{\mathrm{T}}$. The main properties of the *dagger* or *transpose-conjugate* operation are

1. $(A\,B)^\dagger = B^\dagger A^\dagger$
2. $|v\rangle^\dagger = \langle v|$
3. $\left(A|v\rangle\right)^\dagger = \langle v|A^\dagger$
4. $\left(|w\rangle\langle v|\right)^\dagger = |v\rangle\langle w|$
5. $\left(A^\dagger\right)^\dagger = A$
6. $\left(\sum_i a_i A_i\right)^\dagger = \sum_i a_i^* A_i^\dagger$

The last property shows that the dagger operation is *conjugate-linear* when applied on a linear combination of operators.

Normal Operator

An operator A in V is *normal* if $A^\dagger A = A A^\dagger$.

Spectral Theorem

An operator A in V is diagonalizable if and only if A is normal.

Unitary Operator

An operator U in V is *unitary* if $U^\dagger U = U U^\dagger = I$.

Facts About Unitary Operators

Unitary operators are normal, so they are diagonalizable with respect to an orthonormal basis. Eigenvectors of a unitary operator associated with different eigenvalues are orthogonal. The eigenvalues have unit modulus, that is, their form is $\mathrm{e}^{\mathrm{i}\alpha}$, where α is a real number. Unitary operators preserve the inner product, that is, the inner product of $U|v_1\rangle$ by $U|v_2\rangle$ is equal to the inner product of $|v_1\rangle$ by $|v_2\rangle$. The application of a unitary operator on a vector preserves its norm.

Hermitian Operator

An operator A in V is *Hermitian* or *self-adjoint* if $A^\dagger = A$.

Facts About Hermitian Operators

Hermitian operators are normal, so they are diagonalizable with respect to an orthonormal basis. Eigenvectors of a Hermitian operator associated with different eigenvalues are orthogonal. The eigenvalues of a Hermitian operator are real numbers. A real symmetric matrix is Hermitian.

Orthogonal Projector

An operator P in V is an *orthogonal projector* if $P^2 = P$ and $P^\dagger = P$.

Facts About Orthogonal Projectors

The eigenvalues are equal to 0 or 1. If P is an orthogonal projector, then the *orthogonal complement* $I - P$ is also an orthogonal projector. Applying a projector on a vector either decreases its norm or maintains invariant. In this book, we use the term *projector* as a synonym for *orthogonal projector*. We will use the term *non-orthogonal projector* explicitly to distinguish this case. An example of a non-orthogonal projector on a qubit is $P = |1\rangle\langle +|$.

Positive Operator

An operator A in V is said *positive* if $\langle v|A|v\rangle \geq 0$ for any $|v\rangle \in V$. If the inequality is strict for any nonzero vector in V, then the operator is said *positive definite*.

Facts About Positive Operators

Positive operators are Hermitian. The eigenvalues are nonnegative real numbers.

Exercise A.8. Consider matrix

$$M = \begin{bmatrix} 1 & 0 \\ 1 & 1 \end{bmatrix}.$$

1. Show that M is not normal.
2. Show that the eigenvectors of M generate a one-dimensional space.

Exercise A.9. Consider matrix

$$M = \begin{bmatrix} 1 & 0 \\ 1 & -1 \end{bmatrix}.$$

1. Show that the eigenvalues of M are ± 1.
2. Show that M is neither unitary nor Hermitian.
3. Show that the eigenvectors associated with distinct eigenvalues of M are not orthogonal.
4. Show that M has a diagonal representation.

Exercise A.10.

1. Show that the product of two unitary operators is a unitary operator.
2. The sum of two unitary operators is necessarily a unitary operator? If not, give a counterexample.

Exercise A.11.

1. Show that the sum of two Hermitian operators is a Hermitian operator.
2. The product of two Hermitian operators is necessarily a Hermitian operator? If not, give a counterexample.

Exercise A.12. Show that $A^\dagger A$ is a positive operator for any operator A.

A.12 Pauli Matrices

The *Pauli matrices* are

$$\sigma_0 = I = \begin{bmatrix} 1 & 0 \\ 0 & 1 \end{bmatrix},$$

$$\sigma_1 = \sigma_x = X = \begin{bmatrix} 0 & 1 \\ 1 & 0 \end{bmatrix},$$

$$\sigma_2 = \sigma_y = Y = \begin{bmatrix} 0 & -\mathrm{i} \\ \mathrm{i} & 0 \end{bmatrix},$$

$$\sigma_3 = \sigma_z = Z = \begin{bmatrix} 1 & 0 \\ 0 & -1 \end{bmatrix}.$$

These matrices are unitary and Hermitian, and hence their eigenvalues are equal to ± 1. Putting in another way: $\sigma_j^2 = I$ and $\sigma_j^\dagger = \sigma_j$ for $j = 0, \ldots, 3$.

The following facts are extensively used:

$$X|0\rangle = |1\rangle,\ X|1\rangle = |0\rangle,$$

$$Z|0\rangle = |0\rangle,\ Z|1\rangle = -|1\rangle.$$

Pauli matrices form a basis for the vector space of 2×2 matrices. Therefore, a generic operator that acts on a qubit can be written as a linear combination of Pauli matrices.

Exercise A.13. Consider the representation of the state $|\psi\rangle$ of a qubit in the Bloch sphere. What is the representation of states $X|\psi\rangle$, $Y|\psi\rangle$, and $Z|\psi\rangle$ relative to $|\psi\rangle$? What is the geometric interpretation of the action of the Pauli matrices on the Bloch sphere?

A.13 Operator Functions

If we have an operator A in V, we can ask whether it is possible to calculate $\sqrt{A}$, that is, to find an operator the square of which is A? In general, we can ask ourselves whether it makes sense to use an operator as an argument of a usual function, such as, exponential or logarithmic function. If operator A is normal, it has a diagonal representation, that is, can be written in the form

$$A = \sum_i a_i |v_i\rangle\langle v_i|,$$

where a_i are the eigenvalues and the set $\{|v_i\rangle\}$ is an orthonormal basis of eigenvectors of A. We can extend the application of a function $f : \mathbb{C} \mapsto \mathbb{C}$ to A as follows

$$f(A) = \sum_i f(a_i)|v_i\rangle\langle v_i|.$$

The result is an operator defined in the same vector space V and it is independent of the choice of basis of V.

If the goal is to calculate $\sqrt{A}$, first A must be diagonalized, that is, we must determine a unitary matrix U such that $A = UDU^\dagger$, where D is a diagonal matrix. Then, we use the fact that $\sqrt{A} = U\sqrt{D}\,U^\dagger$, where $\sqrt{D}$ is calculated by taking the square root of each diagonal element.

If U is the evolution operator of an isolated quantum system that is initially in state $|\psi(0)\rangle$, the state at time t is given by

$$|\psi(t)\rangle = U^t|\psi(0)\rangle.$$

The most efficient way to calculate state $|\psi(t)\rangle$ is to obtain the diagonal representation of the unitary operator U

$$U = \sum_i \lambda_i |v_i\rangle\langle v_i|,$$

and to calculate the t-th power U, that is,

$$U^t = \sum_i \lambda_i^t |v_i\rangle\langle v_i|.$$

The system state at time t will be

$$|\psi(t)\rangle = \sum_i \lambda_i^t \left\langle v_i \middle| \psi(0) \right\rangle |v_i\rangle.$$

The *trace* of a matrix is another type of operator function. In this case, the result of applying the trace function is a complex number defined as

$$\mathrm{tr}(A) = \sum_i a_{ii},$$

where a_{ii} are the diagonal elements of A. In the Dirac notation

$$\mathrm{tr}(A) = \sum_i \langle v_i | A | v_i \rangle,$$

where $\{|v_1\rangle, \ldots, |v_n\rangle\}$ is an orthonormal basis of V. The trace function satisfies the following properties:

1. $\mathrm{tr}(aA + bB) = a\,\mathrm{tr}(A) + b\,\mathrm{tr}(B)$, (linearity)
2. $\mathrm{tr}(AB) = \mathrm{tr}(BA)$,
3. $\mathrm{tr}(A\,B\,C) = \mathrm{tr}(CA\,B)$. (cyclic property)

The third property follows from the second one. Properties 2 and 3 are valid even when A, B, and C are not square matrices.

The trace function is invariant under *similarity transformations*, that is, $\mathrm{tr}(M^{-1}AM) = \mathrm{tr}(A)$, where M is an invertible matrix. This implies that the trace does not depend on the basis choice for the matrix representation of A.

A useful formula involving the trace of operators is

$$\mathrm{tr}(A|\psi\rangle\langle\psi|) = \left\langle \psi \middle| A \middle| \psi \right\rangle,$$

for any $|\psi\rangle \in V$ and any A in V. This formula can be easily proved using the cyclic property of the trace function.

Exercise A.14. Using the method of applying functions on matrices described in this section, find all matrices M such that

$$M^2 = \begin{bmatrix} 5 & 4 \\ 4 & 5 \end{bmatrix}.$$

A.14 Tensor Product

Let V and W be finite Hilbert spaces with basis $\{|v_1\rangle, \ldots, |v_m\rangle\}$ and $\{|w_1\rangle, \ldots, |w_n\rangle\}$, respectively. The *tensor product* of V by W, denoted by $V \otimes W$, is an mn-dimensional Hilbert space, for which set $\{|v_1\rangle \otimes |w_1\rangle, |v_1\rangle \otimes |w_2\rangle, \ldots, |v_m\rangle \otimes |w_n\rangle\}$ is a basis. The tensor product of a vector in V by a vector in W, such as $|v\rangle \otimes |w\rangle$, also denoted by $|v\rangle|w\rangle$ or $|v, w\rangle$ or $|v\, w\rangle$, can be calculated explicitly via the Kronecker product, defined ahead. A generic vector in $V \otimes W$ is a linear combination of vectors $|v_i\rangle \otimes |w_j\rangle$, that is, if $|\psi\rangle \in V \otimes W$ then

$$|\psi\rangle = \sum_{i=1}^{m} \sum_{j=1}^{n} a_{ij} |v_i\rangle \otimes |w_j\rangle.$$

The tensor product is *bilinear*, that is, linear in each argument:

1. $|v\rangle \otimes \big(a\,|w_1\rangle + b\,|w_2\rangle\big) \;=\; a\,|v\rangle \otimes |w_1\rangle + b\,|v\rangle \otimes |w_2\rangle$,
2. $\big(a\,|v_1\rangle + b\,|v_2\rangle\big) \otimes |w\rangle \;=\; a\,|v_1\rangle \otimes |w\rangle + b\,|v_2\rangle \otimes |w\rangle$.

A scalar can always be factored out to the beginning of the expression:

$$a\big(|v\rangle \otimes |w\rangle\big) \;=\; \big(a|v\rangle\big) \otimes |w\rangle \;=\; |v\rangle \otimes \big(a|w\rangle\big).$$

The tensor product of a linear operator A in V by B in W, denoted by $A \otimes B$, is a linear operator in $V \otimes W$ defined by

$$\big(A \otimes B\big)\big(|v\rangle \otimes |w\rangle\big) \;=\; \big(A|v\rangle\big) \otimes \big(B|w\rangle\big).$$

A generic linear operator in $V \otimes W$ can be written as a linear combination of operators of the form $A \otimes B$, but an operator in $V \otimes W$ cannot be factored out in general. This definition can easily be extended to operators $A : V \mapsto V'$ and $B : W \mapsto W'$. In this case, the tensor product of these operators is of type $(A \otimes B) : (V \otimes W) \mapsto (V' \otimes W')$.

In quantum mechanics, it is very common to use operators in the form of external products, for example, $A = |v\rangle\langle v|$ and $B = |w\rangle\langle w|$. The tensor product of A by B can be represented by the following equivalent ways:

$$\begin{aligned} A \otimes B &= \big(|v\rangle\langle v|\big) \otimes \big(|w\rangle\langle w|\big) \\ &= |v\rangle\langle v| \otimes |w\rangle\langle w| \\ &= |v, w\rangle\langle v, w|. \end{aligned}$$

If A_1, A_2 are operators in V and B_1, B_2 are operators in W, then the composition or the matrix product of the matrix representations obey the property

$$(A_1 \otimes B_1) \cdot (A_2 \otimes B_2) = (A_1 \cdot A_2) \otimes (B_1 \cdot B_2).$$

The inner product of $|v_1\rangle \otimes |w_1\rangle$ by $|v_2\rangle \otimes |w_2\rangle$ is defined as

$$\left(|v_1\rangle \otimes |w_1\rangle\,,\, |v_2\rangle \otimes |w_2\rangle\right) = \langle v_1|v_2\rangle\langle w_1|w_2\rangle.$$

The inner product of vectors written as a linear combination of basis vectors are calculated by applying the linear property in the second argument and the *conjugate-linear* property in the first argument of the inner product. For example,

$$\left(\left(\sum_{i=1}^{n} a_i|v_i\rangle\right) \otimes |w_1\rangle\,,\, |v\rangle \otimes |w_2\rangle\right) = \left(\sum_{i=1}^{n} a_i^* \langle v_i|v\rangle\right)\langle w_1|w_2\rangle.$$

The inner product definition implies that

$$\| |v\rangle \otimes |w\rangle \| = \| |v\rangle \| \cdot \| |w\rangle \|.$$

In particular, the norm of the tensor product of unit-norm vectors is a unit-norm vector.

When we use matrix representations for operators, the tensor product can be calculated explicitly via the *Kronecker product*. Let A be a $m \times n$ matrix and B a $p \times q$ matrix. Then,

$$A \otimes B = \begin{bmatrix} a_{11}B & \cdots & a_{1n}B \\ & \ddots & \\ a_{m1}B & \cdots & a_{mn}B \end{bmatrix}.$$

The dimension of the resulting matrix is $mp \times nq$. The Kronecker product can be used for matrices of any dimension, particularly for two vectors,

$$\begin{bmatrix} a_1 \\ a_2 \end{bmatrix} \otimes \begin{bmatrix} b_1 \\ b_2 \end{bmatrix} = \begin{bmatrix} a_1 \begin{bmatrix} b_1 \\ b_2 \end{bmatrix} \\ a_2 \begin{bmatrix} b_1 \\ b_2 \end{bmatrix} \end{bmatrix} = \begin{bmatrix} a_1 b_1 \\ a_1 b_2 \\ a_2 b_1 \\ a_2 b_2 \end{bmatrix}.$$

The tensor product is an associative and distributive operation, but noncommutative, that is, $|v\rangle \otimes |w\rangle \neq |w\rangle \otimes |v\rangle$ if $v \neq w$. Most operations on a tensor product are performed term by term, such as

$$(A \otimes B)^\dagger = A^\dagger \otimes B^\dagger.$$

If both operators A and B are special operators of the same type, as the ones defined in Sect. A.11, then the tensor product $A \otimes B$ is also a special operator of the same type. For example, the tensor product of Hermitian operators is a Hermitian operator.

The trace of a Kronecker product of matrices is

$$\mathrm{tr}(A \otimes B) = \mathrm{tr}A \ \mathrm{tr}B,$$

while the determinant is

$$\det(A \otimes B) = (\det A)^m \ (\det B)^n,$$

where n is the dimension of A and m of B.

The direct sum of a vector space V with itself n times is a particular case of the tensor product. In fact, a matrix $A \oplus \cdots \oplus A$ in $V \oplus \cdots \oplus V$ is equal to $I \otimes A$ for any A in V, where I is the $n \times n$ identity matrix. This shows that, somehow, the tensor product is defined from the direct sum of vector spaces, analogous to the product of numbers which is defined from the sum of numbers. However, the tensor product is richer than the simple repetition of the direct sum of vector spaces. Anyway, we can continue generalizing definitions: It is natural to define tensor potentiation, in fact, $V^{\otimes n}$ means $V \otimes \cdots \otimes V$ with n terms.

If the *diagonal state* of the vector space V is $|\mathrm{D}\rangle_V$ and of space W is $|\mathrm{D}\rangle_W$, then the diagonal state of space $V \otimes W$ is $|\mathrm{D}\rangle_V \otimes |\mathrm{D}\rangle_W$. Therefore, the diagonal state of space $V^{\otimes n}$ is $|\mathrm{D}\rangle^{\otimes n}$.

Exercise A.15. Let H be the Hadamard operator

$$H = \frac{1}{\sqrt{2}} \begin{bmatrix} 1 & 1 \\ 1 & -1 \end{bmatrix}.$$

Show that

$$\langle i | H^{\otimes n} | j \rangle = \frac{(-1)^{i \cdot j}}{\sqrt{2^n}},$$

where n represents the number of qubits and $i \cdot j$ is the binary inner product, that is, $i \cdot j = i_1 j_1 + \cdots + i_n j_n \mod 2$, where $(i_1, \ldots, i_n)$ and $(j_1, \ldots, j_n)$ are the binary decompositions of i and j, respectively.

A.15 Registers

A *register* is a set of qubits treated as a composite system. In many quantum algorithms, the qubits are divided into two registers: one for the main calculation from where the result comes out and the other for the draft (calculations that will be erased). Suppose we have a register with two qubits. The computational basis is

$$|0,0\rangle = \begin{bmatrix} 1 \\ 0 \\ 0 \\ 0 \end{bmatrix} \quad |0,1\rangle = \begin{bmatrix} 0 \\ 1 \\ 0 \\ 0 \end{bmatrix} \quad |1,0\rangle = \begin{bmatrix} 0 \\ 0 \\ 1 \\ 0 \end{bmatrix} \quad |1,1\rangle = \begin{bmatrix} 0 \\ 0 \\ 0 \\ 1 \end{bmatrix}.$$

A generic state of this register is

$$|\psi\rangle = \sum_{i=0}^{1}\sum_{j=0}^{1} a_{ij}|i,j\rangle$$

where coefficients a_{ij} are complex numbers that satisfy the constraint

$$|a_{00}|^2 + |a_{01}|^2 + |a_{10}|^2 + |a_{11}|^2 = 1.$$

To help generalizing to n qubits, it is usual to compress the notation by converting binary-base representation to decimal-base. The computational basis for two-qubit register in decimal-base representation is $\{|0\rangle, |1\rangle, |2\rangle, |3\rangle\}$. In the binary-base representation, we can determine the number of qubits by counting the number of digits inside the *ket*, for example, $|011\rangle$ refers to three qubits. In the decimal-base representation, we cannot determine what is the number of qubits of the register. This information should come implicit. In this case, we can go back, write the numbers in the binary-base representation and explicitly retrieve the notation. In the compact notation, a generic state of a n-qubit register is

$$|\psi\rangle = \sum_{i=0}^{2^n-1} a_i|i\rangle,$$

where coefficients a_i are complex numbers that satisfy the constraint

$$\sum_{i=0}^{2^n-1} |a_i|^2 = 1.$$

The *diagonal state* of a n-qubit register is the tensor product of the diagonal state of each qubit, that is, $|\mathrm{D}\rangle = |+\rangle^{\otimes n}$.

Exercise A.16. Let f be a function with domain $\{0,1\}^n$ and codomain $\{0,1\}^m$. Consider a 2-register quantum computer with n and m qubits, respectively. Function f can be implemented by using operator U_f defined in the following way:

$$U_f|x\rangle|y\rangle = |x\rangle|y \oplus f(x)\rangle,$$

where x has n bits, y has m bits, and $\oplus$ is the binary sum (bitwise *xor*).

1. Show that U_f is a unitary operator for any f.
2. If $n = m$ and f is injective, show that f can be implemented on a 1-register quantum computer with n qubits.

Further Reading

There are many good books about linear algebra. For an initial contact, we suggest [11, 12, 37, 72]; for a more advanced approach, we suggest [36]; for those who have mastered the basics and are only interested in the application of linear algebra on quantum computation, we suggest [64].

References

1. Aaronson, S., Ambainis, A.: Quantum search of spatial regions. Theory of Computing, **1**, 47–79 (2003)
2. Abal, G., Donangelo, R., Marquezino, F.L., Portugal, R.: Spatial search on a honeycomb network. Math. Struct. Comput. Sci. **20**(Special Issue 06), 999–1009 (2010)
3. Aharonov, D., Ambainis, A., Kempe, J., Vazirani, U.: Quantum walks on graphs. In: Proceedings of 33th STOC, pp. 50–59. ACM, New York (2001)
4. Aharonov, D.: Quantum computation – a review. In: Stauffer, D. (ed.) Annual Review of Computational Physics, vol. VI, pp. 1–77. World Scientific, Singapore (1998)
5. Aharonov, Y., Davidovich, L., Zagury, N.: Quantum random walks. Phys. Rev. A **48**(2), 1687–1690 (1993)
6. Aldous, D.J., Fill, J.A.: Reversible Markov Chains and Random Walks on Graphs. Book in preparation, http://www.stat.berkeley.edu/~aldous/RWG/book.html (2002)
7. Ambainis, A., Bach, E., Nayak, A., Vishwanath, A., Watrous, J.: One-dimensional quantum walks. In: Proceedings of 33th STOC, pp. 60–69. ACM, New York (2001)
8. Ambainis, A., Backurs, A., Nahimovs, N., Ozols, R., Rivosh, A.: Search by quantum walks on two-dimensional grid without amplitude amplification. arxiv:1112.3337 (2011)
9. Ambainis, A.: Quantum walk algorithm for element distinctness. In: FOCS '04: Proceedings of the 45th Annual IEEE Symposium on Foundations of Computer Science, pp. 22–31. IEEE Computer Society, Washington, DC (2004)
10. Ambainis, A., Kempe, J., Rivosh, A.: Coins make quantum walks faster. In: Proceedings of the Sixteenth Annual ACM-SIAM Symposium on Discrete Algorithms, pp. 1099–1108. SIAM, Philadelphia (2005)
11. Apostol, T.M.: Calculus, vol. 1: One-Variable Calculus with an Introduction to Linear Algebra. Wiley, New York (1967)
12. Axler, S.: Linear Algebra Done Right. Springer, New York (1997)
13. Bednarska, M., Grudka, A., Kurzynski, P., Luczak, T., Wójcik, A.: Quantum walks on cycles. Phys. Lett. A **317**(1–2), 21–25 (2003)
14. Bednarska, M., Grudka, A., Kurzynski, P., Luczak, T., Wójcik, A.: Examples of non-uniform limiting distributions for the quantum walk on even cycles. Int. J. Quant. Inform. **2**(4), 453–459 (2004)
15. Benioff, P.: Space searches with a quantum robot. (ed.) Samuel J. Lomonaco, Jr. and Howard D. Brandt Contemporary Mathematics, AMS, as a special session about Quantum Computation and Information, vol. 305, pp. 1–12. Washington, D.C (2002)
16. Bennett, C.H., Bernstein, E., Brassard, G., Vazirani, U.V.: Strengths and weaknesses of quantum computing. SIAM J. Comput. **26**(5), 1510–1523 (1997)

R. Portugal, *Quantum Walks and Search Algorithms*, Quantum Science and Technology, DOI 10.1007/978-1-4614-6336-8,

17. Boyer, M., Brassard, G., Høyer, P., Tapp, A.: Tight bounds on quantum searching. Forstschritte Der Physik **4**, 820–831 (1998)
18. Brassard, G., Høyer, P., Mosca, M., Tapp, A.: Quantum amplitude amplification and estimation. Quant. Comput. Quant. Inform. Sci., Comtemporary Mathematics **305**, 53–74, (2002), quant-ph/0005055
19. Carteret, H.A., Ismail, M.E.H., Richmond, B.: Three routes to the exact asymptotics for the one-dimensional quantum walk. J. Phys A: Math. General **36**(33), 8775–8795 (2003)
20. Childs, A.: On the relationship between continuous- and discrete-time quantum walk. Commun. Math. Phys. **294**, 581–603 (2010)
21. Childs, A.M.: Universal computation by quantum walk. Phys. Rev. Lett. **102**, 180501 (2009)
22. Childs, A.M., Farhi, E., Gutmann, S.: An example of the difference between quantum and classical random walks. Quant. Informa. Process. **1**(1), 35–43 (2002)
23. Diu, B., Cohen-Tannoudji, C., Laloe, F.: Quantum Mechanics. Wiley-Interscience, New York (2006)
24. Cover, T.M., Thomas, J.: Elements of Information Theory. Wiley, New York (1991)
25. d'Espagnat, B.: Conceptual Foundations of Quantum Mechanics. Westview Press, Boulder (1999)
26. Farhi, E., Gutmann, S.: Quantum computation and decision trees. Phys. Rev. A **58**, 915–928 (1998)
27. Feller, W.: An Introduction to Probability Theory and Its Applications, vol. 1, 3rd edn. Wiley, New York (1968)
28. Forets, M., Abal, G., Donangelo, R., Portugal, R.: Spatial quantum search in a triangular network. Math. Struct. Comput. Sci. **22**(03), 521–531 (2012)
29. Gould, H.W.: Combinatorial Identities. Morgantown Printing and Binding Co., Morgantown (1972)
30. Graham, R.L., Knuth, D.E., Patashnik, O.: Concrete Mathematics: A Foundation for Computer Science, 2nd edn. Addison-Wesley Professional, Reading (1994)
31. Griffiths, D.: Introduction to Quantum Mechanics, 2nd edn. Benjamin Cummings, Menlo Park (2005)
32. Grover, L.K.: Quantum computers can search arbitrarily large databases by a single query. Phys. Rev. Lett. **79**(23), 4709–4712 (1997)
33. Grover, L.K.: Quantum mechanics helps in searching for a needle in a haystack. Phys. Rev. Lett. **79**(2), 325–328 (1997)
34. Grover, L.K.: Quantum computers can search rapidly by using almost any transformation. Phys. Rev. Lett. **80**(19), 4329–4332 (1998)
35. Hein, B., Tanner, G.: Quantum search algorithms on a regular lattice. Phys. Rev. A **82**(1), 012326 (2010)
36. Hoffman, K.M., Kunze, R.: Linear Algebra. Prentice Hall, New York (1971)
37. Horn, R., Johnson, C.R.: Matrix Analysis. Cambridge University Press, Cambridge (1985)
38. Hughes, B.D.: Random Walks and Random Environments: Random Walks (Vol 1). Clarendon Press, Oxford (1995)
39. Hughes, B.D.: Random Walks and Random Environments: Random Environments (Vol 2). Oxford University Press, Oxford (1996)
40. Itakura, Y.K.: Quantum algorithm for commutativity testing of a matrix set. Master's thesis, University of Waterloo, Waterloo (2005)
41. Kaye, P., Laflamme, R., Mosca, M.: An Introduction to Quantum Computing. Oxford University Press, Oxford (2007)
42. Kempe, J.: Quantum random walks – an introductory overview. Contemp. Phys. **44**(4), 302–327 (2003) quant-ph/0303081
43. Kempe, J.: Discrete quantum walks hit exponentially faster. Probab. Theor. Relat. Field. **133**(2), 215–235 (2005), quant-ph/0205083
44. Konno, N.: Quantum random walks in one dimension. Quant. Inform. Process. **1**(5), 345–354 (2002)
45. Košík, J.: Two models of quantum random walk. Cent. Eur. J. Phys. **4**, 556–573 (2003)

46. Krovi, H., Magniez, F., Ozols, M., Roland, J.: Finding is as easy as detecting for quantum walks. In: Automata, Languages and Programming. Lecture Notes in Computer Science, vol. 6198, pp. 540–551. Springer, Berlin (2010)
47. Lovász, L.: Random walks on graphs: a survey. Bolyai Society Mathematical Studies, Vol. 2, pp. 1–46. Springer (1993)
48. Lovett, N.B., Cooper, S., Everitt, M., Trevers, M., Kendon, V.: Universal quantum computation using the discrete-time quantum walk. Phys. Rev. A **81**, 042330 (2010)
49. Mackay, T.D., Bartlett, S.D., Stephenson, L.T., Sanders, B.C.: Quantum walks in higher dimensions. J. Phys. A: Math. General **35**(12), 2745 (2002)
50. Magniez, F., Nayak, A.: Quantum complexity of testing group commutativity. Algorithmica **48**(3), 221–232 (2007)
51. Magniez, F., Nayak, A., Richter, P., Santha, M.: On the hitting times of quantum versus random walks. In: Proceedings of the Twentieth Annual ACM-SIAM Symposium on Discrete Algorithms, pp. 86–95. Philadelphia (2009)
52. Magniez, F., Nayak, A., Roland, J., Santha, M.: Search via quantum walk. In: Proceedings of the Thirty-ninth Annual ACM Symposium on Theory of Computing, pp. 575–584. New York (2007)
53. Magniez, F., Santha, M., Szegedy, M.: Quantum algorithms for the triangle problem. SIAM J. Comput. **37**(2), 413–424. New York (2007)
54. Marquezino, F.L., Portugal, R., Abal, G.: Mixing times in quantum walks on two-dimensional grids. Phys. Rev. A **82**(4), 042341 (2010)
55. Marquezino, F.L., Portugal, R., Abal, G., Donangelo, R.: Mixing times in quantum walks on the hypercube. Phys. Rev. A **77**, 042312 (2008)
56. Marquezino, F.L., Portugal, R.: The QWalk simulator of quantum walks. Comput. Phys. Commun. **179**(5), 359–369 (2008), arXiv:0803.3459
57. Mermin, N.D.: Quantum Computer Science: An Introduction. Cambridge University Press, New York (2007)
58. Meyer, C.D.: Matrix Analysis and Applied Linear Algebra. SIAM, Philadelphia (2001)
59. Moore, C., Russell, A.: Quantum walks on the hypercube. In: Rolim, J.D.P., Vadhan, S. (eds.) Proceedings of Random 2002, pp. 164–178. Springer, Cambridge (2002)
60. Moore, C., Mertens, S.: The Nature of Computation. Oxford University Press, New York (2011)
61. Mosca, M.: Counting by quantum eigenvalue estimation. Theor. Comput. Sci. **264**(1), 139–153 (2001)
62. Motwani, R., Raghavan, P.: Randomized algorithms. ACM Comput. Surv. **28**(1), 33–37 (1996)
63. Nayak, A., Vishwanath, A.: Quantum walk on a line. DIMACS Technical Report 2000-43, quant-ph/0010117 (2000)
64. Nielsen, M.A., Chuang, I.L.: Quantum Computation and Quantum Information. Cambridge University Press, New York (2000)
65. Omnès, R.: Understanding Quantum Mechanics. Princeton University Press, Princeton (1999)
66. Peres, A.: Quantum Theory: Concepts and Methods. Springer, Berlin (1995)
67. Preskill, J.: Lecture Notes on Quantum Computation. http://www.theory.caltech.edu/~preskill/ph229 (1998)
68. Rieffel, E., Polak, W.: Quantum Computing, a Gentle Introduction. MIT, Cambridge (2011)
69. Sakurai, J.J.: Modern Quantum Mechanics. Addison Wesley, Reading (1993)
70. Santos, R.A.M., Portugal, R.: Quantum hitting time on the complete graph. Int. J. Quant. Inform. **8**(5), 881–894 (2010), arXiv:0912.1217
71. Shenvi, N., Kempe, J., Whaley, K.B.: A quantum random walk search algorithm. Phys. Rev. A **67**(5), 052307 (2003), quant-ph/0210064
72. Strang, G.: Linear Algebra and Its Applications. Brooks Cole, Belmont (1988)
73. Strauch, F.W.: Connecting the discrete- and continuous-time quantum walks. Phys. Rev. A **74**(3), 030301 (2006)
74. Szegedy, M.: Quantum speed-up of markov chain based algorithms. In: Proceedings of the Fourty-fifth Annual IEEE Symposium on the Foundations of Computer Science, pp. 32–41 (2004). DOI: 10.1109/FOCS.2004.53

75. Szegedy, M.: Spectra of Quantized Walks and a $\sqrt{\delta\epsilon}$ Rule. (2004), quant-ph/0401053
76. Travaglione, B.C., Milburn, G.J.: Implementing the quantum random walk. Phys. Rev. A **65**(3), 032310 (2002)
77. Tregenna, B., Flanagan, W., Maile, R., Kendon, V.: Controlling discrete quantum walks: coins and initial states. New J. Phys. **5**(1), 83 (2003), quant-ph/0304204
78. Tulsi, A.: Faster quantum-walk algorithm for the two-dimensional spatial search. Phys. Rev. A **78**(1), 012310 (2008)
79. Venegas-Andraca, S.E.: Quantum walks: a comprehensive review. Quantum Information Processing **11**(5), 1015–1106 (2012), arXiv:1201.4780
80. Venegas-Andraca, S.E.: Quantum Walks for Computer Scientists. Morgan and Claypool Publishers, San Rafael (2008)
81. Štefaňák, M., Kollár, B., Kiss, T., Jex, I.: Full revivals in 2d quantum walks. Phys. Scripta **2010**(T140), 014035 (2010)
82. Štefaňák, M.: Interference phenomena in quantum information. PhD thesis, Czech Technical University (2010), arXiv:1009.0200
83. Zalka, C.: Grover's Quantum Searching Algorithm is Optimal. Phys. Rev. A **60**, 2746–2751 (1999)

Index

R. Portugal, *Quantum Walks and Search Algorithms*, Quantum Science and Technology, DOI 10.1007/978-1-4614-6336-8,